Innate immune potential of bovine respiratory epithelial cells: role in viral infection

Trinity College Dublin
Coláiste na Tríonóide, Baile Átha Cliath
The University of Dublin

This thesis is submitted to The University of Dublin for the degree of Doctor of Philosophy (Ph.D.)

2023

Sarah Swoboda

B.Sc., M.Sc.

School of Biochemistry and Immunology

Trinity College Dublin

Supervisors: Prof. Cliona O'Farrelly and Dr. Kieran Meade

Declaration

I declare that this thesis has not been submitted as an exercise for a degree at this or any other university and it is entirely my own work.

I agree to deposit this thesis in the University's open access institutional repository or allow the Library to do so on my behalf, subject to Irish Copyright Legislation and Trinity College Library conditions of use and acknowledgement.

I consent to the examiner retaining a copy of the thesis beyond the examining period, should they so wish (EU GDPR May 2018).

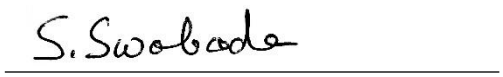

Sarah Swoboda

October 2022

Abstract

Respiratory epithelial cells have important defence activities against respiratory viruses. While their physical barrier function is well described, the molecular mechanisms responsible for how epithelial cells initiate, mediate and regulate local immune activity to viral infection are poorly defined, particularly in livestock species. This lack of knowledge contributes to the challenge in controlling respiratory infections, including bovine herpesvirus 1 (BoHV-1) in cattle. Our study hypothesises that bovine respiratory epithelial cells can respond directly to viral infections and have potent innate molecular antiviral activity. The overall aim was to characterise innate antiviral immune potential of primary bovine respiratory epithelial cells in responding to purified live BoHV-1 and viral ligands.

A cell culture model of primary bovine tracheal epithelial cells was established in order to provide physiologically relevant insight into immune mechanisms. These cultures retain the same genetic and physiological characteristics of their *in-vivo* host. While demonstrating significant inter-animal variation reflective of the outbred animal population, our primary culture model is reproducible and easily available, with low costs, from abattoir by-products. Using this model, we demonstrated that BoHV-1 is able to infect primary tracheal epithelial cells and went on to examine the transcriptomic changes induced early in infection.

Bulk next generation RNA sequencing analysis of epithelial cells infected with purified live BoHV-1 (MOI 7) for 6 hours revealed after correction or multiple testing, differential expression of nine genes. The heat shock protein family A (Hsp70) member 6 gene *HSPA6* demonstrated a fold change of 16 (adj. p-value = 2.59E-45) and was the most upregulated gene. We went on to investigate other heat shock proteins (GRP78/HSPA5 and GRP94/HSP90B1) that are involved in stress responses occurring during viral infections as part of the unfolded protein response (UPR). The UPR is a fundamental cellular defence mechanism activated by disrupted ER homeostasis caused by the accumulation of mis- and unfolded proteins during viral replication. Previously considered reflective of non-specific stress in the host promoting cell survival or

initiating cell death, it has become clear that viruses can disarm the UPR in order to assist their replication. We found that infection with purified live BoHV-1 virus downregulated genes involved in the UPR in primary bovine tracheal epithelial cells (*ATF6*, *DDIT3*, *sXBP1* and *HERPUD1*). Thapsigargin (Tg) is an ER stressor which inhibits the sarcoplasmic/endoplasmic reticulum Ca^{2+} ATPase pump. Pre-treatment of primary cells with Tg partly counteracted the virally-induced downregulation of *GRP78*, *sXBP1*, *HERPUD1* and *GRP94*. Pre-treatment with Tg also significantly decreased viral genome expression. Further investigations of the UPR manipulation by viruses and UPR targeting agents may identify new strategies for preventing infection by respiratory viruses.

Innate immune mechanisms active in bovine tracheal epithelial cells were further investigated by qPCR analysis and results showed that these cells are equipped with membrane associated and cytosolic pathogen recognition receptors (PRRs). While infection with BoHV-1 failed to upregulate expression of *IL6, TNF, IFNB1* and *IFNB3* genes in primary bovine tracheal epithelial cells, the gene encoding interferon λ3 (*IFNL3*), was upregulated by > 30 fold after 24 hours. Interferon stimulated genes *RSAD2, ISG15* and *USP18* were also significantly upregulated as was *IDO1,* an important enzyme in several metabolic pathways and a key immunosuppressor. In recent years, modulation of cellular metabolic pathways, including the synthesis of cholesterol, polyamines and tryptophan by ISGs has been discovered to have exciting potential as a novel antiviral strategy and our results support this approach.

Our results also emphasise an important role for IFN-λ at epithelial surfaces during BoHV-1 infection. However, it is unclear what signalling pathways lead to IFN-λ upregulation and to which extent it might contribute to antiviral innate immunity in epithelial cells. We found that stimulation with Poly(dA:dT), a synthetic dsDNA sequence capable of stimulating multiple cytosolic DNA sensors, and 3p-hpRNA, a 5' triphosphate hairpin RNA as a RIG-I agonist, induced significant expression of *IFNL3* in tracheal epithelial cells, while type I interferons were not significantly induced. Stimulation with Poly(I:C), a synthetic nucleic acid molecule with similar structure to viral dsRNA and TLR3 agonist, upregulated the viral sensing genes *DDX58*, *IFIH1*, *IFI16* and *MB21D1* and induced the interferon-stimulated genes *ISG15, RSAD2, USP18* and *IDO1*. Regulation of

IFNB1 or *IFNB3* was not detected. In contrast, *IFNL3* expression was significantly increased by over 9,000-fold in response to Poly(I:C) at 6 hours. A 6-hour pre-treatment with Poly(I:C) also significantly decreased viral genome abundance. This inhibition indicates that activation of the TLR3/RIG-like receptor signalling pathways induces an antiviral state effective against BoHV-1 replication in tracheal epithelial cells.

Our study highlights the importance of epithelial cells for local innate antiviral activity in the respiratory tract due to their ability to detect and respond to viral infection. Our studies using the infection model of primary bovine tracheal epithelial cells demonstrate the significant innate immune potential of bovine tracheal epithelial cells against viral pathogens characterised by significant *IFNL3* upregulation. We demonstrate protective antiviral potential against viral infection in these cells through activation of the TLR3/RIG-like receptor signalling pathway. Further characterisation of antiviral innate immune potential of respiratory epithelial cells including definition of the signalling pathways underpinning inter-animal variation will ultimately contribute to breeding and immunotherapeutic strategies capable of preventing and better treatment of BoHV-1 infection in livestock.

Table of Contents

Acknowledgements

Everyone told me doing a PhD can be difficult, infuriating, rewarding and exciting at the same time. The reality is, I had no idea what this meant when I started nearly 5 years ago. I can't believe that I'm actually submitting a thesis at the end of this journey, and I wouldn't have been able to do this without the help and support of so many people.

Firstly, I would like to thank my supervisors Cliona O'Farrelly and Kieran Meade. Cliona for her incredible enthusiasm for all results and all directions this project went through. Thank you for everything you taught me, as a scientist and as a human. Thank you, Kieran, for providing the focus and making sure I don't forget that there is a bovine world out there. I know I wasn't the easiest student along the way, so thank you for sticking with me and pushing me through the difficult times. Gerald Barry, thank you so much for the ideas, questions to think about and most importantly for the support and optimism along the way.

Thank you to the best lab group I could have asked for! You all played such an important part, I definitely couldn't have got through the last years without you! Mag, thank you for literally always being there for me, all the life-advice, counselling or small talk when needed. Thank you, Paul, for getting me started in the lab and you probably don't realise how helpful your messages were in the last years! Jamie, my PhD buddy, everyone needs a PhD buddy like you! Thank you for understanding my problems and cheering me up – we made it! Mihai, thank you for bringing the craziness back into the lab and for letting me think about new avenues for my project when I couldn't see them. Federica, thank you so much for everything! You not only sorted out the lab when needed, you also were there for the fun, hugs and girl talks. The time wouldn't have been the same without you. Emer and Sarah, thank you for bringing so much fun into the lab life. You all together were an incredible group to be part of and making my last 5 years really special – including my wedding!

A big thank you to the bovine team – Charlotte, Megan, Amy, Susana and Cian! It was a pleasure to meet you all and thank you for all the help!

I have to mention the best German lab crew, you tought me so much and prepared me so well for my PhD life! You wouldn't believe how many times I did things your way! Cell plates need an eight and a cross. Thank you Sven, Birgit and Patricia!

To all my friends in the real world, I know this PhD thing wasn't easy to understand, but you all had such an important part in keeping me motivated and picking me up. Thank you Brian and Debbie for the best and longest possible Sundays. I wouldn't have managed the time without always looking forward to the next weekend. Brian, thank you so much for all you've done for me. Hannah, for over 20 years now we've shared everything and I'm so lucky to have you as my best friend. There was no question we would manage these 5 years as well - thank you for always being there for me.

Nothing would have been possible without the unbelievable support of my family – my grandparents, parents and my husband. I can't thank you enough for everything. Matt, I don't even know where to start in describing how you helped me over the last years to be able to do this. Thank you for going on this journey with me, I love you.

It wouldn't be me if I didn't finish on something to do with horses! You all made it possible in some shape or form for me to be able to have my horse-time beside doing a PhD and staying sane! I can't thank you all enough for it!

To everyone who has helped me over the last years: thank you!

Abbreviations

°C	Degrees Celsius
µm	Micron
AEC	Airway epithelial cells
ANOVA	Analysis of variance
BCA	Bicinchoninic acid assay
BCoV	Bovine coronavirus
BiP	Immunoglobulin heavy chain binding protein
BLAST	Basic Local Alignment Search Tool
BoHV-1	Bovine herpes virus 1
bp	Base-pair
BRD	Bovine respiratory disease
BRSV	Bovine coronavirus
BSA	Bovine serum albumin
BVDV	Bovine viral diarrhoea virus
cDNA	Complementary deoxyribonucleic acid
cGAS	Cyclic GMP-AMP synthase
CPE	Cytopathic effect
DAB	3,3'-Diaminobenzidine
DAMP	Danger-associated molecular patterns
DC	Dendritic cell
DDT	DL-Dithiothreitol
DMEM	Dulbecco's Modified Eagle's Medium
DMSO	Dimethyl sulfoxide
DNA	Deoxyribonucleic acid
dsDNA	Double-stranded DNA
dsRNA	Double-stranded RNA
EDTA	Ethylenediaminetetraacetic acid
EGFR	Epidermal growth factor receptor
eIF2a	Eukaryotic translation-initiation factor 2α

ELISA	Enzyme linked immunosorbent assay
ER	Endoplasmic reticulum
ERAD	ER-associated protein degradation
ERK	Extracellular regulated protein kinase
FADD	Fas-associated death domain
FBS	Fetal bovine serum
g	Gram or gravity (nominal)
GAPDH	Glyceraldehyde 3-phosphate dehydrogenase
gB	Glycoprotein B
GOI	Gene of interest
h	Hour
H1N1	Influenza A
H3F3A	H3 histone family member 3A
HCV	Hepatitis C virus
HS	Horse serum
HSF	Heat shock factor
HSP	Heat shock protein
HSR	Heat shock response
HSV-1	Herpes simplex virus 1
IAV	Influenza A virus
IBR	Infectious bovine rhinotracheitis
iDEP	Integrated Differential Expression and Pathway analysis
IDO1	Indoleamine-2,3-dioxygenase
IFNAR	Interferon-α/β receptor
IL	Interleukin
IRF	Interferon regulatory factor
ISG	Interferon-stimulated gene
kDa	Kilo-Dalton
KRT18	Keratin 18
LC-MS	Liquid chromatography - mass spectrometry
LDH	Lactate Dehydrogenase

LPS	Lipopolysaccharide
MAVS	Mitochondrion-associated antiviral signalling protein
MDA5	Melanoma differentiation-associated protein 5
MDBK	Madin-Darby bovine kidney
mg/µg/ng/pg	Milli-/micro-/nano-/pico-gram
Min	Minute
ml/µl	Milli-/micro-litre
mm/cm/µm/nm	Milli-/centi-/micro-/nano-meter
mRNA	Messenger ribonucleic acid
NCBI	National Centre for Biotechnology Information
NFκB	Nuclear factor kappa B
NK	Natural killer cell
NLR	Nod like receptor
p	p-value
PAMP	Pathogen associated molecular pattern
PBMC	Peripheral blood mononuclear cell
PBS	Phosphate buffered saline
PCA	Principal component analysis
PCR	Polymerase chain reaction
pDC	Plasmacytoid dendritic cell
PERK	Pancreatic ER kinase
PIV-3	Bovine parainfluenza virus 3
PMN	Polymorphonuclear cells
Poly(dA:dT)	Poly(deoxyadenylic-deoxythymidylic) acid sodium salt
Poly(I:C)	Polyinosinic-polycytidylic acid
PRR	Pattern recognition receptor
qPCR	Quantitative polymerase chain reaction
RIG-I	Retinoic acid inducible gene I
RLH	RIG-like helicase
RLR	RIG-like receptor
RNA	Ribonucleic acid

RNA-seq	RNA sequencing
RSV	Respiratory syncytial virus
SARS-CoV-2	Severe acute respiratory syndrome coronavirus 2
SDS-PAGE	Sodium dodecyl sulfate polyacrylamide gel electrophoresis
Sec	Second
siRNA	Short-interfering ribonucleic acid
SNP	Single-nucleotide polymorphism
ssRNA	Single-stranded RNA
TEER	Trans-epithelial electrical resistance
Tg	Thapsigargin
TLR	Toll-like receptor
TNF	Tumour necrosis factor
Trp	Tryptophan
UPR	Unfolded protein response
v/v	Volume per volume
VZV	Varicella zoster virus
w/v	Weight per volume

List of Figures

List of Tables

Chapter 1. Introduction

1.1. The role of viral infections in the bovine respiratory disease complex (BRD)

Bovine respiratory disease (BRD) is a multi-factorial disease complex and one of the most frequent diseases of cattle impacting animal welfare, performance, and economic parameters. Annually, it costs the American feedlot industry $800-900 million due to loss of production, increased labour expenses, medication costs and death (Health, 2020). BRD is behind about 75% of illness and up to 70% of cattle deaths in feedlots (Loneragan et al., 2001). It occurs as shipping fever pneumonia of feedlot cattle, enzootic pneumonia of dairy and beef calves and pneumonia of adult cows (Caswell, 2014). In 2020, 457 carcases were diagnosed with BRD based on *post-mortem* examination and subsequent laboratory test results in Ireland. The number of cases and percentage (%) by age of the general pathogenic groups detected are shown in **Tab. 1.1**.

Table 1.1 BRD cases in Ireland in 2020
Number of cases and percentage (%) by age of the general pathogenic groups detected in the BRD cases diagnosed on post-mortem examination (n=457). Adapted from SurveillanceReport2020.pdf (agriculture.gov.ie)

Aetiology	Neonatal (0-1 month old)	Calves (1-5 months old)	Weanling (6-12 months old)	Adult Cattle (over 12 months old)	Total
Bacterial	37 (72.5)	**107 (58.5)**	76 (51.0)	45 (60.8)	265 (58.0)
Parasitic	0 (0.0)	**32 (17.5)**	40 (26.8)	13 (17.6)	85 (18.6)
Viral	7 (13.7)	**22 (12.0)**	23 (15.4)	6 (8.1)	58 (12.7)
No agent identified	7 (13.7)	**21 (11.5)**	9 (6.0)	8 (10.8)	45 (9.8)
Other	0 (0.0)	**1 (0.5)**	0 (0.0)	2 (2.7)	3 (0.7)
Fungal	0 (0.0)	**0 (0.0)**	1 (0.7)	0 (0.0)	1 (0.2)

During the pathogenesis of BRD, immunosuppressive stress and adverse environmental conditions predispose the animal to viral infections. Stress can be induced by factors such as poor nutrition, early weaning, dehydration, weather, and transportation. Modern farming with large group sizes, high stocking density and mixing of animals of different age and different sources cause stress and high infection pressure (Caswell, 2014). In addition to direct mortality, viral infections damage the respiratory mucosa and alters host immunity. Commensal or environmental bacteria become pathogens and cause bronchopneumonia (Mosier, 2015) (**Fig. 1.1**). Besides reducing the epithelial barrier function, virus infection leads to an aberrant immune response. Feedback mechanisms prevent over-activation which can lead to a lack or delay in the response to secondary infections (Bellinghausen et al., 2016). Therefore, the long-term consequences of respiratory disease are of major welfare as well as economic concern. Critical for successful antibiotic treatment of bacterial pneumonia is the early treatment and the first treatment success since the outcome for those animals that fail to respond to the first treatment is poor (Lorenz et al., 2011). The common practise of metaphylaxis, blanket medication of all animals, leads to decreased mortality and morbidity and higher weight gain in calves (Wileman et al., 2009). However, the European Parliament called for a review of current practises of prophylactic use of antimicrobials, noting that this use of antibiotics promotes the selection of antibiotic-resistant strains of bacteria (Mateu and Martin, 2001; Parliament, 2011). Focusing on the improvement of animal management and prevention and treatment of the primary viral infections can provide an alternative to the use of antimicrobials for prevention. A study comparing 50 animals with BRD symptoms versus 50 location-matched healthy controls found viruses present in nasal secretions in 68% of BRD-affected animals versus 16% of healthy control animals. 38% of sick animals versus 8% of controls were infected with multiple respiratory viruses (Ng et al., 2015). Alone or in association with other pathogens, the following viruses could be associated with BRD: bovine respiratory syncytial virus (BRSV), bovine herpes virus 1 (BoHV-1), bovine parainfluenza virus 3 (PIV-3), bovine coronavirus (BCoV), bovine viral diarrhoea virus (BVDV). These viruses belong to different virus families and are therefore different in pathogenesis, clinical signs and associated immune responses in the host (**Tab. 1.2**).

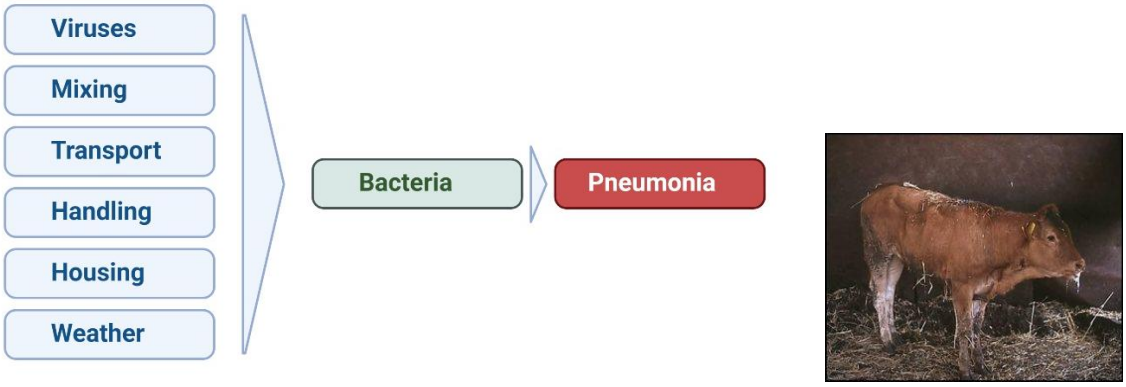

Figure 1.1 Bovine respiratory disease (BRD) as multi-factorial disease complex
Immunosuppressive stress in combination with high infection pressure predisposes the animal to respiratory infections. The pathogenesis typically consists of a primary viral infection targeting the respiratory epithelium and a secondary bacterial infection leading to pneumonia.

Table 1.2: Bovine respiratory viruses associated with BRD

Virus		Virus family	Genome
BRSV	Bovine respiratory syncytial virus	*Paramyxoviridae* (*Pneumovirus*)	Enveloped ssRNA (-RNA) virus
BoHV-1	Bovine herpes virus 1	*Herpesviridae* (*Varicellovirus*)	Enveloped dsDNA virus
PIV-3	Bovine parainfluenza virus 3	*Paramyxoviridae* (*Respirovirus*)	Enveloped ssRNA (-RNA) virus
BCoV	Bovine coronavirus	*Coronaviridae* (*Coronavirus*)	Enveloped ssRNA (+RNA) virus
BVDV	Bovine viral diarrhea virus	*Flaviviridae* (*Pestivirus*)	Enveloped ssRNA (+RNA) virus

1.2. Innate antiviral immunity

The immune system evolved to protect the host against potential pathogenic organisms, including bacteria and viruses. Exposure to these pathogens can occur through a variety of routes, including direct entry through the skin, via the respiratory tract and gastrointestinal mucosa. Diverse repertoires of cells and molecules at these sites cooperate to recognise and eliminate infectious agents and provide local surveillance systems to monitor the integrity of host tissue. Immune responses are tailored towards specific classes of infectious agent and undergo constant refinement. Species-specific differences in immune system repertoires can have important implications for differing susceptibility to infection and associated tissue damage but overall, innate and adaptive immune systems are surprisingly well conserved across species. This ensures the continued ability to respond to the diversity of infectious agents, which have their own evolving strategies to evade host defence mechanisms. During recognition, elimination and the formation of specific memory to infectious agents, immune responses are subject to several layers of regulatory mechanisms. Immune checkpoints set thresholds for the deployment of immune responses to ensure that responses are proportional to the level of threat and not directed against self (Medzhitov and Janeway, 2000).

The immune system has classically been divided into two arms, innate or non-specific immunity and adaptive immunity or acquired specific immunity. Innate immunity is relatively broad-acting and provides highly effective defence; it includes physical barriers, soluble mediators and cellular defences. Physical and chemical barriers are represented by epidermis, epithelium, endothelium and the mucous secretions with an armoury of antimicrobial peptides (Basset et al., 2003). Proteins which are part of the complement and coagulation system, help to opsonise pathogens and to localise infected tissue. Innate immune cells include granulocytes, monocytes/macrophages, dendritic cells and natural killer cells (Chaplin, 2003). While these cells have phagocytotic functions, they also express pattern recognition receptors (PRRs), including the major and most extensively studied family of TLRs (Toll-like receptors). PRRs have evolved to detect conserved components of pathogens, so called pathogen-associated molecular patterns (PAMPs) and danger-associated molecular patterns (DAMPs), not present within the host under normal conditions or present in aberrant

locations, e.g. endosomal DNA (Takeuchi and Akira, 2010). Viral PAMPs can be surface structures, virus genomic material, replication products and capsids which are rarely mutated in the pathogen. Upon PAMP recognition, PRRs activate a multitude of intracellular signaling pathways, including adaptor molecules, kinases and transcription factors (Mogensen, 2009). This ultimately results in the activation of transcription factors which mediate gene expression and synthesis of a broad range of defence-related molecules, including cytokines, chemokines, cell adhesion molecules and immunoreceptors. This pro-inflammatory environment results in the recruitment of cells of the innate and adaptive immune system (Whitsett and Alenghat, 2015), their activation, the production of effector molecules and, in most cases ultimate control of early infection (**Fig. 1.2**).

Epithelial cells have traditionally been considered as an important part of defence due to their function as a physical barrier with a mucosal surface, creating an environment not favourable for the attachment and growths of pathogens. An immunologically mediated defence role for epithelial cells was only proposed when it was shown that they were capable of secreting cytokines and anti-microbial peptides. Cytokine production by epithelial cells was first described in the 1990s with IL-6 cytokine production by epithelial cells using epithelial cell lines from the human urinary tract responding to bacteria (Hedges et al., 1990) and IL-8 production of cells from the lung cancer cell line A549 in response to IL-1 and TNF (Standiford et al., 1990). Our group examined the production of IL-1α, IL-1β and IL-6 in primary human small intestinal epithelial cells. While mRNA of all three was detected, only IL-6 protein expression increased in two out of three samples following activation with LPS (Madrigal-Estebas et al., 2002). In 1993 it was found that IL-8 was readily secreted by isolated human nasal epithelium upon infection with respiratory syncytial virus (RSV) or stimulation with IL-1 and TNF (Becker et al., 1993). In 2000 it was shown that intestinal epithelial cell lines expressed PRRs (Cario et al., 2000). A review in 1995 pointed out that epithelial cells are a source of chemokines and cytokines and cannot be ignored as immunological mediators while studying mucosal infections (Hedges et al., 1995). Our group observed that bovine endometrial epithelial cells are potent producers of β-defensins in response to *E. coli* stimulation (Chapwanya et al., 2013). Recently the immune potential has been

emphasised during the COVID-19 pandemic as primary target cells for SARS-CoV-2 infection and their role as innate immune cells during infection (Bridges et al., 2022; Gallo et al., 2021; Yao et al., 2020). In the following we review the critical role of epithelial cells in the innate immune response to viral infection.

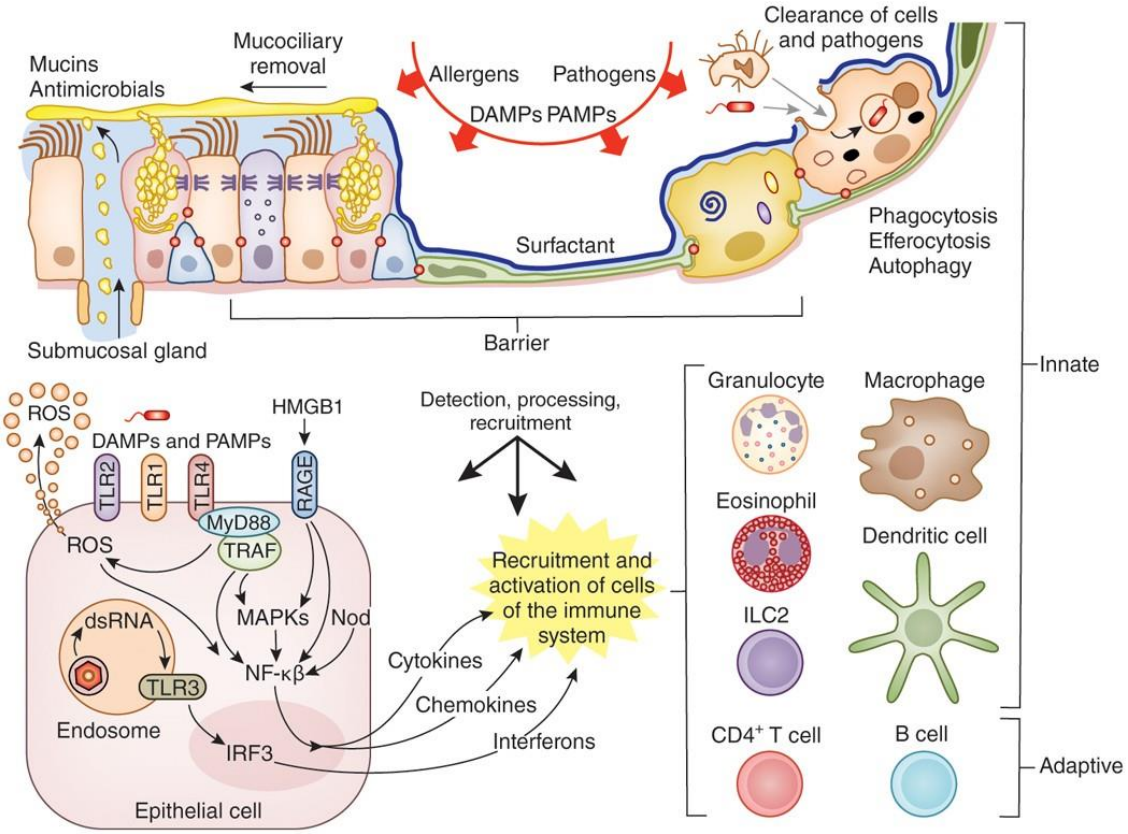

Figure 1.2 Epithelial cells recognise pathogens, recruit immune cells and connect innate and adaptive immune responses

Following recognition of PAMPs and DAMPs, respiratory epithelial cells mediate and regulate innate immune responses through production of antimicrobial substances, cytokines and chemokines, which recruit and activate immune cells. Image from (Whitsett and Alenghat, 2015).

1.3. Respiratory epithelial cells as part of the antiviral innate immune system

1.3.1. Physical and chemical barrier function of respiratory epithelial cells

The respiratory system can be divided into upper and the lower respiratory tract regions. The upper respiratory tract consists of the nasal cavity, pharynx and larynx, whereas the trachea, lungs and bronchi constitute the lower respiratory tract. The conducting airways consist of the upper respiratory tract, trachea and bronchi and the respiratory part consists mainly of alveoli (Weitnauer et al., 2016). The upper airway epithelial barrier is comprised of ciliated cells, olfactory cells, mucus-secreting goblet cells and basal cells with progenitor capacity (Laulajainen-Hongisto et al., 2020) (**Fig. 1.3**). Basal cells have a critical role in regeneration of the airway epithelium, serving as progenitors of both ciliated and secretory cells (Hogan et al., 2014). The composition of the epithelium of the lower respiratory tract varies across the conducting and respiratory regions. Cartilaginous airways from terminal bronchioles to the trachea are lined by pseudostratified epithelium, which forms a complex physiochemical barrier. The main airway cells in the pseudostratified epithelium are ciliated epithelial cells, non-ciliated mucous goblet cells, club cells, also known as clara cells, and undifferentiated basal cells (**Fig. 1.3**). The alveolar epithelium is composed of type I and type II alveolar cells (Weitnauer et al., 2016).

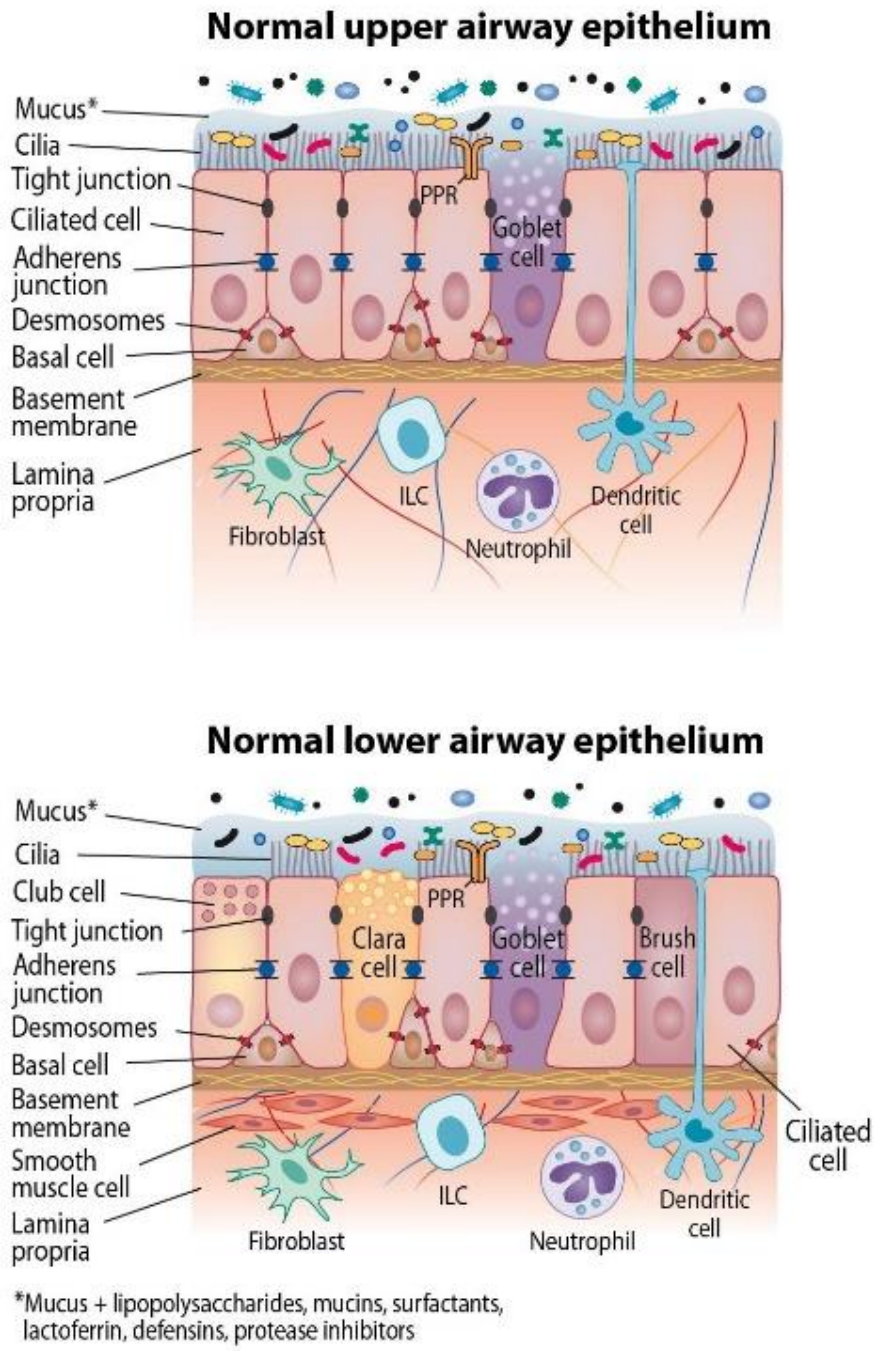

Figure 1.3 Cell composition of the upper and lower airway epithelium

The upper airway epithelial barrier compromises ciliated cells, olfactory cells, mucus-secreting goblet cells and basal cells with progenitor capacity. The main cells in the pseudostratified epithelium of the lower airway epithelium are ciliated epithelial cells, non-ciliated mucous goblet cells, club cells, also known as clara cells, and undifferentiated basal cells. Image modified from (Laulajainen-Hongisto et al., 2020).

Besides the vital function of gaseous exchange, respiratory epithelial cells function as the first line of defence against airborne pathogens, by forming a complex physicochemical barrier. The epithelial cells are attached to their neighbours by cell-cell junctions, including tight junctions, adherence junctions and gap junctions and form an effective physical barrier (Roche et al., 1993). Tight junctions maintain epithelial integrity, consisting of various proteins ensuring impermeability, while enabling communication and intercellular transport between adjacent cells. Located below adherence junctions gap junctions provide adhesive contracts and allow diffusion of small molecules between neighbouring cells. Ciliated epithelial cells and secretory cells facilitate transport of approximately 90% of inhaled particles, including respiratory viruses, away from the bronchioles via cilial movement and mucus secretion (Voynow and Rubin, 2009). Mucus displays a complex composition consisting out of almost 200 different proteins, which includes antimicrobial substances, such as lysozyme and defensins, cytokines and antioxidant proteins (Nicholas et al., 2006). The mucus overlaying the airway epithelium creates a semi-permeable barrier that enables the exchange of nutrients, water and gases while being impermeable to most pathogens. Rhinovirus (RV) replication in primary human epithelial cells reportedly induces mucin expression, which is dependent on TLR3 and the activation of the epidermal growth factor receptor (EGFR), suggesting the involvement of dsRNA signalling on mucus production (Zhu et al., 2009).

1.3.2. Innate sensing of viruses by epithelial cells

As the first cells to encounter respiratory viruses, respiratory epithelial cells have a critical role in the defence against many viral infections. While providing a physical barrier against pathogens was considered their primary defence mechanism, it has increasingly become clear that epithelial cells have additional active roles in mediating and regulating both innate and adaptive immune activity (Proud and Leigh, 2011; Weitnauer et al., 2016; Whitsett and Alenghat, 2015). Innate immune cells recognise invading viruses by several germline encoded different families of PPRs located at the cell surface and within the cell which recognise viral PAMPs (**Tab. 1.3**). PRRs detect molecules expressed during multiple steps in the virus life cycle (**Fig. 1.4**). All viruses consist of a capsid, a protein shell enclosing the nucleic acids, either DNA or RNA. Many

viruses are also enclosed by a phospholipid envelope containing embedded viral glycoproteins. Cell surface TLRs recognise attaching viruses by interaction with envelope glycoproteins. After successful cell entry, most commonly by receptor-mediated endocytosis, TLRs recognise viral nucleic acids within the endosome. Once the virus is released into the cytoplasm, intracellular receptors of the RIG-like helicase (RLH) family recognise dsRNA (Thompson and Locarnini, 2007). Inside the cell the viral DNA is uncoated and rapidly translocated to the nucleus, followed by transcription of viral genes in the nucleus and their translation in the cytosol. The new viral genome is cleaved, assembled with viral proteins and packed inside the nucleus. After viral maturation the nucleocapsid buds out of the nucleus and obtains a primary envelope. After a maturation phase in the cytoplasm, mature virions are released from the cell via an exocytosis-like pathway. Protein translation, proteolytic processing, new genomic synthesis, viral assembly and release are likely to be recognised by further ligand-specific PRRs. Even though PRRs are tightly conserved among species, it is not clear if all cell types utilise the same viral sensing system.

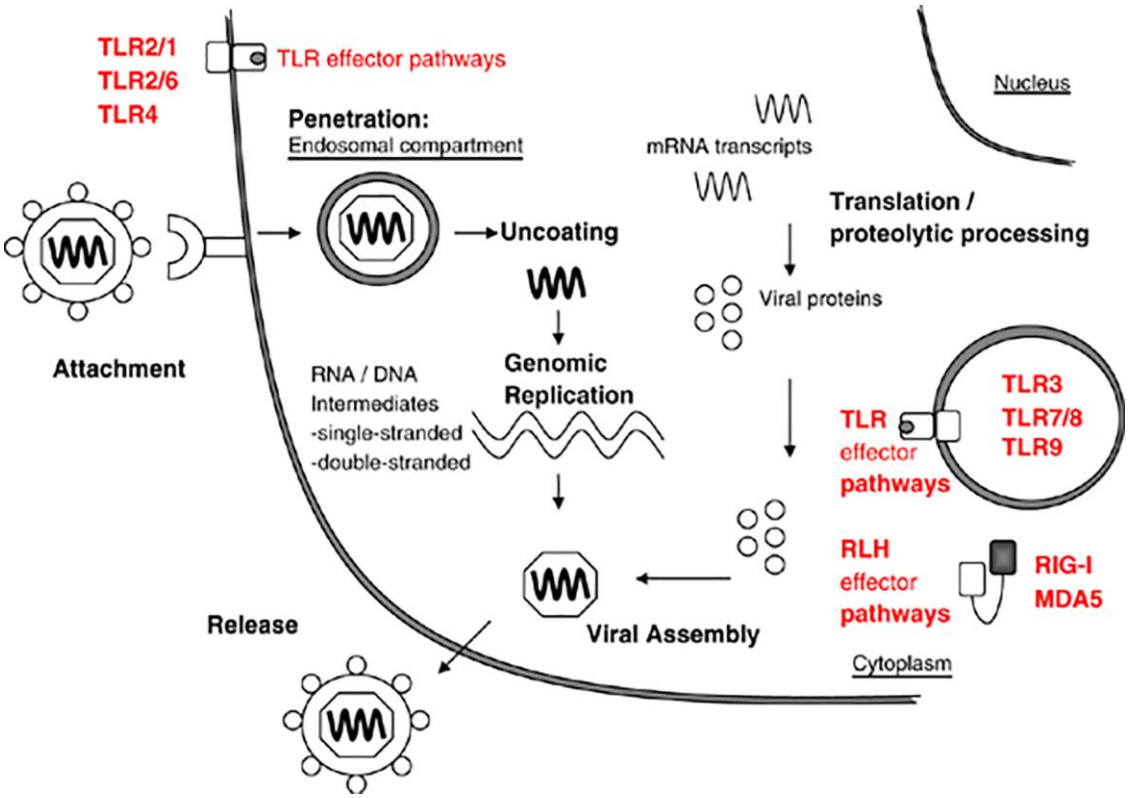

Figure 1.4 PRRs detect different stages of the viral life cycle

Pattern recognition receptors (PRRs) recognise molecules across multiple steps in the viral life cycle. While glycoproteins on the external virion surface may be recognised by surface receptors, the viral genome, replication intermediates and protein products are recognised intracellularly, either in the endosome or cytosol. Image modified from (Thompson and Locarnini, 2007).

Table 1.3 PPR detection of viral PAMPs (small excerpt)

Receptor	Location	Viral PAMP	Ref
TLR2	Cell surface	Glycoproteins, virion component, haemagglutinin	(Bieback et al., 2002; Dolganiuc et al., 2004; Murawski et al., 2009)
TLR3	Endosome	dsRNA	(Alexopoulou et al., 2001)
TLR4	Cell surface	Fusion protein, envelope glycoproteins	(Kurt-Jones et al., 2000)
TLR7/8	Endosome	ssRNA	(Heil et al., 2004; Lund et al., 2004)
TLR9	Endosome	CpG DNA	(Hemmi et al., 2000)
RIG-1	Cytoplasm	dsRNA (short), 5'-triphosphate RNA	(Hornung et al., 2006; Yoneyama et al., 2004)
MDA5	Cytoplasm	dsRNA (long)	(Kato et al., 2006)
AIM2	Cytoplasm	Genomic DNA	(Bürckstümmer et al., 2009)
IFI16	Cytoplasm, Nucleus	Genomic DNA	(Unterholzner et al., 2010)
DAI	Cytoplasm	Genomic DNA	(Takaoka et al., 2007)
cGAS	Cytoplasm	Genomic DNA	(Wu et al., 2013)

Of the PRRs, the TLRs are the most extensively studied. TLRRs located on the cell surface membrane, e.g., TLR2 and -4, detect hydrophobic lipids. Even though the extracellular receptors TLR2 and -4 are known to be activated by bacterial products, they are also involved in the recognition of respiratory viruses. The fusion protein of RSV (respiratory syncytial virus) interacts with TLR4 (Kurt-Jones et al., 2000) and activates innate immunity through TLR2 in macrophages (Murawski et al., 2009). This allows the cells to respond to components of the viral envelope such as fusion machinery at their surface and detect viral genomes in the endosome. TLR3, TLR7, TLR8 and TLR9 are located in the cytoplasmic endosome, where TLR3 recognises double-stranded RNA (dsRNA) (Alexopoulou et al., 2001), TLR7 and TLR8 single-stranded RNA (ssRNA) (Heil et al., 2004) and TLR9 CpG DNA (Hemmi et al., 2000) (**Tab. 1.2**). The expression of each TLR has been investigated in various primary cells and cell lines from the upper and lower airways. TLR2, -3, -4, -5 and -6 have the highest expression, while the expression of TLR7, -8, -9 and -10 is variable depending on the cell type (Armstrong et al., 2004; Muir et al., 2004).

Mayer and colleagues showed that human bronchial epithelial cells express functional TLR1, -2, -3, -4, -5 and -6, while TLR7 and TLR8 could not be detected (Mayer et al., 2007). A study in 2013 found TLR3, TLR7 and TLR9 mostly expressed on the apical side of epithelial cells in the human trachea and in primary polarised airway epithelial cells (Ioannidis et al., 2013).

TLR3 plays an important role in viral recognition of various viruses in many cell types. It responds to the presence of many respiratory viruses, including rhinovirus (Hewson et al., 2005), RSV (Groskreutz et al., 2006) and influenza viruses (Guillot et al., 2005) in human respiratory epithelial cells. A susceptibility to herpes simplex virus-1 (HSV-1) encephalitis was associated with the deficiency of TLR3 protein due to a dominant-negative TLR3 allele in otherwise healthy children (Zhang et al., 2007). TLR3 signals via the MyD88-independent pathway using the adaptor protein TRIF. TRIF interacts with TRAF3 (tumour necrosis factor (TNF) receptor associated factor 3) to activate TBK1 (TRAF-family-member-associated NFκB activator (TANK)-binding kinase 1) and IKKi (non-canonical inhibitor of NFκB (IκB) kinase). These kinases directly phosphorylate IRF3 (interferon regulatory factor-3), which forms a dimer before translocating to the nucleus and inducing IFN transcription. Beside TRAF3, TRIF is also able to interact with TRAF6 and TAK1 (TGF-β-activated kinase). Activated TAK1, in complex with the TAK-1 binding proteins, TAB1 and TAB2, phosphorylates the IKK complex and the MAP kinases JNK, ERK and p38. This leads to the activation of the transcription factors NFκB and AP-1 (activating protein-1), inducing the genes involved in the inflammatory response e.g. TNFα, IL-1, and IL-6 (Thompson and Locarnini, 2007) (**Fig. 1.5**). TLR3 ligands give the strongest pro-inflammatory response as a potential by-product of continual viral presence (Sha et al., 2004; Wang et al., 2007).

TLR7/8 and TLR9 use the adaptor protein MyD88 which forms a signalling complex with IRAK-1, IRAK4, TRAF6, TRAF3 and IKKα. The MyD88- IRAK4 and TRAF6 complex activates NFκB and AP-1 as described above. Additionally, recruitment of IRAK1, TRAF3 and IKKα leads to activation of IRF7, which translocates to the nucleus to regulate the expression of type I IFN genes (Thompson et al., 2011) (**Fig. 1.5**).

Once the virus has entered the cytoplasm of airway epithelial cells, other intracellular located receptors can initiate an innate immune response. Cytoplasmic PRRs include NOD-like receptors, the cytosolic DNA sensor cyclic GMP-AMP synthase (cGAS), NLRP1, and RIG-I-like receptors. In experiments on the cell line L-929, mouse fibroblasts from subcutaneous connective tissue, RIG-I (retinoic acid inducible gene I) and MDA5 (melanoma differentiation-associated gene 5) belonging to the RIG-I-like receptors (Yoneyama et al., 2004) were discovered. Interestingly, a high concentration of RIG-I has been demonstrated at tight junctions, suggesting that these might also interact with antiviral innate responses (Mukherjee et al., 2009). Induction of an antiviral response via RIG-I or MDA5 has been shown for several respiratory viruses, for example, RSV activates the IFN-β promoter via RIG-I (Sasai et al., 2006). MDA5 is a receptor for long dsRNAs of approximately 500-1,000 bp, whereas RIG-I recognises shorter dsRNAs of approximately 22-500 bp and 5'-triphosphate groups (5'ppp) (Jensen and Thomsen, 2012). 5'ppp is present in all transcripts but is removed from host RNAs during normal 5' processing. Whereas viral RNAs often retain 5'ppp and do not undergo 5' processing (Chen and Hur, 2022; Hornung et al., 2006). Following binding, both RIG-I and MDA5 undergo conformational changes allowing interaction of their recruitment domain (CARD) with the downstream adapter protein IPS-1 (IFNB promoter stimulator), also known as MAVS (Kawai et al., 2005). The C-terminal hydrophobic trans membranous region targets IPS-1 to the mitochondrion, which localisation is required for activity. IPS-1 interacts with TRAF3 to activate TBK1 and IKKi which phosphorylate IRF3 and IRF7, inducing a type I IFN response (Saha et al., 2006). A second pathway activated by IPS-1 is the activation of RIP1, in a complex with the Fas-associated death domain (FADD), leading to NFκB nuclear translocation (Jensen and Thomsen, 2012) (**Fig. 1.5**). Infection of primary tracheal epithelial cells with rhinovirus increases IFN and ISG mRNA expression, while it was found that TLR3 and MDA5, but not RIG-I, are required for maximal sensing of rhinovirus dsRNA in these cells (Wang et al., 2009). TLR3, TLR7, and MDA5 contributed to the innate immunity against H9N2 viruses in apically differentiated primary human tracheobronchial epithelial culture (Xing et al., 2011). RIG-I mediates early antiviral responses and TLR3 expression in respiratory syncytial virus (RSV) infected airway epithelial cells (Liu et al., 2007).

Intracellular DNA is an important PAMP during viral infection and can in addition act as 'danger' signal during cell death when DNA from dead cells is not effectively cleared (Unterholzner, 2013). The detection of exogenous DNA inside the cytoplasm initiates two distinct innate signalling pathways. The first involves activation of IRF3 and NFκB which results in the transcription of IFNs, chemokines and pro-inflammatory cytokines. The second results in formation of an inflammasome complex, activating the protease caspase-1 which processes pro-IL-1β and pro-IL-18 to active cytokines causing a rapid, pro-inflammatory form of cell death called pyroptosis (Latz et al., 2013). The inflammasome family includes the NOD-like receptor family of inflammasomes, which include NLRP1B, NLRP1B, NLRP3 and NLRC4, and the PYHIN family of inflammasomes, which include AIM2 and IFI16. Inflammasome complexes can be activated through a variety of stimuli e.g., extracellular ATP, pore-forming toxins and reactive oxygen species. The predominant sensors for cytosolic DNA are the PYHIN family protein AIM2 (Bürckstümmer et al., 2009) and IFI16 (Unterholzner et al., 2010). AIM2 and IFI16 recruit ASC (apoptosis-associated speck-like protein containing CARD) followed by the activation of caspase-1. IFI16 shuttles between the nucleus and the cytoplasm, being predominantly nuclear present at steady state and able to sense DNA in both locations (Unterholzner, 2013). While AIM2 only induces inflammasome activation, IFI16 has been shown to induce inflammasome activation or IFN type I responses. IFI16 recruits STING for DNA-mediated IFN-β induction via TBK1, IRF3 and NFκB activation, e.g., in response to live HSV-1 (herpes simplex virus) (Unterholzner et al., 2010). Another example of viral DNA detection is the cGAS-STING pathway, whereby cGAS binds to dsDNA. cGAS dimers rearrange the dsDNA into a high affinity form suitable for binding other cGAS. The cGAS-DNA complex condensates and forms droplet structures where cGAS 2'-3'cGAMP is produced from ATP and GTP. 2'-3'cGAMP binds to STING, leading to the translocation of activated STING from the ER to the ER-Golgi intermediate compartment and the phosphorylation of TBK1 and IRF3 (Huérfano et al., 2022) (**Fig. 1.5**).

The expression of pattern recognition receptors by bovine epithelial cells has also been investigated, mainly with a focus on the TLR expression. Bovine tracheal epithelial cells have been shown to express the PRRs TLR1 to 10 like their human airway epithelial cell

counterparts (Berghuis et al., 2014; Ma et al., 2016). A summary of a conducted literature research can be seen in **Tab. 1.4**.

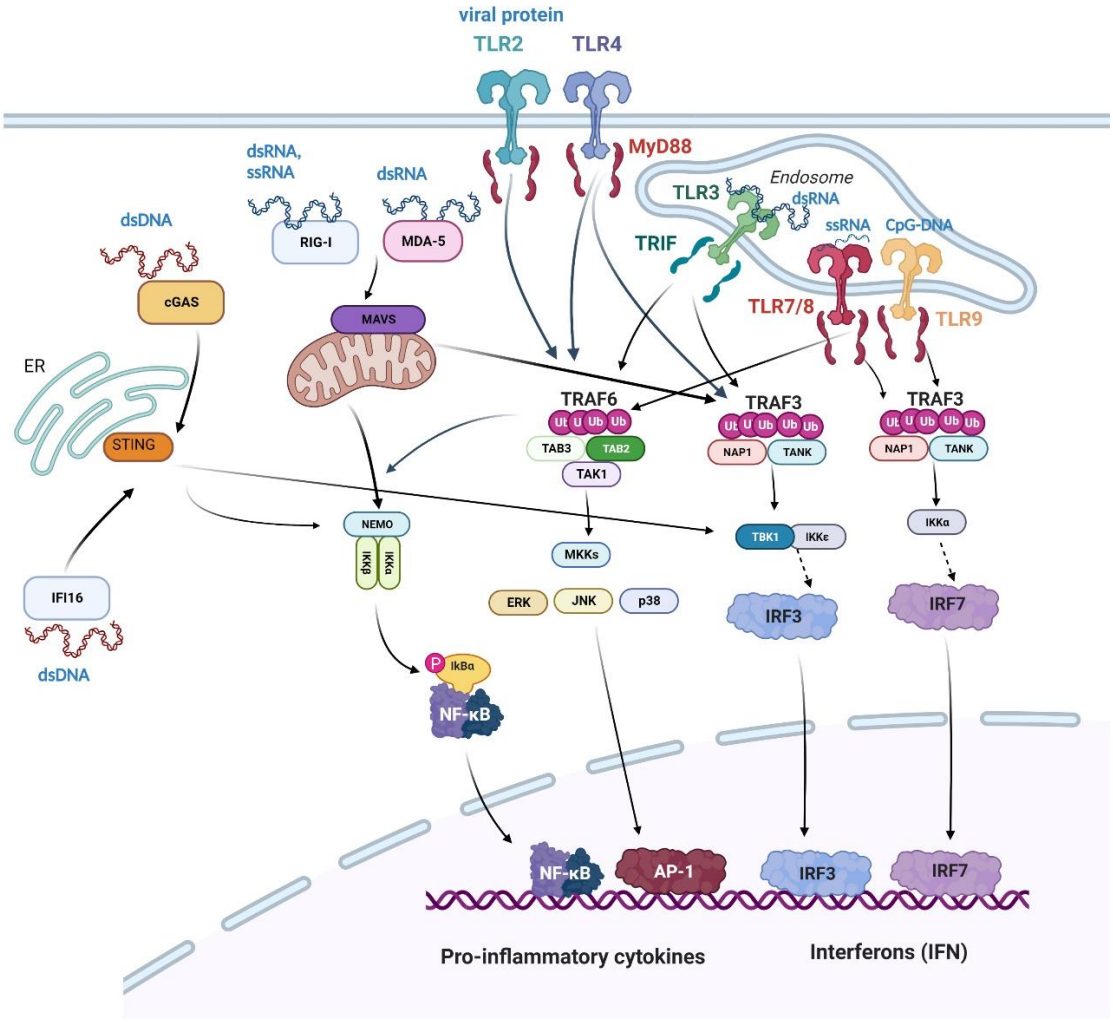

Figure 1.5 PRR activated signaling and antiviral responses during virus infection

PRR activated signaling and antiviral responses during virus infection. An overview of signaling pathways triggering IFN and cytokine production after sensing viral proteins, viral genome and replication intermediates. TLR2, TLR4, TLR7/8, and TLR9 signal via the adaptor molecule Myd88 and via TRAF6 and/or TRAF3. TLR2 primarily mediates activation of NFκB, whereas TLR3 and TLR4 mediate activation of NFκB and of IRF3 via the adaptor molecule TRIF. TLR3 and TLR4 stimulation induce IFN production. TLR7/8 and TLR9 primarily activate IRF7 leading to immediate IFN expression, but also NFκB activation leading to stimulation of proinflammatory cytokines. RNA sensors and DNA sensors lead to activation of both IRF3 and NFκB thus regulating both IFN and cytokine production. DNA sensors IFI16 and cGAS signal via STING located at the ER whereas the RNA sensors RIG-I and MDA5 signal via MAVS. ER = endoplasmic reticulum. This figure was created with BioRender.com.

Table 1.4 Pattern recognition receptor expression in bovine epithelial cells

Cell type	Method	TLR1	TLR2	TLR3	TLR4	TLR5	TLR6	TLR7	TLR8	TLR9	TLR10	NOD-1	NOD-2	RIG-I	Publication
Tracheal epithelial cells (primary)	PCR Agarose gel	Y	Y	Y	Y	Y	Y	Y	Y	Y	Y				(Berghuis et al., 2014) 2014
Bronchial epithelial cells (primary)	qPCR partly Western Blot		Y		Y		Y		Y						(Ma et al., 2016) 2016
Endometrial epithelial (primary)	PCR Agarose gel	Y	Y	Y	Y	Y	Y		N	Y	N				(Davies et al., 2008) 2008
	Western Blot													Y	(Carneiro et al., 2017) 2017
Mammary epithelial cells (bMECs)	qPCR		Y		Y										(Gondaira et al., 2018) 2018
	qPCR	Y	Y				Y								(Zbinden et al., 2015) 2015
	qPCR		Y		Y							Y	Y		(Deng et al., 2016) 2016
Intestinal epithelial cell line (BIE cells)	qPCR partly fluorescent localisation	Y	Y	Y	Y	Y	Y	Y	Y	Y	Y				(Takanashi et al., 2013) 2013
Intestinal epithelial cells (primary)				Y										Y	(Kobayashi et al., 2017) 2017
	qPCR	Y	Y	Y	Y	Y	Y	Y	Y	Y	Y				(Yang et al., 2015) 2015

As the surfaces of respiratory epithelial cells are in constant contact with the environment, any immune activity must be tightly regulated to prevent hyperactivation of the immune response (Weitnauer et al., 2016). In addition, local harmless microbiomes need to be tolerated. Diverse tolerance mechanisms have been discovered for intestinal epithelial cells. They mediate microbial signals to mucosal immune cells and promote the coordination of appropriate immune responses against commensal bacteria and enteric pathogens of both innate and adaptive effector cells (Okumura and Takeda, 2017). Analogous to the gut, the airways are colonized by diverse communities of microbes, whereby the colonisation is less in the lower respiratory tract and is altered in diseases (Wang et al., 2017). However, the molecular mechanisms regulating the activation of the immune response of respiratory epithelial cells are poorly defined.

The antiviral immune response of epithelial cells is influenced by the virus type, host, cell location and the environment to which the cells are exposed (Vareille et al., 2011). A study looking at the innate immune response in the respiratory epithelium of human, porcine and bovine during influenza virus infection found predominantly ciliated cells being infected in all hosts. However, detailed time-resolved transcriptome analysis revealed species-specific and species-uniform host responses. The infection induces species-specific host responses, as the number of common identified differential expressed genes among the different host species was low. However, subsequent pathway enrichment analysis of the different DE gene clusters revealed that most genes are associated with the innate immune regulatory and response pathways. The results indicate that the host transcriptional response during the infection with two different influenza virus strains in human, porcine and bovine airway epithelial cells is influenced by temperature and is both species- and virus-specific (Laloli et al., 2022).

1.3.3. Type I and III interferon production by respiratory epithelial cells

As previously described, various signalling cascades can induce interferon expression upon virus detection. In 1963, two separate groups reported that DNA and RNA derived from pathogens were capable of inducing IFN production in fibroblasts (Jensen et al., 1963; Rotem et al., 1963). IFNs belong to the family of cytokines and are grouped into three families, type I, II and III. All types can promote autocrine or paracrine signalling

leading to the induction of ISGs. All types also cooperate synergistically to promote antiviral activities. Because of their importance at respiratory surfaces during viral infection, we discuss type I and III in more detail in the following section.

Type I IFNs consist of 13 IFN-α, IFN-β1, IFN-ε, IFN-κ and IFN-ω in the human and 7 IFN-α, IFN-β1 and -3, IFN-ε, IFN-κ, IFN-τ1-3, IFN-ω, IFN-δ and IFN-χ in the bovine (Takaoka and Yanai, 2006). They all share the same heterodimeric receptor complex consisting of one chain of the IFN-α receptor 1 (IFNAR1) and one chain of the IFNα receptor 2 (IFNAR2), which is ubiquitously expressed on all cells. They all signal through the JAK/STAT pathway and activate the heterotrimeric transcription factor complex ISGF3, which translocates to the nucleus and binds IFN-stimulated response elements in the upstream promoter regions of interferon-stimulated genes (ISGs) (Schoggins, 2019). Type I IFNs have a broad range of functions including antiviral, antibacterial, antifungal, antiproliferative activities as well as the ability to modulate innate and adaptive immunity (Takaoka and Yanai, 2006).

Beside the well-known type I interferons IFN-α and IFN-β, type III interferon IFN-λ was discovered in 2003 (Kotenko et al., 2003; Sheppard et al., 2003). This family includes IFN-λ1 to -3, also known as interleukins IL-29, IL-28A, and IL-28B in the human. In the bovine only the reference sequence of *IFNL3* has been known, while the sequences of *IFNL1* and *IFNL4* have only been modelled and predicted in the bovine genome (**Tab. 5.1**). In comparison to the ubiquitously expressed type I IFN receptor, the type III IFN receptor expression is limited to epithelial cells and a subset of immune cells (i.e., NK cells, pDCs, and DCs) (Sommereyns et al., 2008; Zhou et al., 2007). The heterodimeric receptor complex consists of one chain of IFNLR1 and one chain of IL10Rβ. Even though IFN-λ is produced in response to various viral pathogens e.g., HCV (hepatitis C virus) (Marcello et al., 2006), enteric virus (Mahlakõiv et al., 2015) or metapneumovirus (Baños-Lara Mdel et al., 2015), the most insight has been gained in the context of influenza A virus (IAV). Production of IFN-λ upon IAV infection is a characteristic response of lung epithelial cells (Crotta et al., 2013). Epithelial cells in the respiratory tract express higher levels of IFN-λ transcripts and protein than of type I IFNs during IAV infection, shown *in-vitro* for primary tracheal epithelial cells (Crotta et al., 2013) and

in-vivo for bronchial epithelial cells (Galani et al., 2017). Also in response to RSV IFN-λ is preferentially secreted by primary epithelial cells (Okabayashi et al., 2011). Interestingly, it has been shown that the RSV-induced EGFR activation suppresses the IRF1-dependent IFN-λ secretion in order to escape the control by type III IFNs (Kalinowski et al., 2018).

Both type I and III IFNs induce the JAK/STAT signalling cascade through the activation of the heterotrimeric transcription factor complex ISGF3, comprised of phosphorylated STAT1 and STAT2 and interferon regulatory factor 9 (IRF9). Activated ISGF3 translocates to the nucleus binding to IFN-stimulated response elements (ISREs) in the upstream promoter regions of ISGs (Lazear et al., 2019) (**Fig. 1.6**). The transcriptional responses induced by type I and III IFNs are similar and no signature unique to IFN-λ has been identified (Lazear et al., 2015).

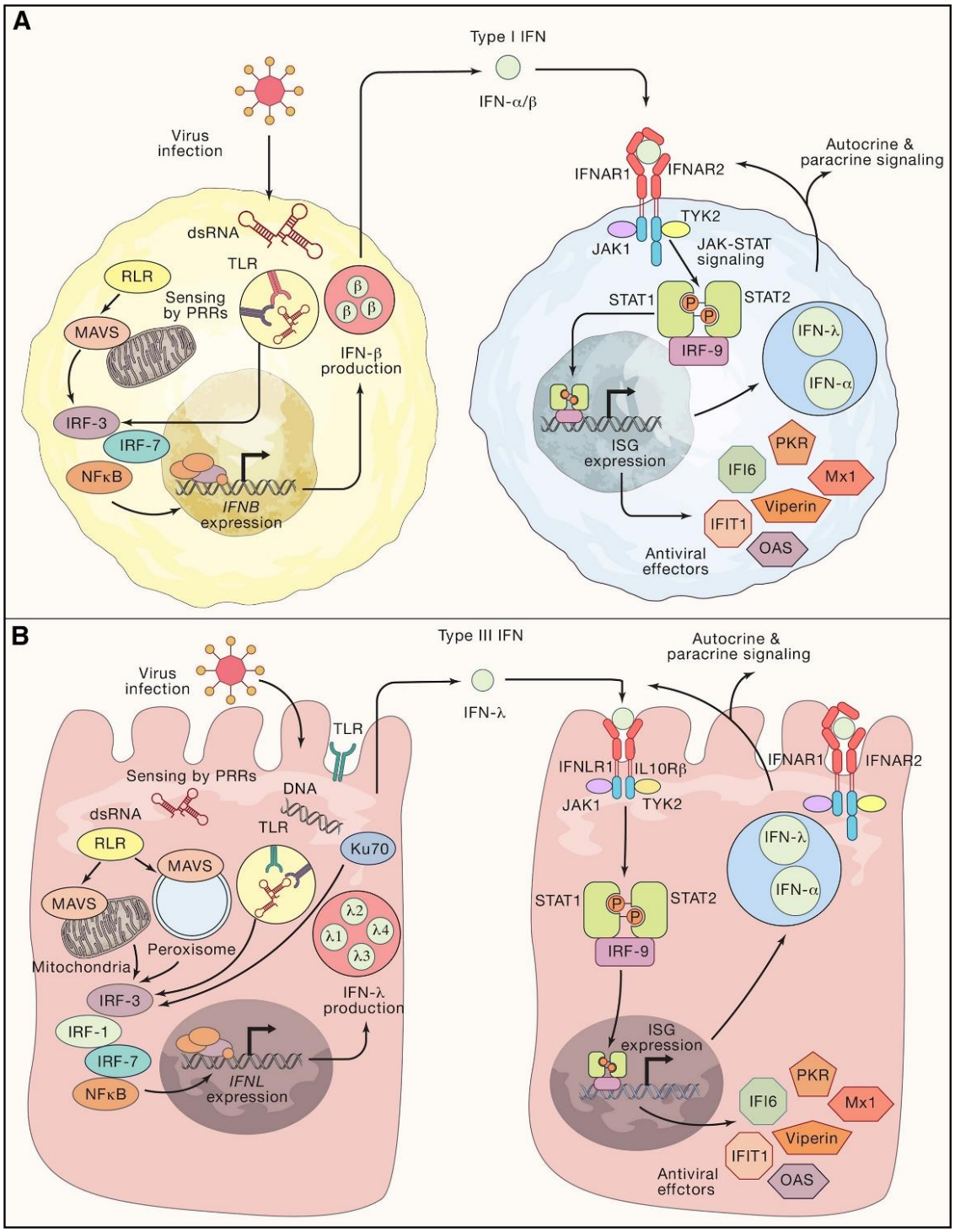

Figure 1.6 Signal transduction of type I and III IFNs

Viral PAMPs are sensed by PRRs, activating signalling cascades leading to IFN induction and secretion by infected cells. Both type I (A) and type III (B) IFN induce the activation of the JAK/STAT signalling pathway upon binding to their receptor. Activated STATs dimerise and bind to IRF9, forming the ISGF3 complex which translocates into the nucleus and drives ISG production, mediating antiviral effects of IFNs. Image taken from (Lazear et al., 2019).

It is thought that cell-, virus- and species-specific antiviral responses are achieved with different magnitudes of induced ISGs, kinetics of ISG transcription and degradation and the composition of ISGs expressed (Mesev et al., 2019). Whereas type I IFN activity is characterised by fast induction and fast decrease in ISG expression with a high magnitude, type III IFNs show a slow but sustained induction of ISGS with a low magnitude (Stanifer et al., 2020a). The induced ISGs can target most steps of viral replication, amplifying IFN signalling cascades to strengthen the host response and control a negative feedback-loop to control IFN release (Schoggins and Rice, 2011; Zhou et al., 2007). For example MX1 targets early viral gene expression, the IFN-inducible DNA sensor IFI16 interferes with virus gene transcription and Viperin inhibits viral gene replication (Schoggins, 2019). SOCS1 and USP18 are examples for ISGs with negative regulatory functions. Possible explanations for the negative feedback function of some ISGs are that the viruses have evolved to hijack these effectors, the increased viral uptake may stimulate a more robust adaptive immune response or the immune response can be controlled via this mechanism (Schoggins, 2019). USP18 has been shown to inhibit the IFN induced Jak/Stat signalling, desensitising cells to further IFN-α stimulation while not influencing IFN-λ signalling (François-Newton et al., 2011). A study comparing ISGs induced after IFN type I stimulation of fibroblasts from 10 different species (human, rat, cow, sheep, pig, horse, micro bat, fruit bat and chicken) found a conserved core of 62 genes. This highlights on the one hand the longstanding conserved role of the IFN system and on the other hand important species-specific differences. IFN repressing genes, e.g. USP18, were also part of core genes, which demonstrates the importance of avoiding excess stimulation in the evolution of all species (Shaw et al., 2017).

In addition to ISG induction, IFN-λ stimulates long-lasting adaptive immunity via an indirect mechanism. The majority of immune cells, including B-cells, do not respond to IFN-λ. IFN-λ induces thymic stromal lymphopoietin (TSLP) secretion by airway M cells and TSLP acts on CD103+ dendritic cells (DCs) to promote their maturation and migration to draining lymph nodes. Activated DCs enhance CD8+ T cell maturation in the draining lymph nodes and promote germinal centre reactions through effects on T

follicular helper cells, resulting in the increased production of virus-specific IgG1 and IgA (Ye et al., 2019a; Ye et al., 2019b).

Due to the shared characteristics in expression patterns, signalling cascades and antiviral functions, it has been complicated to identify unique non-redundant roles for type I and III IFNs (Lazear et al., 2015). Galani et al. recently detailed the different timing during viral infection and activation of an inflammatory state upon release as important differences in type I and III IFN functions. IFN-λ is induced first, at a lower viral burden compared to type I IFNs and seems to limit initial infection spread (Galani et al., 2017). In line with these findings, it has been reported that IFN-λs are essential for preventing virus transmission from the upper airways to the lungs early during infection (Klinkhammer et al., 2018). Interestingly, IFN-λs mount an antiviral state without activating inflammation, while type I IFNs enhance the antiviral defences and trigger a pro-inflammatory response if the infection escapes the IFN-λ control and high virus titres are present (Galani et al., 2017). The suppression of innate pro-inflammatory response and the limited host damaging effects associated with IFN-λs are largely due to their selective action on neutrophils which prevents their pro-inflammatory activation (Galani et al., 2017). Thus, IFN-λ is more efficient in controlling sublethal infections at the site of exposure, whereas type I IFNs become essential once the infection spreads to the lower respiratory tract. This complex interplay demonstrates the importance for both IFNs types for optimal viral clearance with minimal host damage in the respiratory tract (Andreakos et al., 2017) (**Fig. 1.7**).

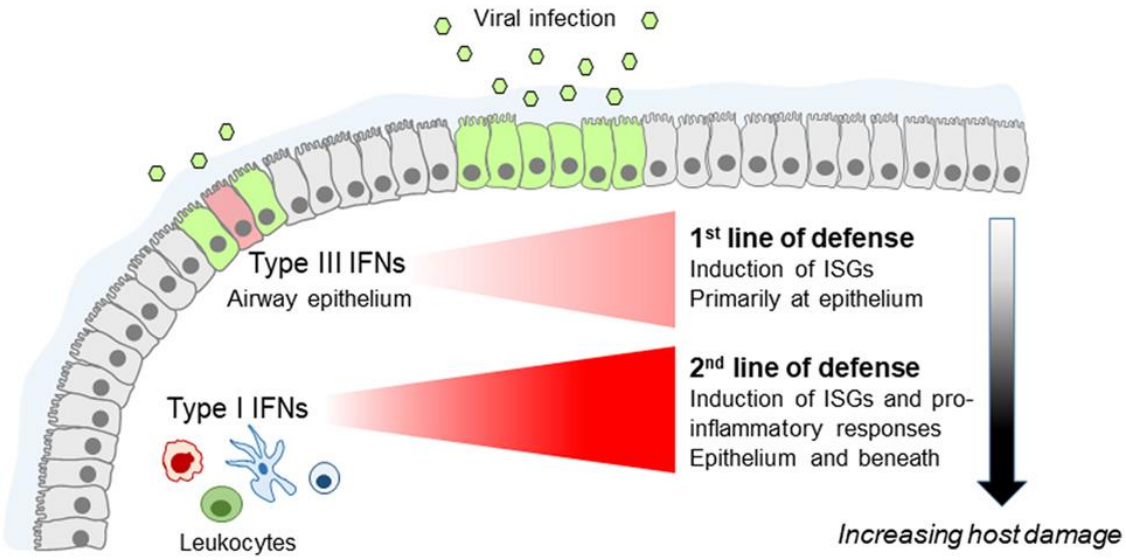

Figure 1.7 Signal transduction downstream of type I and II IFN receptors
Type III interferons are first to be produced after viral infection by epithelial cells to limit virus spread without triggering inflammation. If infections escape the IFN type III mechanism, type I IFNs are induced. The pro-inflammatory response activated by type I IFNs is essential for providing protection but can also cause increased host damage and immunopathology. Image from (Andreakos et al., 2017).

1.4. Bovine herpes virus 1 (BoHV-1)

1.4.1. Epidemiology and vaccination

Bovine herpesvirus 1 (BoHV-1) belongs to the *Herpesviridae* family and the *Alphaherpesvirinae* subfamily. It causes significant economic losses to the cattle industry, particularly due to its association with BRD. An Irish study estimated a reduction of 250 L per cow per year in IBR-positive herds, which amounts to an annual cost of €62 million to the Irish dairy industry (Sayers, 2017). BoHV-1 is one of eight herpesviruses isolated from naturally infected cattle in 1956 (Madin et al., 1956). The virus occurs worldwide and is endemic in several countries (Ackermann and Engels, 2006). However, there is limited data available which determines the exact extent of exposure to endemic diseases among cattle. Two studies conducted on Irish beef (O'Grady et al., 2008) and dairy herds (Cowley et al., 2011) both reported herd level seroprevalence of approximately 75% consistent throughout the country. In 2018, 6049 cows in 161 beef cow herds from across the island of Ireland were sampled and found a herd seroprevalence of 90% (at least one seropositive case within the herd). At an individual herd level, the overall mean BoHV-1 seroprevalence was 39.8% (median 38.1%) (Barrett et al., 2018). This study also found 18% of herds vaccinated for BHV-1, ranging from 11.5% in the Republic of Ireland to 45.5% in Northern Ireland. Several conventional modified live and inactivated IBR vaccines as well as subunit vaccines and gE-deleted marker vaccines, that lack the viral structural glycoprotein gE, are on the market (Belknap et al., 1999; van Drunen Littel-van den Hurk et al., 1997). Vaccination is able to reduce disease severity and virus replication and transmission and makes it less likely that latent carrier will reactivate and shed the virus (Ackermann and Engels, 2006). Vaccinated animals can still become infected and become a latent carrier (Muylkens et al., 2007). To accomplish eradiation, culling seropositive animals without vaccination has been the most successful method. However, this can only be considered if the seroprevalence of BoHV-1 is relatively low. At this moment in time there is no national programme for BoHV-1 control in Ireland (www.animalhealthireland.ie /assets/uploads/2021).

1.4.2. Clinical manifestation

While BoHV-1 infection can sometimes result in no clinical signs at all, it also has been associated with several different clinical complications including infectious bovine rhinotracheitis, pneumonia, abortion, and systemic infection in neonates. There are three recognised subtypes of BoHV-1: BoHV-1.1, BoHV-1.2a and BoHV-1.2b. BoHV-1.1 mainly causes IBR (infectious bovine rhinotracheitis), while the latter cause IPV (infectious pustular vulvovaginitis) and IPB (infectious pustular balanoposthitis). The enveloped dsDNA virus is transmitted directly by aerosol or by close contact between animals with initial viral replication occurring in epithelial cells at the point of entry such as muzzle, nose, nasopharynx, trachea and first bronchi (Turin et al., 1999). Clinical symptoms of the respiratory disease occurring after 2 to 6 days may include pyrexia, anorexia, dyspnoea, cough, bilateral nasal discharged or depression. Auscultation reveals the presence of a tracheitis. Animals usually recover within 2 weeks, except in approximately of 10% of cases when a secondary bacterial infection manifestation and bronchopneumonia occurs (Turin et al., 1999). Infection in females may lead to infertility and abortion. A meta-analysis in 2017 of over 7500 animals showed an overall decrease in abortion risk of 60% in pregnant cattle vaccinated against BoHV-1 (Newcomer et al., 2017). After primary infection all animals subsequently develop a latent infection of nervous sensory ganglia cells, re-emerging to cause disease periodically in association with decreases in animal well-being for example stress and immunosuppression (Jones, 2003).

1.4.3. Pathogenesis

Alpha herpesviruses are large (135kB) double-stranded DNA viruses consisting of nucleocapsid, connected to the envelop by a tegment. BoHV-1 is characterised by a relatively large host range, a short replication cycle and the ability to induce latent infection (Muylkens et al., 2007). Entry of BoHV-1 into epithelial cells happens in a three-step process

a. low affinity binding of the viral envelop proteins gC and gB to heparin-like sugar moieties on the cell surface,

b. high affinity binding between gD and the cellular receptor nectin-1 and

c. fusion of the of the viral envelop with the cell membrane involving gB, gD, gH and gL (Ellis, 2009).

BoHV-1 does not have a specific cell tropism, can infect a variety of cell types and is able to spread cell-to-cell via tight junctions, possibly due to the use of multiple cell surface receptors by the virus (Spear, 2004). After entry into the target epithelial cells and uncoating, the viral genome enters the nucleus and sets up a lytic replication cycle. The tightly regulated phases of the herpes virus gene transcription are immediate early (IE), early (E) and late (L). The viral structural protein VP16 stimulates IE RNA expression in the first 2-4 hours after infection (Roizman et al., 2005). The encoded proteins stimulate expression of E and L genes and block host cell silencing by the PML-NBs (nuclear domain ten protein of promyelocytic leukemia (PML) nuclear bodies). PML-NBs are cellular proteins that counteract herpes viral infections by inhibiting viral replication at different stages (Tavalai and Stamminger, 2009). E genes encode non-structural proteins that stimulate viral DNA replication and L proteins make up the virion particle (Jones, 2013). Intracellular BoHV-1 virions can be detected at 10 hours post infection and extracellular at 12-13 hours, leading to the infection of adjacent and non-adjacent cells (Babiuk et al., 1975). Although most animals are able to clear the primary infection, herpes viruses establish a life-long latent infection in approximately 40% of ganglionic sensory neurons (Maggioncalda et al., 1996). Latency-related (LR) gene products, e.g. LAT (latency-associated transcript) in HSV-1 and LR in BoHV-1, inhibit cell proliferation, bICP0 RNA expression and apoptosis (Jones et al., 2006; Lovato et al., 2003).

The cytopathic effect (CPE) caused by BoHV-1 was described as early as 1978 as result of inhibition of proteosynthesis (Fenwick and Walker, 1978). It is characterised by cell ballooning and the rise of intracellular inclusions. The cell death results both from necrosis and apoptosis during the BoHV-1 replication cycle (He and Han, 2020; Muylkens et al., 2007). The shut-off of cellular protein synthesis is partly caused by the so called VHS (virion shut off) tegument protein in BoHV-1 infected cells (Hinkley et al., 2000). Apoptosis is currently considered as a critical cellular defence mechanism against viral invasion. Killing of virally infected cells by apoptosis leads to reduction of inflammation, alteration of immune recognition and prevention of virus spread. Members of the *Alphaherpesvirinae* subfamily are known to induce or inhibit apoptosis depending on

the life cycle stage of the virus in a cell-type-dependent manner (Galvan and Roizman, 1998).

During herpes virus infection there is a balance between pro- and anti-apoptotic mechanisms that delays apoptosis until the virus has replicated. Anti-apoptotic proteins encoded by the virus are for example BICP0, gD, gJ and as previously mentioned LAT (He and Han, 2020). The mechanisms by which BoHV-1 induces apoptosis are less defined. It has been reported that BoHV-1 decreases the level of the anti-apoptotic protein Bcl-2 and increases the level of pro-apoptotic protein Bax (Xu et al., 2012). Besides inducing the CPE directly, BoHV-1 is also able to inhibit the repair of the airway epithelium by reducing epithelial cell migration (Spurzem et al., 1995).

1.4.4. Innate immune response and immune evasion strategies

In addition to inducing apoptosis, BoHV-1 infected cells mount an innate antiviral response as described in 1.3.2. However, BoHV-1 counteracts immune responses and immune-surveillance to enhance pathogenesis and virus transmission. DNA sensors IFI16 and NLRP3 were induced in bovine kidney cells within eight hours after infection with BoHV-1 (Wang et al., 2014) and TLR activation and expression in bovine alpha-herpesvirus infections suggest the involvement of TLR7 and TLR9 in the recognition of BoHV-1 and -5 (Marin et al., 2014). The major pro-inflammatory cytokines during the early response are IL-1α, IL-1β, IL-6 and TNF which cause an influx of polymorphonuclear leukocytes and induce ICAM-1 on epithelial cells, to which leucocytes adhere (Levings and Roth, 2013).

The immunosuppressive effects of BoHV-1 infection favour secondary bacterial infection and are thought to correlate with depressed cell-mediated immunity. BoHV-1 impairs CD8+ T-cell recognition of infected cells by repressing expression of major histocompatibility complex class I molecules (Hariharan et al., 1993). CD4+ T-cell function is impaired due to induction of apoptosis (Winkler et al., 1999). BoHV-1 encodes several genes that impair innate immune responses during infection (Jones, 2019). The viral gene product BICP0 interacts with IRF3 and IRF7, leading to reduced promoter activity of IFN-β and a downregulation of IFN-β (Henderson et al., 2005; Saira

et al., 2007). Also bICP27 can inhibit the IFN-β1 and IFN-β3 promoter activity (da Silva et al., 2012). In addition, the viral protein VP8 has been shown to downregulate expression of STAT1 causing inhibition of the IFN-β signalling (Afroz et al., 2016). The viral glycoprotein gG is able to interfere with chemokine to their specific receptors (Bryant et al., 2003). In summary, the presence of various viral proteins throughout infection allows for high levels of virus replication during the acute phase. Immune activity and immune evasion strategies during BoHV-1 infection are summarised in **Tab. 1.5**.

Table 1.5 Immune activity and viral immune evasion strategies during BoHV-1 infection

Components of the immune response		BoHV-1 immune evasion strategies	References
Soluble factors of the innate immunity	Type I-IFN	Downregulation of type I IFN by BICP0	(Henderson et al., 2005; Saira et al., 2007)
	Chemokines	Chemokine binding activity of gG	(Bryant et al., 2003)
	Complement system	Interaction of gC with bovine C3b	(Huemer et al., 1993)
	PML-NBs	Antagonization by BICP0 and VP8	(Tavalai and Stamminger, 2009)
Cells of the innate immunity	Monocytes-macrophages	PBMC apoptosis	(Hanon et al., 1996)
	Polymorphonuclear cells	Interference with alveolar macrophages and PMN activities	(Brown and Ananaba, 1988; Warren et al., 1996)
Antigen presentation	MHC class I pathway	Inhibition of TAP by UL49.5	(Koppers-Lalic et al., 2001)
		Decrease of MHC class I Presentation by UL41 (vhs)	(Hinkley et al., 2000)
	MHC class II pathway	Decrease of MHC class II presentation by UL41 (vhs)	(Hinkley et al., 2000)
Adaptive immune cells	Helper T lymphocytes (CD4+)	Infection and apoptosis of CD4+	(Winkler et al., 1999)
	Cytotoxic T lymphocytes (CD8+)	Downregulation of MHC class I impairs the activation of CD8+	(Hariharan et al., 1993)
	B cells		
Adaptive humoral factors	Antibodies	The direct cell-to-cell spread mediated by gB, gD, gH/gL, gE/gI allow spreading of BoHV-1 in the presence of neutralising Abs	(Trapp et al., 2003)
Apoptosis of infected cells		ICP6, gD, Us3, gJ, LAT, latency related gene inhibits apoptosis in latently infected cells	(Ciacci-Zanella et al., 1999)

1.5. Cell culture models for respiratory viral infections

While *in-vivo* models have classically been used to characterise the overall complexity of immune mechanisms, experimental infection models are expensive and require dedicated research facilities which preclude their widespread adoption. Furthermore, due to the increasingly stringent regulations in order to reduce the use of live animals in research, reproducible and physiologically relevant *in-vitro* culture models as alternatives are required. Such models are particularly limited in livestock species.

With the focus on the cultivation of viruses in a laboratory setting at the time, organ cultures of trachea from human embryos were originally developed for growing, isolation and characterisation of new respiratory viruses by Hoorn and Tyrrell in 1965 (Tyrrell and Bynoe, 1965). Hoorn pointed out the advantage of studying the specificity of viral infections in histological and functionally intact organ cultures, thereby avoiding experimental animals or human volunteers and providing the possibility of quantitative measurements under bacteria-free conditions (Hoorn, 1964). Shortly thereafter, animals like ferret, chicken, cow and pig were used to obtain more easily available and larger tracheal organ cultures (Reed, 1969). Even though, tissue explants can provide the physiological link to the *in-vivo* situation, the reduced viability of the explants *in-vitro* may limit their use and thereby restrict the investigation of signalling pathways, particularly in single cell populations. While cell lines are commonly used and provide a good basis for investigation, they cannot capture true inter-animal variation and lack many characteristics of their primary cell counterparts. The genetic changes due to the process of immortalising can cause an altered phenotype, immune function and responsiveness (Kaur and Dufour, 2012). In addition, the contamination with other cell lines, such as HeLa cells, has been a known issue for many years (Nelson-Rees et al., 1981). To address this need for representative options, primary airway epithelial cells models from both human and bovine have been developed to facilitate the investigation of events happening during viral infection (Cozens et al., 2018; de Courcey et al., 2012). For studies of the human epithelium the accessibility of bronchial brushings and endobronchial biopsies is critical. The invasive procedure of bronchoscopies is carried out in the context of clinic care and acquiring healthy controls is challenging (Hewitt and Lloyd, 2021). Submerged tissue culture systems, even using primary epithelial cells, also

have numerous limitations, such as they do not reflect three-dimensional architecture and physiological conditions (Al-Haddawi et al., 2007; de Courcey et al., 2012; Mitchell et al., 2007; Taha-Abdelaziz et al., 2016). In addition to submerged cell cultures, differentiated airway epithelial cells (AECs) are being increasingly used. The exposure to an air-liquid interface (ALI) over 21 days, specific growth factors and hormones trigger differentiation into ciliated, goblet and basal cells and possess the typical pseudostratified architecture (Cozens et al., 2018). Primary cell cultures provide a more physiologically relevant insight into innate immune mechanisms, retaining the genetic background, an unaltered cellular physiology and capture inter-animal variation, which is more reflective of true *in-vivo* responses.

1.6. Rationale

Respiratory tract infections in cattle by various bacterial and viral pathogens are economically important. Traditionally, research focus has been on classical immune cells. More recent recognition of the importance of the defence role of epithelial cells at the primary site of infection has been growing. It has become clear that epithelial cells play an important role in the initiation and orchestration of local innate and adaptive immune activity. We aim to characterise the response mechanisms of virally infected epithelial cells of the bovine, an understudied important livestock species. Further characterisation of antiviral innate immune potential of respiratory epithelial cells will ultimately contribute to breeding and immunotherapeutic strategies capable of preventing and better treatment of respiratory virus infection in livestock.

1.7. Hypothesis and overall aims

Hypothesis:

We propose here that bovine respiratory epithelial cells can respond directly to viral infections and have potent innate molecular antiviral activity.

The overall aims were to:

1. Establish and characterise an appropriate culture model of bovine respiratory epithelial cells to allow for hypothesis testing.
2. Characterise innate antiviral immune potential of primary bovine respiratory epithelial cells in responding to purified live BoHV-1 and viral ligands.
3. Investigate targeting innate antiviral pathways and antiviral defense mechanisms in respiratory epithelial cells as potential antiviral strategies.

Chapter 2. Materials and Methods

2.1. Organ and cell culture

2.1.1. Ethics statement

All tissue was collected post-mortem for which ethical approval is not required.

2.1.2. Cell line culture

Cell culture was carried out in sterile conditions using laminar air flow hoods and sterile or autoclaved materials and reagents. The bovine neonate nasal turbinate epithelial like BT cell line (CRL 1390™) was purchased from ATCC® for this project and cultured in vented 75 cm2 flasks in an incubator at 37°C with 5% CO2. Growth media consisted of Dulbecco's Modified Eagle's Medium (DMEM) with 10% horse serum (HS). BT cells were sub-cultivated every 4 days with media changing every 48 hours. MDBK (NBL-1) (Madin-Darby bovine kidney) epithelial cells were supplied by Dr Gerald Barry, University College Dublin and originally purchased from ATCC® (CCL-22™). Growth media consisted of Eagle's Minimum Essential Medium (MEM) with 10% horse serum (HS). MDBK cells were sub-cultivated every 4 days with media changing every 48 hours.

2.1.3. Primary epithelial cell culture

Tracheal sections from clinically healthy animals were collected at the abattoir within 15 min of euthanasia. The tracheal segment was rinsed with phosphate-buffered saline (PBS) supplemented with 50 IU penicillin, 50 µg/ml streptomycin and 2.5 µg/ml amphotericin B prior to cutting the tissue lengthwise. Sterile scissors and forceps were used to strip off the epithelial layer. Dissection was performed at the abattoir with the tissue harvested into a 50 ml tube containing 20 ml of DMEM supplemented with antibiotics, as described above. Samples were transported to the laboratory at room temperature within 120 min of collection. On arrival at the laboratory, tissue was washed in PBS supplemented with antibiotics, as described above, and dissected into fine pieces (1-3 mm^3 in size), before placing it in pre-warmed 0.25% trypsin in a shaking incubator at 150 rpm and 37°C for 1 hour. Tissue pieces were separated from single cells using a 70 µm nylon mesh strainer, collecting the filtrate in fetal bovine serum (FBS) for

trypsin inactivation. The cells were pelleted by centrifugation at 1,000 x g for 10 min and resuspended in LHC-9 media supplemented with antibiotics as above, 5% FBS and Insulin-Transferrin-Selenium-Ethanolamine (ITS-X) solution. Cells were counted using trypan blue staining and seeded in 12 well plates in a 37°C incubator in 5% CO_2. The cells were washed with PBS and growth media was changed to remove any debris after 24 hours, following media change every 2-3 days. Visual examination of cell morphology under the light microscope was used to check purity of cultures in addition to characterisation based on expression of the differing cytoskeletal proteins cytokeratin and vimentin. Once the cells reached approximately 85% confluency, cells were used for experiments.

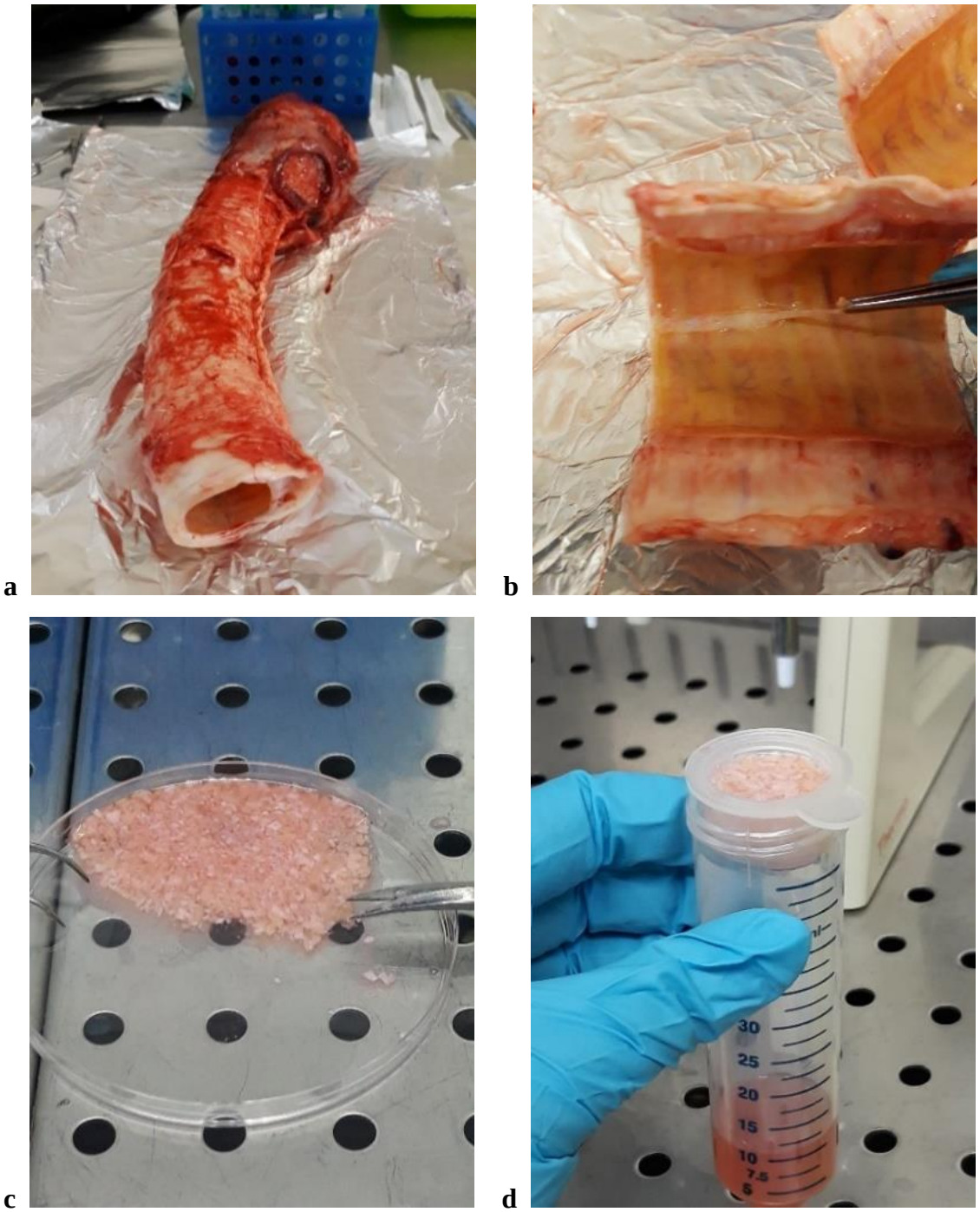

Figure 2.1 Isolation of primary bovine tracheal epithelial cells

(a) The inside of the trachea was rinsed with phosphate-buffered saline (PBS) supplemented with 50 IU penicillin, 50 µg/ml streptomycin and 2.5 µg/ml amphotericin B. (b) Sterile scissors and forceps were used to open the trachea and to strip off the epithelial layer. (c) Sterile scissors were used to dissect the tissue into 1-3 mm^3, before incubating in 0.25% trypsin placed in a 37°C shaking incubator at 150 rpm for 1 h. (d) The resulting mixture was filtered through a 70 µm nylon mesh strainer, collecting the filtrate with isolated cells.

2.1.4. Polarised primary epithelial cell culture

Polarised epithelial cell cultures were prepared by seeding 1 x 10^5 cells onto each hanging cell culture insert, which had previously been coated with 50 µl of matrigel diluted 1:8 in LHC-9 media and left at room temperature for 1 hour before the remaining matrigel was aspirated. Inserts were placed in 24 well plates, with 300 µl and 800 µl of culture medium in the apical and basolateral compartment respectively. Cells reaching confluency and polarisation were determined by examining the trans-epithelial electrical resistance (TEER) of the epithelial barrier using the EVOM2 epithelial volt/ohmmeter. 1,000 Ωcm^2 were considered as confluent.

2.1.5. Explant culture

Tracheal sections from clinically healthy animals were collected at the abattoir within 15 min of euthanasia. The tracheal segment was rinsed with phosphate-buffered saline (PBS) supplemented with 50 IU penicillin, 50 µg/ml streptomycin and 2.5 µg/ml amphotericin B prior cutting the tissue lengthwise. A sterile scalpel was used to dissect the inside of the trachea down to the cartilage. Dissection was performed at the abattoir with the tissue harvested into a 50 ml tube containing 20 ml of DMEM supplemented with antibiotics, as described above. Samples were transported to the laboratory at room temperature within 120 min of collection. On arrival at the laboratory, tissue was washed in PBS supplemented with antibiotics and dissected into pieces approximately 3 mm^3 in size before transferred to 6-well tissue culture plates (**Fig. 2.2**). The explants were cultures with LHC-9 media supplemented with antibiotics as above, 5% FBS and Insulin-Transferrin-Selenium-Ethanolamine (ITS-X) solution at 37°C with 5% CO_2. The explants were orientated with the epithelial surface uppermost and the culture medium was changed every before treatments. The organ cultures were treated within 24 hours of culture to avoid unwanted cell death. Following treatments, the tissue samples were stored in 2 ml of RNAlater at -80°C.

a

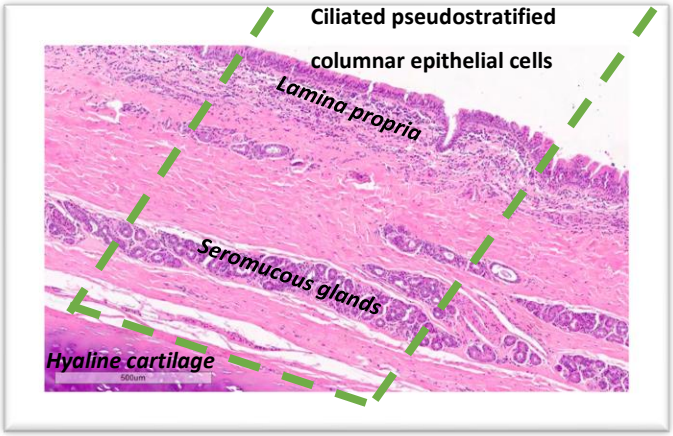

b

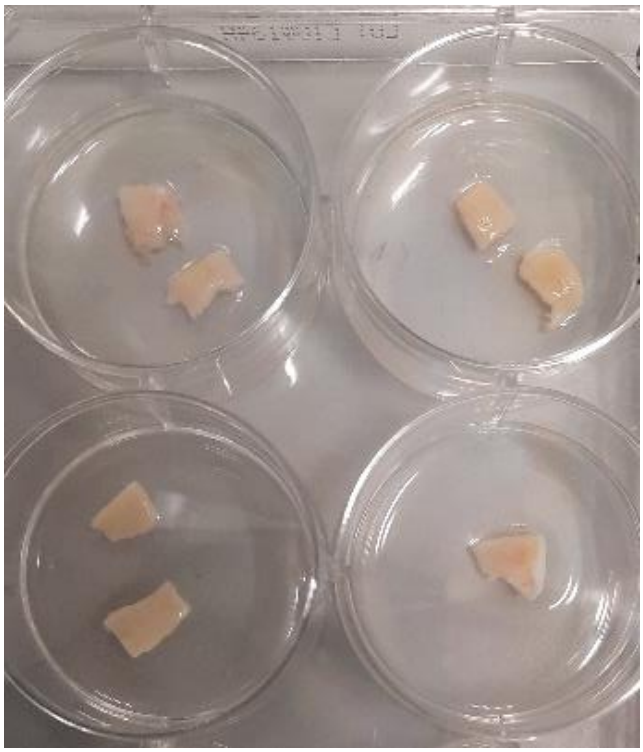

Figure 2.2 Bovine tracheal organ cultures

(a) Marked tissue part was dissected from a tracheal segment for tracheal organ cultures. (b) Cell culture of bovine tracheal organ explants in 6 well tissue culture plates, orientated with the epithelial surface uppermost.

2.1.6. Stimulations and treatments

For time-point stimulations cells were seeded in 12 well plates after the cell isolation from tissue and grown up to 80-90% confluency before stimulation. Media was removed and replaced with control media or media containing the treatment. The relevant stimulations were applied at a range of concentrations and incubated for 1, 3, 6, 12, 24 or 48 hours. Following stimulation, the cells were lysed in 1 ml TRIzol per well for mRNA extraction and stored at -80°C. Supernatants were harvested and stored at -20°C for further analysis.

2.1.7. Viability assays

The CellTiter-Blue® Cell Viability Assay was used according to manufacturer's instructions. Briefly, 1 x 10^4 cells were seeded into each well of a 96 well tissue culture plate and treatments conducted. Following treatments, 10 µl of Cell Titer Blue dye was added and plates incubated at 37°C with 5% CO_2 for 3 hours before fluorescence was recorded at 560/590 nm.

The LDH Glo™ Cytotoxicity Assay was used according to manufacturer's instructions. Briefly, cell culture supernatants were diluted in storage buffer and stored at -20°C. LDH activity was measured by adding an equal volume of LDH detection reagent to the diluted sample. The luminescence was recorded after 30-60 min.

For the MTT Assay 1 x 10^4 cells were seeded into each well of a 96 well plate. At each time point 20 µl of 6 mM Thiazolyl Blue was added to 100 µl growth media and incubated for 4 h. Following incubation, the media was aspirated and 150 µl Dimethyl sulfoxide (DMSO) added. The plate was photometrically measured at 595 nm after shaking the plate in the plate reader for 15 s to dissolve the crystals.

2.1.8. siRNA treatments

siRNA duplexes were designed using https://horizondiscovery.com/en/ordering-and-calculation-tools/sidesign-center. The specificity of the designed siRNA complex was confirmed by using the program BLAST https://blast.ncbi.nlm.nih.gov/Blast.cgi. A

non-targeting siRNA (scramble) was used as a control. For optimisation cells were seeded in 24 well tissue culture plates to be at different degrees of confluences ranging from 40-90% at the time of transfection. Lipofectamine (RNAiMax) was diluted by adding 3 µl lipofectamine to 50 µl Opti-mem medium. siRNA targeting TLR3, DDX58, IFNAR1, IFNLR1 or non-targeting siRNA was diluted 1:50 in Opti-mem medium. The diluted siRNA was added to the diluted lipofectamine (1:1 ratio) and incubated for 5 min at room temperature. The siRNA complex was then added dropwise to cells (100 µl of siRNA complex added to 1 ml complete LHC-9 media) to give a final concentration of 5 or 10 pmol siRNA in each well. Cells were incubated for 24, 48 or 72 h at 37°C before stimulation. Following stimulation cells were harvested in TRIzol for qPCR analysis.

2.2. Bovine herpes virus 1 culture

2.2.1. Propagation and purification

Bovine herpesvirus 1, sub-type BoHV-1.1, was supplied by Dr. Ronan O'Neill (Department of Agriculture, Food and the Marine, Ireland). MDBK (Madin-Darby bovine kidney) cells were used for virus expansion. Briefly, MDBK cells were infected at a low MOI with BoHV-1 for 24 h until cytopathic effect (CPE) was visible. Supernatant was collected and debris removed by a centrifugation at 27,000 x g for 20 min. A sucrose cushion was used for purification. Briefly, supernatant, containing the virus, was layered on TNE buffer (Tris 10 mM, EDTA 1 mM, NaCl 100 mM) pH 8.0 with 20% sucrose in an ultracentrifugation tube. Virus was pelleted down by centrifugation at 82,000 x g for 90 min without brakes in an ultracentrifuge with a horizontal rotor. The virus pellet was resuspended in TNE buffer, incubated on ice for 2 h and stored in aliquots at -20°C.

2.2.2. TCID50 Assay

For the virus titre determination, a serial virus dilution was performed in a 96 well cell culture plate and incubated with 5,000 MDBK cells per well in a 37°C incubator in 5% CO_2 for 4 to 7 days. The TCID50 was calculated using the Reed-Muench calculation (REED and MUENCH, 1938) recording the cell death.

2.3. Quantitative polymerase chain reaction (PCR)

2.3.1. RNA extraction and cDNA synthesis

Total RNA was extracted using Trizol reagent according to manufacturer's instructions. Briefly, cells were lysed into Trizol and chloroform was added, followed by phase separation by centrifugation. RNA was precipitated with isopropanol and pelleted by centrifugation. Pellets were washed with 80% ethanol and redissolved in RNase-free water. RNA quantity was determent by measurement of the absorbance at 260 nm using a NanoDrop spectrophotometer. A260/280 nm and A260/230 ratios were checked to assess presence of non-nucleic acid contamination, with ratio ≥ 1.8 indicating high purity. RNA quality was evaluated by 1.5% agarose gel electrophoresis with SybrSAFE DNA gel stain. One microgram of RNA was reverse transcribed into cDNA using the Omniscript cDNA synthesis kit with Oligo (dT) primers according to manufacturer's instructions. The cDNA solutions were diluted 1:10 before qPCR analysis.

2.3.2. Primer design and optimisation

Primers were designed using the Primer BLAST software to be intron spanning where possible. Primer details are recorded in **Tab. 2.1**. Lyophilised primers were re-suspended to a working concentration of 50 µM. Primer mixes were prepared by adding 25 µl each of forward and reverse primer to 200 µl dH_2O to achieve a final concentration of 5 µM for each primer. Optimal primer concentration was optimised for each primer pair by titration of 100, 300, 500 and 700 nM final concentrations with an annealing temperature of 60°C. The concentration which achieved the lowest Cq value while still generating a single peak on dissociation curve was selected. The efficiency of each primer set with the specific reaction conditions was determined by running a reaction with 5 point, 2-fold or 10-fold serial dilutions of the positive control cDNA. The standard curves were represented as the semi-log regression line plot of Cq value vs. Log of the relative input cDNA concentration. The efficiencies were calculated using the formula:

$E = 10^{(-1/Slope)}-1$;

$\%E = (10^{(-1/Slope)}-1) \times 100$

Efficiencies between 85 and 110% were considered acceptable. The specificity of each primer set was determined by Sanger sequencing (GATC Biotech, Konstanz, Germany)

of PCR products, examining electropherograms for single peaks at each position to confirm a single amplicon and running the returned sequence through BLAST to ensure the desired gene target was amplified.

Table 2.1 Primer sequences and conditions for qPCR

Gene	Primer Sequence	Product Size (bp)	Concentration (nm)
ACTB	F- GGACTTCGAGCAGGAGATGG	151	700
	R- GGATTCCATGCCCAGGAAGG		
ATF4	F- CCCAAACCCTACGACCCTCCTG	140	300
	R- TCCTGTTCCGCCCTCTTCTTCTG		
ATF6	F- GAGGAGCAAGACACATCGGATGAC	131	500
	R- TGACAGGGAGGCGGAGGAATATAG		
BAX	F- GCCCTTTTGCTTCAGGGTTT	179	500
	R- ACAGCTGCGATCATCCTCTG		
BoHV-1 gC	F- ATGTTAGCGCTCTGGAACC	79	500
	R- CTTTACGGTCGACGACTCC		
BCL2	F- CTCCACAAAGGCGTCCCAG	134	700
	R- CTCCACAAAGGCGTCCCAG		
CASP1	F- ACAGCTATGGATAGAGCCCGAG	177	500
	R- GACCACTGCTTGGGGTTTTTG		
CASP4	F- TATAAAAGCTCCTGAGGAAACT	268	700
	R- TTCCACAGTGTAGCCAAGAC		
CASP8	F- TGAGGGCCCTGGGATTTTAT	105	300
	R- TGTAGTTGTTACCAGAGGCG		
CCL2	F- CTGTGCCTGCTACTCACAGT	70	500
	R- GGGAGTTAATTGCATCTGGCTG		
CXCL10	F- GCACCATGAACAAAAGCGGT	194	300
	R- TGTGGCAATAATCTCGACACG		
CXCL8	F- ATTCCACACCTTTCCACCCC	176	300
	R- TTGCTTCTCAGCTCTCTTCACA		
DDIT3	F- CCTGAGGAGAGAGTGTTCCAG	219	500
	R- CTCCTTGTTTCCAGGGGGTG		
DDX58	F- TCCCAGCAATGAGAACGCTA	219	400
	R- GGGAGCGTCATTCCCATTGT		

EGR1	F- GCCCACCATGGACAACTACC R- CAGGAAAGGACTCTGCGGTC	242	500
EPSTI1	F- ACTCCAACTACCCACCCACT R- GCATCAAGTGACTCCCTGCT	218	500
ERK2	F- CAAACCTTCCAACCTGCTGC R- GGACTTGGTGTAGCCCTTGG	175	500
FAS	F- AAATGCCCACATGGCTGGTA R- TTTTCCGTTTGCCAGGAGGA	131	500
GADD45G	F- CGCCCTCTGTTCTTGTGGAT R- CAGGACTTTGGCTGACTCGT	191	300
GAPDH	F- ATCAAGTGGGGTGATGCTGG R- GGCGTGGACAGTGGTCATAA	288	100
H3F3A	F- CATGGCTCGTACAAAGCAGA R- ACCAGGCCTGTAACGATGAG	136	100
HIF1A	F- CCTCTGATCTCACGAGGGGT R- TCGACGTTCAGAACTTATCTTTTTC	204	500
HSPA6	F- GCCTGCCTACTTCAACGACT R- CCCACCCAGGTCGAAAATGA	169	500
IDO1	F- TACTTTGCAGAAAGCGCTGC R- GGTTGCCTTTCCAACCAGAC	140	300
IFI16	F- GGAAGTCGTGGTTTATGGACAGCG R- CCTTGGTGACCTTGATGAAACTAT	146	300
IFI44	F- GCTCACGCATGTGGATACCT R- TGTGAACTGCCTCTAGCTGAA	98	500
IFIH1	F- AGCCCATGACACAGAATGAACA R- CTCATCAGCTCTGGCTCGAC	191	400
IFNA	F- TGGCTGTGAGGAAATACTTCCAGAG R- CAGTCCTTTCTCCTGAAACTCTCCTG	148	500
IFNAR1	F- ACAGGCGGAATAAAGGGAGC R- GGCTGATCGGAGAAATACTCG	220	300

IFNB1	F- AGAAGCAAAACTCCACTACGGA R- CAGGCACACCTGTCGTACTC	106	300
IFNB3	F- AGCCCTGTGCCTGTTTTCAT R- TGGTTCATCTCCTCAGGGACT	221	500
IFNL3	F- AGGCCATGGCTAACTCATCC R- GGCAACACATTTCAGGTCCC	245	500
IFNLR1	F- CCCCAGCTATTAGAAGCCGT R- CGTTTCACGGTGTCCAGAGA	197	700
IL1A	F- TGAACGACGCCCTCAATCAA R- GGTGTCTCAGGCATCTCCTTT	226	700
IL1B	F- AACGTCCTCCGACGAGTTTC R- GCTCATGCAGAACACCACTTC	163	500
IL33	F- CAAAACAAGATCACAAGGATTGCC R- GGCTTCCTGTTGTCCACACT	135	300
GRP78/HSPA5	F-CGGAGGAGGAGGACAAGAAGGAGC R- ATAAGACGGCGTGATGCGGTTG	143	500
GRP94/HSP90B1	F- CAAGATCGAGAAGGCTGTGGTGTC R- GATGTCCTTGCCTGTCTGGTATGC	133	500
HERPUD1	F- ATCAGAACGCTGCTCCACAAGTG R- TAGCGGCTGAGTAGGTCCAATCC	138	500
IL6	F- CAGGAACGAAAGAGAGCTCCA R- AATGGAGTGAAGGCGCTTGT	76	500
IRF1	F- GTGGATGGGAAGGGGTATCTG R- TATCAGGCCAATATAACCCCCA	120	300
IRF3	F- ACCCAACACTTAGGCCAGAC R- GTCGGGCTTATCCTTCCCAG	237	500
IRF7	F- ACCACGGAGGGCCCAG R- AGAGAGAGGAGGGCTGTCTG	195	300
ISG15	F- GGCCATGGGCGGGGA R- TTCTGGGCGATGAACTGCTT	108	500

KRT18	F- ATTTCAGTCTTGGCGACGCT R- GCCTCAGTGCCTCAGAACTT	131	300
MAVS	F- GCGGCTACCCAAGCCTTTAT R- GAAGAGGTTCCAGAGGGTGC	247	300
MB21D1	F- ACTTCTGATTAGAAAACCTAGAGAA ATATCTGTGG R- CGCCATGTTTCTTCTTGGAAAAGACT	207	400
MX1	F- GGGGACGGGCGGTGTT R- GGTTGCTCTTGGACTCCATATCT	181	300
NFKB1	F- GTGTCTGCACTTGGCCTCTA R- GGGATTCTGCAGGTCCACTG	136	100
NFKBIA	F- GGACGAGCTTCCCTACGATG R- ATGTTCCAGACCAGGCAGTG	191	300
NOD1	F- TCTTTGAAGTGGGGATGTGGG R- GCTCTCTGCCACTTCGTCAT	221	500
NOD2	F- CGCCAAAGGACTTGCAAGA R- CCTCGGAGCCAGACTTCCA	135	500
OAS1Z	F- GTCCTGCCCGCCTTTGAT R- TCCCATGTCTCTTCTTACACTGTT	229	500
PERK	F- GCCGTGCGGCAGATCATTAG R- GGCTGGATGACACCAAGGAA	128	500
PPIA	F- TTATGTGCCAGGGTGGTGAC R- TGCCATCCAACCACTCAGTC	195	100
RPS9	F- GCGTCTGTTCGAAGGTAATGC R- AAGTCGATGTGCTTCTGCGA	370	200
RSAD2	F- TGGTTCCAGAAGTACGGTGAA R- TCCTCGTCCACGTTGAATCG	203	300
STAT1	F- AGTCTTGGCATCTGACGTGC R- GCAGCATGCTCCCAGTCTT	220	500
TAP	F-GTCTGCTTGGTTAGGATTTACTCAAGG R- CCCGCCCAACACAGGTG	125	700

TGFB1	F- ACAATTCCTGGCGCTACCTC	200	300
	R- GCCGGAACTGAACCCGTTA		
TLR3	F- CAGCTCCAACTGGAGAACCT	148	400
	R- ACCCAGGAGAGAACTCTTTGATT		
TLR4	F- ACCCTTGCGTACAGGTTGTT	80	300
	R- GGGGATGTTGTCGGGGATTT		
TLR7	F- TCTTGAGGAAAGGGACTGGTTA	205	700
	R- AAGGGGCTTCTCAAGGAATATC		
TLR8	F- TAACCTTCGGAATGTCTCCAGT	232	700
	R- GTGGGAAATTCTGTTTCGACTC		
TLR9	F- CTGACACCTTCAGTCACCTGAG	156	500
	R- TGGTGGTCTTGGTGATGTAGTC		
TMEM173	F- AGGTAGAAGATGCCTCACTCCA	102	300
	R- CACCAGACAGGCACTTAGCA		
TNF	F- CTGGTTCAAACACTCAGGTCCTC	84	300
	R- CCCCGGAGAGTTGATGTCG		
TP53	F- ACTTGTGGAACCTACTTCCTG	211	300
	R- GAGGGGACAAAGGACGACAG		
USP18	F- CCCGGTCGGTTTACACAACA	111	500
	R- CCTGGCACCGTTATCCTCTT		
VIM	F- TGCGCTCAAAGGGACTAACG	189	300
	R- TCGAGCGCCATCTTGACATT		
XBP1 spliced	F- GCTGAGTCCGCAGCAGGT	130	700
	R- CTGGGTCCAAGTTGAACAGAAT		
XBP1 total	F- TGAAAAACAGAGTAGCAGCTCAGA	181	500
	R- CCCAACCGCTGTCTCAACTC		
XBP1 unspliced	F- CAGACTACGTGCACCTCTGC	139	500
	R- CTGGGTCCAAGTTGAACAGAAT		

2.3.3. Quantitative real time PCR (qPCR)

Quantitative PCR was run using the PowerUp SYBR Green Master Mix on a StepOnePlus Real Time PCR System using the following parameters: 95°C for 20 s, followed by 40 cycles of 95°C for 3 s and 60°C for 30 s and a final amplicon dissociation step at 95°C for 15 s, 60°C for 1 min and 95°C for 15 s. A non-template control was included in each gene assay to detect molecular contamination. All reactions were carried out in triplicate. Levels of gene of interest (GOI) expression were determined using the delta delta Ct method (2^-ΔΔCt) (Schmittgen and Livak, 2008). A ratio of GOI relative to the reference gene was generated by normalising the gene of interest to a stable internal reference control gene.

2.3.4. GeNorm analysis

A stable internal reference control gene was determined using GeNorm analysis from a panel of possible reference genes: beta-actin (ACTB), Glyceraldehyde 3-phosphate dehydrogenase (GAPDH), peptidylprolyl isomerise A protein (PPIA), ribosomal protein S9 (RPS9) and H3 histone, family 3A (H3F3A). The cDNA was synthesised from RNA extracted from stimulated primary cell cultures and PCR was performed using primers for the panel of reference genes. The software GeNorm calculates the gene expression stability measure M for a reference gene as the average pairwise variation for that gene with all other tested reference genes. Stepwise exclusion of the gene with the highest M value allows ranking of the tested genes according to their expression stability. M values were used to determine stable gene expression with lower M values indicating a more stable reference gene. H3F3A was found to be the most stable reference gene across the primary bovine tracheal epithelial cell culture stimulations (**Fig. 2.3**).

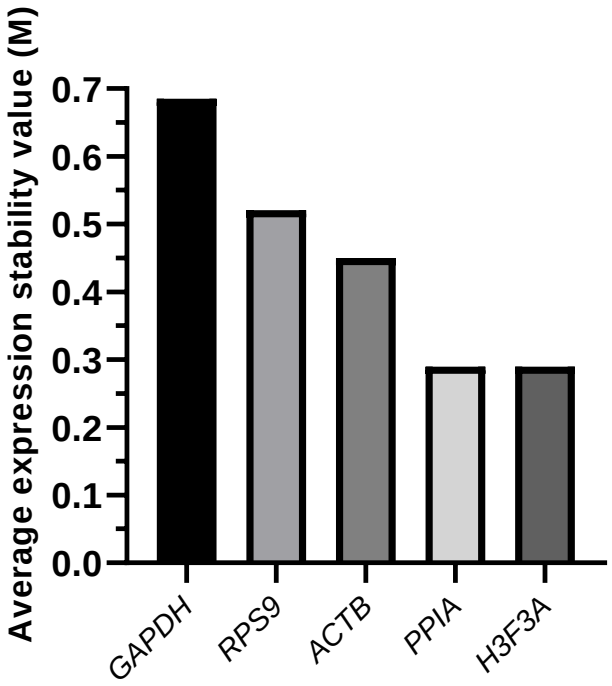

Figure 2.3 GeNorm analysis of stability of reference gene expression in primary tracheal epithelial cells

cDNA was synthesised from RNA extracted from stimulated primary bovine tracheal epithelial cell cultures and PCR was performed using primers for the panel of reference genes. The quantities obtained were used by GeNorm software to determine respective M values for each gene, with lower M values indicating a more stable reference gene. H3F3A was found to be the most stable reference gene from the tested panel.

2.3.5. Detection of leukocyte contamination of primary epithelial cell cultures via PTPRC polymerase chain reaction (PCR)

The HotStar Master Mix PCR kit was used to carry out a PCR reaction to detect transcription of the protein tyrosine phosphatase receptor type C (*PTPRC*) gene, encoding the pan-leukocyte marker CD45, within primary cell cultures. A 20 µl reaction volume was prepared containing 0.6 µl cDNA, 1X CarolLoad reaction buffer, 200 µM dNTP solution, 300 nM *PTPRC* specific primers and 0.6 µl HotStarTaq polymerase enzyme, with nuclease free water making up the remainder. cDNA prepared from bovine PBMCs was used as a positive control for PRPTC amplification. The reference gene *H3F3A* was amplified from all samples to ensure poor cDNA quality did not account for a lack of amplification. A non-template control was included for both gene assays. The PCR reaction was carried out in a Techne Prime thermocycler using the following thermocycling conditions: 95°C for 5 min and 40 cycles of 95°C for 30 s, 60°C for 1 min, 72°C for 1 min. Results were assessed by presence or absence of a PCR product of expected size on a 1.5% agarose gel with SybrSafe staining after electrophoresis.

2.4. Cell imaging

2.4.1. Histological processing of tracheal samples

Tracheal biopsies were removed from formalin and immersed in 70% ethanol for 24 h before overnight paraffin wax embedding in Surgipath cassettes. Embedded biopsies were sectioned at 3 µm and dried overnight at 60°C. An automated staining system was used to dewax by immersion in histoclear, rehydration by immersion in 100%, 90%, 80% and 75% ethanol, applying a haematoxylin and eosin staining and progressively dehydrated by a reversal of the ethanol immersion steps used previously. Slides were mounted with Surgipath mounting medium and examined using an Olympus BX51 upright microscope.

2.4.2. Immunohistochemistry staining of cell cytoskeleton proteins

Primary tracheal cells were grown confluent in wells of the Millicell EZ SLIDE 4 well glass culture slides. Cells were washed three times in PBS before being fixed in ice-cold methanol for 10min at room temperature. Cells were then washed a further three times in PBS before incubation in 3% H_2O_2 for 20 min at room temperature, followed by blocking in 10% BSA for 1 h at room temperature. Cells were incubated overnight with mouse anti-human cytokeratin antibody, mouse anti-human vimentin antibody or IgG1 isotype control using 100 µl per well of a 1:100 dilution in PBS. Cells were washed three times in PBS before incubation with the secondary antibody, Dako, for 30 min at room temperature. Following washing three times, slides were mounted with Surgipath mounting medium and examined using an Olympus BX51 upright microscope.

2.5. Next generation sequencing analysis

Data on sex, age and breed of animals used for tracheal epithelial cell culture was made available in the abattoir immediately following slaughter. Four animals were used for next generation sequencing analysis, three male and one female, Simmental, Hereford and Friesian Cross with an age ranging from 33 to 104 months. Tissue samples were directly collected in RNAlater and tested negative for BoHV-1 and BoHV-4 by the

Virology Division, Laboratories Backweston, Dept. of Agriculture, Food and Marine, Celbridge, Co. Kildare, Ireland.

Next generation sequencing paired end reads of 151 bp was conducted by Macrogen Europe using an Illumina platform with the Illumina package bcl2fastq and Sanger Quality (ASCII Character Code = Phred Quality Value + 33). TrueSeq Stranded mRNA LT Sample Prep Kit was used as library kit and TrueSeq Stranded mRNA Sample Preparation Guide, Part # 15031047 rev. E as library protocol (**Tab. 2.2**).

Quality control of raw data was carried out using the program FastQC. Fragments mapped and alignments assigned with the program Subread in Rstudio using the bovine genome Bos taurus ARS-UCD1.2 (2018) with a percentage of successfully mapped fragments of ≥ 96.9% and assigned alignments ≥ 74.8% (**Tab. 2.3**). The principal component analysis (PCA) was carried out using the program iDEP (integrated Differential Expression and Pathway analysis) in Rstudio. Differently expressed gene analysis was conducted with the program Limma voom and Deseq2 in Rstudio.

Table 2.2 Raw data information from next generation sequencing

Sample	Total Bases	Read Count
1_Animal 4520_Control	18,540,524,732	122,784,932
2_Animal 4520_BoHV-1 MOI7	18,020,628,410	119,341,910
3_Animal 4620_Control	19,910,103,188	131,854,988
4_Animal 4620_BoHV-1 MOI7	18,985,073,866	125,728,966
5_Animal 4720_Control	19,960,177,506	132,186,606
6_Animal 4720_BoHV-1 MOI7	18,170,578,054	120,334,954
7_Animal 4820_Control	16,075,852,902	106,462,602
8_Animal 4820_BoHV-1 MOI7	18,115,878,002	119,972,702

Table 2.3 Successfully mapped fragments and assigned alignments with the program Subread in Rstudio using the genome Bos taurus ARS-UCD1.2 (2018)

	Successfully mapped fragments [%]	Successfully assigned alignments [%]
Ctr 1	98.9	77.9
Ctr 2	98.8	77.9
Ctr 3	98.8	77.9
Ctr 4	98.7	79.2
BoHV-1 1	97.4	76.3
BoHV-1 2	96.9	76.0
BoHV-1 3	97.6	74.8
BoHV-1 4	98.1	75.6

2.6. TCA protein precipitation

The TCA protein precipitation method was used to concentrate proteins from cell culture supernatants. Briefly, 1 volume of 100% (w/v) Trichloroacetic acid (TCA) was added to 4 volumes of supernatant (250 µl TCA to 1 ml sample) and incubated for 10 min at 4°C. After a centrifugation at 10,0000 x g for 5 min, the supernatant could be removed, leaving the protein pellet intact. The pellet was washed twice with 200 µl cold acetone, following centrifugation as previously described and dried by placing the tube in 95°C heat block for 5-10 min. The pellet was stored at -20°C until further analysis via SDS PAGE or mass spectrometry analysis.

2.7. SDS PAGE and Coomassie staining

The protein pellets obtained from the TCA protein precipitation from cell culture supernatants were resuspended or cells scrapped off in loading buffer and heated at 95°C for 5 min. A 14% resolving gel, topped with a 4% stacking gel were prepared (**Tab. 2.4, Tab. 2.5**). The gels were loaded with the molecular marker and samples in a running tank with 1X running buffer in the upper and lower reservoirs of the apparatus. The gel was run at 110 V for 45 min. Following electrophoresis, Coomassie Brilliant Blue R-250 Staining Solution was used by shaking the gel in a tray with staining solution on a laboratory shaker for approximately 2 hours and de-stained with a 7% (v/v) acetic acid in 5% (v/v) methanol solution.

Table 2.4 Resolving and stacking gel for SDS PAGE

	14% resolving gel	**4% stacking gel**
TrisHCl 1.5M	3.8 ml	750 µl
Acrylamide	7 ml	1 ml
10% SDS	150 µl	60 µl
10% APS	150 µl	60 µl
TEMED	6 µl	12 µl
dH_2O	3.9 ml	4.61 ml

Table 2.5 Sample loading and running buffer for SDS PAGE

5x sample loading buffer	
Glycerol	5 ml
SDS (10%) in H_2O	10 ml
Bromophenol blue	10 mg
Tris HCl 1 M pH 6.8	6.25 ml
H_2O	28.75 ml

10x running buffer	
MES	*0.5 mM 47.6 g*
Tris	*500 mM 60.6 g*
EDTA	*10 mM 2.92 g*
SDS	*1% 10 g*
H_2O	*Up to 1 L*

2.8. Mass spectrometry analysis

For mass spectrometry analysis of supernatant proteins, the protein pellet following TCA precipitation was resuspended in 50 µl of 6 M urea in 50 mM Ammonium bicarbonate. The BCA Protein Assay was used to determine protein concentration. Briefly, BCA reagent B was diluted 1:50 in BCA reagent A and 200 µl solution used per well in a 96 well plate. 3 µl of each sample and standard curve samples was added into the reagent mix and the plate placed in an incubator at 37°C for 30 min. Following incubation, the absorbance was measured at 562 nm on a plate reader. A standard curve was generated each time with BSA standards and the protein concentration of each sample calculated accordantly. The Preomics iST Sample Preparation Kit was used to lyse, reduce, alkylate, digest and purify 100 µg protein per sample for mass spectrometry analysis. The mass spectrometry analysis was conducted by the mass spectrometry core facility at the Conway Institute of Biomolecular and Biomedical Research at the University College Dublin, Ireland.

2.9. Bioinformatic tools

Gene and protein sequences were obtained from the GenBank database (part of the National Centre for Biotechnology Information (NCBI) (www.ncbi.nlm.nih.gov/genbank) and Ensembl (www.ensembl.org/index.html). The UCSC genome browser (https://genome.ucsc.edu/) was used to further probe genes across species. BLAST (basic local alignment tool) (https://blast.ncbi.nlm.nih.gov/Blast.cgi) was used to find homologous sequences to the bovine sequences of interest. Alignment of sequences of

interest was performed using ClustalOmega (www.ebi.ac.uk/Tools/msa/clustalo/). Phylogenetic analysis was performed using MEGA-X (www.megasoftware.net/).

2.10. Statistical analysis

Statistical analysis was carried out using Graphpad Prism 8.0.1 software and indicated in each figure legend. All data were tested for normality of distribution in order to decide whether to apply parametric and non-parametric tests accordantly.

For stimulation experiments with one stimulus concentration and multiple time points or multiple stimuli/concentrations at one time point, a one-way ANOVA followed by Sidak's multiple comparison test and the Friedman (matched) or Kruskal-Wallis test (not matched) for non-parametric data followed by Dunn's multiple comparison test was used. For stimulation experiments with multiple concentrations of stimulus and multiple time points, the two-way ANOVA or with missing values, the mixed-effects model with the Geisser-Greenhouse correction followed by the Sidak's multiple comparisons test was used. The paired t test for parametric data or for non-parametric data, the Wilcoxon matched-pairs signed rank test were used for the comparison of two matched datasets. For analysing of two not matched and non-parametric datasets the Mann-Whitney test was used.

Chapter 3. Optimisation of primary bovine tracheal epithelial cell culture model for *in-vitro* research: cytosolic and endoplasmic reticulum stress responses in primary bovine tracheal epithelial cells infected with bovine herpesvirus 1

3.1. Introduction

Respiratory tract infections in cattle by various bacterial and viral pathogens are economically important. In addition to direct mortality, they can cause immune suppression and tissue damage, resulting in secondary infections in the respiratory tract (Bellinghausen et al., 2016; Mosier, 2015). Comprehensive knowledge about disease pathogenesis and immune defence systems at the site of infection is needed to improve animal health. While *in-vivo* models have classically been used to capture the overall complexity of immune mechanisms, experimental infection models are expensive and require dedicated research facilities which preclude their widespread adoption. Furthermore, due to the increasingly stringent regulations in order to reduce the use of live animals in research, reproducible and physiologically relevant alternatives are required. Additionally, a traditional focus has been applied to classical immune cells but due to the growing recognition of their importance in the initiation and orchestration of the innate immune system at the primary site of infection, understanding response mechanisms of virally infected epithelial cells may lead to improved insights into the pathogenesis of respiratory infections. Such models are particularly limited in livestock species.

One mechanism being activated in epithelial cells upon viral infection are so called stress proteins (SPs), a diverse group of proteins including heat shock proteins (HSPs), RNA chaperone proteins (RNPs) and ER associated stress proteins (Wan et al., 2020). Ubiquitously expressed they get activated in response to a disruption in cell homeostasis and they trigger signalling cascades to either promote cell survival or alternatively to initiate cell death - all in order to secure tissue survival. The disruption of cell homeostasis can be caused by the effects of environmental and physiological stresses, resulting in increased expression of misfolded proteins, high rate of protein translation,

disruption to the redox state of the cell or an intracellular pH drop (Lang et al., 2021). The proteotoxic stress leads to the activation of the heat shock factor (HSF) and synthesis of HSPs. During homeostasis HSF1 exists as inert monomers which oligomerise to a trimeric state and the proteins becomes phosphorylated during the stress response (Baler et al., 1993). HSF trimers then bind to heat shock elements located upstream of heat shock responsive genes and induce transcription of HSPs (Kline and Morimoto, 1997) (**Fig. 3.1**). Many HSPs function as molecular chaperones to guide conformational states of proteins and are classified based on their molecular weight, including HSP100s, HSP90s, HSP70s, HSP60s, HSP40s and some smaller HSPs (Wan et al., 2020). Even though the heat shock response (HSR) is considered as a fundamental cellular defence mechanism, reflecting a non-specific stress situation of the host cell, the interaction between viruses and HSR remains unclear. It has been hypothesised that HSPs can be induced by the virus to regulate and assist with the virus life cycle and therefore be detrimental to the host (Santoro et al., 2010; Wan et al., 2020).

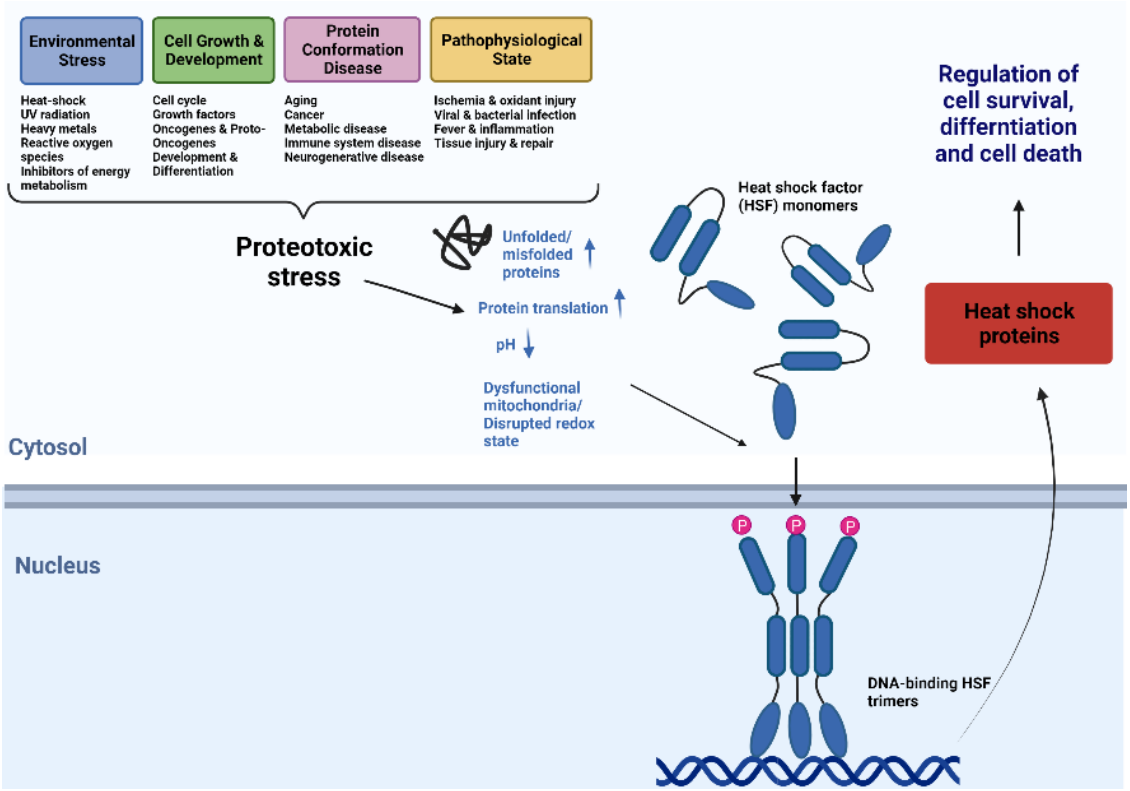

Figure 3.1 Cytosolic stress response – Heat shock response (HSR)

Environmental and physiological stress results in the disruption of cell homeostasis leading to the appearance of increased levels of non-native proteins, high rate of protein translation, disrupted redox state of the cell or an intracellular pH drop. The proteotoxic stress leads to the activation of the heat shock factor (HSF) and synthesis of heat shock proteins. During homeostasis the heat shock factor 1 (HSF1) exists as inert monomers which oligomerise to a trimeric state and become phosphorylated during the stress response. The HSF trimers bind to heat shock elements located upstream of heat shock responsive genes and induce transcription of heat shock proteins. Created with BioRender.com.

A similar mechanism gets activated during ER (endoplasmic reticulum) stress to re-establish ER homeostasis. The ER stress response or also called unfolded protein response (UPR) gets triggered when one of the primary functions of the ER – such as protein synthesis and transport, protein modification, lipid and steroid synthesis or Ca^{2+} homeostasis is disrupted (Raghunath et al., 2018). Such perturbations can be caused by increased protein translation, inhibition of degradation of misfolded proteins, hypoxia, nutrient depravation or disruption of the ER-Ca^{2+} buffering capacity. The UPR molecular mechanism consists of three parts: the pancreatic ER kinase (PERK), activating transcription factor 6 (ATF6) and inositol-requiring transmembrane kinase/endonuclease 1 (IRE1), as reviewed in (Malhotra and Kaufman, 2007; Raghunath et al., 2018). These three ER-localised transmembrane proteins are bound to the chaperone BiP (immunoglobulin heavy chain binding protein), also called GRP78 (glucose-regulated protein 78) or HSPA5 (heat shock protein family A member 5). During ER stress misfolded proteins bind to BiP, releasing the three UPR sensors. ATF6 then translocates to the Golgi where it is proteolytically cleaved by S1P and S2P (site-1 and site-2 proteases) (Chen et al., 2002). ATF6 activates the transcription of UPR genes including GRP78, GRP94 and XBP1 (X-box binding protein 1) (Yoshida et al., 2001). The UPR activation results among other things in the transcription of genes involved in ER-associated protein degradation (ERAD) and redox homeostasis to promote cell survival. Following dissociation, PERK homo-oligomerises, auto-phosphorylates and inactivates elF2a (eukaryotic translation-initiation factor 2α) by phosphorylation. The inhibition of elF2a attenuates the synthesis of most proteins, alleviating ER protein synthesis burden (Shi et al., 1998). An exception of this are specific mRNAs such as *ATF4*, *ATF3* and its target gene *DDIT3* (CHOP, C/EBP homologous protein) which control the transcriptional component of ER stress (Ubeda et al., 1996). In addition to elF2a, PERK activates another transcription factor NRF2 (nuclear factor erythroid 2-related factor 2), which leads to an upregulation of antioxidant genes and the promotion of cell survival during ER stress (Cullinan et al., 2003). Activated IRE1a can initiate two major events, autophagy and apoptosis. After dimerization of IRE1a and auto-phosphorylation, the activated IRE1a splices *XBP1* mRNA to form the more stable *sXBP1* mRNA, encoding a potent transcription factor. Depending on the level of ER stress and reversibility the IRE1a axis can offer cytoprotection or apoptosis. In the case of apoptosis CHOP activates

the pro-apoptotic proteins BAX and BAK and downregulates Bcl2 (Hetz et al., 2006). Autophagy is initiated when IRE1a binds to TRAF2 (tumour-necrosis factor receptor associated factor 2) and activates JNK (JUN N-terminal kinase) (Ogata et al., 2006) (**Fig. 3.2**).

On one hand, the viral accumulation of mis- and unfolded proteins in the ER during viral replication can trigger the UPR, similar to the heat shock response in the cytosol. On the other hand, it has been shown that viruses are able to disarm the UPR or to customise it for their own benefit. Whereas, blocking as well as activation of the UPR can be pro-viral, the mechanisms are virus and cell specific (Johnston and McCormick, 2019). This makes physiological relevant infection models important to investigate the interplay of economically relevant viral infections in livestock species with the cytosolic and endoplasmic reticulum stress responses in epithelial cells.

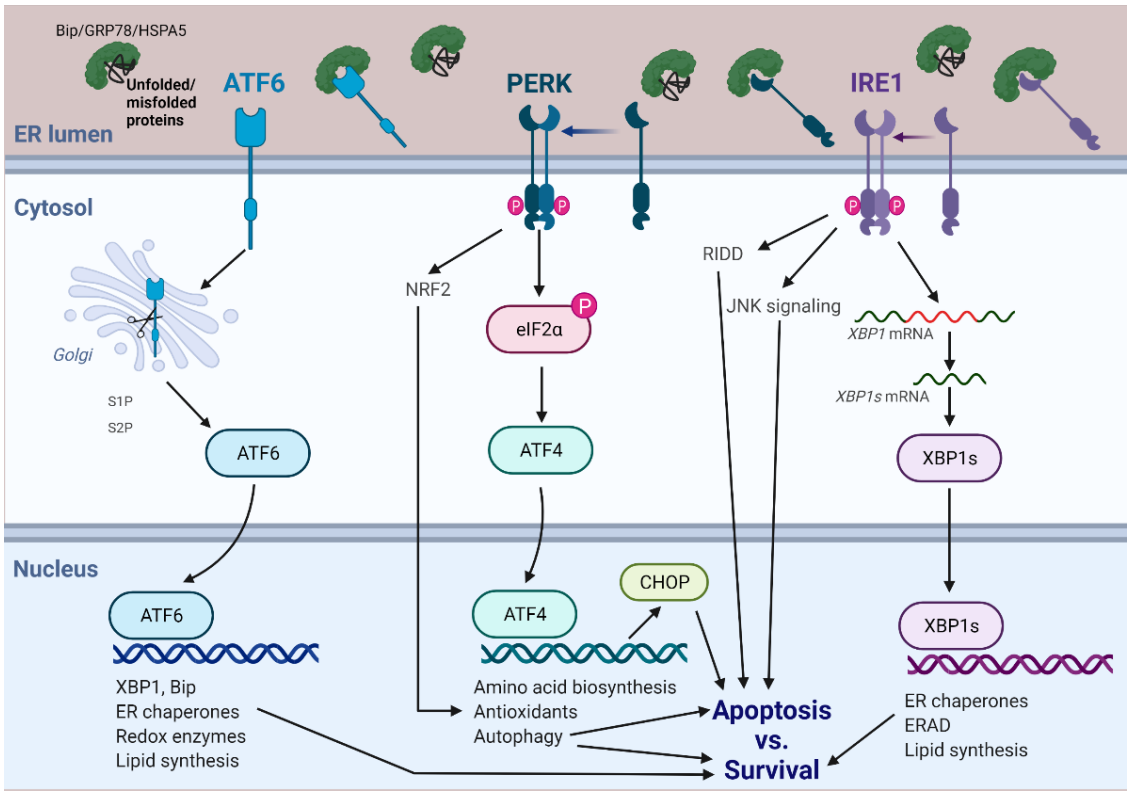

Figure 3.2 ER stress response – Unfolded protein response (UPR)

The UPR molecular mechanism consists of three arms: the pancreatic ER kinase (PERK), activating transcription factor 6 (ATF6) and inositol-requiring transmembrane kinase/endonuclease 1 (IRE1). During ER stress misfolded proteins bind to BiP, releasing the three UPR sensors which activate signalling pathways. Transcription factors lead to the upregulation of different genes, promoting either cell survival or cell death in response to ER stress. Created with BioRender.com.

3.2. Rationale

Here, we aimed to establish a cell culture model of primary bovine tracheal epithelial cells, which can provide a realistic insight into immune mechanisms in response to bovine herpesvirus 1 infection. With next generation sequencing analysis of epithelial cells infected with purified live BoHV-1 we investigated the transcriptomic changes early after infection. Next, we examined gene expression of proteins involved in the stress responses occurring during viral infections as part of the unfolded protein response (UPR). We tested the influence of Thapsigargin (Tg), an ER stressor, on tracheal epithelial cells and its antiviral potential.

3.3. Hypothesis and specific aims

Hypothesis:

Bovine herpesvirus 1 infection influences the cytoplasmic and endoplasmic reticulum stress response in bovine respiratory epithelial cells.

The specific aims were to:

1. Establish and characterise a tracheal explant model to study the innate antiviral immune responses in the intact bovine tracheal tissue.
2. Establish and characterise a primary culture model of tracheal epithelial cells.
3. Investigate the conserved defence mechanisms during viral replication as part of the innate antiviral activity in respiratory epithelial cells.
4. Investigate targeting the UPR as a potential antiviral strategy.

3.4. Results

3.4.1. Characterisation of tracheal organ cultures and primary bovine tracheal epithelial cells as post-mortem culture models

Bovine tracheas were collected from recently slaughtered animals, readily available as unused by-products of the slaughtering process. Data on sex, age and breed of animals was made available by the abattoir. Due to the SARS-CoV-2 pandemic data was not available on 31 of the 75 animals used for this project. 55% of all recorded animals were female, approximately 6-8 years old and over 30% were of Friesian or Friesian-cross breed (**Fig. 3.3**).

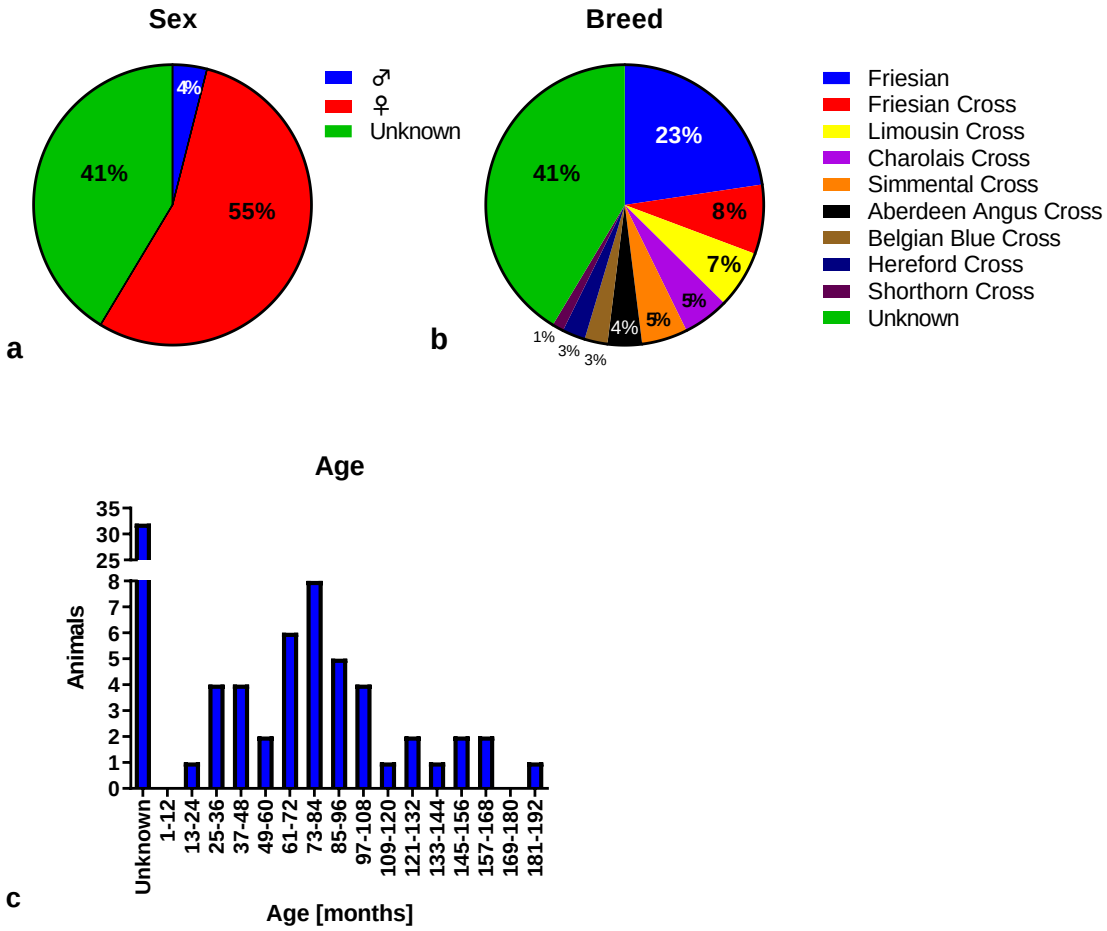

Figure 3.3 Sex, breed and age of animals from which trachea was processed for tissue culture *Data on sex, age and breed of animals was made available in the abattoir immediately following slaughter. Due to the SARS-CoV-2 pandemic data was not available on all animals. (a-b) Details of sex and breed of cows from which tracheal samples were obtained, n=75. (c) Histogram detailing the age categories of cows from which tracheal samples were collected, n=75.*

Because the isolation of pure cell populations involves significant disruption to the tissue architecture, we decided to investigate the use of a tracheal organ culture model in addition to isolated tracheal epithelial cells. The explant model maintains the functional important cell types in the physiological correct arrangement and enables normal cell-cell interaction between other important cell types such as fibroblasts. Previously published protocols were used as guidelines (Di Teodoro et al., 2018; Fulton and Pearson, 1980).

Guided by a previously published protocol (Berghuis et al., 2014; Mitchell et al., 2007), we established a reproducible primary culture model of bovine tracheal epithelial cells, easily obtainable from abattoir by-products. To maximise cell viability the dissection was performed at the abattoir and the dissected tissue transported back in culture media with penicillin G, streptomycin and amphotericin B. There was no issue with bacterial or fungal contamination in the isolated cultures.

During the process of the epithelia cell isolation histology images were taken before and after dissection of the upper functional epithelial layer of the inside of the trachea and can be seen in **Fig. 3.4**. The uppermost functional layer containing the luminal cilliated pseudostratified columnar epithelium overlaying the stroma is successfully removed during dissection. After disruption of the harvested tissue using both mechanical and enzymatic dissociation in trypsin solution the average cell yield was 42.6 x 10^6 per animal (n=60), while the yield was proportional to the amount of processed tissue (**Fig. 3.5 a**-**b**). The ability of cell populations to proliferate in culture is shown by the growth curve in Figure 3.5 c obtained by the MTT-Assay. Epithelial cell populations were easily identified by morphology. A representative morphological image of epithelial cells grown in small islands that ultimately combine to form a confluent monolayer can be seen in **Fig. 3.5 d**.

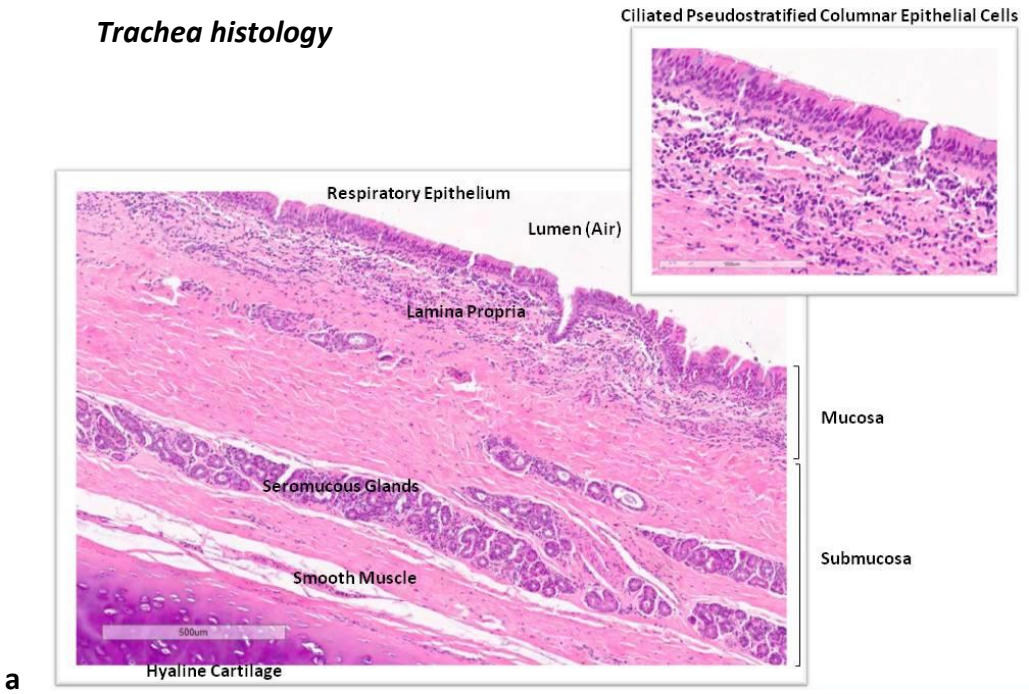

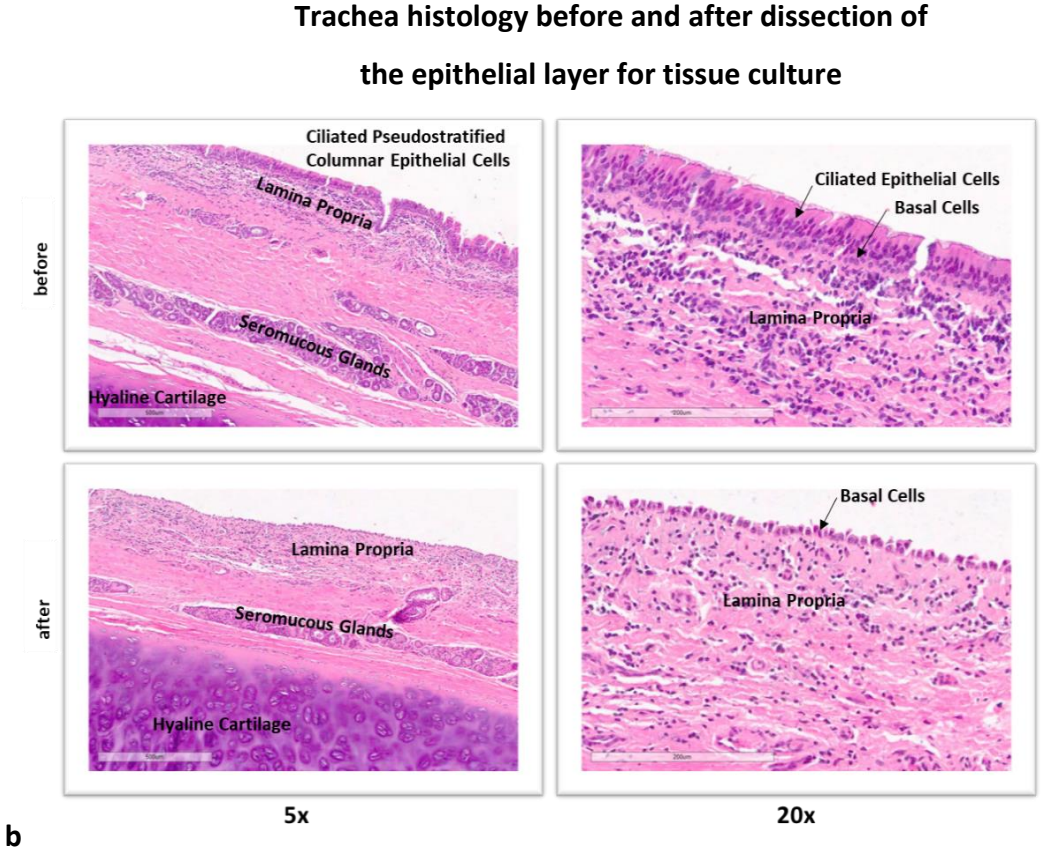

Figure 3.4 Bovine trachea before and after dissection of epithelial layer for tissue culture
Prior to and following dissection of the trachea, cross sections were collected, formalin fixed, and paraffin embedded, before being sectioned into 4 µm sections using a microtome. Sections were then mounted onto glass slides, de-paraffinized and stained with haematoxylin and eosin before being imaged under an Olympus BX51 upright microscope. (a) Histological image of bovine trachea. (b) Representative histological image of bovine trachea before and after dissection of epithelial layer for tissue culture.

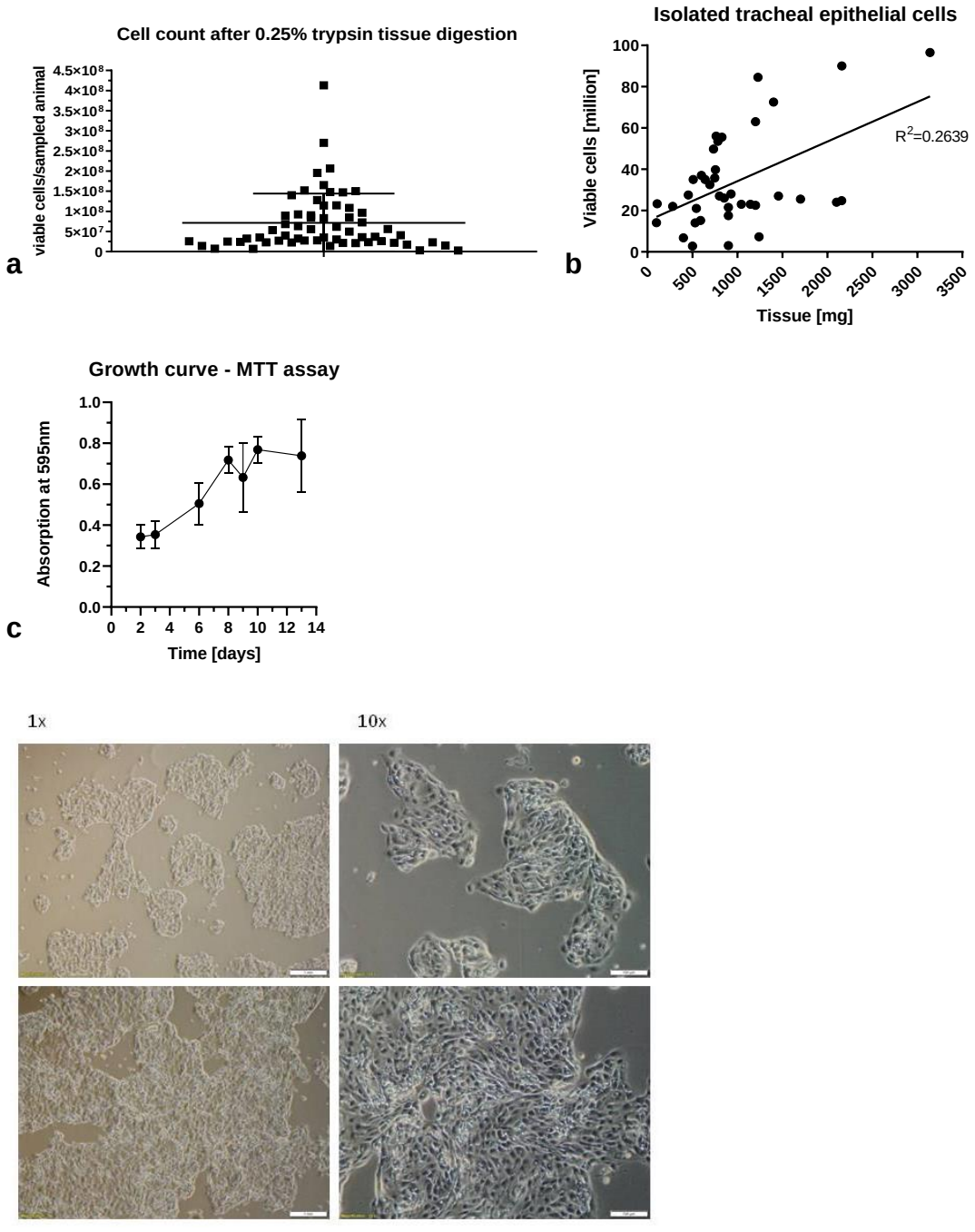

Figure 3.5 Cell yields and proliferation in culture of tracheal epithelial cells following isolation
(a) Average cell yield isolated from tissue was 42.6 x 10^6 ± 55.3 x 10^6, n=60. (b) Isolated epithelial cells per mg digested tissue, n=38. (c) Growth curve showing the increase in cell populations over 10 to 13 days. The cell proliferation was measured via MTT assay. 1 x 10^4 cells were seeded in each well of a 96 well plate. At each time point 20 µl of 6 mM Thiazolyl Blue was added to 100 µl growth media and incubated for 4 h. Following incubation, the media was aspirated and 150 µl Dimethyl sulfoxide (DMSO) added. The plate was photometrical measured at 595 nm, n=3-6 for each time point. (d) Representative images of pure bovine tracheal epithelial cells showing characteristic morphology after 5 days of culture. Following the cell isolation protocol, cells were seeded in 6 well tissue culture plates. Images were taken using an Olympus IX81 inverted microscope.

Purity of the epithelial cell populations was demonstrated by the expression of cell specific cytoskeleton proteins. Epithelial cells are known to express cytokeratin while stromal cells are known to express vimentin. Therefore, vimentin expression could be used to identify pure populations of tracheal epithelial cells. In **Fig. 3.6 a** representative cell cultures with high or low vimentin expression are shown after an immunohistochemistry staining for cytokeratin and vimentin. Cell cultures with high vimentin expression showed two cell populations, one staining positive for cytokeratin and the other for vimentin, indicating a contamination with stromal cells.

Beside isolated epithelial cell cultures, whole pieces of tracheal tissue of mucosa, submucosa and smooth muscle cells were grown as organ cultures. Tracheal organ cultures showed a 10 times higher *VIM* (vimentin) abundance compared to isolated epithelial cells (**Fig. 3.6 b**). A relative *VIM* mRNA abundance < 0.02 were considered as pure tracheal epithelial cell cultures and used for further experiments.

As we aim to use our primary culture model to investigate the innate immune response of the cells, the cell cultures were checked for immune cell contamination. A PCR for *PTPRC*, the gene encoding for CD45, a marker of immune cells, was conducted. PBMC cDNA was included as a positive control. The housekeeping gene *H3F3A* was included to ensure cDNA quality was adequate. As sown in **Fig. 3.7** five out of seven cultures were negative for the presence of *PTPRC* indicating an abscence of immune cell contamination. Two cultures were positive for *PTPRC*. Through optimisation of cell isolation and cell culture less time, approximately 6-8 days instead of previously 10-20 days, was needed to reach confluency of cells. This resulted in less media changes and the possibility of blood cell contamination. For cell cultures used in this thesis more washing steps were included during the cell culture period to remove any immune cells.

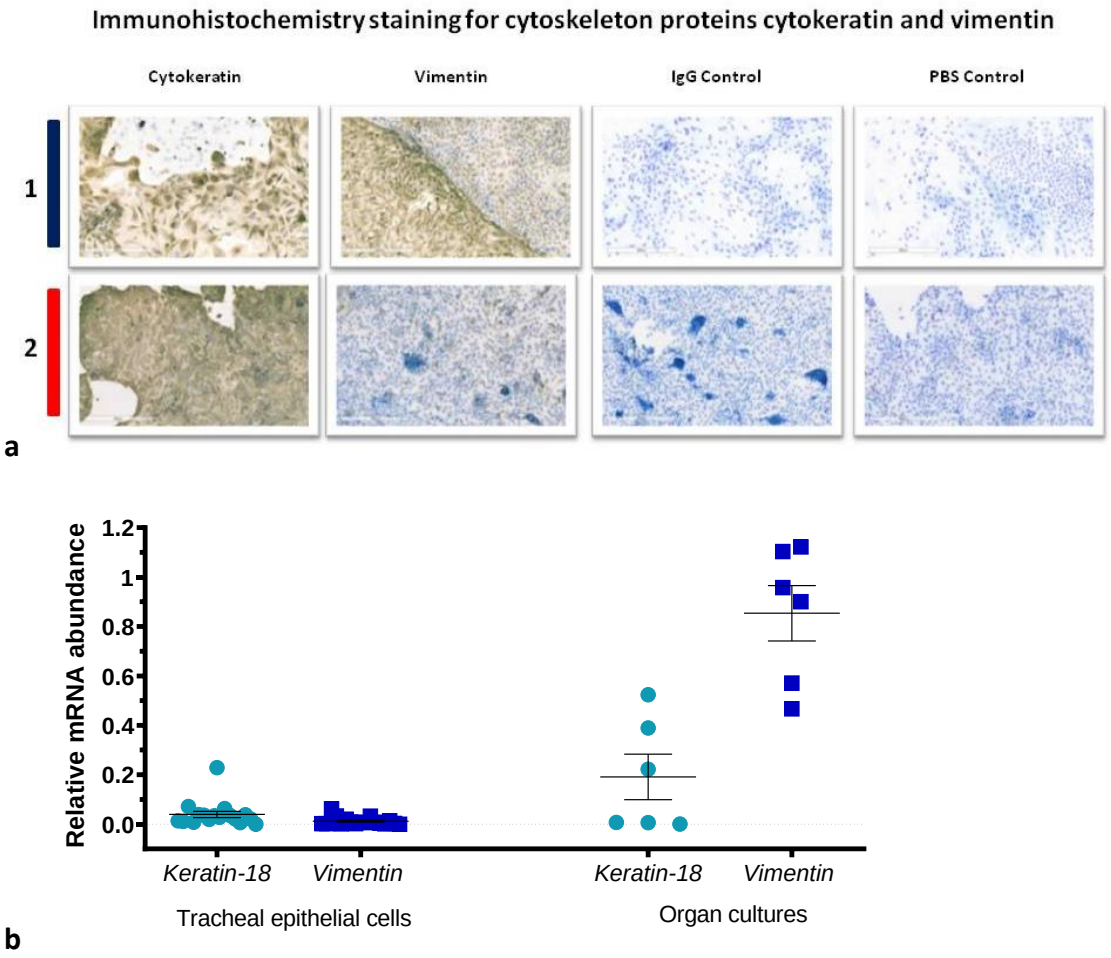

Figure 3.6 Keratin and vimentin expression in primary bovine tracheal epithelial cell populations and in tracheal organ cultures

(a) Tracheal cell populations can be identified based on their differential expression of cytoskeletal proteins by immunocytochemistry. 1 – Mixed epithelial and stromal cells; 2 – epithelial cells. Cells were seeded into wells of the Millicell EZ SLIDE 4 well glass culture slides and allowed to grow up to confluency. Cells were then fixed in ice cold methanol before blocking in 3% H_2O_2 for 20 mins followed by blocking in 10% BSA for 1 hour. Cells were incubated overnight with antibodies against human cytokeratin and vimentin cytoskeleton proteins. Cells were then washed in PBS before incubation with the secondary antibody for 30 mins followed by incubation with the chromogen DAB for 10 mins. Slides were mounted using Surgipath mounting medium before being examined using an Olympus BX51 upright microscope. (b) Relative KRT18 (keratin 18) and VIM (vimentin) mRNA gene expression in tracheal cell populations and tracheal organ cultures. Organ cultures were collected in RNAlater, homogenised and harvested into Trizol. Cells were harvested into Trizol following cell culture. RNA was extracted and first strand cDNA reverse transcribed. qPCR was carried out on KRT18 (keratin 18), a marker of epithelial cells and VIM (vimentin), a marker of stromal cells, gene Cq values were normalised to the reference gene H3F3A. Error bars indicate standard error of the mean.

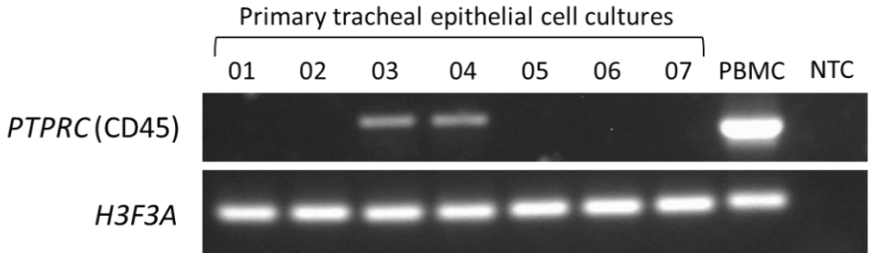

Figure 3.7 Gel electrophoresis of PTPRC and H3F3A PCR products amplified from cDNA made from tracheal epithelial cells after cell culture

Total RNA was extracted from tracheal epithelial cell cultures of seven animals and first stand cDNA reverse transcribed. PCR was carried out for PTPRC and H3F3A to detect leukocyte contamination. PBMC cDNA was used as a positive control for PTPRC amplification. Following PCR amplification, 1.5% agarose gel electrophoresis allowed confirmation of expected amplicon size.

3.4.2. Bovine herpesvirus 1 (BoHV-1) infects primary bovine tracheal epithelial cells and tracheal organ cultures *in-vitro* and results in cell death

In order to investigate the influence of BoHV-1 on bovine tracheal tissue, we developed a viral infection model using our established tracheal organ cultures and purified tracheal epithelial cultures. Purified live bovine herpes virus-1 was able to infect and replicate within both culture models. The infection of organ cultures with 10,000,000 PFU reached in the qPCR analysis a relative abundance of the viral genome of 1.41 after 24 hours and higher concentration of LDH in the supernatant compared to unstimulated organ cultures (**Fig. 3.8**). Within the primary tracheal epithelial cells, the relative abundance of the viral genome reached 0.16 after 6 hours and 216.14 after 24 hours with an infection of BoHV-1 MOI 70 (**Fig. 3.9 a**).

Measuring the cell metabolic activity via MTT assay revealed an activity of 86.88% after an infection with BoHV-1 MOI 70 at 25 hours and 56.20% at 48 hours compared to the uninfected control (**Fig. 3.9 b**). Bovine tracheal epithelial cells infected with live BoHV-1 MOI 7 showed microscopically visible signs of cytopathic effects after 48 hours seen in **Fig. 3.10**. Conventional agarose gel electrophoresis was used to characterise a potential DNA fragmentation, characteristic for the apoptosis progress. After 72, 96 hours and 7 days genomic DNA isolated from BoHV-1 infected cells showed unresolved HMW DNA, whereas unfragmented DNA was present in uninfected cells at all tested time points (**Fig. 3.11**). The apoptosis genes *BCL2*, *BAX* and *FAS* were downregulated at 24 hours in BoHV-1 infected tracheal epithelial cells (**Fig. 3.12**).

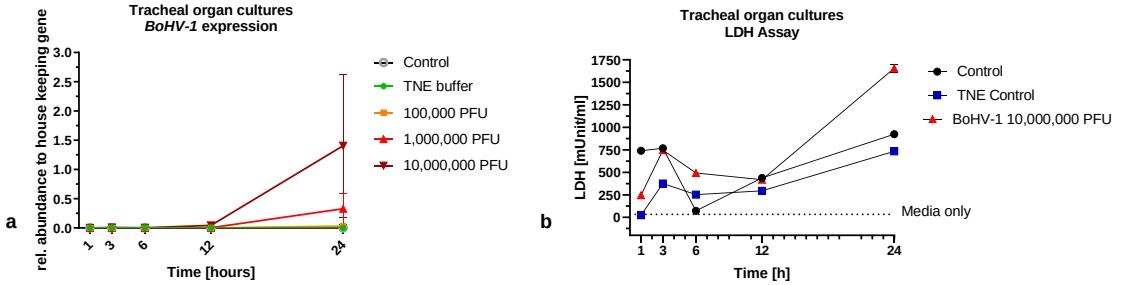

Figure 3.8 Bovine herpesvirus 1 infects tracheal organ cultures in-vitro

(a) BoHV-1 expression relative to the reference gene in infected bovine tracheal organ cultures. Cultures were infected with purified live BoHV-1 and homogenised and harvested into Trizol. RNA was extracted and first strand cDNA reverse transcribed. qPCR was carried out and gene Cq values were normalised to the reference gene H3F3A; n=3. (b) LDH assay of BoHV-1 infected bovine tracheal organ cultures. Each data point represents a different animal. Error bars indicate standard error of the mean; n=1.

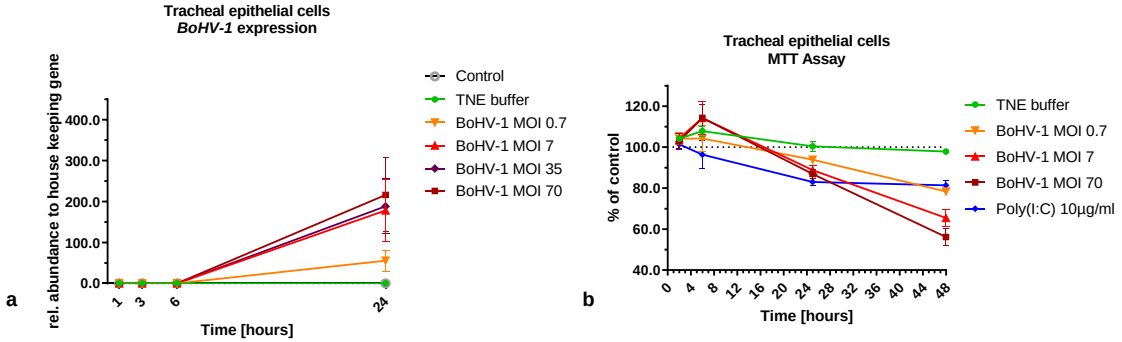

Figure 3.9 Bovine herpesvirus 1 infects primary bovine tracheal epithelial cells in-vitro

(a) BoHV-1 expression relative to the reference gene in infected bovine epithelial cells. Cells were infected with purified live BoHV-1 and harvested into Trizol. RNA was extracted and first strand cDNA reverse transcribed. qPCR was carried out and gene Cq values were normalised to the reference gene H3F3A. (b) MTT assay of BoHV-1 infected bovine tracheal epithelial cells. Each data point represents a different animal. Error bars indicate standard error of the mean; n=4.

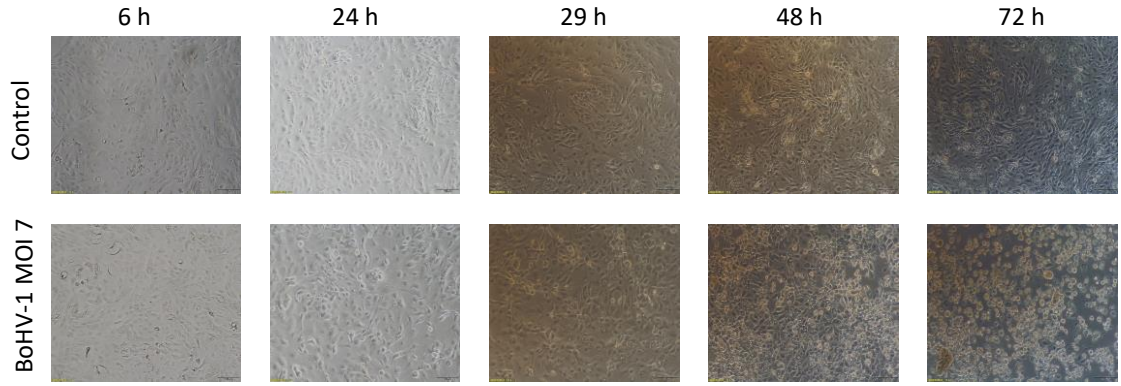

Figure 3.10 Bovine herpesvirus 1 infection causes morphological changes in primary bovine tracheal epithelial cells in-vitro

Representative images of bovine tracheal epithelial cells infected with live BoHV-1 showing signs of the cytopathic effect. Primary bovine epithelial cells were seeded in 12 well tissue culture plates and infected with purified live BoHV-1. Images were taken using an Olympus IX81 inverted microscope.

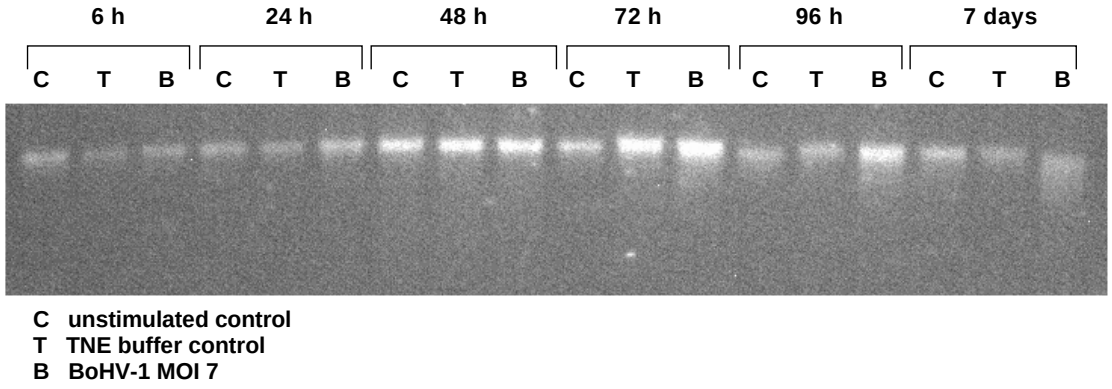

Figure 3.11 Gel electrophoresis of genomic DNA extracted from primary bovine tracheal epithelial cell infected with live bovine herpesvirus 1 in-vitro

Representative image of genomic DNA agarose gel electrophoresis of bovine tracheal epithelial cells infected with live BoHV-1. Primary bovine epithelial cells were seeded in 12 well tissue culture plates and infected with purified live BoHV-1. DNA was extracted with the Invitrogen Pure Link™ Genomic DNA Mini kit and DNA quality was evaluated by 1.5% agarose gel electrophoresis with SYBR™ Safe DNA Gel staining.

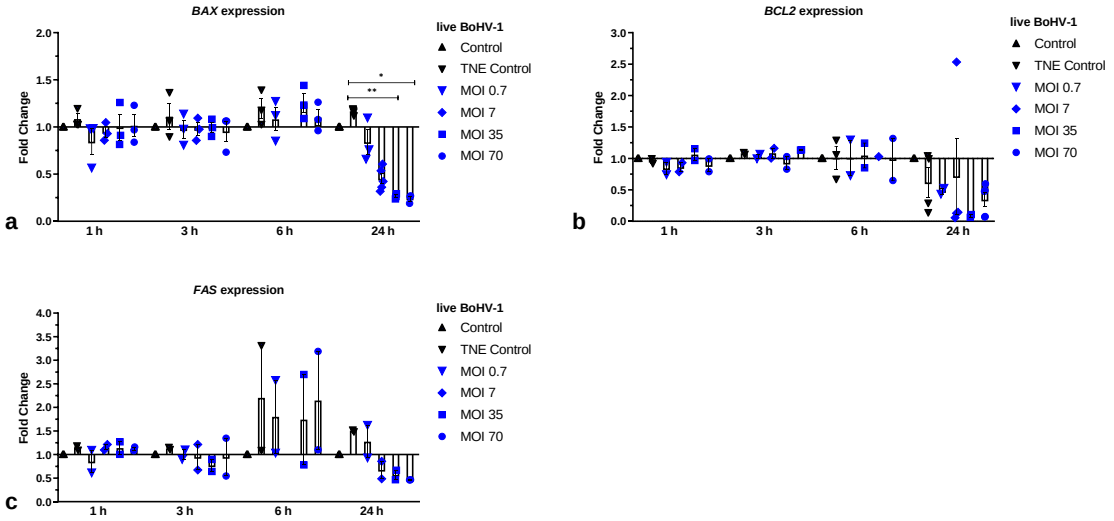

Figure 3.12 Expression of apoptosis genes in primary tracheal epithelial cells infected with purified live bovine herpes virus 1

*Confluent tracheal epithelial cells were infected with purified live bovine herpes virus 1 for 1, 3, 6 or 24 hours. Cells were harvested into Trizol. RNA was extracted and first strand cDNA reverse transcribed. qPCR was carried out and gene Cq values were normalised to the reference gene H3F3A and values normalised to the untreated control. Each data point represents a different animal. Error bars indicate standard error of the mean. Statistical analysis was performed on the ΔCt values using the mixed-effects model with the Geisser-Greenhouse correction followed by Sidak's multiple comparisons test. Asterisks indicate statistically significant differences relative to the untreated control and the TNE buffer control: *= adjusted p<0.05; **= adjusted p<0.01.*

3.4.3. Next generation sequencing analysis reveals 9 significantly differentially expressed genes in primary tracheal epithelial cells infected with BoHV-1

After having shown that BoHV-1 is able to infect primary tracheal epithelial cells, we were interested in the transcriptomic changes early after infection. Epithelial cells infected with purified live BoHV-1 MOI 7 6 hours were sent for next generation sequencing analysis. The four animals used were three male and one female, Simmental, Hereford and Friesian Cross with an age ranging from 33 to 104 months. Tissue samples were directly collected in RNAlater and tested negative for BoHV-1 and BHV-4 by the Virology Division, DAFM Laboratories Backweston, Dept. of Agriculture, Food and Marine, Celbridge, Co. Kildare, Ireland (**Tab. 3.1**).

Table 3.1 Animals used for next generation sequencing experiment

Animal	Sex	Breed	D.o.B	Age in months	BoHV-1 and BoHV-4 test
4520	♀	Simmertal Cross	05.06.11	104	neg
4620	♂	Friesian Cross	14.03.17	35	neg
4720	♂	Hereford Cross	18.04.17	34	neg
4820	♂	Friesian Cross	12.05.17	33	neg

The principial component analysis (PCA) (**Fig. 3.13**) showed animals clustered together and the infection with BoHV-1 did not result in a separation between uninfected and infected samples.

Differently expressed gene analysis with the program Limma voom in Rstudio with the criteria of > 10 counts/gene in > 2 samples resulted in 9488 genes with 0 significantly differently expressed with adj. P value < 0.05. In **Tab. 3.2** are shown the top 10 genes sorted by p-value. Differently expressed gene analysis with the program Deseq2 in Rstudio with the criteria of > 10 counts/gene in > 2 samples resulted in 17961 genes with 9 significantly differently expressed with adj. P value < 0.05 (**Tab 3.3**). The heat shock protein family A (Hsp70) member 6 gene *HSPA6* was with a fold change of 15.96 the most upregulated gene. A pathway enrichment analysis could not be conducted due to the small number of differentially expressed genes.

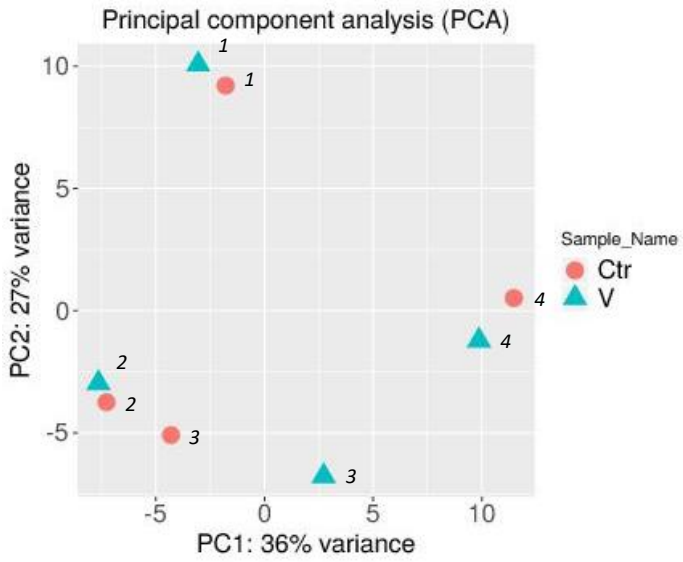

Figure 3.13 Principal component analysis (PCA)

PCA plot obtained with the program iDEP (integrated Differential Expression and Pathway analysis) in Rstudio using the first and second principal components. Primary tracheal epithelial cells infected with purified live BoHV-1 MOI 7 for 6 hours, four animals (1-4) unstimulated control (Ctr) and virally infected (V).

Table 3.2 DEG analysis with Limma voom of primary tracheal epithelial cells infected with BoHV-1

top 10 genes sorted by p-value, 0 significantly differently expressed genes with adj. p-value < 0.05

Gene symbol	Gene name	Log2 FC	FC	P-value	Adj. p-value
HSPA6	Heat shock protein family A (Hsp70) member 6	3.92	15.14	2.30E-05	0.22
EGR1	Early growth response 1	1.93	3.81	7.70E-05	0.37
MYLIP	Myosin regulatory light chain interacting protein	0.83	1.78	2.40E-04	0.76
PTHR	Parathyroid hormone-related protein	-0.38	0.77	7.80E-04	1
ID2	DNA-binding protein inhibitor ID-2	0.5	1.41	1.10E-02	1
CCNL1	Cyclin-L1	0.3	1.23	1.40E-02	1
TACC3	TACC3 protein	-0.43	0.74	2.20E-02	1
EPG5	Ectopic P-granules autophagy	0.24	1.18	2.40E-02	1
KIFC1	Kinesin-like protein	-0.3	0.81	2.60E-02	1
LOC112443783	Uncharacterized protein	0.28	1.21	2.60E-02	1

Table 3.3 DEG analysis with Deseq2 of primary tracheal epithelial cells infected with BoHV-1
9 significantly differently expressed genes with adj. p-value < 0.05

Gene symbol	Gene name	Log2 FC	FC	P-value	Adj. p-value
HSPA6	heat shock protein family A (Hsp70) member 6	4.00	15.96	1.45E-49	2.59E-45
SNAI1	snail family trans-criptional repressor 1	3.07	8.38	1.66E-07	0.000496293
HBA	hemoglobin, alpha 2	2.37	5.16	5.10E-06	0.011405684
ARC	activity regulated cytoskeleton associated protein	2.28	4.84	4.87E-08	0.000174311
EGR1	early growth response 1	1.93	3.82	3.02E-13	2.70E-09
EGR3	early growth response 3	1.90	3.73	5.88E-06	0.011707798
GADD45G	growth arrest and DNA damage-inducible protein GADD45 gamma	1.75	3.36	1.00E-09	5.97E-06
MYLIP	myosin regulatory light chain interacting protein	0.83	1.78	1.62E-08	7.25E-05
PTHR	parathyroid hormone-related protein	-0.39	0.77	3.04E-06	0.007786541

From the 9 differential expressed genes, we validated the genes *HSPA6* and *EGR1* via PCR analysis. *HSPA6* was significantly upregulated in tracheal epithelial cells infected with BoHV-1 for 24 hours, whereas in tracheal organ cultures no differential expression could be detected. In both culture models the viral dsRNA viral analogue Poly(I:C) did not induce *HSPA6* expression (**Fig. 3.14**).

EGR1 was significantly upregulated in tracheal epithelial cells stimulated with Poly(I:C) and infected with BoHV-1 after 6 hours (**Fig. 3.15**).

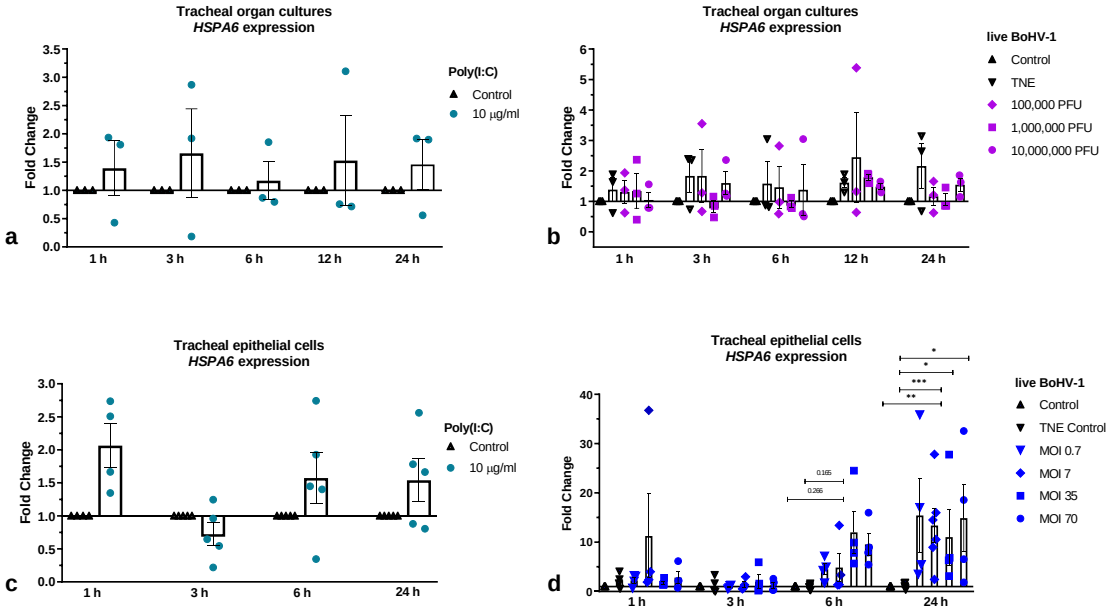

Figure 3.14 Expression of HSPA6 gene in bovine tracheal organ cultures and tracheal epithelial cells stimulated with Poly(I:C) or infected with live BoHV-1

Bovine tracheal organ cultures and confluent tracheal epithelial cells were stimulated for 1, 3, 6, 12 or 24 hours with 10 µg/ml Poly(I:C) or infected with purified live BoHV-1. Organ cultures were collected in RNAlater and homogenised and harvested into Trizol. Cells were directly harvested into Trizol. RNA was extracted and first strand cDNA reverse transcribed. qPCR was carried out and gene Cq values were normalised to the reference gene H3F3A and values normalised to the untreated control. Each data point represents a different animal. Error bars indicate standard error of the mean. Statistical analysis was performed on the ΔCt values using a mixed-effects model with the Geisser-Greenhouse correction followed by Sidak's multiple comparisons test. Asterisks indicate statistically significant differences relative to the untreated control:= adjusted p<0.05; **= adjusted p<0.01; ***=adjusted p<0.001.*

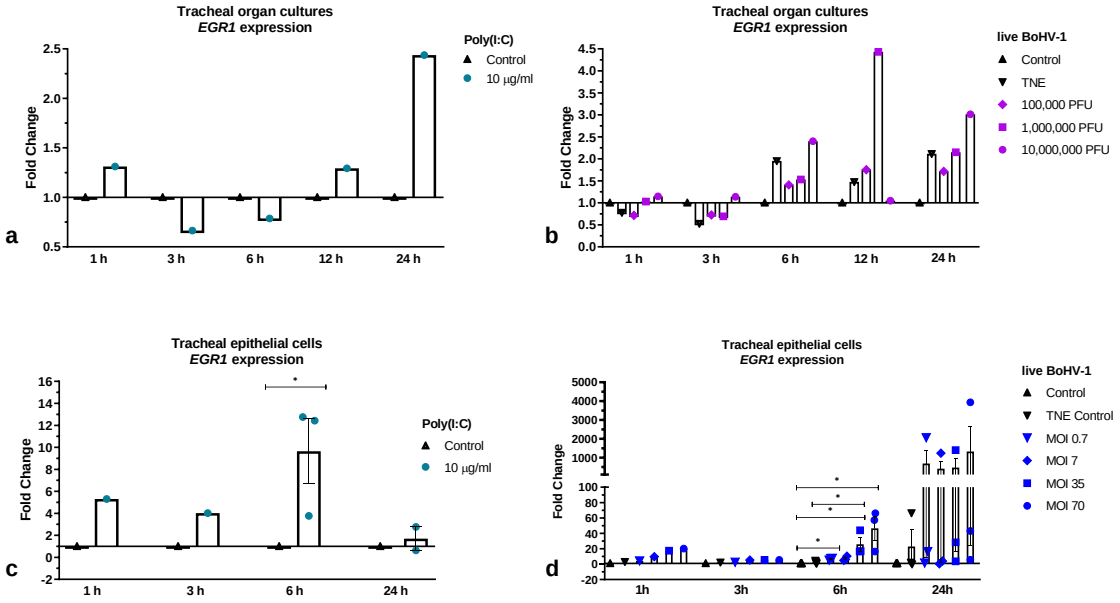

Figure 3.15 Expression of EGR1 gene in bovine tracheal organ cultures and tracheal epithelial cells stimulated with Poly(I:C) or infected with live BoHV-1

*Bovine tracheal organ cultures and confluent tracheal epithelial cells were stimulated for 1, 3, 6, 12 or 24 hours with 10 µg/ml Poly(I:C) or infected with purified live BoHV-1. Organ cultures were collected in RNAlater and homogenised and harvested into Trizol. Cells were directly harvested into Trizol. RNA was extracted and first strand cDNA reverse transcribed. qPCR was carried out and gene Cq values were normalised to the reference gene H3F3A and values normalised to the untreated control. Each data point represents a different animal. Error bars indicate standard error of the mean. Statistical analysis was performed on the ΔCt values using a mixed-effects model with the Geisser-Greenhouse correction followed by Sidak's multiple comparisons test. Asterisks indicate statistically significant differences relative to the untreated control: *= adjusted p<0.05.*

We found *HSPA6* to be significantly upregulated in tracheal epithelial cells treated with the transfection reagent Lipofectamine, containing lipid subunits forming liposomes in an aqueous environment. The positively charged surface and a neutral co-lipid of the liposomes facilitate the fusion and entry through the negatively charged cell membrane (Dalby et al., 2004). Following a Lipofectamine treatment for 48 hours *HSPA6* was significantly upregulated with a fold change of 12. There were no transcriptomic changes for the tested proteins involved in the unfolded protein response (**Fig. 3.16**).

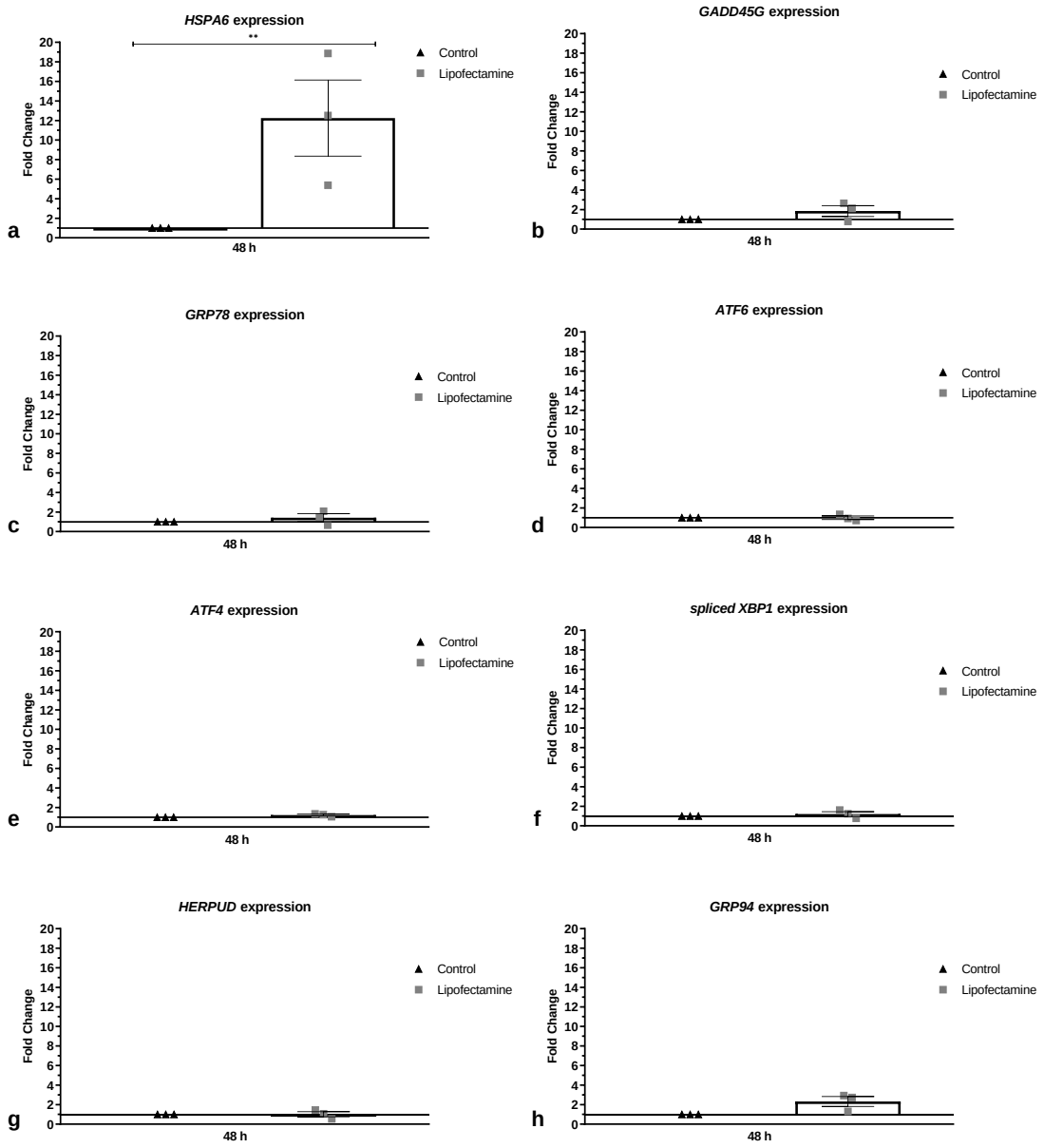

Figure 3.16 HSPA6 gene expression is upregulated in primary bovine tracheal epithelial cells in response to Lipofectamine

*HSPA6, GADD45G, GRP78, ATF6, ATF4, spliced XBP1, HERPUD and GRP94 mRNA expression levels in primary bovine tracheal epithelial cells were examined by qPCR following treatment with Lipofectamine for 48 hours. Cells were harvested into Trizol, RNA extracted and first strand cDNA reverse transcribed. Gene Cq values were normalised to the reference gene H3F3A and values normalised to the untreated control. Error bars indicate standard error of the mean. Statistical analysis was performed on the ΔCt values using a paired t test. Asterisks indicate statistically significant differences relative to the untreated control: *= adjusted p<0.05; **= adjusted p<0.01.*

3.4.4. BoHV-1 infection downregulates UPR genes in primary tracheal epithelial cells

Since we found the heat shock protein HSPA6 being significantly upregulated in epithelial cells infected with BoHV-1, we wanted to examine other heat shock proteins involved in stress responses occurring during viral infections. Looking at the transcriptomic changes of proteins involved in the unfolded protein response, we found BoHV-1 infection caused a downregulation of *GRP78/HSPA5*, *ATF6*, *ATF4*, *DDIT3*, *spliced XBP1*, *HERPUD1* and *GRP94/HSP90B1* in bovine tracheal epithelial cells. *ATF6* was significantly downregulated with a fold change of 0.56, *spliced XBP1* with 0.63 and *DDIT3* with a fold change 0.28 after an infection with BoHV-1 MOI 7 for 24 hours. The stimulation with Poly(I:C) with a concentration of 10 µg/ml had no influence on the gene expression of the tested genes (**Fig. 3.17**).

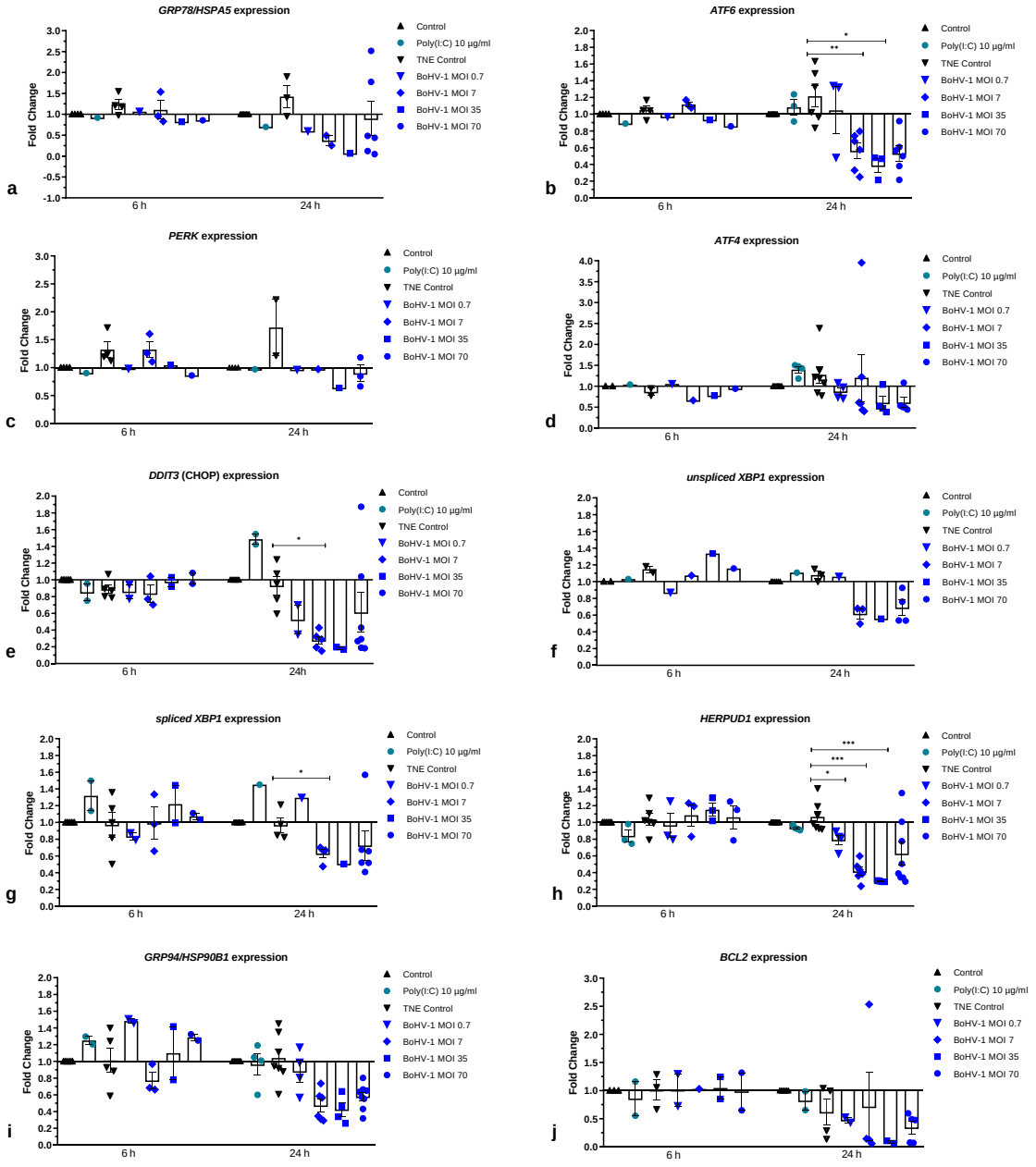

Figure 3.17 BoHV-1 infection downregulates genes involved in the unfolded protein response (UPR) in bovine tracheal epithelial cells

*Confluent tracheal epithelial cells were stimulated with Poly(I:C) 10 µg/ml or infected with purified live bovine herpes virus for 6 or 24 hours. Cells were harvested into Trizol. RNA was extracted and first strand cDNA reverse transcribed. qPCR was carried out and gene Cq values were normalised to the reference gene H3F3A and values normalised to the untreated control. Each data point represents a different animal. Error bars indicate standard error of the mean. Statistical analysis was performed on the ΔCt values using the mixed-effects model with the Geisser-Greenhouse correction followed by Sidak's multiple comparisons test. Asterisks indicate statistically significant differences relative to the untreated control and the TNE buffer control: *= adjusted p<0.05; **= adjusted p<0.01; ***=adjusted p<0.001.*

3.4.5. Thapsigargin partly counteracts the downregulation of UPR genes in BoHV-1 infected primary bovine tracheal epithelial cells

We used Thapsigargin (Tg), a guaianolide, extracted from the plant *Thapsia garganica*, to induce ER stress. Tg inhibits the ubiquitous ER Ca^{2+}-ATPase, resulting in raising cytosolic calcium concentrations. The depletion of ER calcium stores leads to ER stress activating the UPR (Sehgal et al., 2017). The used concentration of 1 µM for 24 hours did not influence the cell viability of primary tracheal epithelial cells, assessed by the CellTiter-Blue Cell Viability Assay (**Fig. 3.18**).

The treatment with 1 µM Tg alone upregulated *GRP78*, *PERK*, *DDIT3*, *spliced XBP1* and *HERPUD1* at 6 hours and *GRP94* at 6 and 24 hours. *Spliced XBP1* was significantly upregulated with a fold change of 8, *HERPUD1* with a fold change of 9 (**Fig. 3.19**).

A 2-hour pre-treatment with 1 µM Tg before BVH-1 MOI 7 infection for 24 hours let partly to a compensation of the downregulation of UPR related genes caused by the virus infection. *GRP78*, *spliced XBP1*, *HERPUD1* and *GRP94* were downregulated in response to DMSO control pre-treatment before BoHV-1 infection compared to an upregulation after pre-treatment with Tg prior to BoHV-1 infection. *GRP78* and *spliced XBP1* were rarely regulated after an infection with BoHV-1 after 24 hours pre-treated with DMSO control and significantly upregulated with a pre-treatment of Tg with a fold chance of 4 and 5 respectively. The DMSO control pre-treatment let to a downregulation of 0.58 fold compared to an upregulation of HERPUD1 of 2 fold after pre-treatment with Tg. *GRP94* was significantly upregulated with Tg treatment alone after 24 hours with a fold change of 10. BoHV-1 infection, pre-treated with control DMSO, resulted in a downregulation with a fold change of 0.79 of *GRP94*, whereas Tg pre-treatment before BoHV-1 infection let to a significantly different gene expression compared to Tg alone or DMSO pre-treatment with an upregulation with 18 fold (**Fig. 3.19**).

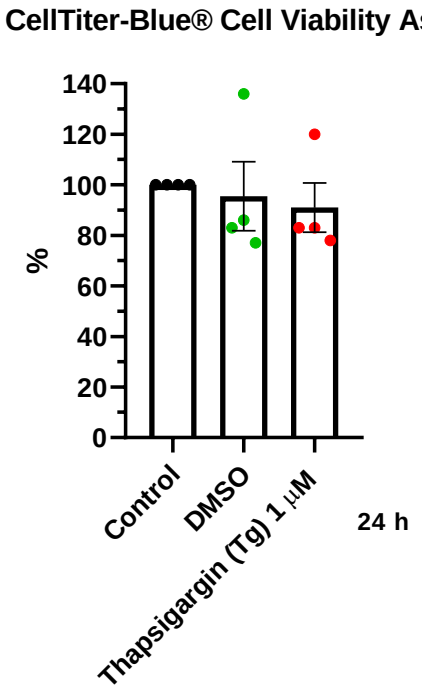

Figure 3.18 Thapsigargin does not influence the cell viability of primary bovine tracheal epithelial cells

CellTiter-Blue® Cell Viability assay of bovine tracheal epithelial cells treated with Thapsigargin 1 µM for 24 hours. Each data point represents a different animal. Error bars indicate standard error of the mean; n=4.

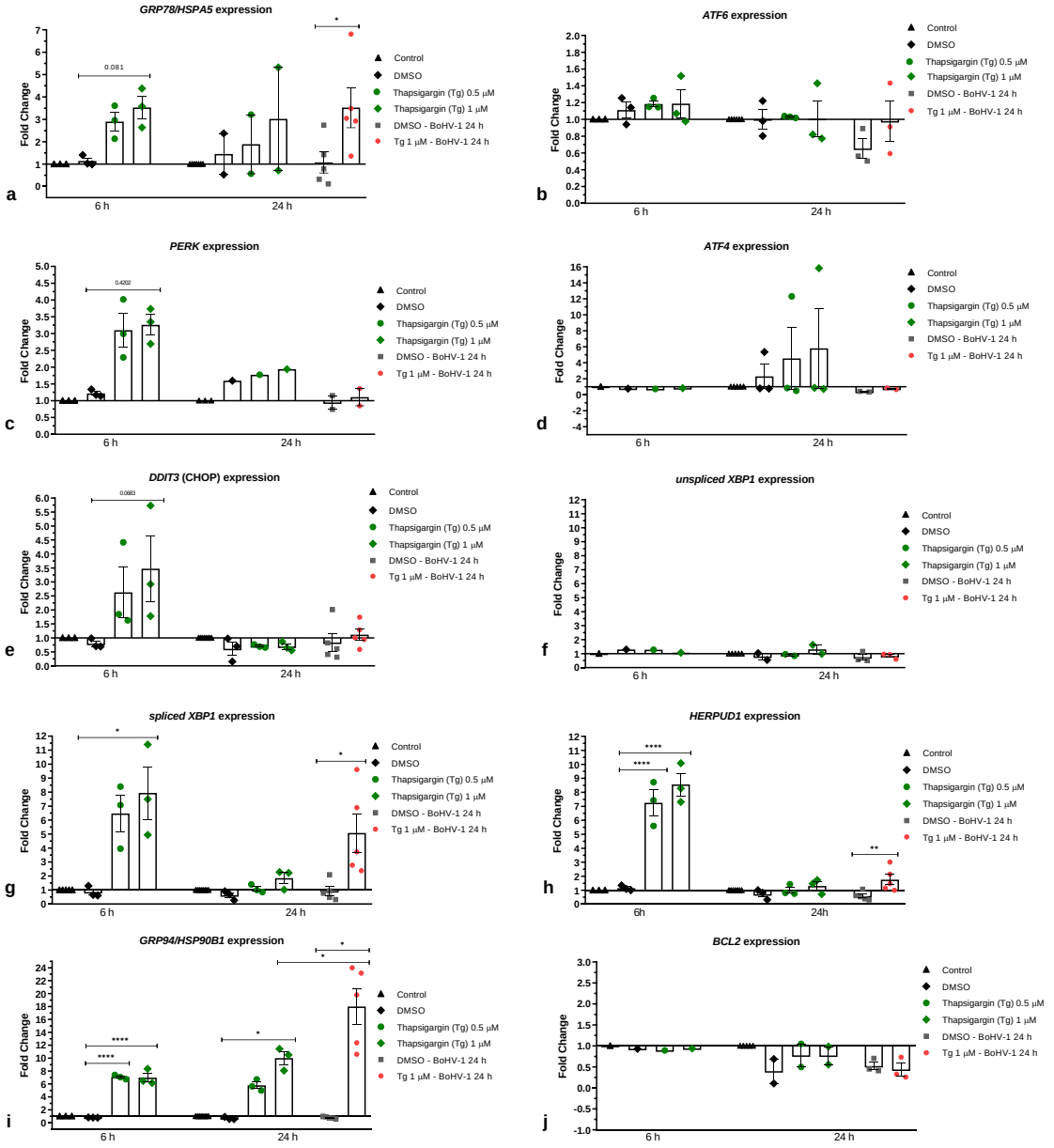

Figure 3.19 Thapsigargin partly counteracts the downregulation of UPR genes in BoHV-1 infected primary bovine tracheal epithelial cells

*Bovine tracheal epithelial cells were stimulated for 6 or 24 hours with 0.5 µM or 1 µM Tg or pre-treated 2 hours with Tg prior to infection with purified live BoHV-1 MOI 70 for 24 hours. Cells were harvested into Trizol, RNA was extracted and first strand cDNA reverse transcribed. qPCR was carried out and gene Cq values were normalised to the reference gene H3F3A and values normalised to the untreated control. Each data point represents a different animal. Error bars indicate standard error of the mean. Statistical analysis was performed on the ΔCt values using a Friedman test followed by a Dunn's multiple comparisons test. Asterisks indicate statistically significant differences relative to the untreated control: *= adjusted p<0.05; **= adjusted p<0.01; ***=adjusted p<0.001; ****=adjusted p<0.0001.*

We have shown that Thapsigargin treatment upregulated gene expression of heat shock proteins part of the UPR. Next, we examined the influence of Tg on the gene expression of the heat shock protein HSPA6, EGR1 and GADD45G. Genes, which were significantly upregulated in the next generation sequencing analysis of tracheal epithelial cells infected with BoHV-1 (**Tab. 3.3**). Whereas Poly(I:C) and Tg stimulation alone did not influence the gene expression of these genes. A pre-treatment with Tg before BoHV-1 infection did not significantly influence the upregulation of *EGR1* and *GADD45G*. However, *HSPA6* was upregulated with a fold change of 65 in response to DMSO control pre-treatment before BoHV-1 infection compared to 117 in cells pre-treated with Tg before BoHV-1 infection (p=0.0625, Wilcoxon test) (**Fig. 3.20**).

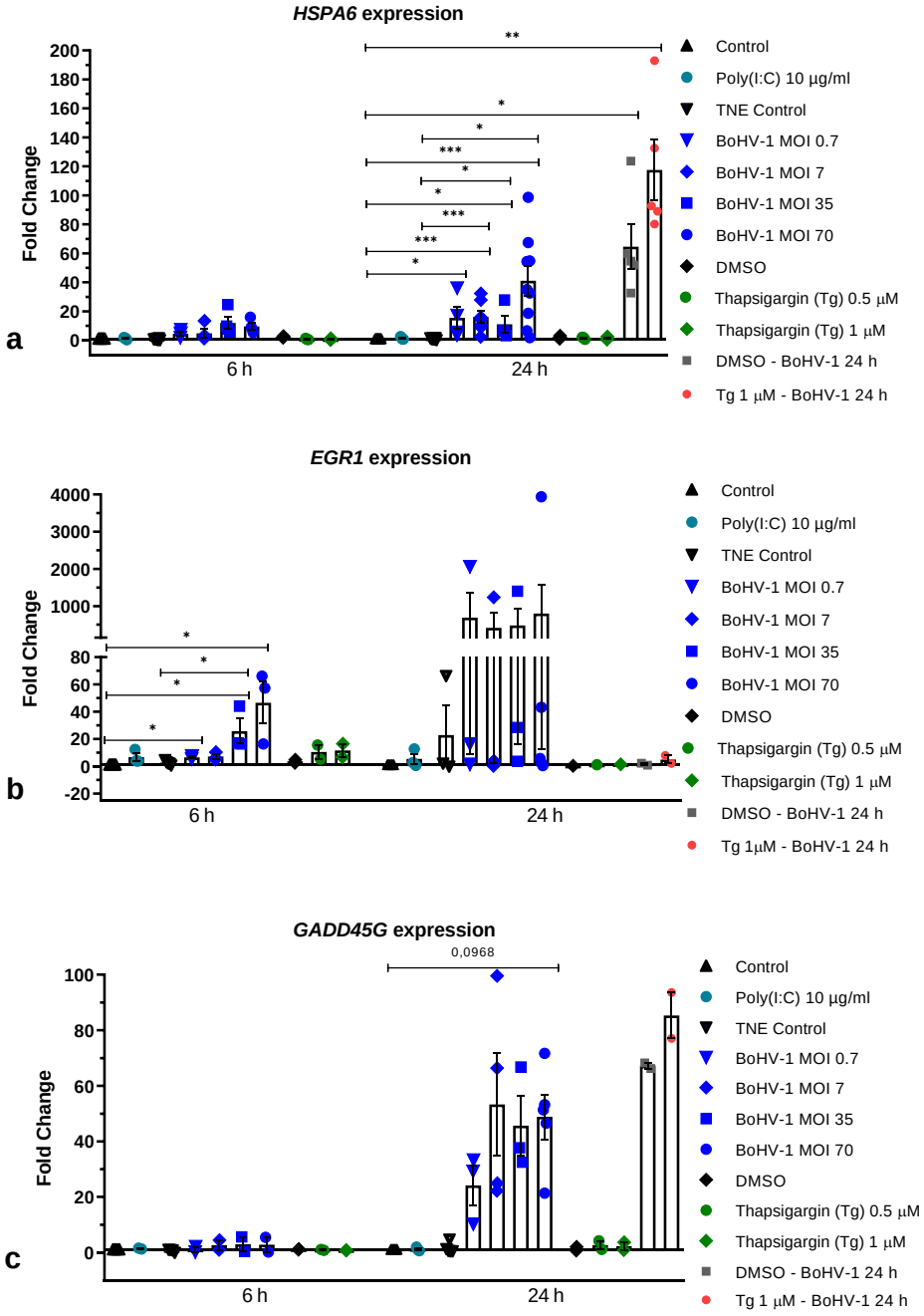

Figure 3.20 HSPA6, EGR1 and GADD45G expression in bovine tracheal epithelial cells stimulated with Thapsigargin (Tg), Poly(I:C) or infected with live BoHV-1

*Bovine tracheal epithelial cells were stimulated for 6 or 24 hours with 0.5 µM or 1 µM Tg, 10 µg/ml Poly(I:C) or infected with purified live BoHV-1. Cells were harvested into Trizol, RNA was extracted and first strand cDNA reverse transcribed. qPCR was carried out and gene Cq values were normalised to the reference gene H3F3A and values normalised to the untreated control. Each data point represents a different animal. Error bars indicate standard error of the mean. Statistical analysis was performed on the ΔCt values using a mixed-effects model with the Geisser-Greenhouse correction followed by Sidak's multiple comparisons test. Asterisks indicate statistically significant differences relative to the untreated control: *= adjusted p<0.05; **= adjusted p<0.01; ***=adjusted p<0.001.*

3.4.6. Thapsigargin inhibits the replication of BoHV-1 in primary tracheal epithelial cells

After having shown that in primary bovine epithelial cells gene expression of proteins involved in the UPR were downregulated in response to BoHV-1 infection and a Tg pre-treatment resulted partly in a cancellation of the downregulation, we assessed the viral genome presence of BoHV-1. A pre-treatment with Tg 1 µM significantly decreased the viral genome presence with a log2 fold change of -1.57 (adj. p-value = 0.0089) compared to BHV-infection alone. However, the downregulation was not significant compared to the DMSO control pre-treatment with a fold change of 0.88 (**Fig. 3.21**).

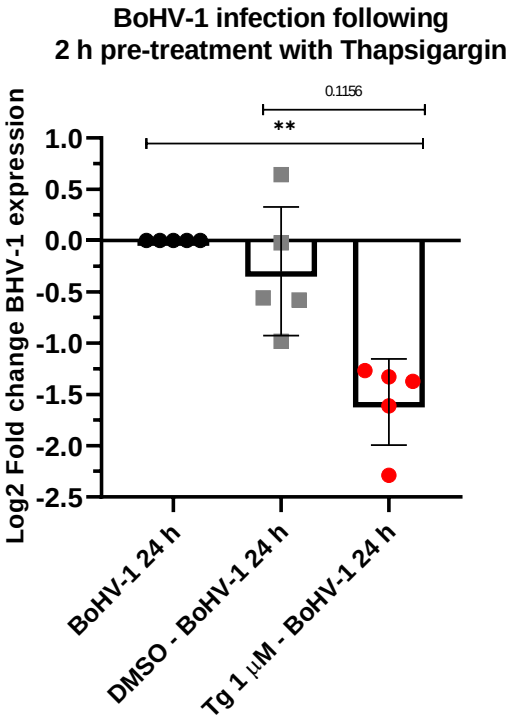

Figure 3.21 Thapsigargin treatment inhibits the replication of live bovine herpes virus 1 in primary tracheal epithelial cells

*Confluent primary bovine tracheal epithelial cells were treated with 1 µM Tg 2 hours prior infection with purified live bovine herpes virus 1. Cells were harvested into Trizol. RNA was extracted and first strand cDNA reverse transcribed. qPCR for BoHV-1 expression was carried out and gene Cq values were normalised to the reference gene H3F3A. Values were normalised to the BoHV-1 infected control. Each data point represents a different animal. Error bars indicate standard error of the mean. Statistical analysis was performed on the 2^-ΔCT values using the Friedman test followed by the Dunn's multiple comparison test, n=5. Asterisks indicate statistically significant differences relative to the BoHV-1 infected control: **= adjusted p<0.01.*

3.5. Discussion

Our established cell culture model of primary bovine tracheal epithelial cells enables us to investigate the role of epithelial cells in the innate immune defence in a physiological relevant context. Our results demonstrate that respiratory epithelial cells play an important role in the innate immune defence against viral infections. We found an interaction between the unfolded protein response (UPR) in epithelial cells and bovine herpesvirus-1 infection, which provides a potential antiviral target option. Genes involved in the UPR were downregulated in response to BoHV-1 infection, while pre-treatment with Thapsigargin was able to counteract the BoHV-1 mediated downregulation of *sXBP1*, *HERPUD1* and *GRP94*. Interestingly, quantifying the viral genome presence via qPCR of BoHV-1 showed that pre-treatment with Tg had a protective antiviral activity against BoHV-1 infection.

The recent outbreak of SARS-CoV-2 (severe acute respiratory syndrome coronavirus 2) in 2020 highlighted the important role of the respiratory epithelium in respiratory viral infections and emphasised the need of further research into this cell type (Bridges et al., 2022). Tracheal explants can provide the closest approach to model *in-vivo* conditions, allowing the crosstalk between epithelial cells and underlaying stromal cells. However, using explants for infection models are greatly restricted by their limited viability *in-vitro*. We have found that stimulation within 12 hours of collection showed the least cell death. In addition, achieving consistent cell composition and size in order to accomplish a reproducible experimental setup has been problematic. Based on these observations, we decided to focus on pure populations of tracheal epithelial cells for the examination of cell specific responses and signalling pathways operating within a distinct cell population. Models of primary airway epithelial cells have been previously developed for the use in human and bovine. Thus, bovine cells derived from abattoir material represent a more accessible alternative to human cells. In addition, bovine animal models are also used to study the pathogenesis of the human respiratory syncytial virus (RSV) as bovine and human viruses are closely related viruses and cause similar infections in cattle and humans (Bem et al., 2011; Taylor, 2017). Our model of primary respiratory epithelial cells provides realistic insight into early immune activity in response to viral exposure as they retain the physiology and genetic characteristics of

their cellular counterparts *in-vivo.* The isolated cell yield allowed reliable generation of confluent cell cultures for stimulation experiments. This model demonstrates significant inter-animal variation, indicating more physiological relevance than commonly used cell lines. The model is reproducible and easily available with low costs from abattoir by-products. The established cell culture model of primary bovine tracheal epithelial cells gives the basis for the investigation of the role of epithelial cells and their innate immune pathways for respiratory diseases in cattle.

We found BoHV-1 to be infecting and replicating in tracheal organ cultures as well as tracheal epithelial cells using qPCR and observing a cytopathic effect. While PCR based assays are a sensitive, discriminative and rapid tool for epidemiological studies, further methods can be used to evaluate the viral infection in more detail in cell culture models. Direct visualation of viral antigen using immunohistochemistry or immunofluorescence would have allowed to determine the frequency of infected cells within the culture. A study in 2004 produced murine monoclonal antibodies against BoHV-1 and other related alphaherpesviruses which showed viral specificity using enzyme-linked immunosorbent assay and indirect immunofluorescence staining of virus infected cells (Keuser et al., 2004). The selected antibodies were found to be directed against glycoprotein C (gC) or gD showing that antibodies against virus antigens are suitable to allow discrimination of alphaherpesviruses. Beside direct visualisation of virus antigens, the expression of viral regulatory proteins, e.g. bICP0 and bICP27, can be used to determine infected cells. Confocal microscopy of bovine kidney cells infected with BoHV-1 showed bICP0 primarily localised in the nucleus of infected cells (Wang et al., 2014). In another study BoHV-1-GFP was used to determine the infection rate of epithelium (Keil, 2000; Kirchhoff et al., 2014). Future investigations are necessary to validate the infection rate in our cell culture model with the used BoHV-1 concentrations.

We used virus concentrations ranging from MOI 0.7 to 70 to investigate the effects in our cell culture model of primary bovine tracheal epithelial cells. In literature ALI cultures of bovine airway epithelial cells inoculated with BoHV-1-GFP with MOI 0.1 and MOI 1 showed no infected cell after 2 days and occasionally infected cells 5 days post infection. A MOI of 10 led to a few cells being infected on day 1 and appearance of

infected foci suggested the spread within the culture after 5 days (Kirchhoff et al., 2014). *In-vivo* aerosol challenge of calves with BoHV-1 (5 x 10^7 p.f.u./animal) led to visible focal staining of epithelial cells in tissue samples of nasal turbinates and trachea in 4 to 6 out of 6 animals 5 days post infection. Immunohistochemistry staining of nasal turbinate tissue confirmed infected foci within the mucosal epithelial layer (Osman et al., 2017).

After approximately 24 hours we observed a morphological cytopathic effect (CPE) in tracheal epithelial cell cultures infected with BoHV-1 with a concentration of MOI 7 and detached rounded cells after 48 hours. The term cytopathic effect summarises characteristic biochemical and morphological changes in virally infected cells. Dependent on cell type, virus type and concentration, the CPE can range from alteration of growth kinetics and metabolic activity up to cell death (Agol, 2012). The DNA fragmentation during apoptosis occurs in several stages, starting with the generation of high-molecular-weight DNA fragments, undetectable by conventional agarose gel electrophoresis, and the end-point of fragmentation, appearing as characteristic "DNA ladder" during agarose gel electrophoresis (Matassov et al., 2004). In our infection model genomic DNA isolated from BoHV-1 infected cells showed unresolved HMW DNA after 72, 96 hours and 7 days. Whereas, MDBK (Madin-Darby bovine kidney) cells, used for BoHV-1 virus propagation, agarose gel electrophoresis exhibited the characteristic laddering of degraded high-molecular-weight DNA at 48 hpi (Devireddy and Jones, 1999). As not all cell types undergoing apoptosis degrade their DNA to this extent, further methods detecting apoptosis are needed for our infection model.

HSPA6 was with a fold change of 15.96 the most upregulated gene in the next generation sequencing analysis of BoHV-1 infected primary bovine tracheal epithelial cells. The heat shock protein family A (Hsp70) member 6 gene (HSPA6, also known as Hsp70B') is a member of the highly conserved heat shock protein 70kDa (Hsp70) family with 14 other isoforms identified in the human (Radons, 2016). The HSPA70 family is known to protect cells against stress (Daugaard et al., 2007) and was found to be highly expressed in many tumours, promoting progression of malignancy partly due to inhibiting apoptosis (Albakova et al., 2020). HSP70s are also involved in different steps of the virus replication cycle. The different isoforms are associated with various functions, although there is a

high sequence homology (Radons, 2016). For example, HSPA1A (Hsp70-1), the major cytoplasmic stress-inducible Hsp70s, has a role in replication complex formation for hepatitis C virus (HCV) (Chen et al., 2010) and in DNA repair and tumour immune response (Duan et al., 2014). Whereas, HSPA9 (Hsp70-9) is expressed in mitochondria, not inducible by heat stress and is correlated with mitochondrial respiration (Radons, 2016). Both HSPA1 and HSPA6 share 85% sequence identity (Daugaard et al., 2007). However, compared to the widely studied HSPA1A and its functions in the viral life cycle (reviewed in (Santoro et al., 2010)), little is known about HSPA6. HSPA6 itself is stress-inducible (Ramirez et al., 2015) and has been reported to protect human neuronal cells from cellular stress (Deane and Brown, 2018) and to correlate with the malignant progression and immune microenvironment of gliomas (Zhou et al., 2022). Very little is known about its possible functions in the viral life cycle, a study found HSPA6 induced during enterovirus A71 infection in the RD cell line (human rhabdomyosarcoma) with positive regulatory effects (Su et al., 2021). Interestingly, we found *HSPA6* being upregulated in bovine tracheal epithelial cells after treatment with the transfection reagent Lipofectamine, which contains lipid subunits forming liposomes in an aqueous environment to facilitate the entry through the cell membrane. Whereas no heat shock proteins or other proteins involved in the unfolded protein response were differentially expressed. It has been suggested that heat shock can change the fluidity of membranes, which leads to a re-organisation of membrane lipids (Bromberg and Weiss, 2016). Considerable evidence was found that the HSR is induced in response to alterations to the plasma membrane and lipids modulate the transient receptor potential channels (reviewed in (Török et al., 2014)). Our results indicate that HSPA6 expression can be influenced by agents changing the lipid membrane constellation.

Our transcriptomic analysis of proteins involved in the unfolded protein response showed a downregulation in BoHV-1 infected bovine respiratory epithelial cells. On one hand, the viral accumulation of mis- and unfolded proteins in the ER during viral replication can trigger the UPR. On the other hand, it has been shown that viruses are able to disarm the UPR or to customise it for their own benefit. Whereas, blocking as well as activation of the UPR can be pro-viral, the mechanisms are virus and cell specific (Johnston and McCormick, 2019). This makes physiological relevant infection models

important to address economically relevant viral infections in livestock species. While the mechanisms of bovine herpes virus require further investigation, human herpesviruses have been studied more intensely. The alphaherpesvirus HSV-1 expresses γ34.5, an ortholog of GADD34, causing eIF2a dephosphorylation in order to ensure ongoing protein synthesis even if eIF2a kinases become activated during viral infection (He et al., 1997). Salubrinal, a small chemical compound was found to specially suppress HSV-1 γ34.5-mediated eIF2a dephosphorylation and significantly reduce HSV-1 replication (Boyce et al., 2005). The HSV-1 protein UL41 is able to inhibit the IRE1-dependent pathway by decreasing the expression of XBP1 and blocking XBP1 splicing. Wild-type HSV-1 but not UL41-null mutant HSV-1 decreased XBP1 mRNA induced by Tg (Zhang et al., 2017). Our results showed a downregulation of *sXBP1* during infection, indicating a potential similar mechanism used by BoHV-1. The additional downregulation of *ATF6* in our infection model might add to this effect, as ATF6 has been shown to transactivate *XBP1* and heterodimerises with XBP1 (Yoshida et al., 2001). In comparison, another human alphaherpesvirus, varicella zoster virus (VZV), induces the UPR in order to promote viral replication by upregulating autophagy and an autophagy inhibitor reduced the viral titre (Buckingham et al., 2014).

Early experimental use of Thapsigargin at high concentrations inducing apoptosis as end-stage of extreme ER-stress has been described in targeted cancer therapy (Lindner et al., 2020). In the previous years, its antiviral effect on respiratory syncytial virus, influenza viruses and coronaviruses in non-toxic concentrations was reported (Al-Beltagi et al., 2021a; Al-Beltagi et al., 2021b). The induced ER stress response was thought to be the driver for the activation of downstream host antiviral defences, but the exact mechanism remained unclear. In 2021, a study validated the antiviral effects of Tg against HCoV-229E, MERS-CoV and SARS-CoV-2 in different cell types including primary human bronchial epithelial cells and demonstrated the influence of Tg on several central mechanisms required for CoV replication (Shaban et al., 2021). Their proteome wide analyses revealed specific pathways and components that likely mediate the Tg induced antiviral state, including HERPUD1, UBA6 and ZNF622, factors of ER quality control. The results pointed out that Tg largely overrides virus induced modulation and counteracted

the CoV-mediated downregulation of HERPUD1 and GRP78 (Shaban et al., 2021) in line with our results using the BoHV-1 infection model.

Our study highlights the importance of epithelial cells for the innate antiviral activity in the respiratory tract due to their conserved defence mechanisms in case of interruption of cell homeostasis during viral replication. BoHV-1 infection caused an upregulation of the heat shock protein HSPA6 and a downregulation of proteins involved in the UPR in primary bovine tracheal epithelial cells, supporting an important role for the HSP and UPR in viral replication in epithelial cells. We demonstrated protection against BoHV-1 infection in these cells through Thapsigargin mediated induction of ER genes, which was able to override the suppressive effects of BoHV-1. Further investigations of the UPR manipulation by viruses and UPR targeting agents will help to identify improved strategies to prevent infection of respiratory viruses involved in BRD.

Chapter 4. Immune response of primary bovine tracheal epithelial cells to live bovine herpes 1 virus (BoHV-1) infection

4.1. Introduction

As the first cells to be infected, respiratory epithelial cells have a critical role in the defence against BoHV-1 infection (Turin et al., 1999). While their barrier function is well described, innate antiviral immune mechanisms have not been well defined. However, it has increasingly become clear that epithelial cells have active roles in initiating, mediating and regulating both innate and adaptive immune activity (Proud and Leigh, 2011; Weitnauer et al., 2016; Whitsett and Alenghat, 2015). Here we aimed to define the innate antiviral immune potential of bovine respiratory epithelial cells during infection by measuring the ability of bovine tracheal epithelial cells to express various innate immune genes and to respond to a viral infection.

Tolerance of commensals, early detection of potential pathogens and the activation of an appropriate immune response are critical functions of these non-traditional immune cells. As the surface of respiratory epithelial cells is in constant contact with the environment, any immune activity must be tightly regulated to prevent inappropriate activation of the immune system by harmless antigens. While the molecular mechanisms regulating the activation of the immune response of intestinal epithelial cells have been studied more intensely, mechanisms of respiratory epithelial cells are poorly defined, particularly in livestock species.

In recent years, the role of intracellular metabolites in the complex regulation of immune cells has become an important research focus, reviewed in (O'Neill et al., 2016). Cellular metabolism supports immune cell maintenance and development, guiding activation and differentiation (Jung et al., 2019). While the focus to date has been on classical immune cells, metabolomic responses in bovine epithelial cells during viral infections remains largely uncharacterised. Moreover, immunometabolism analysis of immune cells have essentially focused on the glycolysis and the oxidative phosphorylation pathways. Interestingly, it has been found that tryptophan catabolism

in host cells may play an important role as a component of the immune response to pathogens. The enzyme called indoleamine-2,3-dioxygenase (IDO1), responsible for the rate-limiting step of tryptophan catabolism, is long known to be stimulated by LPS exposure and IFN-γ (Werner et al., 1989; Yoshida and Hayaishi, 1978; Yoshida et al., 1981). We propose that the activity of IDO1 might therefore be important in regulating epithelial cell antiviral immunity and aimed to explore it in our model.

The main biochemical function of the ISG IDO1 is to catalyse the degradation of Tryptophan (Trp) and promote kynurenine (Kyn) synthesis. Therefore, IDO1 is significantly important for tryptophan homoeostasis. Tryptophan (Trp), as an essential amino acid, involved in several metabolic pathways, primarily protein, kynurenine and serotonin synthesis. On the one hand, it has been shown, that IDO1 mediated Trp deprivation suppresses pathogen replication, as viruses are dependent on amino acids of the host (Rabbani et al., 2016). On the other hand, IDO1 is also well-recognised as immunosuppressant. Tryptophan is required for successful lymphocyte proliferation. The IDO1 produced by many regulatory immune cell populations inhibits lymphocyte proliferation, thereby facilitating immunological tolerance by preventing T cell activity (Munn and Mellor, 2013). It is also thought that the immunosuppressive activity provides a possible mechanism for feedback counter-regulation during IFN activation. During immune activation and IFN production, IFN upregulates IDO1 expression, resulting in immunosuppression (Raniga and Liang, 2018) (**Fig. 4.1**).

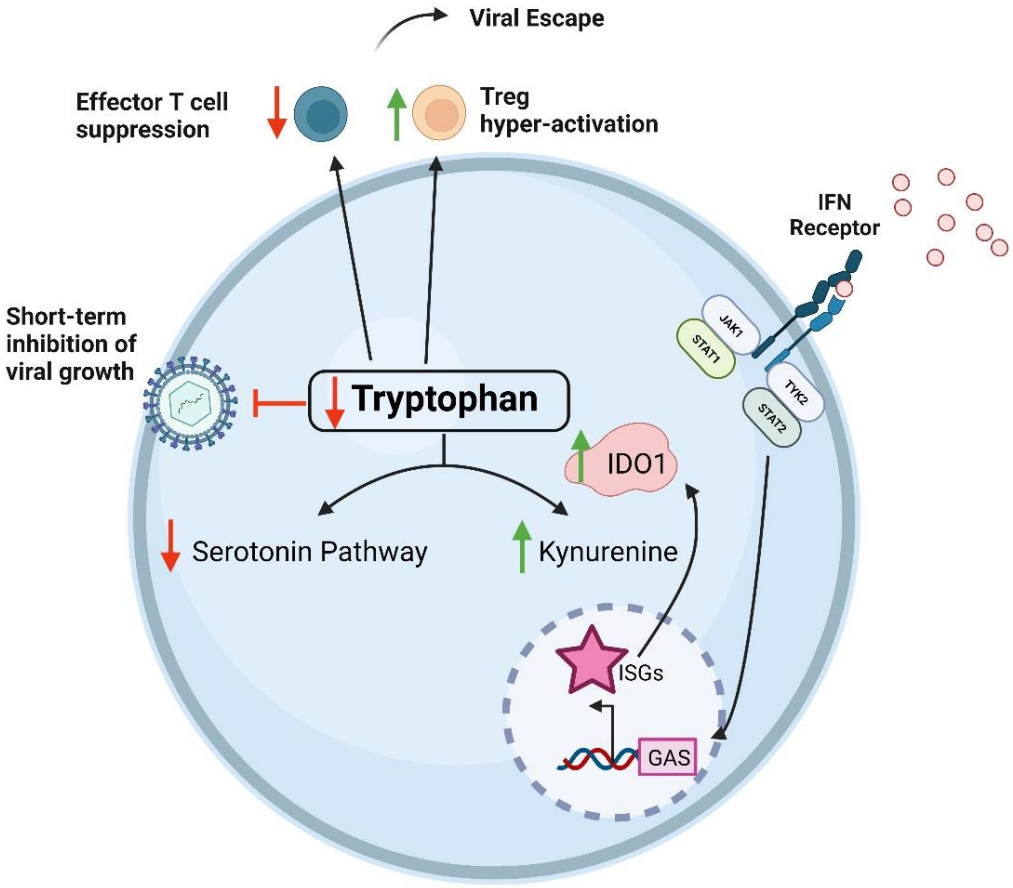

Figure 4.1 IDO1-Mediated Tryptophan Depletion

Tryptophan is metabolised by the serotonin and kynurenine pathway, whereby IDO1 converts tryptophan into kynurenine. IFN-induced IDO1 gene expression decreases tryptophan availability for viral replication as well as reducing serotonin synthesis and T cell proliferation. Red arrows, downregulation; green arrows, upregulation; T bar, inhibition. This figure was created with BioRender.com.

4.2. Rationale

In order to characterise bovine respiratory epithelial cells as non-classical immune cells, we investigated the basal gene expression of several proteins with roles in epithelial defence. With further qPCR analysis of epithelial cells infected with purified live BoHV-1, we investigated the transcriptomic changes early after infection. We also aimed to further investigate the gene expression of indoleamine 2,3 dioxygenase-1 (IDO1) in response to viral stimulation, as an ISG playing a role in the tryptophan metabolism.

4.3. Hypothesis and specific aims

We hypothesise that bovine herpesvirus 1 infection activates the innate immune response in bovine respiratory organ cultures and bovine respiratory epithelial cells.

The specific aims were to:

1. Investigate the basal gene expression of genes involved in the innate immune response in bovine tracheal organ mixed cell cultures and in primary bovine tracheal epithelial cells.
2. Define the innate antiviral immune response to infection with purified live BoHV-1 in both bovine tracheal organ cultures and tracheal epithelial cells across a time course.
3. Investigate the gene expression of indoleamine 2,3 dioxygenase-1 (IDO1), an enzyme initiating the tryptophan catabolism, in response to BoHV-1 infection and stimulation with synthetic viral analogues.

4.4. Results

4.4.1. Tracheal epithelial cells and tracheal organ cultures express several genes involved in the innate immune response

While viral PAMPs are capable of triggering an antiviral activity in most cells of the infected host, sensing mechanisms are species and cell-type specific. These differences are largely dependent on the gene expression and activation of the viral sensing proteins. TLR gene expression in tracheal epithelial cells has been previously profiled (Berghuis et al., 2014), however, expression of other viral sensing genes has not. To establish baseline levels, gene expression in unstimulated primary bovine tracheal epithelial cells was measured. Some innate immune receptor and inflammatory cytokine genes were constitutively expressed (**Fig. 4.2 a-b**). The cells showed expression of type I and type III interferon genes as well as their receptors and genes involved in immune related signalling pathways e.g. *STAT1, IRF3, IRF7* and *MAVS* and the interferon-stimulated genes *CXCL10, ISG15, RSAD2, MX1, OAS1Z, USP18* and *IFI44* (**Fig. 4.2 c**). The relative mRNA abundance measurement of *CXCL10* and *INFL3* was low or not detectable via qPCR in unstimulated cells.

Comparing the expression levels of innate immune genes in isolated tracheal epithelial cells and tracheal organ explants, we found specific genes to be differentially expressed. *TLR3*, *IFNAR1*, *ISG15* and *TNF* had significantly higher basal expression levels in epithelial cells compared to organ cultures. Furthermore, IFNLR1 and IFNL had higher expression levels in isolated epithelial cells, however, these differences were not statistically significant. In tracheal organ explants *IFNA*, *IFNB1*, *CXCL10*, *IL1B* and *IL6* showed higher basal expression levels compared to isolated primary epithelial cells (**Fig. 4.3**).

We compared our primary cell culture model with the bovine neonate nasal turbinate epithelial-like BT cell line (CRL-1390™). BT cells showed morphological characteristics of stromal-like cells (**Fig. 4.4 b**). The analysis of cytokeratin and vimentin gene expression revealed that cytokeratin, an epithelial cell marker, was undetectable and the stromal cell marker vimentin was expressed approximately 300 times higher than in primary tracheal epithelial cells (**Fig. 4.4 a**). Expression of TLR3, IFNAR1 and IFNLR1, IFNAR1 was higher in the BT cell line compared to primary cell cultures (**Fig. 4.4 c**)

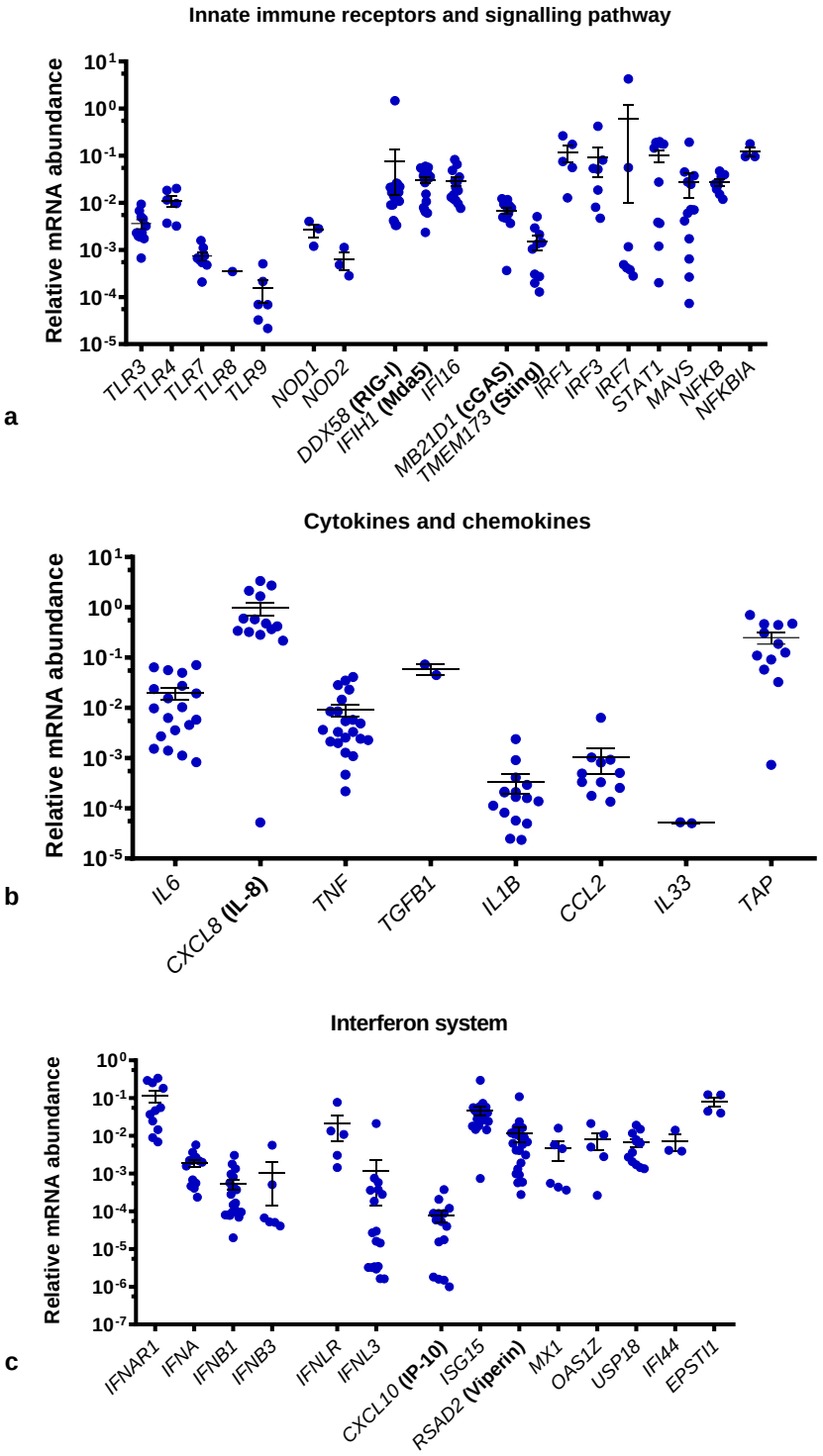

Figure 4.2 Primary bovine tracheal epithelial cells constitutively express several genes involved in the antiviral innate immune response

mRNA baseline expression of genes involved in the innate immune response relative to the reference gene across unstimulated cell cultures of primary bovine tracheal epithelial cells. Cells were harvested into Trizol. RNA was extracted and first strand cDNA reverse transcribed. qPCR was carried out and gene Cq values were normalised to the reference gene H3F3A and the 2^-ΔCT graphed. Each data point represents a different animal. Error bars indicate standard error of the mean; n=2-24.

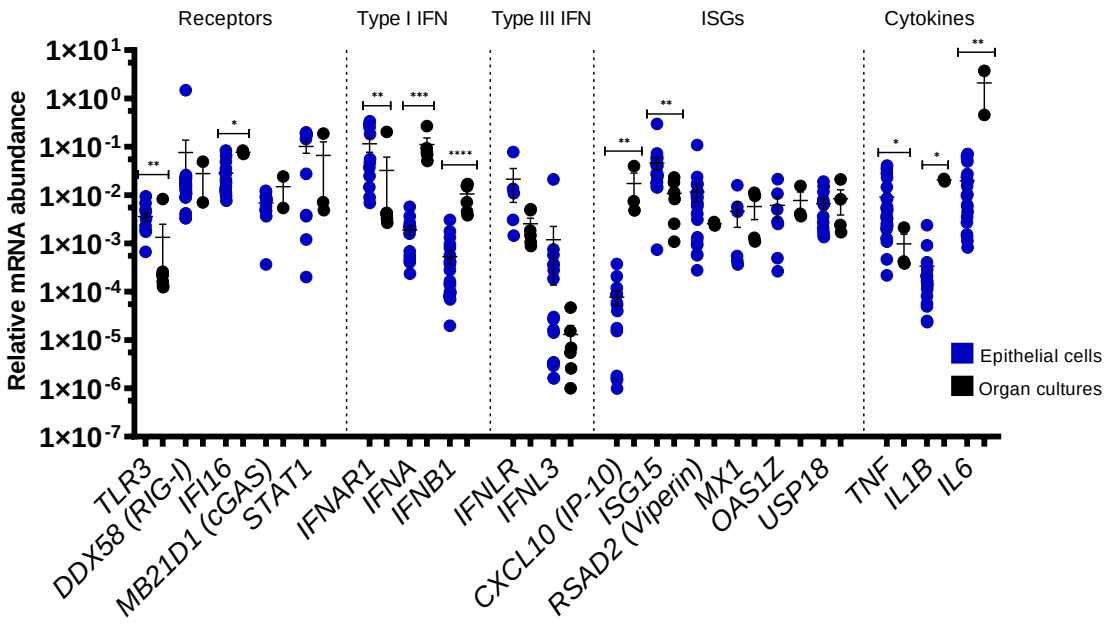

Figure 4.3 Primary bovine tracheal epithelial cells constitutively express different levels of innate immune gene transcripts compared to tracheal organ cultures

mRNA baseline expression of genes involved in the innate immune response relative to the reference gene across unstimulated primary bovine tracheal epithelial cell cultures and tracheal organ cultures. Organ cultures were collected in RNAlater and homogenised and harvested into Trizol after 2-3 days of cell culture. Cells were harvested into Trizol following growing up confluent cell cultures for 2-3 weeks. RNA was extracted and first strand cDNA *reverse transcribed. qPCR was carried out and gene Cq values were normalised to the reference gene H3F3A and the 2^-ΔCT graphed. Each data point represents a different animal. Error bars indicate standard error of the mean. Statistical analysis was performed using Mann-Whitney test. Asterisks indicate statistically significant differences between the two groups: *= adjusted p<0.05; **= adjusted p<0.01; ***=adjusted p<0.001; ****=adjusted p<0.0001; n=2-24.*

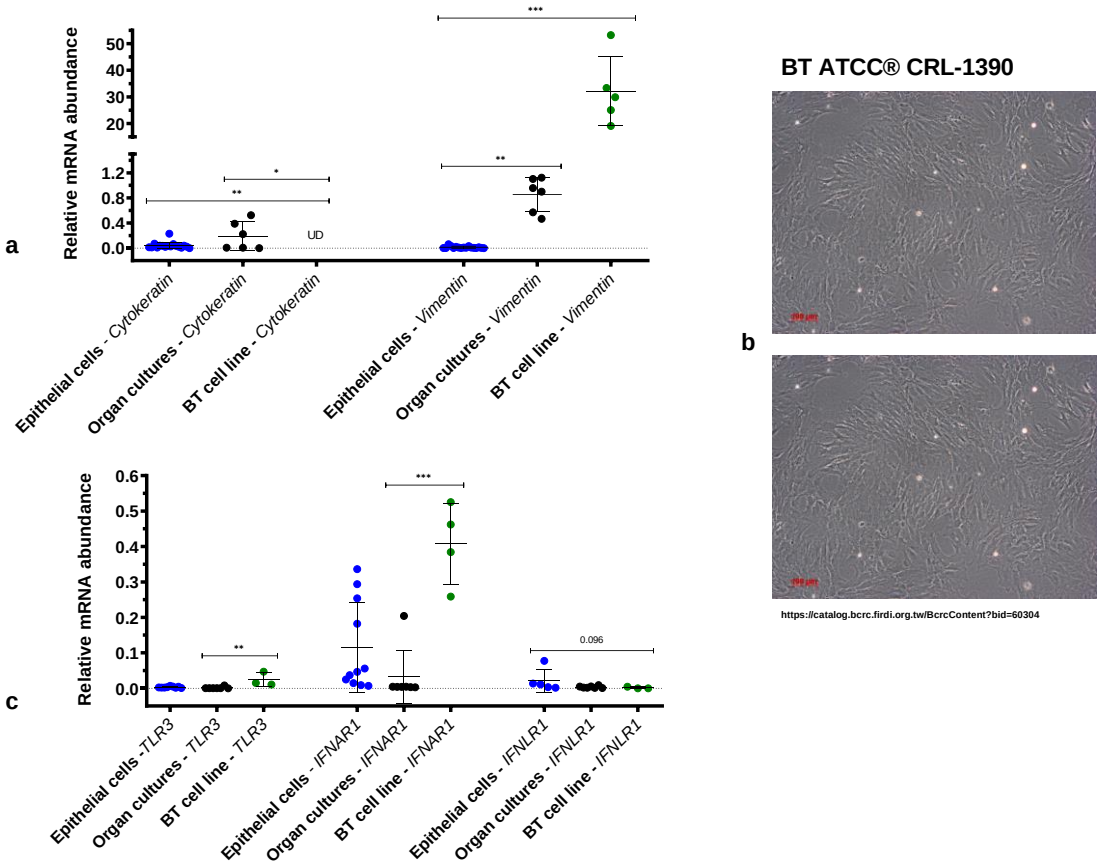

Figure 4.4 Characterisation of the cell line BT ATCC® CRL-1390

(A) Relative keratin-18 and vimentin mRNA gene expression and (B) relative gene expression of TLR3, IFNAR1 and IFNLR1 in tracheal cell populations, tracheal organ cultures and the cell line BT. Organ cultures were collected in RNAlater, homogenised and harvested into Trizol. Cells were harvested into Trizol following cell culture. RNA was extracted and first strand cDNA reverse transcribed. qPCR was carried out on keratin-18, a marker of epithelial cells and vimentin, a marker of stromal cells, gene Cq values were normalised to the reference gene H3F3A and the 2^-ΔCT graphed. Error bars indicate standard error of the mean. Statistical analysis was performed using a Kruskal-Wallis test followed by the Dunn's multiple comparison test. Asterisks *indicate statistically significant differences between the two groups: *= adjusted p<0.05; **= adjusted p<0.01; ***=adjusted p<0.001; n=3-17. (C) Representative images of the BT cell line showing characteristic morphology obtained from https://catalog.bcrc.firdi.org.tw /BcrcContent?bid=60304.*

4.4.2. Expression of cytokines, interferons and interferon-stimulated genes (ISGs) in organ cultures infected with BoHV-1

Tracheal organ cultures were infected with BoHV-1 with concentrations ranging from 100,000 to 10,000,000 PFU for 1 up to 24 hours and gene expression assessed via qPCR. The immune receptors RIG-I, cGAS and IFI16 were significantly upregulated at 12 and 24 hours (**Fig. 4.5 a-c**), while the cytokines IL-6, TNF and IL-1B were not significantly differentially regulated (**Fig. 4.5 d-f**). While *IFNB1* was not differential expressed during BoHV-1 infection, *IFNL3* gene expression was significantly upregulated at 24 hours by 26 fold. All tested ISGs, IP-10, ISG15, Viperin, USP18, MX1 and OAS1Z, were significantly upregulated at 24 hours after infection **(Fig. 4.6**).

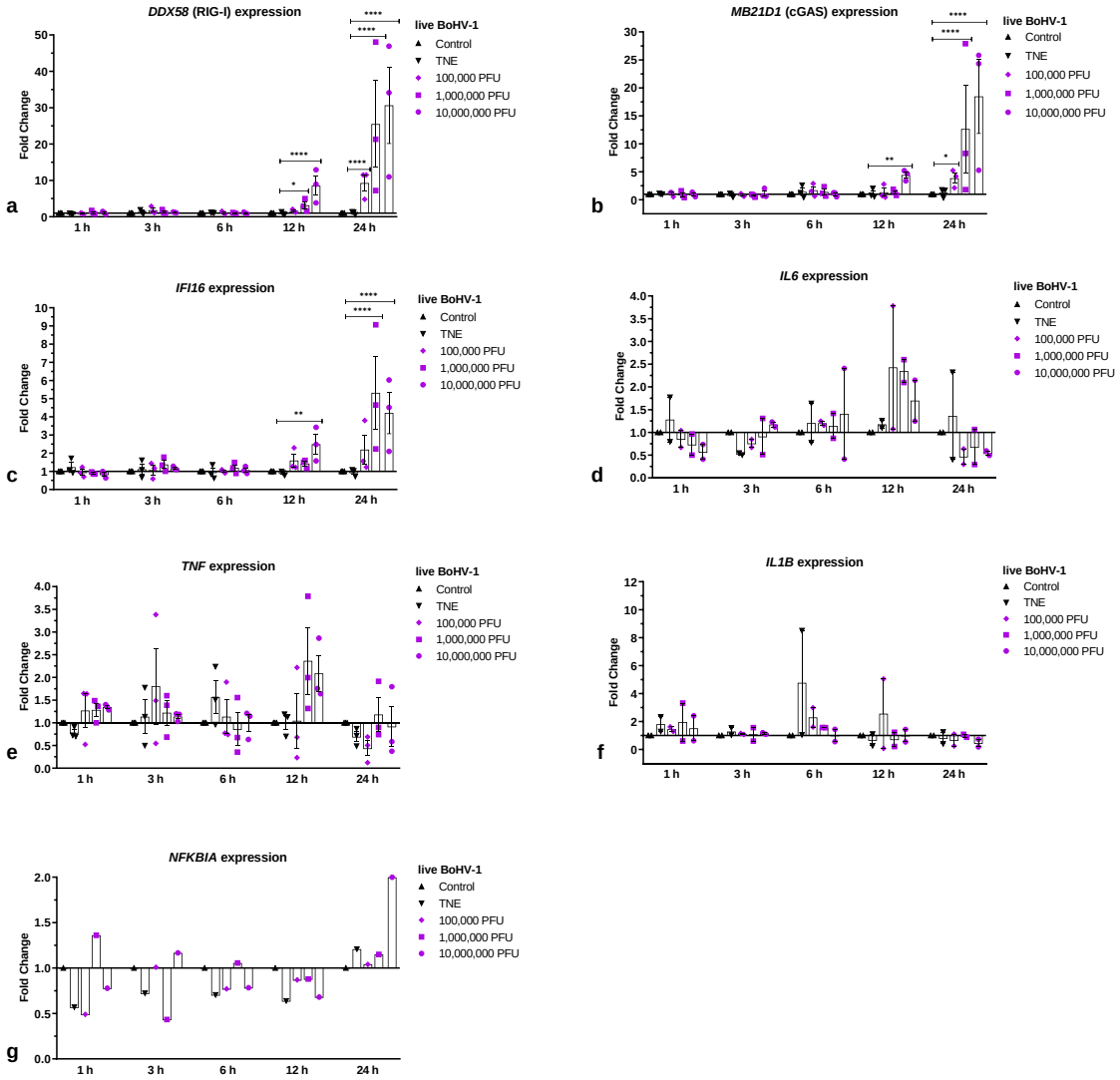

Figure 4.5 Expression of immune receptor and cytokine genes in bovine tracheal organ cultures infected with live bovine herpesvirus 1

*Tracheal organ cultures were infected for 1, 3, 6, 12 or 24 hours with purified live bovine herpesvirus 1. Organ cultures were collected in RNAlater and homogenised and harvested into Trizol. RNA was extracted and first strand cDNA reverse transcribed. qPCR was carried out and gene Cq values were normalised to the reference gene H3F3A and values normalised to the untreated control. Each data point represents a different animal. Error bars indicate standard error of the mean. Statistical analysis was performed on the ΔCt values using a repeated measures two-way ANOVA followed by Sidak's multiple comparisons test. Asterisks indicate statistically significant differences relative to the untreated control: *= adjusted p<0.05; **= adjusted p<0.01; ***=adjusted p<0.001; ****=adjusted p<0.0001; n=1-3.*

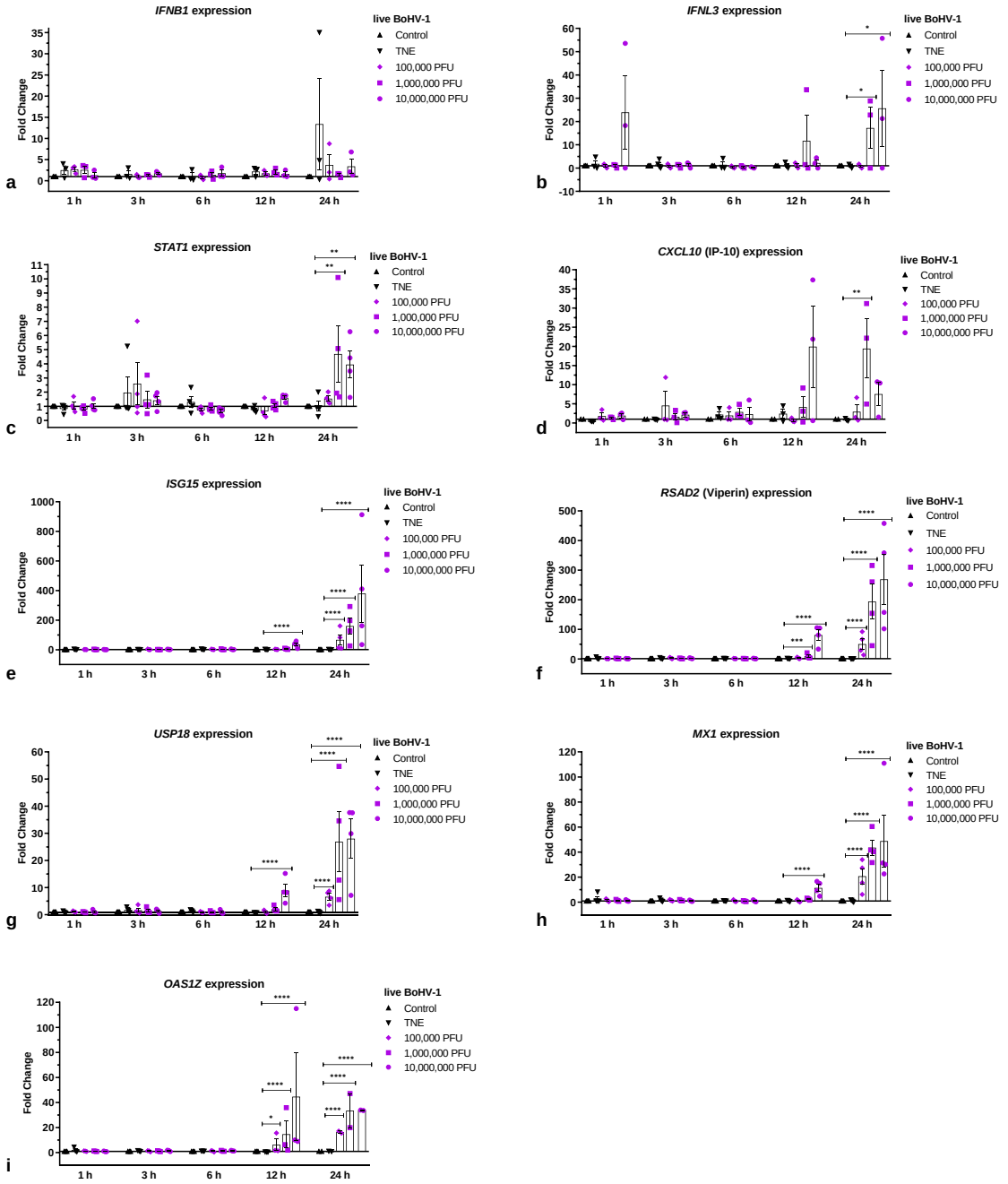

Figure 4.6 Expression of interferon genes and interferon stimulated genes (ISGs) in bovine tracheal organ cultures infected with live bovine herpesvirus 1

*Tracheal organ cultures were infected for 1, 3, 6, 12 or 24 hours with purified live bovine herpesvirus 1. Organ cultures were collected in RNAlater and homogenised and harvested into Trizol. RNA was extracted and first strand cDNA reverse transcribed. qPCR was carried out and gene Cq values were normalised to the reference gene H3F3A and values normalised to the untreated control. Each data point represents a different animal. Error bars indicate standard error of the mean. Statistical analysis was performed on the ΔCt values using a repeated measures two-way ANOVA followed by Sidak's multiple comparisons test. Asterisks indicate statistically significant differences relative to the untreated control: *= adjusted p<0.05; **= adjusted p<0.01; ***=adjusted p<0.001; ****=adjusted p<0.0001; n=2-4.*

4.4.3. Expression of interferon genes and interferon stimulated genes (ISGs) in bovine tracheal organ cultures infected with live bovine herpesvirus 1

Having shown that BoHV-1 infection leads to activation of innate immune activity in whole tracheal organ explants, we analysed gene expression in infected isolated pure tracheal epithelial cells. qPCR analysis showed no significant changes in expression of *IL6, CXCL8, TNF, IL1B, CCL2* or *TAP* with a trend towards downregulation 24with live BoHV-1 *IFNA, IFNB1* and *IFNB3* were not significantly upregulated, *IFNL3* was significantly upregulated by 33 fold after BoHV-1 MOI 7 infection at 24 hours (**Fig. 4.8 a-d**). Analysis of the interferon stimulated genes *ISG15*, *RSAD2* and *USP18* showed a significant upregulation for each at 24 hours (**Fig 4.8 j-l**).

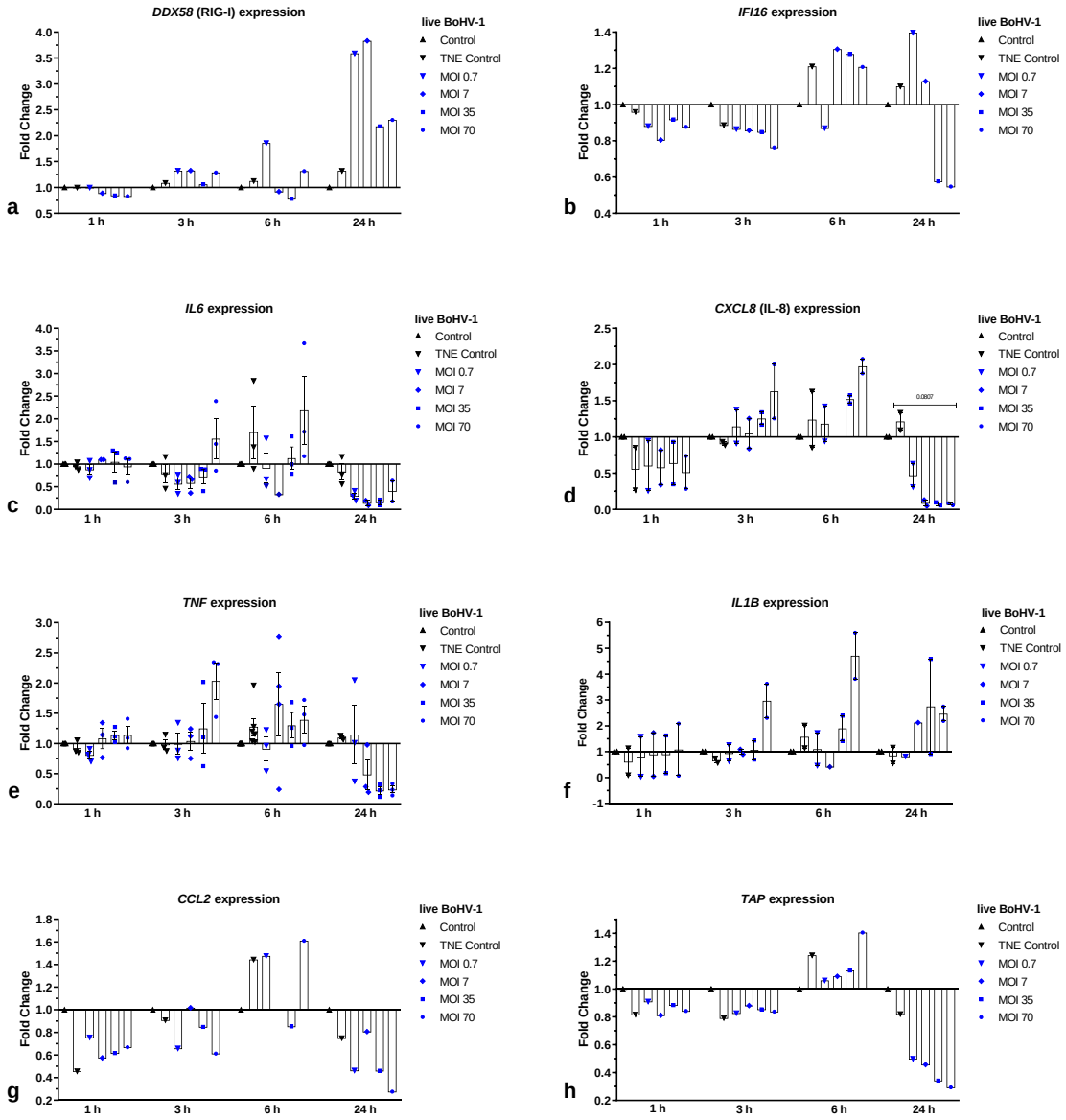

Figure 4.7 Expression of immune receptors, cytokines and chemokines genes in primary tracheal epithelial cells infected with purified live bovine herpes virus 1

*Confluent tracheal epithelial cells were infected with purified live bovine herpes virus 1 for 1, 3, 6 or 24 hours. Cells were harvested into Trizol. RNA was extracted and first strand cDNA reverse transcribed. qPCR was carried out and gene Cq values were normalised to the reference gene H3F3A and values normalised to the untreated control. Each data point represents a different animal. Error bars indicate standard error of the mean. Statistical analysis was performed on the ΔCt values using the mixed-effects model with the Geisser-Greenhouse correction followed by Sidak's multiple comparisons test. Asterisks indicate statistically significant differences relative to the untreated control and the TNE buffer control: *= adjusted p<0.05; **= adjusted p<0.01; ***=adjusted p<0.001; n=1-3.*

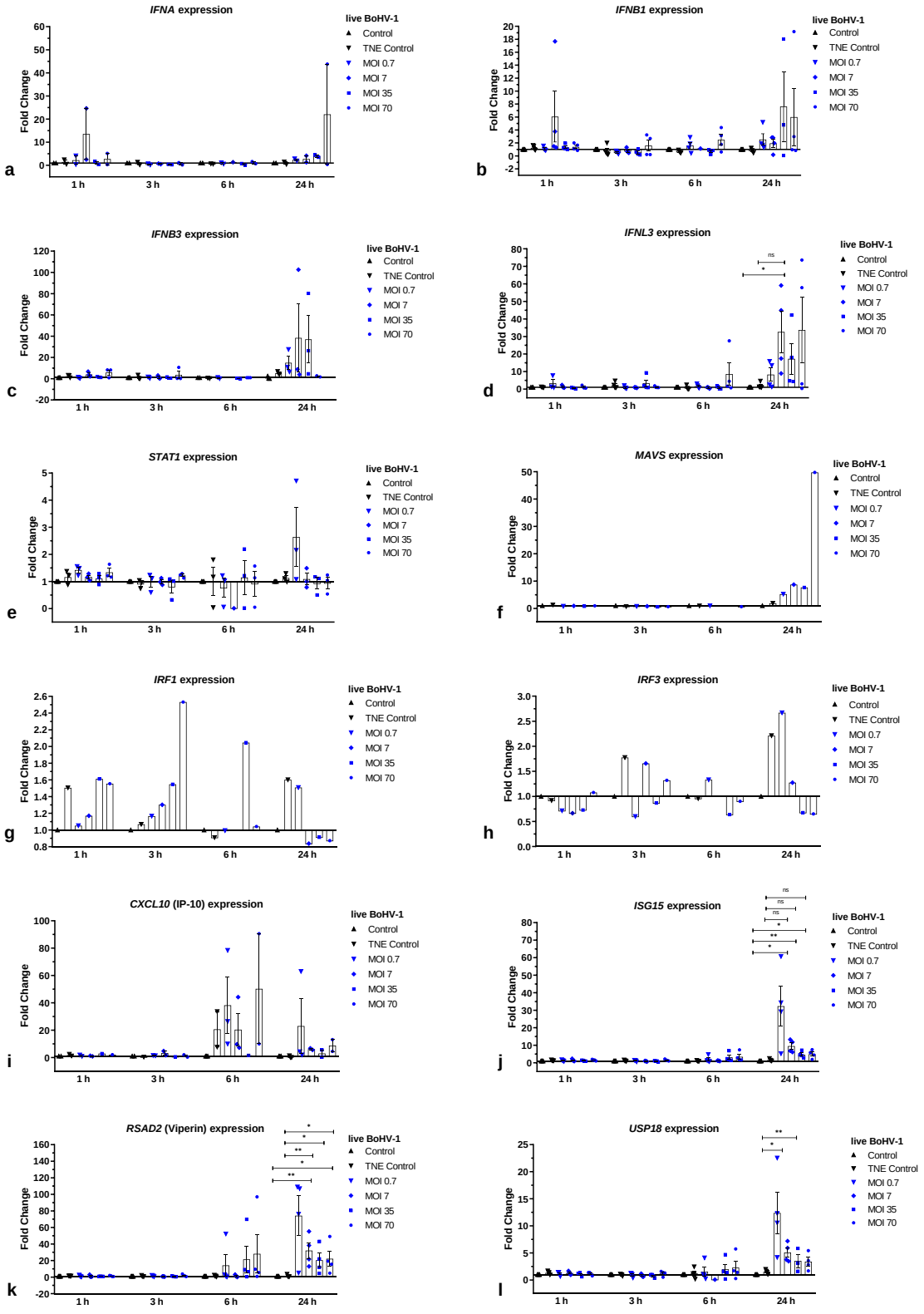
a
IFNA expression
b
IFNB1 expression
c
IFNB3 expression
d
IFNL3 expression
e
STAT1 expression
f
MAVS expression
g
IRF1 expression
h
IRF3 expression
i
CXCL10 (IP-10) expression
j
ISG15 expression
k
RSAD2 (Viperin) expression
l
USP18 expression
Fold Change
1 h
3 h
6 h
24 h
live BoHV-1
Control
TNE Control
MOI 0.7
MOI 7
MOI 35
MOI 70
ns
*
**

Figure 4.8 Gene expression of interferons and interferon stimulated genes (ISGs) in primary tracheal epithelial cells infected with purified live bovine herpes virus 1

*Confluent primary bovine tracheal epithelial cells were infected with purified live bovine herpes virus 1 for 1, 3, 6 or 24 hours. Cells were harvested into Trizol. RNA was extracted and first strand cDNA reverse transcribed. qPCR was carried out and gene Cq values were normalised to the reference gene H3F3A and values normalised to the untreated control. Each data point represents a different animal. Error bars indicate standard error of the mean. Statistical analysis was performed on the ΔCt values using the mixed-effects model with the Geisser-Greenhouse correction followed by Sidak's multiple comparisons test. Asterisks indicate statistically significant differences relative to the untreated control and the TNE buffer control: *= adjusted p<0.05; **= adjusted p<0.01; ***=adjusted p<0.001; n=1-4.*

4.4.4. BoHV-1 infection changes the metabolism in primary bovine tracheal epithelial cells

The CellTiter-Blue® Cell Viability Assay was used to measure the metabolic capacity of primary tracheal epithelial cells infected with BoHV-1. Viable cells are able to reduce the contained resazurin into resorufin, which is highly fluorescent. While Poly(I:C) stimulation caused a slight reduction in the metabolic capacity, BoHV-1 infection MOI 70 for 24 hours led to increased metabolic capacity of 160% (**Fig. 4.9**).

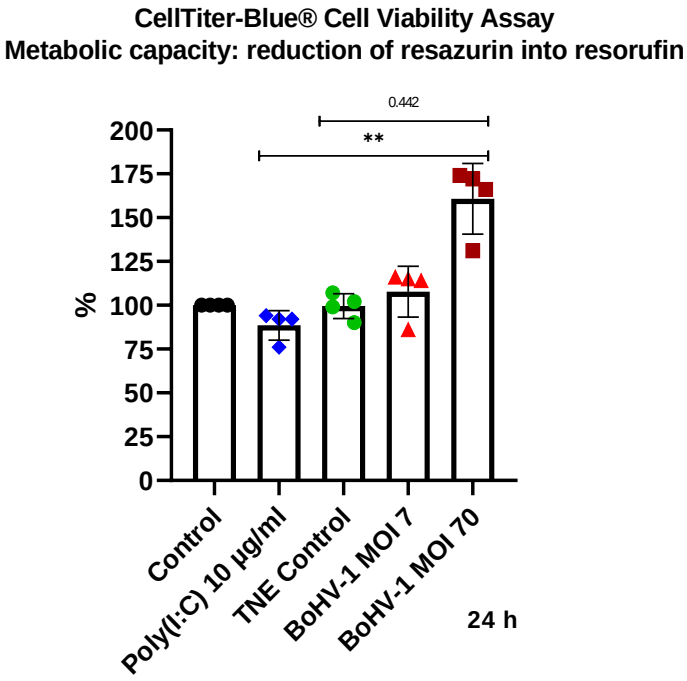

Figure 4.9 Bovine tracheal epithelial cells infected with BoHV-1 show an increased metabolic capacity

*CellTiter-Blue® Cell Viability assay of BoHV-1 infected bovine tracheal epithelial cells for 24 hours. Each data point represents cells from a different animal. Error bars indicate standard error of the mean; n=4. Statistical analysis was performed using a Friedman test followed by Dunn's multiple comparisons test. Asterisks indicate statistically significant differences relative to the untreated control: **= adjusted p<0.01; n=4.*

4.4.5. IDO1 gene expression is upregulated in response to BoHV-1 infection and synthetic viral PAMPS in tracheal organ cultures and tracheal epithelial cells

In order to investigate the increased metabolic capacity in respiratory epithelial cells early after BoHV-1 infection, we analysed expression of indoleamine 2,3 dioxygenase-1 (IDO1), an enzyme responsible for tryptophan catabolism. In tracheal organ cultures, *IDO1* was significantly upregulated by 5 fold 12 hours after Poly(I:C) stimulation and 25 fold 24 hours after BoHV-1 infection (**Fig. 4.10**). Isolated tracheal epithelial cells upregulated *IDO1* expression in response to multiple synthetic viral PAMPs. Poly(I:C), as synthetic analog of dsRNA, led to an upregulation of 23,580 fold after 12 hours and transfected Poly(I:C) to 1,180 fold at 24 hours (**Fig. 4.11 a-b**). Stimulation with transfected Poly(dA:dT), a synthetic dsDNA, for 12 hours resulted in an upregulation of 72 fold (**Fig. 4.11 c**) and 41 fold after 6 hours of stimulation with 3-p-hpRNA, a specific RIG-I agonist (**Fig. 4.11 e**). BoHV-1 infection of respiratory epithelial cells caused an upregulation of 18 fold after 24 hours (**Fig. 4.11 d**).

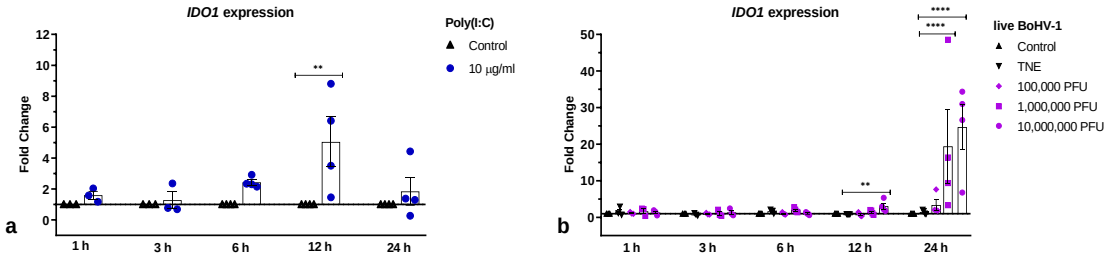

Figure 4.10 IDO1 gene expressions in bovine tracheal organ cultures stimulated with Poly(I:C) or infected with BoHV-1

*Tracheal organ cultures were stimulated for 1, 3, 6, 12 or 24 hours with 10 µg/ml Poly(I:C) or infected with purified live BoHV-1. Organ cultures were collected in RNAlater and homogenised and harvested into Trizol. RNA was extracted and first strand cDNA reverse transcribed. qPCR was carried out and gene Cq values were normalised to the reference gene H3F3A and values normalised to the untreated control. Each data point represents a different animal. Error bars indicate standard error of the mean. Statistical analysis was performed on the ΔCt values using a repeated measures two-way ANOVA followed by Sidak's multiple comparisons test. Asterisks indicate statistically significant differences relative to the untreated control: *= adjusted p<0.05; **= adjusted p<0.01; ***=adjusted p<0.001; ****=adjusted p<0.0001; n=3-4.*

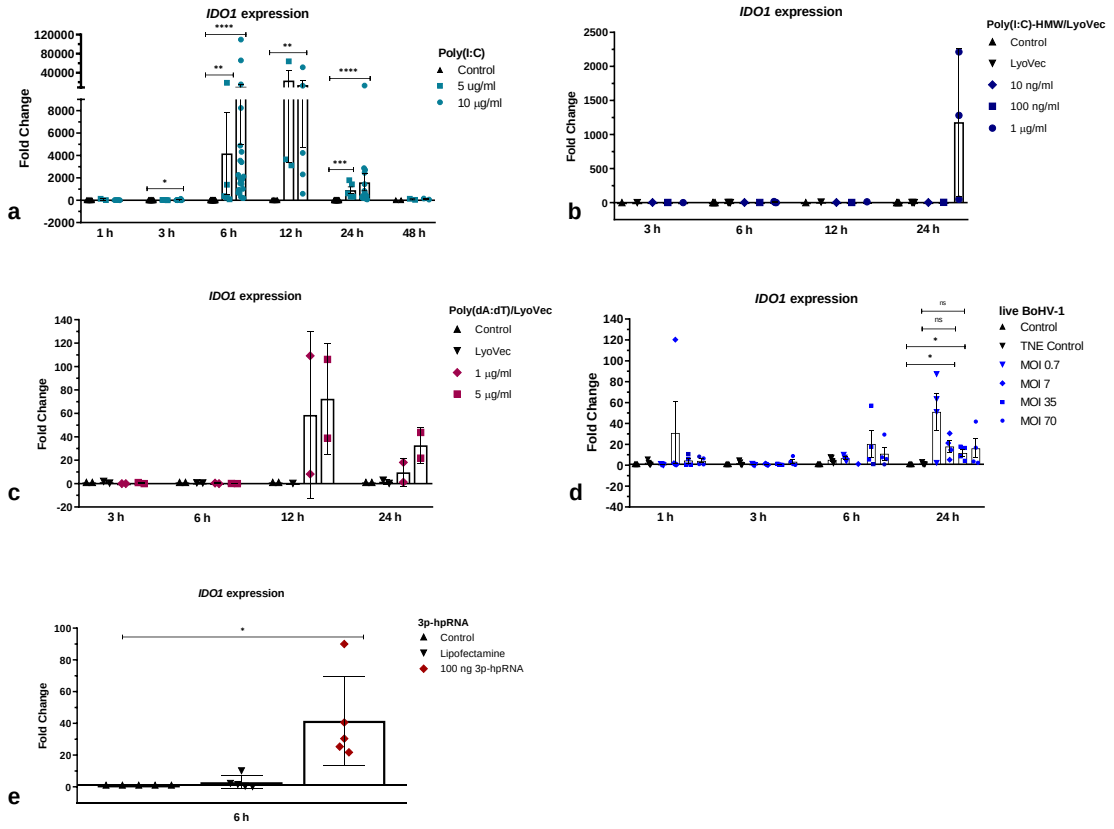

Figure 4.11 IDO1 expression in primary bovine tracheal epithelial cells stimulated with Poly(I:C), Poly(dA:dT), 3p-hpRNA, IFNB1 or infected with live BoHV-1

*Confluent primary tracheal epithelial cells were stimulated for 1, 3, 6, 12, 24 or 48 hours with Poly(I:C), Poly(dA:dT), 3p-hpRNA or infected with live purified BoHV-1. Cells were harvested into Trizol. RNA was extracted and first strand cDNA reverse transcribed. qPCR was carried out and gene Cq values were normalised to the reference gene H3F3A and values normalised to the untreated control. Each data point represents a different animal. Error bars indicate standard error of the mean. Statistical analysis was performed on the ΔCt values using a mixed-effects model with the Geisser-Greenhouse correction followed by Sidak's multiple comparisons test (a-d, f) or using a Friedman test followed by Dunn's multiple comparisons test (e). Asterisks indicate statistically significant differences relative to the untreated control: *= adjusted p<0.05; **= adjusted p<0.01; ***=adjusted p<0.001; n=2-22.*

We looked for correlation between IDO1 upregulation and interferon expression in primary respiratory epithelial cells stimulated with Poly(I:C). We found that *IFNL3* upregulation positively correlated with *IDO1* upregulation with R^2=0.179 (p=0.090) but not with *IFNB1* gene expression with R^2=0.007 (p=0.836) (**Fig. 4.12 a-b**). IDO1 upregulation was positively coregulated with the other ISG Viperin with R^2=0.286 (p=0.049) (**Fig. 4.12 d**).

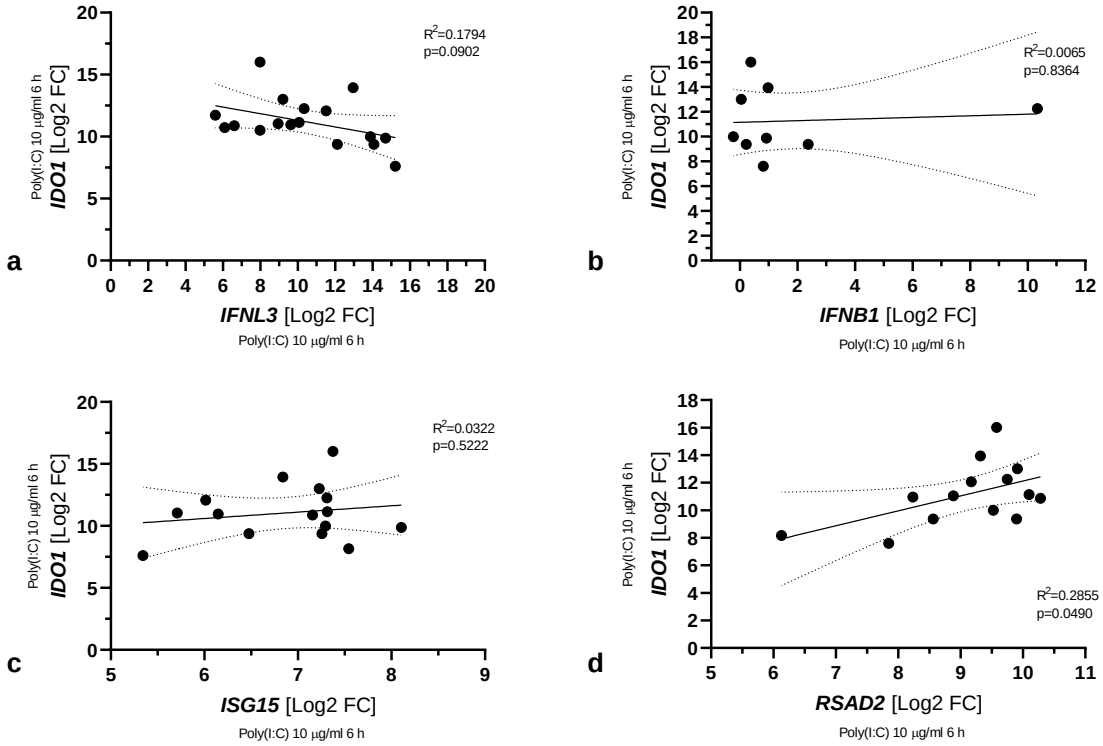

Figure 4.12 Correlation between IDO1 and IFN/ISG upregulation in Poly(I:C) stimulated primary tracheal epithelial cells

Confluent tracheal epithelial cells were stimulated for 6h with 10µg/ml Poly(I:C). Cells were harvested into Trizol. RNA was extracted and first strand cDNA reverse transcribed. qPCR was carried out and gene Cq values were normalised to the reference gene H3F3A and values normalised to the untreated control. Each data point represents a different animal. Statistical analysis was performed on the log2 fold change values using a linear regression, n=9-17.

4.5. Discussion

Our study demonstrates that bovine epithelial cells are capable of detecting and responding to virus infection by mounting an early innate response. We found that significant upregulation of *IFNL3* expression characterises the early innate antiviral innate immune activity induced by BoHV-1 infection. The antiviral state within epithelial cells showed changes in the cell metabolism including significant upregulation of *IDO1*.

While viral PAMPs can trigger antiviral activity in most cells of the infected host, sensing mechanisms are species and cell-type specific and are not defined in many cases. These differences are largely reflected in differences in expression, translation and activation of viral sensing proteins. Here we examined the capability of bovine tracheal epithelial cells to respond to viral infection with BoHV-1. TLR gene expression in these cells has previously been profiled (Berghuis et al., 2014), however, the expression of other viral sensing genes has not. Examining constitutive expression in unstimulated primary bovine tracheal epithelial cells, we found various innate immune receptors, including RIG-I, MDA5 and cGAS, and inflammatory cytokines, such as IL-6, IL-8, TNF, CCL2 and IL-33, to be expressed. The cells show expression of type I and type III interferon genes and their receptors. We also found expression of molecules involved in the interferon signaling pathway, such as STAT1, IRF1, IRF3 and IRF7, confirming innate immune function of respiratory epithelial cells.

We found the receptors TLR3, IFNAR1 and IFNLR1 had higher basal expression levels in epithelial cells compared to organ cultures. The higher expression of *IFNA*, *IFNB1*, *CXCL10*, *IL1B* and *IL6* in tracheal organ cultures compared to isolated tracheal epithelial cells indicate that explants exist in a heightened inflammatory state, possibly due to the presence of DAMPs within the tissue, generated by the tissue dissection released. However, infection with BoHV-1 caused increased upregulation of *IFNL3* and ISGs predominantly 24 hours after infection indicating a functional innate immune potential in tracheal organ explants.

Due to limited access to slaughterhouse material during the SARS-CoV-2 pandemic, we examined the suitability of a commercially available cell line. The BT cell line of bovine

epithelial like turbinate cells represents a cost effective and unlimited supply of respiratory epithelial cells. However, the cell line showed more fibroblast like characteristics with higher levels of vimentin expression and had different expression levels of TLR3, IFNAR1 and IFNLR1 compared to primary tracheal epithelial cells. IFN expression in virally infected epithelial cells was different between cell types. While RSV infection led to upregulation of IFN-λ but not type I IFNs in human nasal epithelial cells, both type I and III IFNs were induced in the human bronchiolar carcinoma cell line A549 (Okabayashi et al., 2011). This demonstrates the importance of establishing primary cell culture models and the differentiation of cell locations to investigate physiologically relevant innate immune responses.

Due to the physiological position of epithelial cells in constant contact with the environment and with commensal microbes and require tight regulation of immune activity in order to avoid unnecessary inflammation stimulated by harmless antigens. It is necessary that epithelial cells modulate the sensitivity of innate immune sensing and are generally hyporesponsive towards prototypical PAMPs and DAMPs (Weitnauer et al., 2016). Only if antigens or pathogens overcome a certain threshold of tolerance, does the inhibitory microenvironment switch to a stimulatory one and initiate immune activity. In our infection model with purified BoHV-1, the virus was able to infect and replicate in the primary bovine tracheal epithelial cells as it would *in-vivo*. We found that infection with BoHV-1 stimulated a relatively muted innate immune response based on gene expression. This could indicate significant suppression of innate immune activity by BoHV-1.

Indeed, it has recently been demonstrated that BoHV-1 encodes several genes that impair innate immune responses during infection, reviewed in (Jones, 2019). The viral gene product BICP0 interacts with IRF3 and IRF7, leading to reduction of the promoter activity of *IFNB* and downregulation of *IFNB* (Henderson et al., 2005; Saira et al., 2007). Also bICP27 was shown to inhibit *IFNB1* and *IFNB3* promoter activity (da Silva et al., 2012). In addition, the viral protein VP8 downregulates expression of *STAT1* thus inhibiting IFN-β signalling (Afroz et al., 2016).

Having demonstrated that BoHV-1 infection upregulates *IFNL* and ISG expression, we aimed to investigate any correlation between expression of type I and III IFN and the upregulation of ISGs. We aimed to establish knockdown of *IFNAR1* and *IFNLR1* in our established primary cell culture model of bovine tracheal epithelial cells. Unfortunately, successful knockdown was not achieved in any of the cell densities, transfection setups or duration of transfection tested. Due to time limitations, other knockdown methods such as lentiviral systems driving shRNAmiRs could not been tested.

Many diverse antiviral mechanisms attributed to ISGs are well described and reviewed in (Schoggins, 2019). Several target distinct steps in the viral replication cycle, e.g. deterring viral entry, inhibiting viral mRNA synthesis and translation or blocking virus release (Schoggins, 2019). Besides the upregulation of the interferon stimulated genes *RSAD2, ISG15* and *USP18*, we found *IDO1* to be upregulated in primary bovine tracheal epithelial cells infected with BoHV-1 and highly upregulated after Poly(I:C) stimulation. Interestingly, tryptophan catabolism in host cells has been shown to prevent the growth of bacterial and parasitic pathogens by denying them a necessary substrate for anabolic growth (Pfefferkorn, 1984; Schroten et al., 2001). This suggests that tryptophan metabolism may play an important role as a component of the immune response to pathogens. Our results show that within bovine epithelial cells, *IFNL3* and *IDO1* gene expressions were highly upregulated in response to virus infection, suggesting a role of metabolic changes in innate antiviral immunity potentially linked with IFN-λ. A previous study found *IDO1* expression was upregulated by recombinant IFN-λ and *IDO1* expression reduced if *IFNL* was silenced in human respiratory epithelial cells during influenza infection (Fox et al., 2015).

Our study highlights the importance of epithelial cells for the innate antiviral activity in the respiratory tract due to their ability to detect and respond to viral infection. Our results with an infection model of primary bovine tracheal epithelial cells support an important role for IFN-λ3 in innate antiviral immune activity in these cells. Further research is needed to investigate the mechanisms of IFN-λ3 regulation and function in the antiviral innate immune response in respiratory epithelial cells. Interestingly, there were clear animal to animal differences in responses to virus and this variability will

likely contribute to susceptibility to infection and immunopathogenesis. Age, breed and sex are likely to contribute to this inter-animal variation in innate immune activity. If more precisely understood, these mechanisms of variability could inform animal breeding programmes as well as enhance our understanding of inter-individual variation in other species including humans.

Chapter 5. Defining the innate immune response in primary bovine respiratory epithelial cells to synthetic viral PAMPs

5.1. Introduction

Viral PAMP sensing mechanisms and antiviral response characteristics are species and cell-type specific (Kato et al., 2005; Nalubamba et al., 2007). Even within a single species and individual cell type, there are regional differences in response to viral infections. For example, primary human nasal epithelial cells mount a more vigorous antiviral response to rhinovirus infection and direct stimulation of the viral RNA sensor RIG-I than do bronchial epithelial cells (Mihaylova et al., 2018). In contrast, RIG-I stimulation triggered a more NRF2-dependent oxidative stress response in bronchial cells (Mihaylova et al., 2018). Based on these findings, Mihaylova and colleagues proposed that epithelial cell-intrinsic defence mechanisms are adjusted for different airway microenvironments to optimise airway protection.

The functionality of the viral sensing genes we have defined in bovine tracheal epithelial cells in response to live virus has not been investigated previously. Commercially available synthetic viral analogues can be used to activate specific cell signalling pathways and thereby delineate the specificity of epithelial cell responses. Poly(I:C) (polyinosinic-polycytidylic acid) is a synthetic analog of double stranded RNA, a molecular pattern associated with viral agents. It induces an innate immune response initiated by two types of pattern recognition receptors (PRRs): the Toll-like receptors (TLRs) and the RIG-I-like receptors (RLRs) (Kawai and Akira, 2007). Naked Poly(I:C) is recognised by TLR3 whereas transfected Poly(I:C) is sensed by RIG-I/MDA-5. In *in-vitro* experiments using Poly(I:C) without transfection reagent in the culture medium, the Poly(I:C) is endocytosed and delivered to TLR3. Some cell types express a small amount of TLR3 on the surface, with the majority being found within endosomes, where TLR3 signalling is initiated (O'Neill et al., 2013). The exact TLR3 signalling pathway activated varies between cell types. Human synovial fibroblasts, endothelial cells and murine DCs activate NFκB in response to Poly(I:C), whereas human DCs and macrophages do not (Lundberg et al., 2007). Several dsRNA helicases of the RIG-like receptor (RLR) family

sense dsRNA generated by viral replication in the cytoplasm (Thompson and Locarnini, 2007). RIG-I activation as well as MDA5 is essential for IFNB production in response to dsRNA stimulation, with IRF3 activity driving *IFNB* expression (Yoneyama et al., 2005; Yoneyama et al., 2004). Viral sensing in the bovine has been best studied in the context of bovine viral diarrhoea virus (BVDV) infection. Expression of RIG-I and MDA-5 genes were upregulated in foetuses whose dams have been infected with BVDV during gestation (Smirnova et al., 2012) and in naturally-infected steers (Shoemaker et al., 2009). Inclusion of plasmids expressing RIG-I agonist in a DNA-based vaccine against bovine viral diarrhoea virus generates an increased antibody response over plasmids encoding BVDV antigen alone (LM et al., 2015).

Using the synthetic analog of viral DNA, Poly(dA:dT), we examined the response of tracheal epithelial cells to activation of cytosolic DNA sensors. Poly(dA:dT) is a poly(deoxyadenylic-deoxythymidylic) acid sodium salt, a repetitive synthetic double-stranded DNA sequence of poly(dA-dT):poly(dT-dA). Poly(dA:dT)/LyoVec is delivered into the cytosol and is recognised by multiple PRRs. In the cytosol, Poly(dA:dT) is recognised by DNA sensors, including cGAS, AIM2, DAI, DDX41 and IFI16 (Unterholzner, 2013; Wu et al., 2013). Whereas indirect sensing by the cytosolic RNA sensor RIG-I can occur upon the transcription of Poly(dA:dT) into dsRNA (Ablasser et al., 2009).

To achieve stimulation of RIG-I, transfected 3p-hpRNA can be used. 3p-hpRNA is a 5'triphosphate hairpin RNA that was generated by *in-vitro* transcription of a sequence from the influenza A (H1N1) virus, a ssRNA virus. The 89-mer RNA oligonucleotide contains an uncapped 5' triphosphate extremity and a double-strand fragment. The 3p-hpRNA sequence self-anneals to form secondary structures such as hairpin or panhandle confirmations. These structural features distinguish viral from mammalian RNA and are recognized by RIG-I (Gebhardt et al., 2017; Hornung et al., 2006).

Although the dsDNA herpesviruses, like BoHV-1, contribute to a wide range of pathologies, DNA-sensing mechanisms are understudied in the bovine. The expression

pattern and function of the wider virus DNA and RNA sensing machinery is unknown in bovine epithelial cells.

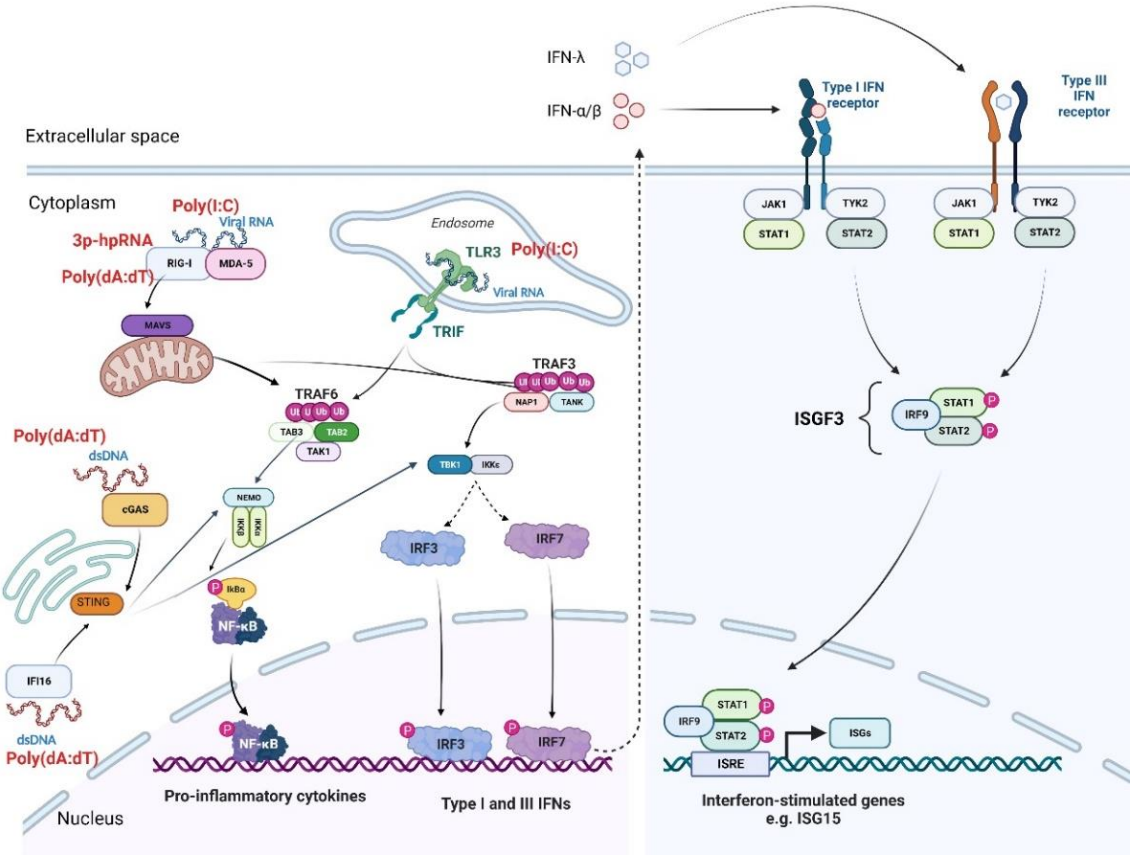

Figure 5.1 Synthetic viral analogues activate specific cell signalling pathways

Host intracellular viral RNA and DNA recognition and innate immune signalling network. The synthetic viral analogue Poly(I:C) untransfected is recognised by TLR3 whereas transfected Poly(I:C) is sensed by RIG-I/MDA-5. This figure was created with BioRender.com

5.2. Rationale

Here, we aimed to define the innate antiviral immune potential of bovine respiratory epithelial cells, in particular type III interferon. We carried out stimulation experiments with multiple synthetic viral analogues for dsRNA, dsDNA and 5'triphosphate hairpin RNA, analysing the gene expression of type I and III interferons and pro-inflammatory genes. Next, we examined the antiviral potential of bovine IFNB1 protein, conditioned media of Poly(I:C) stimulated cells and the treatment with Poly(I:C) against BoHV-1 infection.

5.3. Hypothesis and specific aims

We hypothesise that synthetic viral analogues induce innate immune activity, in particular type III interferon expression, in bovine respiratory epithelial cells, thus activating an antiviral state.

The specific aims were to:

1. Investigate the evolutionary features of type III interferons and the interferon lambda receptor 1.
2. Define the innate antiviral immune response to Poly(I:C), Poly(dA:dT) and 3p-hpRNA stimulation in bovine tracheal organ cultures and tracheal epithelial cells across a time course.
3. Define the innate antiviral immune response to Poly(I:C) in polarised primary bovine tracheal epithelial cells.
4. Investigate the antiviral potential of bovine IFNB1, conditioned media of Poly(I:C) stimulated cells and the treatment with Poly(I:C) against BoHV-1 infection of primary bovine tracheal epithelial cells.

5.4. Results

5.4.1. Sequence alignments of type I and type III interferons human vs. bovine

While the sequences of *IFNL1-4* have been reviewed or validated in the human genome, *IFNL1* and *IFNL4* have only been modelled and predicted in the bovine genome (**Tab. 5.1**). Using five primer sets each to analyse basal expression of *IFNL1* and *IFNL4* in bovine tracheal organ explants, tracheal epithelial cells, lymph node, liver or PBMCs the qPCR results were undetermined.

Human and bovine protein sequences were aligned using BLAST. Human IFNLs showed a 71-96% identity, while bovine IFNLs showed a much lower 31-45% sequence identity. Aligning human and bovine protein sequences of type III interferons show between 30 and 68% identity. Across the IFNL3 protein, there is 68% identity in amino acid sequence between the human and bovine protein (**Tab 5.2**). However, key amino acids, e.g. cystein, were identical, suggesting a similar function of IFN-λs in human and bovine (**Fig. 5.2**).

Table 5.1 Type III interferons in the human and bovine

IFNL1 / IL-29		
	Homo sapiens	**Bos taurus**
Refseq status	reviewed	model
Location	Chromosome 19	Chromosome 13
genomic	NC_000019.10 Reference GRCh38.p13 Primary Assembly	NC_037340.1 Reference ARS-UCD1.2 Primary Assembly PREDICTED: Bos taurus interferon lambda-1-like (LOC112449243)
mRNA	NM_172140.2	XM_025000904
	775 bp mRNA	3436 bp mRNA
Protein	NP_742152.1	XP_024856672.1 LOW QUALITY PROTEIN: interferon lambda-1-like
	200 aa	223 aa

IFNL2 / IL-28A		
	Homo sapiens	**Bos taurus**
Refseq status	validated	
Location	Chromosome 19	
genomic	NC_000019.10 Reference GRCh38.p13 Primary Assembly	
mRNA	NM_172138.2	
	951 bp mRNA	
Protein	NP_742150	
	200 aa	

IFNL3 / IL-28B		
	Homo sapiens	**Bos taurus**
Refseq status	reviewed	provisional
Location	Chromosome 19	Chromosome 18
genomic	NG_042193.1 RefSeqGene	NC_037345.1
mRNA	NM_001346937.2	NM_001281901.1
	953 bp mRNA	588 bp mRNA
Protein	NP_001333866.1	NP_001268830
	200 aa	195 aa

IFNL4		
	Homo sapiens	**Bos taurus**
Refseq status	reviewed	model
Location	Chromosome 19	Chromosome 18
genomic	NG_055295.1 RefSeqGene	NC_037345.1 Reference ARS-UCD1.2 Primary Assembly PREDICTED: Bos taurus interferon lambda-4-like
mRNA	NM_001276254.2	XM_005219126
	1636 bp mRNA	594 bp mRNA
Protein	NP_001263183.2	XP_005219183.1
	179 aa	197 aa

Table 5.2 Significant alignments between human vs. bovine type III interferon amino acid sequences

	IFNL1 Homo sapiens	IFNL2 Homo sapiens	IFNL3 Homo sapiens	IFNL4 Homo sapiens	IFNL1 Bos taurus	IFNL3 Bos taurus	IFNL4 Bos taurus
IFNL1 Homo sapiens	100%	139/196 71%	140/189 74%		104/182 57%	118/196 60%	
IFNL2 Homo sapiens	133/179 74%	100%	192/200 96%		79/149 53%	131/198 66%	47/164 29%
IFNL3 Homo sapiens	136/179 76%	192/200 96%	100%		87/169 51%	134/198 68%	47/165 28%
IFNL4 Homo sapiens				100%		48/160 30%	125/185 68%
IFNL1 Bos taurus	96/163 59%	84/169 50%	87/169 51%		100%	79/177 45%	
IFNL3 Bos taurus	111/174 64%	131/198 66%	134/198 68%	48/160 30%	78/177 44%	100%	56/179 31%
IFNL4 Bos taurus	51/176 29%			125/185 68%		57/182 31%	100%

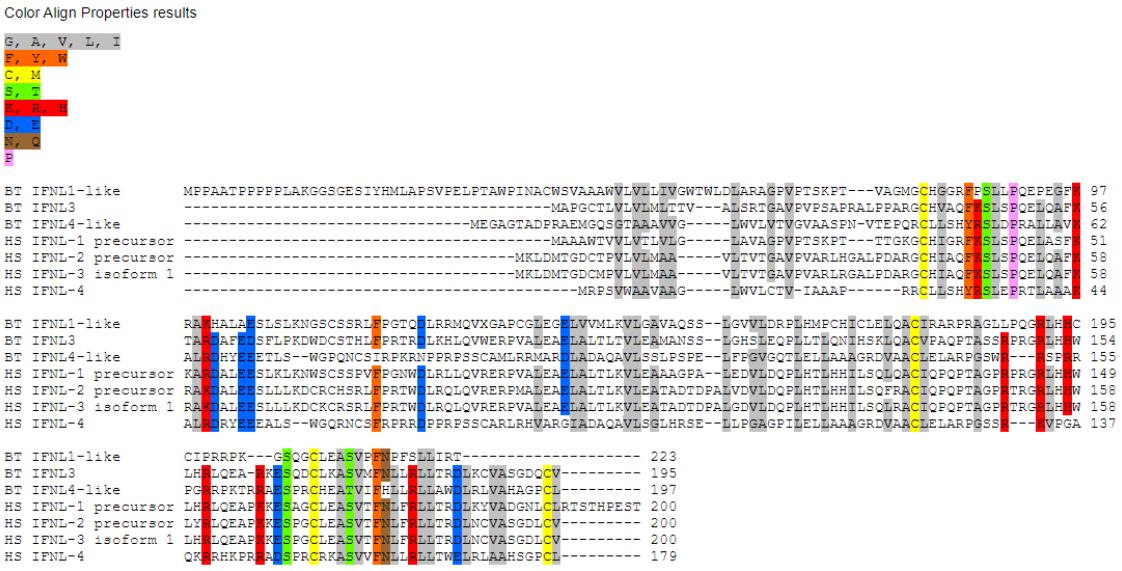

Figure 5.2 Alignment of amino acid sequences of human and bovine type III interferons

Amino acid sequences for human and bovine type III interferons were downloaded from GenBank. The accession numbers are given in Table 5.1. The sequences were aligned using Clustal Omega (http://www.ebi.ac.uk/Tools/msa/clustalo/). Amino acids are coloured according to physicochemical groupings, yellow indicates conserved cysteine residues.

Considering the identity of 68% in amino acid sequence of the IFNL3 protein between human and bovine, we next aligned the amino acid sequences of the interferon lambda receptor 1. We found between 63 and 74% identity between the human IFNLR1 isoforms with the bovine IFNLR1 (**Tab. 5.3**).

Table 5.3 Significant alignments between human vs. bovine IFNLR1 amino acid sequences

	IFNLR1 Isoform 1 Homo sapiens	IFNLR1 Isoform 2 Homo sapiens	IFNLR1 Isoform 3 Homo sapiens	IFNLR1 Bos taurus
IFNLR1 Isoform 1 Homo sapiens NP_734464.1	100%	491/520 100%	224/227 99%	341/534 63%
IFNLR1 Isoform 2 Homo sapiens NP_775087.1	491/520 94%	100%	224/227 99%	341/505 66%
IFNLR1 Isoform 3 Homo sapiens NP_775088.1	224/227 99%	224/227 99%	100%	169/228 74%
IFNLR1 Bos taurus NP_001178426.2	335/534 63%	335/505 66%	169/228 74%	100%

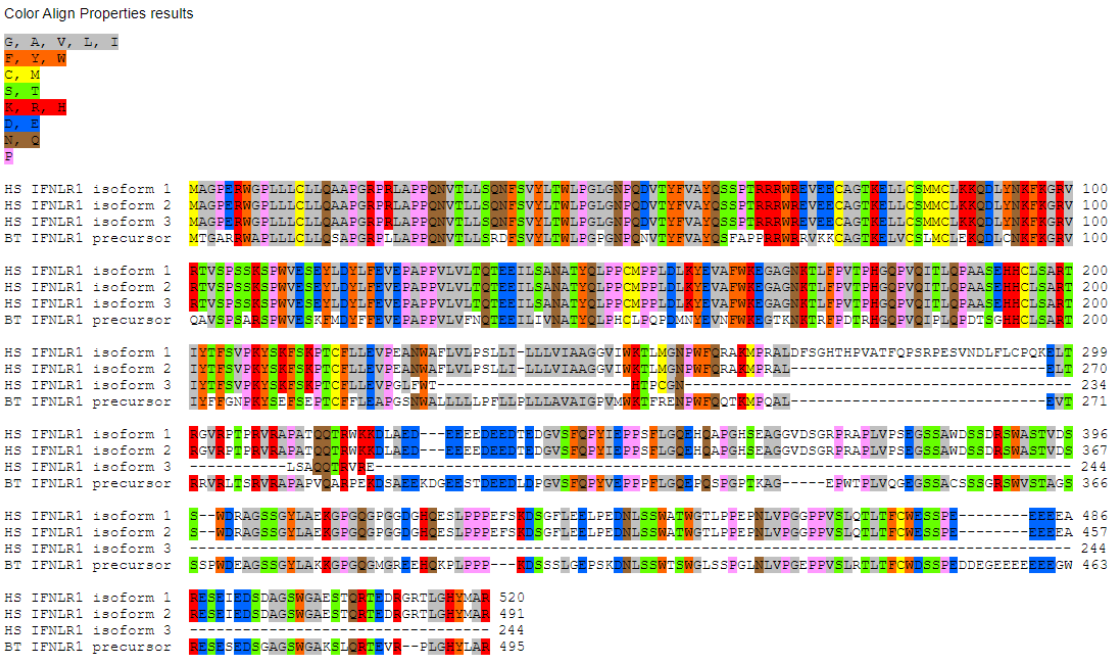

Figure 5.3 Alignment of amino acid sequences of human and bovine IFNLR1

Amino acid sequences for human and bovine IFNAR1 proteins were downloaded from GenBank. The accession numbers are given in Table 5.3. The sequences were aligned using Clustal Omega (http://www.ebi.ac.uk/Tools/msa/clustalo/). Amino acids are coloured according to physicochemical groupings, yellow indicates conserved cysteine residues

5.4.2. Poly(I:C) induced the expression of innate immune genes in tracheal organ cultures

In order to examine type III interferon expression and characterise the innate antiviral immune response in primary bovine tracheal epithelial cells we used Poly(I:C), a synthetic nucleic acid molecule with similar structure to viral dsRNA. This PRR acts as an agonist for TLR3 (Alexopoulou et al., 2001), which is expressed by bovine tracheal epithelial cells as demonstrated in 4.4.1. Bovine tracheal organ cultures were stimulated with Poly(I:C) within 12 hours after collection. We found expression of RIG-I and IFI16 to be significantly upregulated after stimulation for 12 hours after stimulation (**Fig. 5.4**). While expression of *IFNB1* was not influenced by Poly(I:C) stimulation, *IFNL3* was significantly upregulated. *IFNL3* was upregulated 29 fold at 1 hour and 37 fold at 3 hours. We found expression of the ISGs ISG15, Viperin, USP18, MX1 and OAS1Z significantly upregulated, peaking at 12 hours (**Fig. 5.5**).

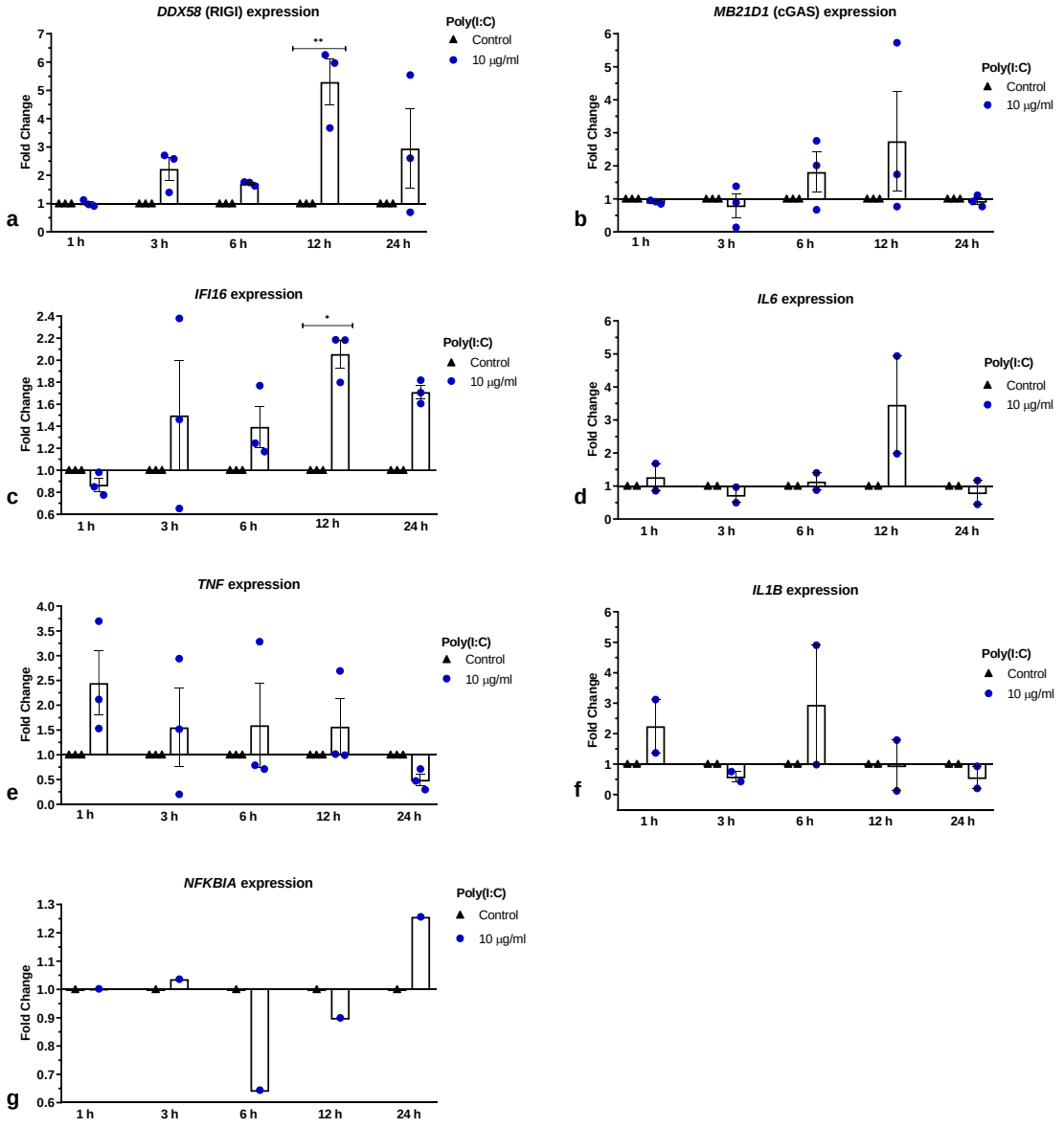

Figure 5.4 Expression of immune receptor and cytokine genes in bovine tracheal organ cultures stimulated with Poly(I:C)

*Tracheal organ cultures were stimulated for 1, 3, 6, 12 or 24 hours with 10 µg/ml Poly(I:C). Organ cultures were collected in RNAlater and homogenised and harvested into Trizol. RNA was extracted and first strand cDNA reverse transcribed. qPCR was carried out and gene Cq values were normalised to the reference gene H3F3A and values normalised to the untreated control. Each data point represents a different animal. Error bars indicate standard error of the mean. Statistical analysis was performed on the ΔCt values using a repeated measures two-way ANOVA followed by Sidak's multiple comparisons test. Asterisks indicate statistically significant differences relative to the untreated control: *= adjusted p<0.05; **= adjusted p<0.01; n=1-3.*

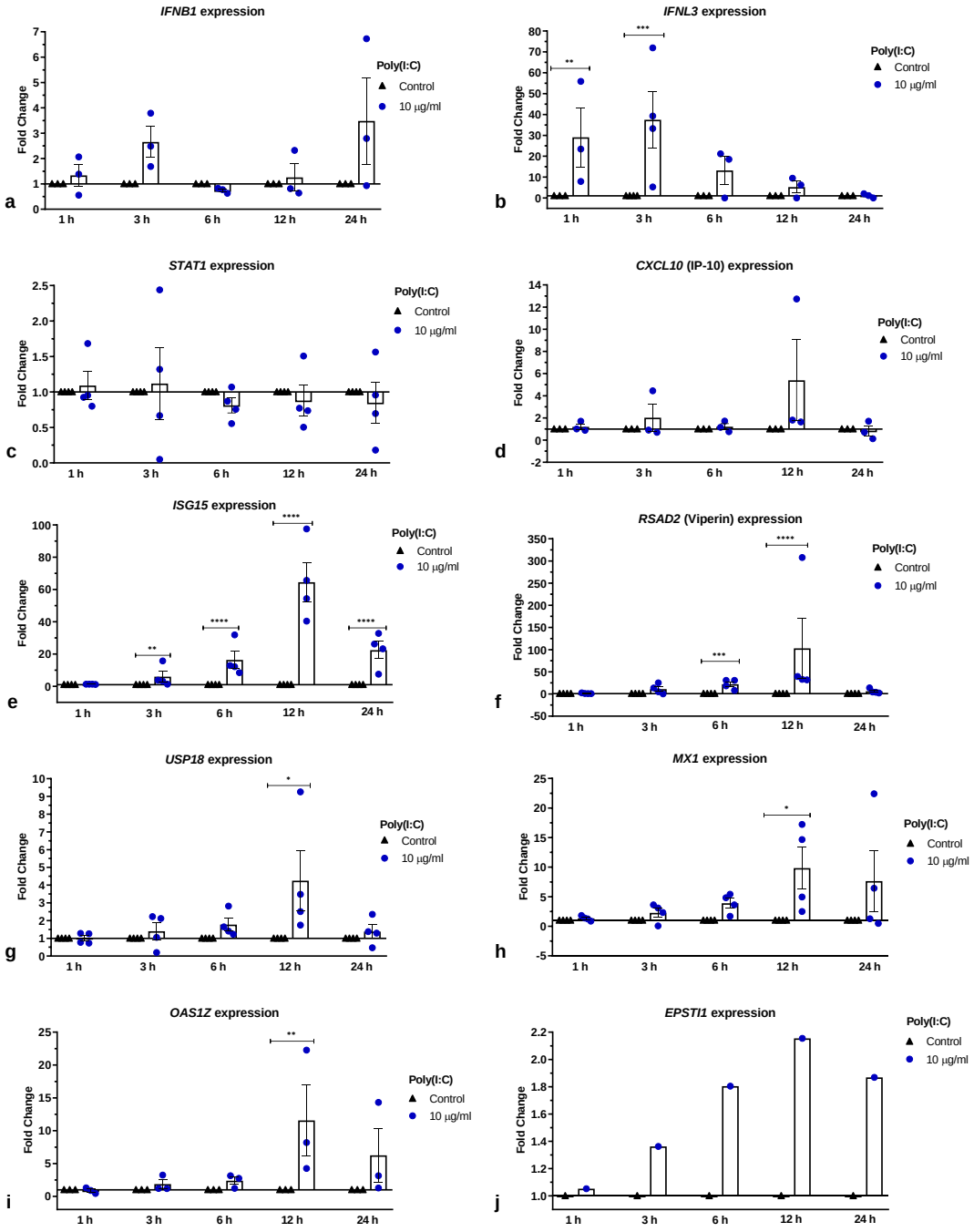

Figure 5.5 Expression of interferon genes and interferon stimulated genes (ISGs) in bovine tracheal organ cultures stimulated with Poly(I:C)

*Tracheal organ cultures were stimulated for 1, 3, 6, 12 or 24 hours with 10 µg/ml Poly(I:C). Organ cultures were collected in RNAlater and homogenised and harvested into Trizol. RNA was extracted and first strand cDNA reverse transcribed. qPCR was carried out and gene Cq values were normalised to the reference gene H3F3A and values normalised to the untreated control. Each data point represents a different animal. Error bars indicate standard error of the mean. Statistical analysis was performed on the ΔCt values using a repeated measures two-way ANOVA followed by Sidak's multiple comparisons test. Asterisks indicate statistically significant differences relative to the untreated control: *= adjusted p<0.05; **= adjusted p<0.01; ***=adjusted p<0.001; ****=adjusted p<0.0001; n=1-4.*

5.4.3. Poly(I:C) induced expression of innate immune genes in primary tracheal epithelial cells

Confluent cell cultures of primary bovine tracheal epithelial cells were stimulated with 5 and 10 µg/ml high molecular weight Poly(I:C) for 1, 3, 6, 12, 24 and 48 hours and qPCR gene expression analysis performed.

While *TLR3* gene expression was not upregulated by Poly(I:C) stimulation at any time point, we found the viral sensing genes *DDX58*, *IFIH1*, *IFI16* and *MB21D1* to be significantly upregulated with a peak at 6 or 12 hours and decreasing again after 48 hours (**Fig. 5.6 a-f**). The gene expression of the transcription factor *NFKB* was significantly upregulated at 3, 6, 12 and 24 hours as well as the pro-inflammatory cytokines *IL6*, *TNF* and *CCL2* (**Fig. 5.6 and 5.7**). *IL6* gene expression was significantly upregulated by 4 fold at 6 hours and *TNF* gene expression was significantly upregulated by 4 fold at 12 hours. Interestingly, *TNF* was significantly downregulated by 0.36 fold 48 hours after Poly(I:C) stimulation (**Fig. 5.7 c**). While *IL1B* was not significantly upregulated, *CASP1* was significantly upregulated peaking at 24 hours by 5 fold (**Fig. 5.7 i-j**).

Measurement of IFN levels showed no significant gene upregulation of *IFNB1* or *IFNB3* at the tested time points. Whereas *IFNL3* was significantly upregulated 8,161 fold at 3 hours, 9,226 fold at 6 hours, 3,549 fold at 12 hours and 82 fold at 24 hours. Looking at gene expressions of proteins being part of the signalling pathway, we found *STAT1* and *IRF1* but not *IRF3* and *IRF7* significantly upregulated (**Fig. 5.8**). *IRF1* was upregulated by 10 fold 6 hours after Poly(I:C) stimulation (**Fig. 5.8 i**). The analysis of the ISGs *CXCL10*, *ISG15*, *RSAD2, USP18, MX1, OAS1Z, IFI44* and *EPSTI1* showed a significant upregulation at multiple timepoints with a peak at 12 hours post-stimulation (**Fig. 5.9**).

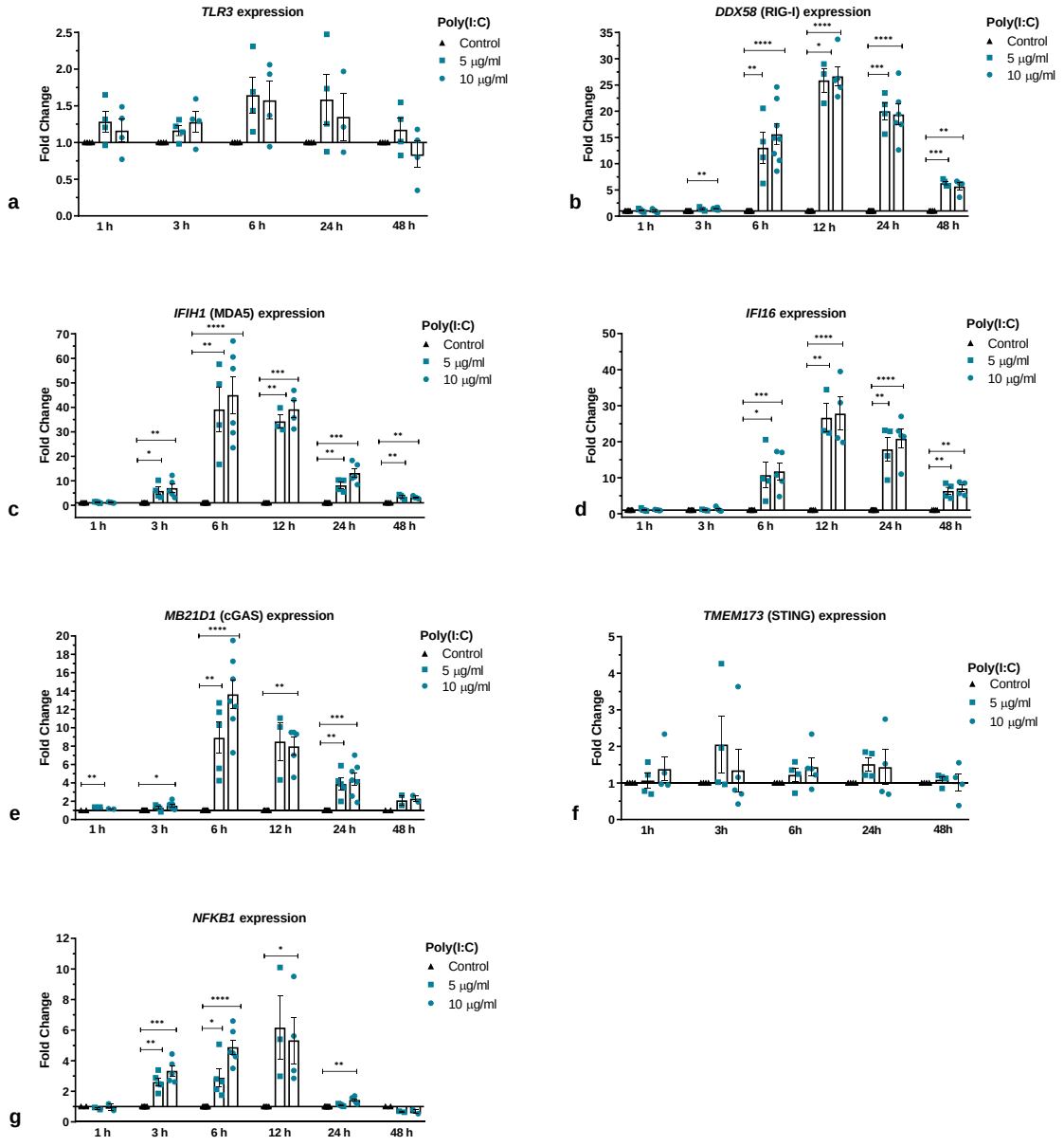

Figure 5.6 Immune receptor gene expression is upregulated in primary tracheal epithelial cells stimulated with Poly(I:C)

*Confluent tracheal epithelial cells were stimulated for 1, 3, 6, 12, 24 or 48 hours with 5 or 10 μg/ml Poly(I:C). Cells were harvested into Trizol. RNA was extracted and first strand cDNA reverse transcribed. qPCR was carried out and gene Cq values were normalised to the reference gene H3F3A and values normalised to the untreated control. Each data point represents a different animal. Error bars indicate standard error of the mean. Statistical analysis was performed on the ΔCt values using a mixed-effects model with the Geisser-Greenhouse correction followed by Sidak's multiple comparisons test. Asterisks indicate statistically significant differences relative to the untreated control: *= adjusted p<0.05; **= adjusted p<0.01; ***=adjusted p<0.001; ****=adjusted p<0.0001; n=2-8.*

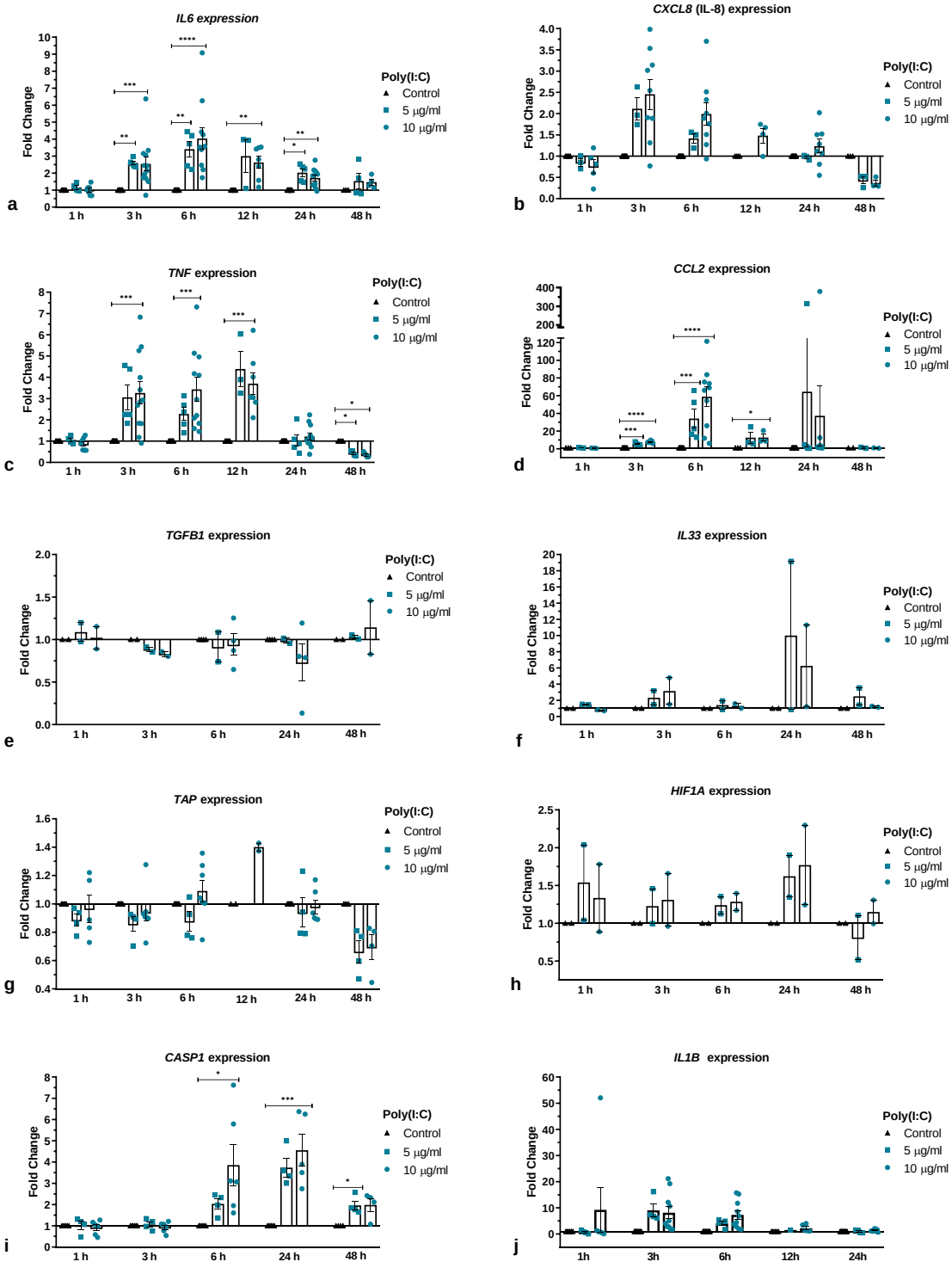
a
IL6 expression
Fold Change
1 h
3 h
6 h
12 h
24 h
48 h
Poly(I:C)
Control
5 μg/ml
10 μg/ml
b
CXCL8 (IL-8) expression
c
TNF expression
d
CCL2 expression
e
TGFB1 expression
f
IL33 expression
g
TAP expression
h
HIF1A expression
i
CASP1 expression
j
IL1B expression
1h
3h
6h
12h
24h

Figure 5.7 Chemokine and cytokine gene expression is upregulated in primary tracheal epithelial cells stimulated with Poly(I:C)

*Confluent tracheal epithelial cells were stimulated for 1, 3, 6, 12, 24 or 48 hours with 5 or 10 µg/ml Poly(I:C). Cells were harvested into Trizol. RNA was extracted and first strand cDNA reverse transcribed. qPCR was carried out and gene Cq values were normalised to the reference gene H3F3A and values normalised to the untreated control. Each data point represents a different animal. Error bars indicate standard error of the mean. Statistical analysis was performed on the ΔCt values using a mixed-effects model with the Geisser-Greenhouse correction followed by Sidak's multiple comparisons test. Asterisks indicate statistically significant differences relative to the untreated control: *= adjusted p<0.05; **= adjusted p<0.01; ***=adjusted p<0.001; ****=adjusted p<0.0001; n=2-11.*

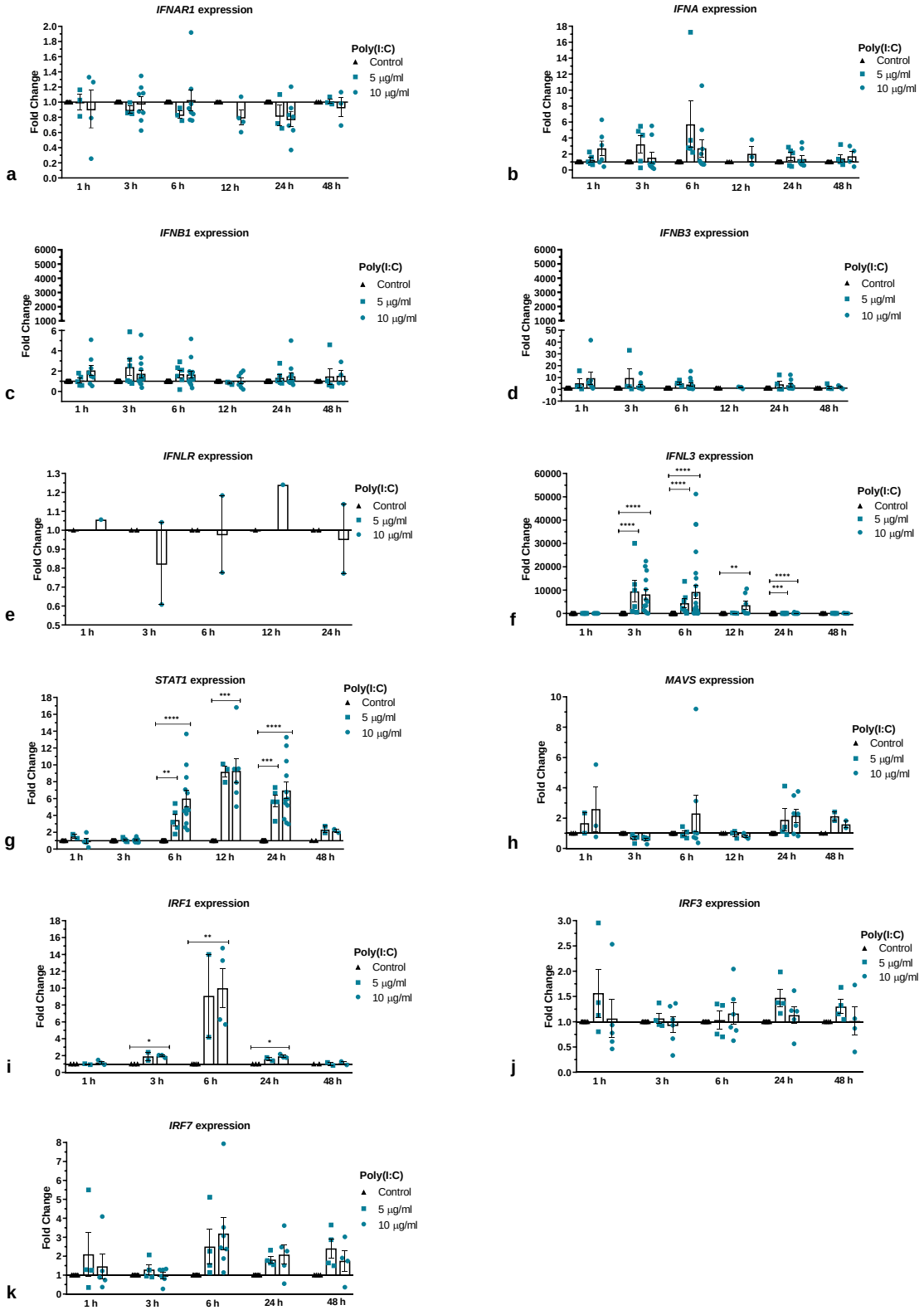
a
IFNAR1 expression
Fold Change
Poly(I:C)
Control
5 μg/ml
10 μg/ml
1 h
3 h
6 h
12 h
24 h
48 h
b
IFNA expression
c
IFNB1 expression
d
IFNB3 expression
e
IFNLR expression
f
IFNL3 expression
g
STAT1 expression
h
MAVS expression
i
IRF1 expression
j
IRF3 expression
k
IRF7 expression

Figure 5.8 Interferon and interferon pathway genes are upregulated in primary tracheal epithelial cells stimulated with Poly(I:C)

*Confluent tracheal epithelial cells were stimulated for 1, 3, 6, 12, 24 or 48 hours with 5 or 10 µg/ml Poly(I:C). Cells were harvested into Trizol. RNA was extracted and first strand cDNA reverse transcribed. qPCR was carried out and gene Cq values were normalised to the reference gene H3F3A and values normalised to the untreated control. Each data point represents a different animal. Error bars indicate standard error of the mean. Statistical analysis was performed on the ΔCt values using a mixed-effects model with the Geisser-Greenhouse correction followed by Sidak's multiple comparisons test. Asterisks indicate statistically significant differences relative to the untreated control: *= adjusted p<0.05; **= adjusted p<0.01; ***=adjusted p<0.001; ****=adjusted p<0.0001; n=1-24.*

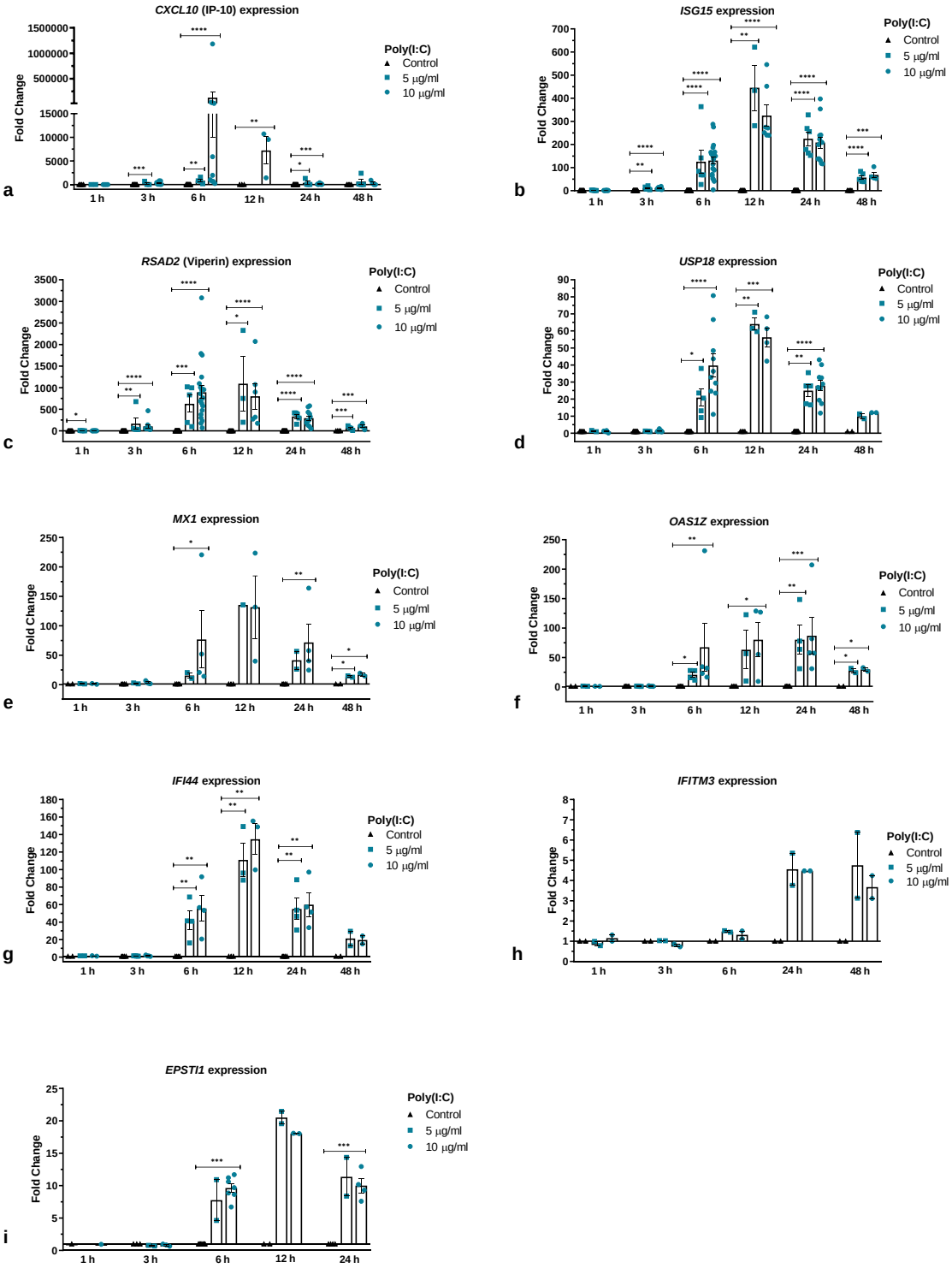
a
CXCL10 (IP-10) expression
Fold Change
1500000
1000000
500000
15000
10000
5000
0
1 h
3 h
6 h
12 h
24 h
48 h
Poly(I:C)
Control
5 μg/ml
10 μg/ml
b
ISG15 expression
700
600
500
400
300
200
100
0
c
RSAD2 (Viperin) expression
3500
3000
2500
2000
1500
1000
500
0
d
USP18 expression
90
80
70
60
50
40
30
20
10
0
e
MX1 expression
250
200
150
100
50
0
f
OAS1Z expression
g
IFI44 expression
180
160
140
120
100
80
60
40
20
0
h
IFITM3 expression
8
7
6
5
4
3
2
1
0
i
EPSTI1 expression
25
20
15
10
5
0

Figure 5.9 Interferon stimulated genes are upregulated in primary tracheal epithelial cells stimulated with Poly(I:C)

*Confluent tracheal epithelial cells were stimulated for 1, 3, 6, 12, 24 or 48 hours with 5 or 10 µg/ml Poly(I:C). Cells were harvested into Trizol. RNA was extracted and first strand cDNA reverse transcribed. qPCR was carried out and gene Cq values were normalised to the reference gene H3F3A and values normalised to the untreated control. Each data point represents a different animal. Error bars indicate standard error of the mean. Statistical analysis was performed on the ΔCt values using a mixed-effects model with the Geisser-Greenhouse correction followed by Sidak's multiple comparisons test. Asterisks indicate statistically significant differences relative to the untreated control: *= adjusted p<0.05; **= adjusted p<0.01; ***=adjusted p<0.001; ****=adjusted p<0.0001; n=1-21*

In order to identify any correlation between type I and type III interferon and the upregulation of ISGs in tracheal epithelial cells after Poly(I:C) stimulation, we conducted linear regression analysis. We could not identify any significant correlation between *IFNB1* or *IFNL3* expression and the expression of the ISGs ISG15 and Viperin. Whereas *ISG15* and *RSAD2* expression positively correlated with each other (**Fig. 5.10**).

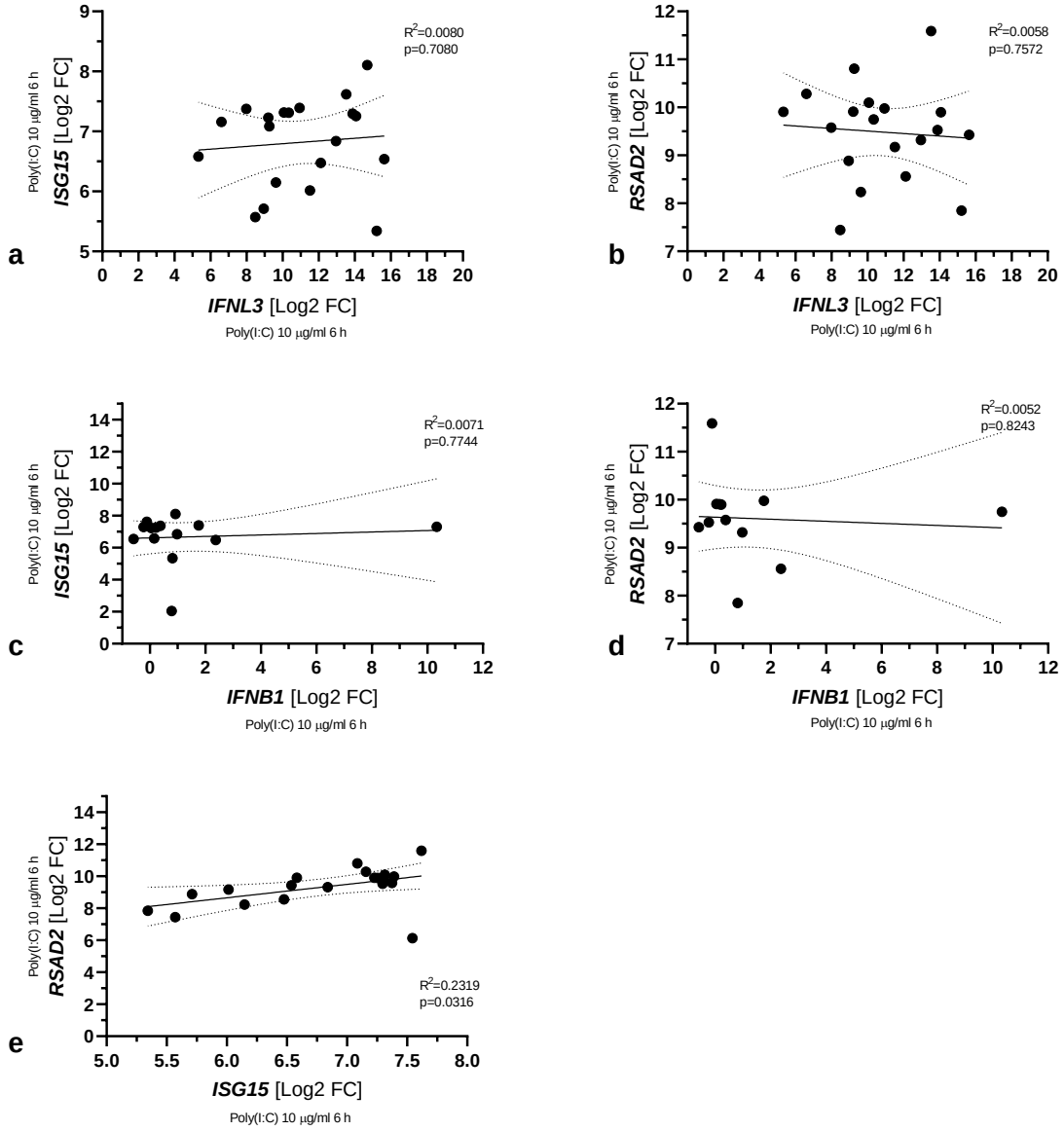

Figure 5.10 IFN and ISG gene upregulation in Poly(I:C) stimulated primary tracheal epithelial cells did not correlate

Confluent tracheal epithelial cells were stimulated for 6 hours with 10 µg/ml Poly(I:C). Cells were harvested into Trizol. RNA was extracted and first strand cDNA reverse transcribed. qPCR was carried out and gene Cq values were normalised to the reference gene H3F3A and values normalised to the untreated control. Each data point represents a different animal. Statistical analysis was performed on the log2 fold change values using a linear regression; n=10-19.

For stimulation and activation via RIG-I and MDA5, we used Poly(I:C)/LyoVec™, which is a complex between Poly(I:C) and the transfection reagent LyoVec™. LyoVec™ protects against degradation and facilitates uptake during transfection.

We found expression of RIG-I and MDA5 significantly upregulated at 24 hours after treatment (**Fig. 5.11 a-b**). The expression of cytokines and chemokines *TNF, IL6, IL8* and *IL1B* were not regulated after transfection of Poly(I:C) between 3 and 24 hours (**Fig. 5.11 c-f**).

Whereas *IFNB1* and *IFNB3* gene expression were not significantly changed after Poly(I:C), *IFNL3* was significantly upregulated at 12 hours by 782 fold and at 24

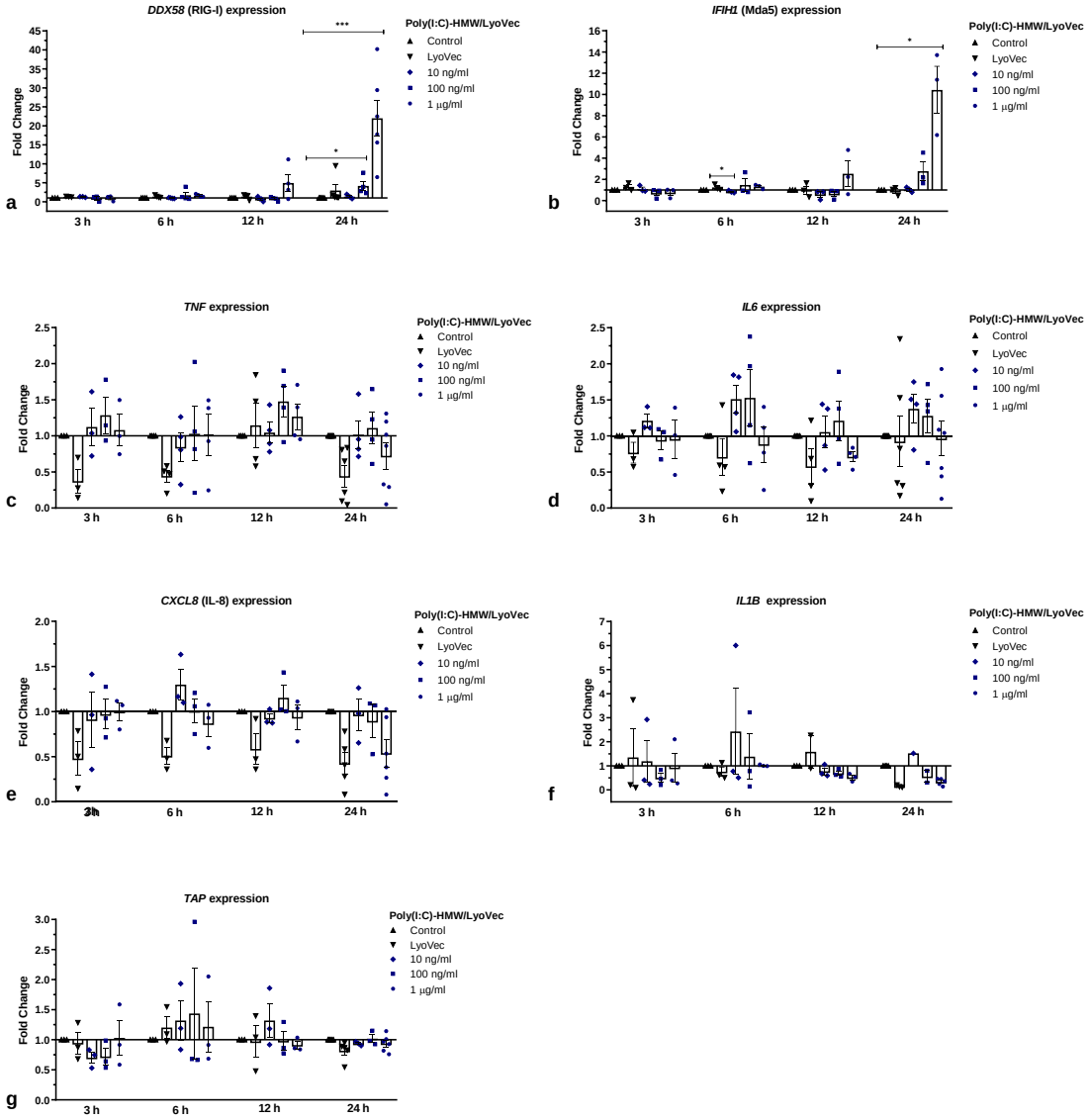

Figure 5.11 Expression of innate immune receptor, chemokine and cytokine genes in primary tracheal epithelial cells stimulated with transfected Poly(I:C)

*Confluent tracheal epithelial cells were stimulated for 3, 6, 12 or 24 hours with 10 ng/ml, 100 ng/ml or 1 µg/ml Poly(I:C)-HMW/LyoVec. Cells were harvested into Trizol. RNA was extracted and first strand cDNA reverse transcribed. qPCR was carried out and gene Cq values were normalised to the reference gene H3F3A and values normalised to the untreated control. Each data point represents a different animal. Error bars indicate standard error of the mean. Statistical analysis was performed on the ΔCt values using a mixed-effects model with the Geisser-Greenhouse correction followed by Sidak's multiple comparisons test. Asterisks indicate statistically significant differences relative to the untreated control: *= adjusted p<0.05; **= adjusted p<0.01; ***=adjusted p<0.001; ****=adjusted p<0.0001; n=1-7*

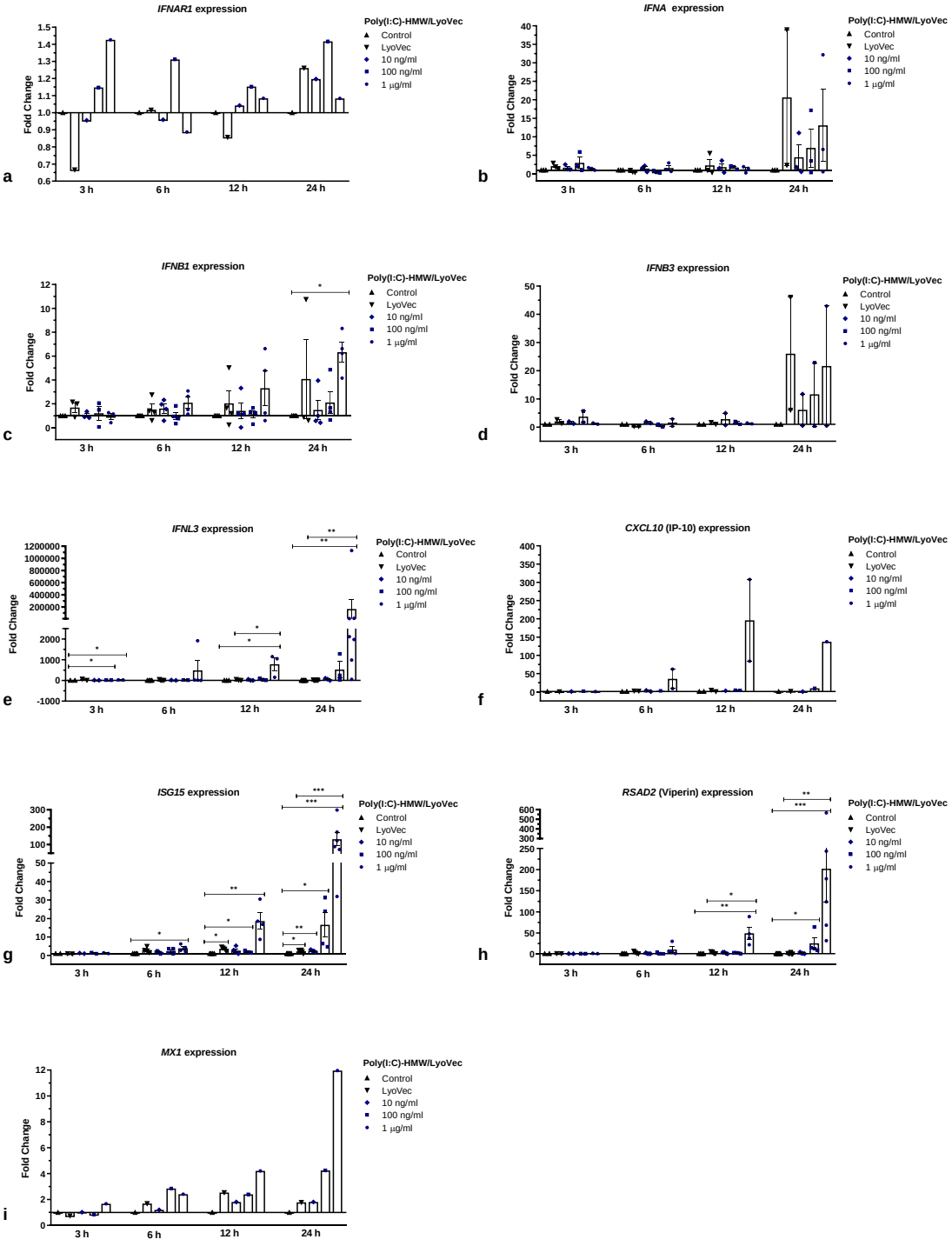
a
IFNAR1 expression
Fold Change
3 h
6 h
12 h
24 h
Poly(I:C)-HMW/LyoVec
Control
LyoVec
10 ng/ml
100 ng/ml
1 µg/ml
b
IFNA expression
c
IFNB1 expression
d
IFNB3 expression
e
IFNL3 expression
f
CXCL10 (IP-10) expression
g
ISG15 expression
h
RSAD2 (Viperin) expression
i
MX1 expression

Figure 5.12 Expression of interferon genes and interferon stimulated genes (ISG)) in primary tracheal epithelial cells stimulated with transfected Poly(I:C)

*Confluent tracheal epithelial cells were stimulated for 3, 6, 12 or 24 hours with 10 ng/ml, 100 ng/ml or 1 µg/ml Poly(I:C)-HMW/LyoVec. Cells were harvested into Trizol. RNA was extracted and first strand cDNA reverse transcribed. qPCR was carried out and gene Cq values were normalised to the reference gene H3F3A and values normalised to the untreated control. Each data point represents a different animal. Error bars indicate standard error of the mean. Statistical analysis was performed on the ΔCt values using a mixed-effects model with the Geisser-Greenhouse correction followed by Sidak's multiple comparisons test. Asterisks indicate statistically significant differences relative to the untreated control: *= adjusted p<0.05; **= adjusted p<0.01; ***=adjusted p<0.001; ****=adjusted p<0.0001; n=1-7.*

5.4.4. Poly(dA:dT) induced expression of innate immune genes in primary tracheal epithelial cells

Using the transfection of synthetic analog of dsDNA, Poly(dA:dT), we examined the response of tracheal epithelial cells to activation of cytosolic DNA sensors. Expression of cGAS, STING, IFI16 and NFκB was not induced at any time point between 3 and 24 hours stimulation (**Fig. 5.13 a-d**). Expression of the cytokines and chemokines *IL6, IL8, TNF, ILB1* and *CCL2* was similarly not upregulated **(Fig. 5.13 e-i**).

While gene expression of the type I interferons IFNA, IFNB1 and IFNB3 did not show significant changes, IFNL3 was significantly upregulated 752 fold after 24 hours stimulation with 5 µg/ml Poly(dA:dT)/LyoVec (**Fig. 5.14 f**). Expression of *STAT1*, *IRF3* and *IRF7* was not induced, although, the ISGs *ISG15* and *RSAD2* were significantly upregulated at 24 hours (**Fig. 5.14**).

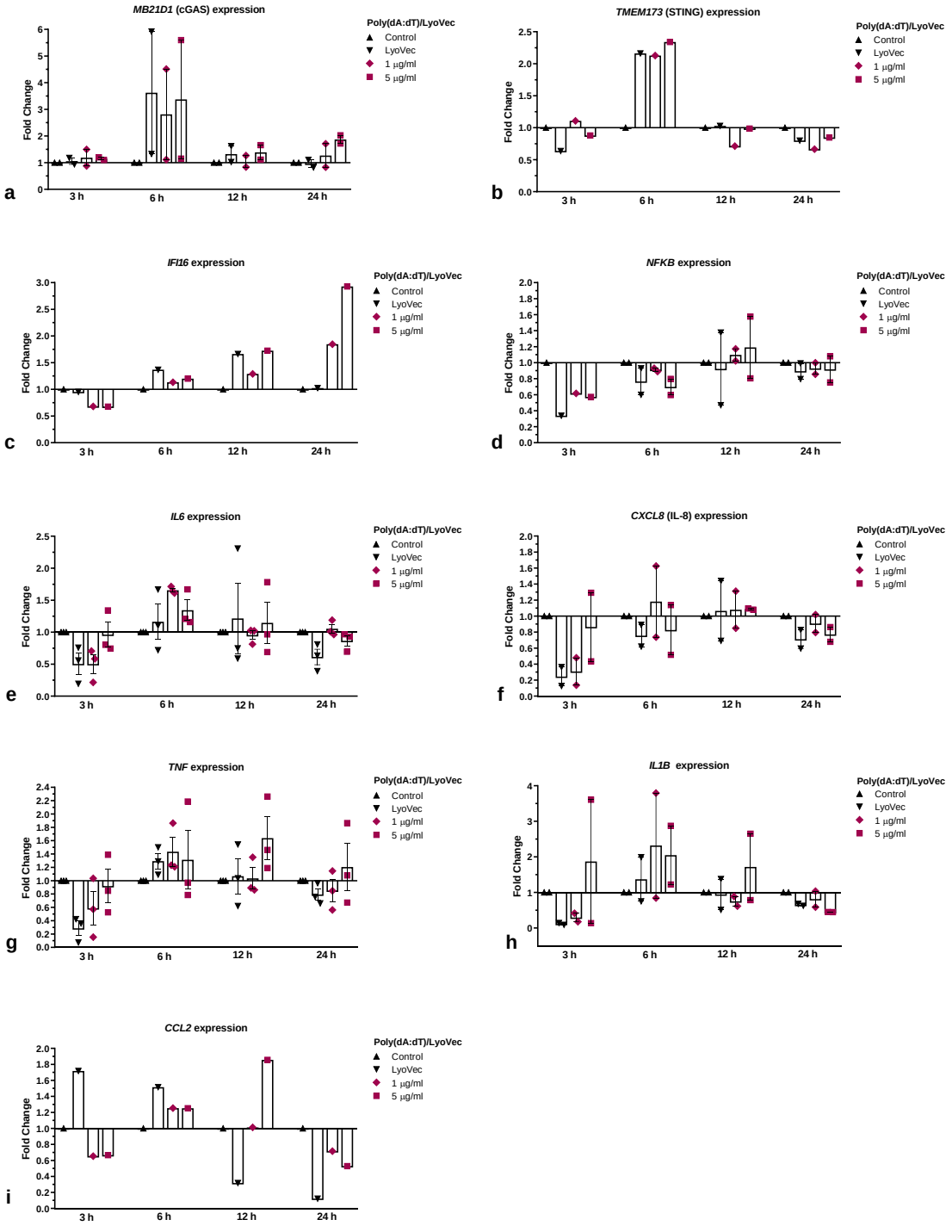
MB21D1 (cGAS) expression
TMEM173 (STING) expression
IFI16 expression
NFKB expression
IL6 expression
CXCL8 (IL-8) expression
TNF expression
IL1B expression
CCL2 expression
Fold Change
3 h
6 h
12 h
24 h
Poly(dA:dT)/LyoVec
Control
LyoVec
1 µg/ml
5 µg/ml
a
b
c
d
e
f
g
h
i

Figure 5.13 Expression of innate immune receptors, chemokines and cytokines genes in primary tracheal epithelial cells stimulated with transfected Poly(dA:dT)

*Confluent tracheal epithelial cells were stimulated for 3, 6, 12 or 24 hours with 1 µg/ml or 5 µg/ml Poly(dA:dT)/LyoVec. Cells were harvested into Trizol. RNA was extracted and first strand cDNA reverse transcribed. qPCR was carried out and gene Cq values were normalised to the reference gene H3F3A and values normalised to the untreated control. Each data point represents a different animal. Error bars indicate standard error of the mean. Statistical analysis was performed on the ΔCt values using a mixed-effects model with the Geisser-Greenhouse correction followed by Sidak's multiple comparisons test. Asterisks indicate statistically significant differences relative to the untreated control: *= adjusted p<0.05; **= adjusted p<0.01; ***=adjusted p<0.001; ****=adjusted p<0.0001; n=1-3.*

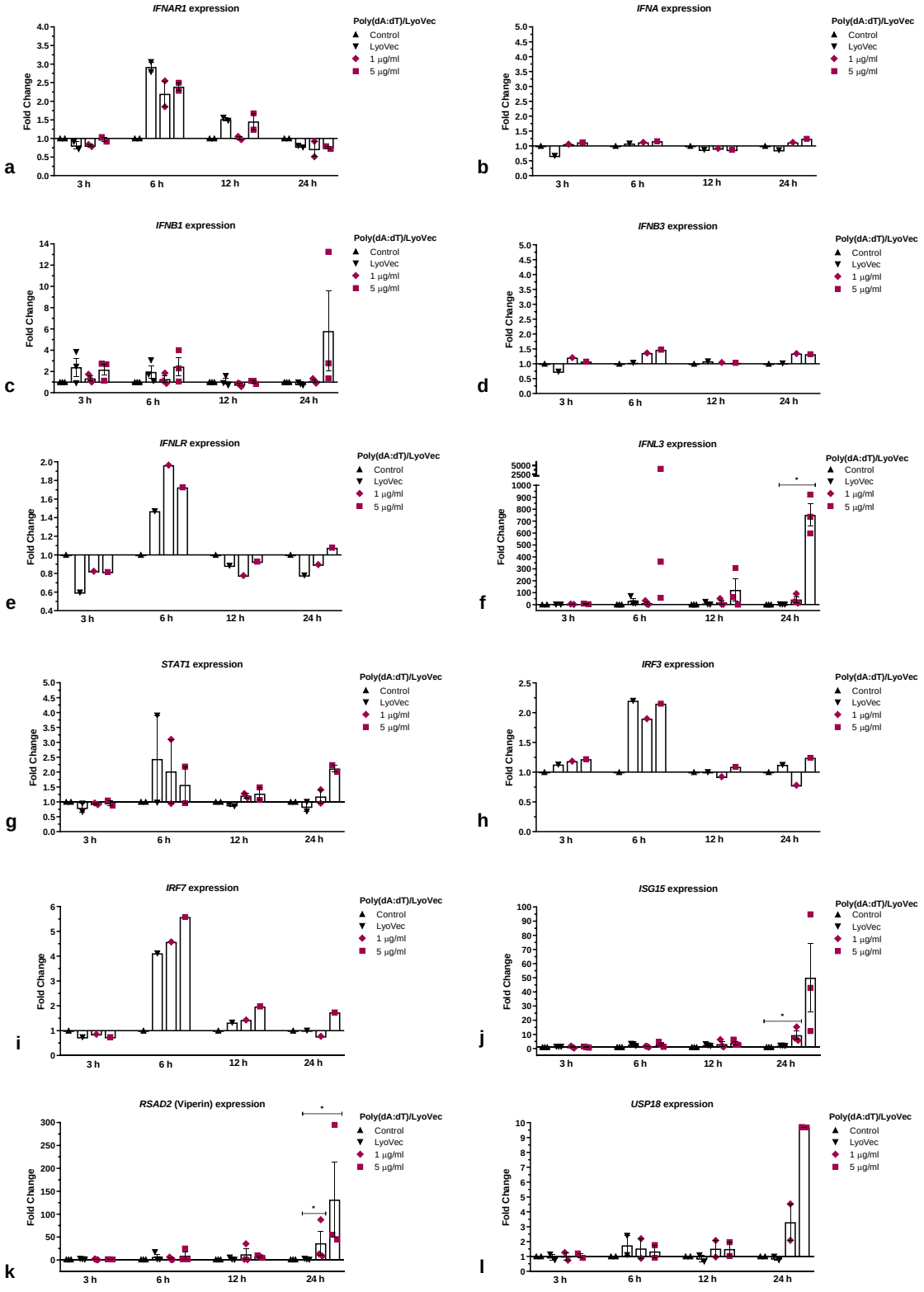
a
IFNAR1 expression
b
IFNA expression
c
IFNB1 expression
d
IFNB3 expression
e
IFNLR expression
f
IFNL3 expression
g
STAT1 expression
h
IRF3 expression
i
IRF7 expression
j
ISG15 expression
k
RSAD2 (Viperin) expression
l
USP18 expression
Fold Change
3 h
6 h
12 h
24 h
Poly(dA:dT)/LyoVec
Control
LyoVec
1 µg/ml
5 µg/ml

Figure 5.14 Expression of interferon genes and interferon stimulated genes (ISGs) in primary tracheal epithelial cells stimulated with transfected Poly(dA:dT)

*Confluent tracheal epithelial cells were stimulated for 3, 6, 12 or 24 hours with 1 µg/ml or 5 µg/ml Poly(dA:dT)/LyoVec. Cells were harvested into Trizol. RNA was extracted and first strand cDNA reverse transcribed. qPCR was carried out and gene Cq values were normalised to the reference gene H3F3A and values normalised to the untreated control. Each data point represents a different animal. Error bars indicate standard error of the mean. Statistical analysis was performed on the ΔCt values using a mixed-effects model with the Geisser-Greenhouse correction followed by Sidak's multiple comparisons test. Asterisks indicate statistically significant differences relative to the untreated control: *= adjusted p<0.05; **= adjusted p<0.01; ***=adjusted p<0.001; ****=adjusted p<0.0001; n=1-3.*

5.4.5. 3p-hpRNA induced the expression of innate immune genes in primary tracheal epithelial cells

After stimulation with 3p-hpRNA, a specific RIG-I agonist, RIG-I gene expression itself was upregulated in primary tracheal epithelial cells 3 fold and Mda5 3 fold after 6 hours (**Fig. 5.15 a-b**). While *NFKB*, *IL6*, *TNF* and *IFNB1* were not significantly regulated, *IFNL3*, *ISG15* and *RSAD2* were significantly upregulated. *IFNL3* was upregulated 36 fold 6 hours after treatment with 3p-hpRNA (**Fig. 5.15 h**).

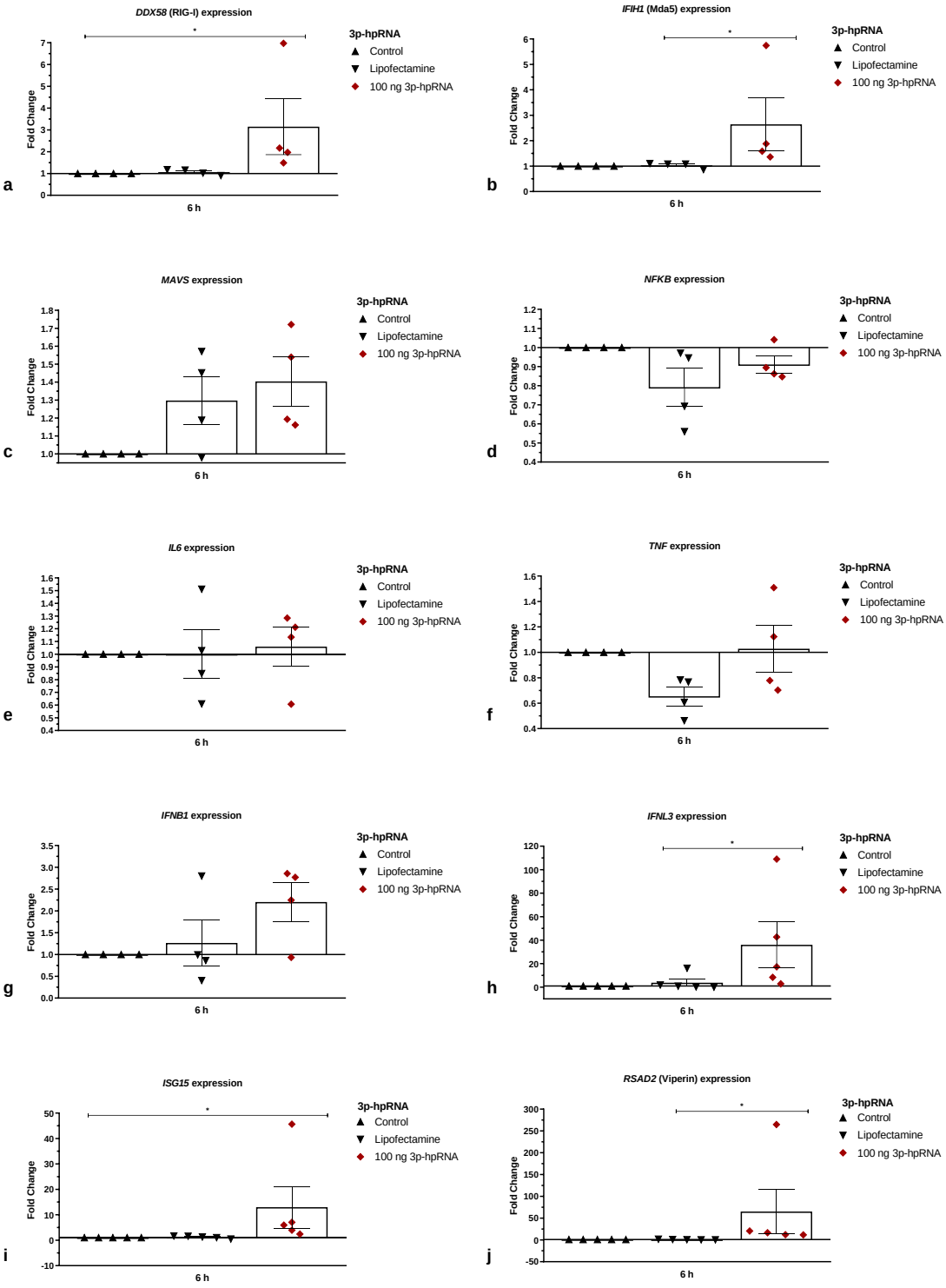
a
DDX58 (RIG-I) expression
Fold Change
6 h
3p-hpRNA
Control
Lipofectamine
100 ng 3p-hpRNA
b
IFIH1 (Mda5) expression
c
MAVS expression
d
NFKB expression
e
IL6 expression
f
TNF expression
g
IFNB1 expression
h
IFNL3 expression
i
ISG15 expression
j
RSAD2 (Viperin) expression

Figure 5.15 Expression of innate immune genes, cytokines, chemokines, interferons and interferon stimulated genes in primary tracheal epithelial cells stimulated with transfected 3p-hpRNA

*Confluent tracheal epithelial cells were stimulated for 6 hours with 100 ng/ml 3p-hpRNA transfected with Lipofectamine. Cells were harvested into Trizol. RNA was extracted and first strand cDNA reverse transcribed. qPCR was carried out and gene Cq values were normalised to the reference gene H3F3A and values normalised to the untreated control. Each data point represents a different animal. Error bars indicate standard error of the mean. Statistical analysis was performed on the ΔCt values using a Friedman test followed by Dunn's multiple comparisons test. Asterisks indicate statistically significant differences relative to the untreated control: *= adjusted p<0.05; n=4.*

5.4.6. The innate immune response to Poly(I:C) stimulation in polarised primary tracheal epithelial cells

Having shown that bovine primary tracheal epithelial cells in a monolayer did not upregulate the analysed chemokines, cytokines and type I interferons while upregulating IFNL3 and ISGs, we established a culture model of polarised primary tracheal epithelial cells. Measuring the trans-epithelial electrical resistance (TEER), we obtained confluent polarised epithelial cells after 14 days of culture with resistance greater than 1,000Ωcm^2, indicating full polarization and confluency of the epithelial barrier (**Fig. 5.16**).

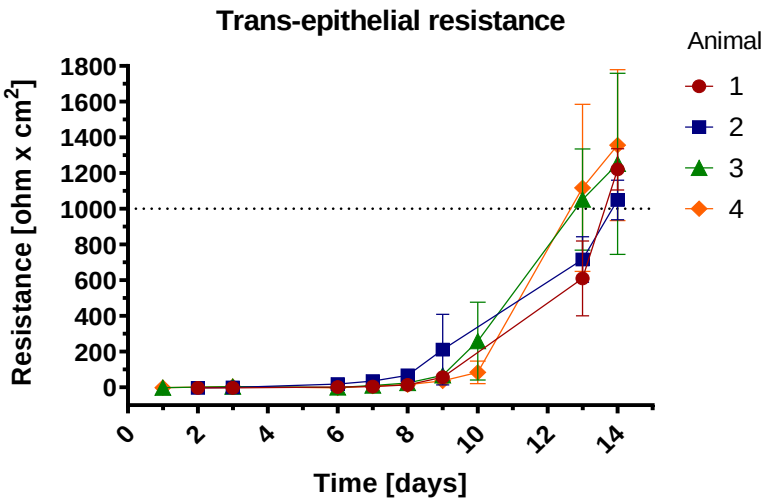

Figure 5.16 Establishment of a model of polarized bovine tracheal epithelial cells

Polarized epithelial cell cultures were prepared by seeding 0.5 × 10^5 cells on each hanging cell culture insert, which had previously been coated with 50 µl of matrigel diluted 1:8 in LH-9 media and left at room temperature for 1 hour before the remaining matrigel was aspirated. Inserts were placed in 24 well plates, with 300 µl and 800 µl of culture medium in the apical and basolateral compartment respectively. Trans-epithelial electrical resistance (TEER) was used to examine the permeability of the epithelial barrier. TEER values were recorded using an epithelial volt-ohm meter. Values were corrected for the area of the transwell insert and baseline levels were accounted for by measuring a blank (containing no cells) insert. A value greater than 1,000Ωcm^2 indicated full polarization and confluency of the epithelial barrier.

Comparing gene expression changes in tracheal epithelial cells stimulated with Poly(I:C) in monolayers compared to polarised cultures revealed that gene expression changed less in polarised cells overall. Comparing apical vs. basolateral stimulation with Poly(I:C), basolateral stimulation caused higher gene upregulation. Expression of *DDX58* and *IFIH1* was upregulated more in cells grown as monolayer compared to apical stimulation of polarised epithelial cells (**Fig. 5.17 a-b**). Type I interferons *IFNA, IFNB1* and *IFNB3* were downregulated in polarised epithelial cells after Poly(I:C) stimulation. Whereas *IFNL3* was upregulated less after apical stimulation and similar after basolateral stimulation compared to the stimulation of monolayered epithelial cells (**Fig. 5.18 e**). A similar trend could be observed in the expression of the ISGs ISG15 and Viperin (**Fig. 5.18 g-h**).

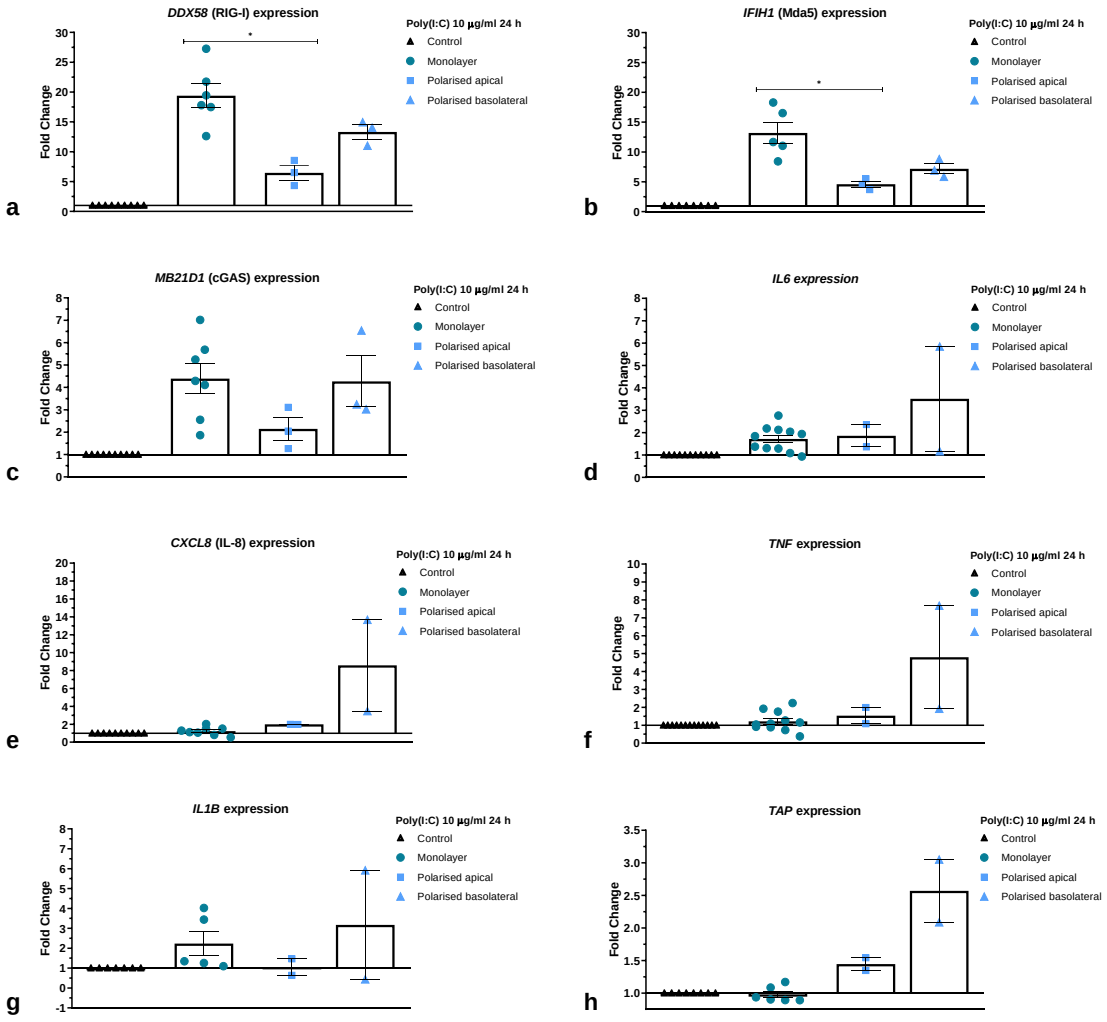

Figure 5.17 Expression of immune receptor, cytokine and chemokine genes in polarised bovine tracheal epithelial cells stimulated with Poly(I:C)

*Epithelial cells were grown to confluency on transwell inserts coated with matrigel and allowed to polarize before stimulation with 10 µg/ml Poly(I:C) in either the apical or basolateral compartment for 24 hours. Following stimulation, the cells were harvested into Trizol. RNA was extracted and first strand cDNA reverse transcribed. qPCR was carried out and gene Cq values were normalised to the reference gene H3F3A and values normalised to the untreated control. Each data point represents a different animal. Error bars indicate standard error of the mean. Statistical analysis was performed using a Kruskal-Wallis test followed by the Dunn's multiple comparison test. Asterisks indicate statistically significant differences between the two groups: *= adjusted p<0.05; **= adjusted p<0.01; ***=adjusted p<0.001; n=2-11.*

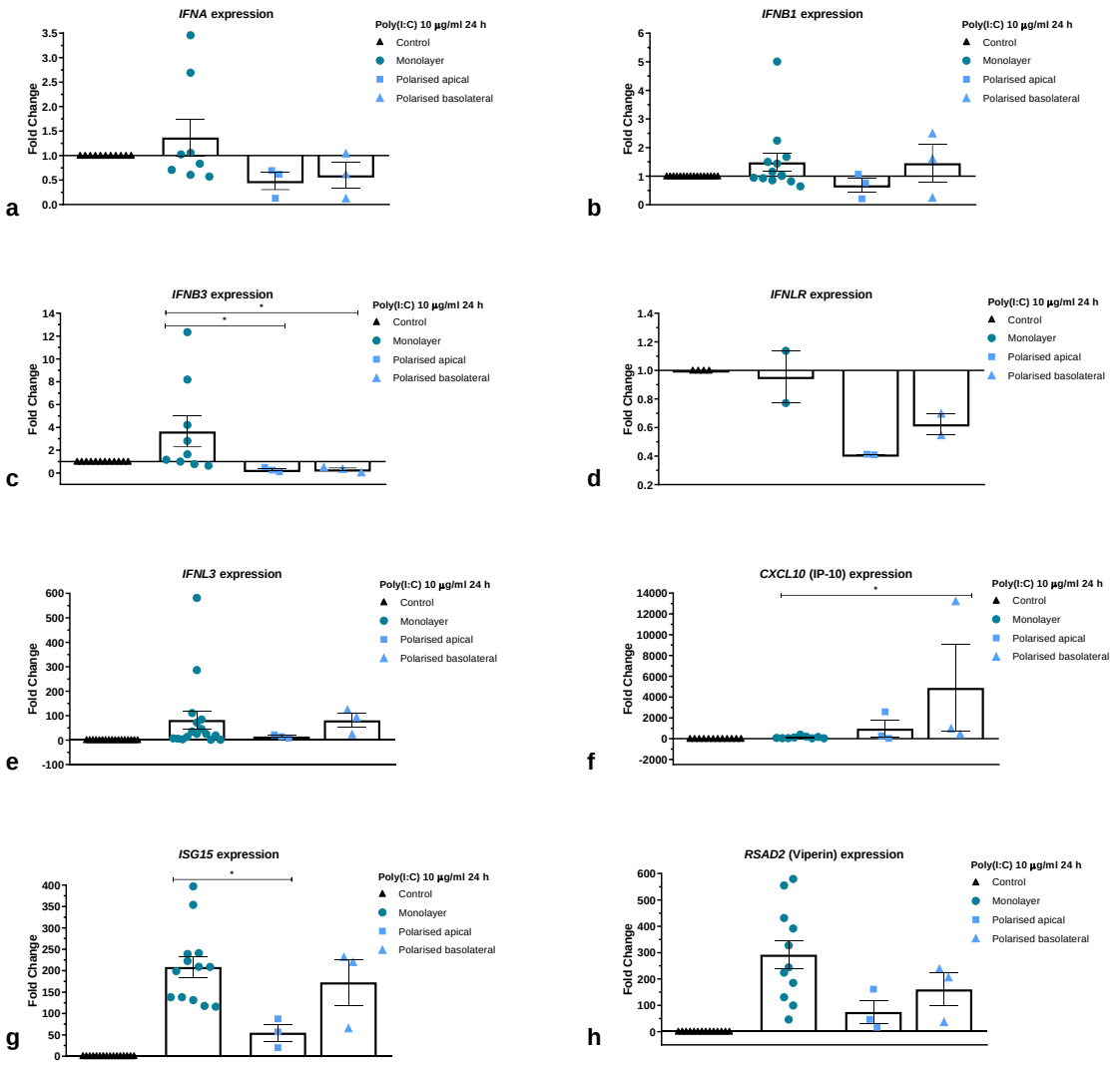

Figure 5.18 Expression of interferon genes and interferon stimulated genes (ISGs) in polarised bovine tracheal epithelial cells stimulated with Poly(I:C)

*Epithelial cells were grown to confluency on transwell inserts coated with matrigel and allowed to polarize before stimulation with 10 µg/ml Poly(I:C) in either the apical or basolateral compartment. Following stimulation, the cells were harvested into Trizol. RNA was extracted and first strand cDNA reverse transcribed. qPCR was carried out and gene Cq values were normalised to the reference gene H3F3A and values normalised to the untreated control. Each data point represents a different animal. Error bars indicate standard error of the mean. Statistical analysis was performed using a Kruskal-Wallis test followed by the Dunn's multiple comparison test. Asterisks indicate statistically significant differences between the two groups: *= adjusted p<0.05; **= adjusted p<0.01; ***=adjusted p<0.001; n=2-13.*

5.4.7. IFNB1 protein does not inhibit the replication of BoHV-1 in primary tracheal epithelial cells

Bovine IFNB1 protein was tested for its antiviral function against BoHV-1 infection of primary tracheal epithelial cells. Cells were pre-treated with IFNB1, or IFNB1 was added simultaneously with the virus to the cell culture media. We could not detect any influence of IFNB1 treatment on the BoHV-1 virus load (**Fig. 5.19**). However, we observed a reduced viral load after pre-treatment of 24 hours by -2.27 log2 fold with the solvent control PBS with 0.1% BSA (**Fig. 5.19 a**).

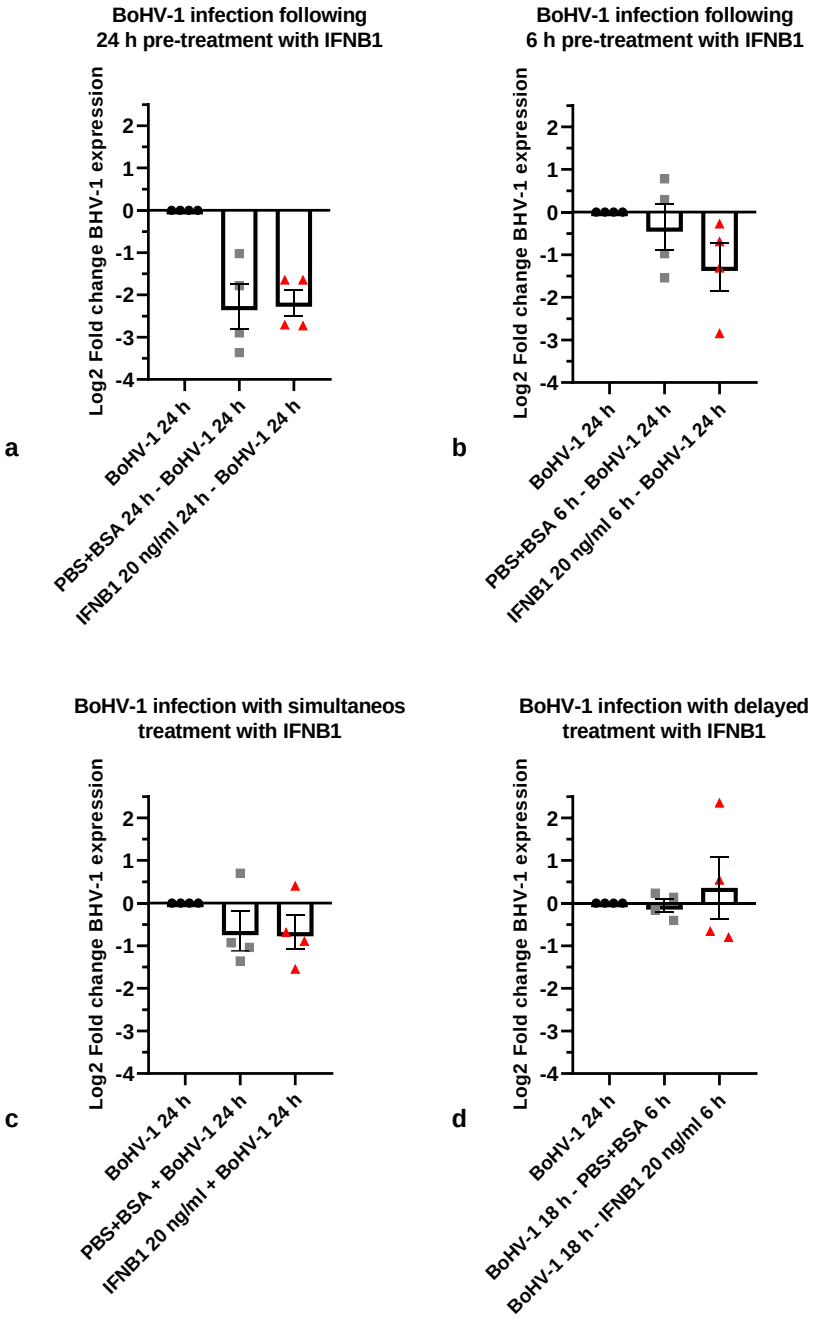

Figure 5.19 IFNB1 stimulation does not inhibit the replication of live bovine herpes virus 1 in primary tracheal epithelial cells

*Confluent primary bovine tracheal epithelial cells were stimulated with IFNB1 prior (A-B), simultaneous (C) and after (D) infection with purified live bovine herpes virus 1. Cells were harvested into Trizol. RNA was extracted and first strand cDNA reverse transcribed. qPCR for BoHV-1 expression was carried out and gene Cq values were normalised to the reference gene H3F3A. Values were normalised to the BoHV-1 infected control. Each data point represents a different animal. Error bars indicate standard error of the mean. Statistical analysis was performed on the 2^-ΔCT values using the Friedman test followed by the Dunn's multiple comparison test. Asterisks indicate statistically significant differences relative to the BoHV-1 infected control: *= adjusted p<0.05; n=4.*

5.4.8. Supernatants from tracheal epithelial cells stimulated with Poly(I:C) do not inhibit the replication of BoHV-1 in primary tracheal epithelial cells

Having shown that Poly(I:C) stimulation upregulates IFNL3 and various ISGs, we aimed to investigate their antiviral abilities. We wondered might the antiviral agent be present in supernatants from stimulated epithelial cells. We therefore tested the influence of conditioned media from cells stimulated with Poly(I:C) on the infection of primary tracheal epithelial cells infected with BoHV-1. The conditioned media was produced by the stimulation of primary tracheal epithelial cells with Poly(I:C) for 3 hours followed by a replacement of the media. The media replacement after 3 hours assured the conditioned media did not have any Poly(I:C) and did not influence the gene expression changes observed in cells stimulated with Poly(I:C). The removal of Poly(I:C) did not influence the upregulation of *DDX58*, *IFNL3*, *ISG15* and *RSAD2* (**Fig. 5.20 a-d**). The conditioned media from epithelial cells stimulated with Poly(I:C) for 6BoHV-1 presence 24 hours after infection (**Fig. 5.20 e**). The conditioned media from epithelial cells stimulated with Poly(I:C) for 24BoHV-1 presence analysed 24 hours after infection ($p=0.275$) (**Fig. 5.20 f**).

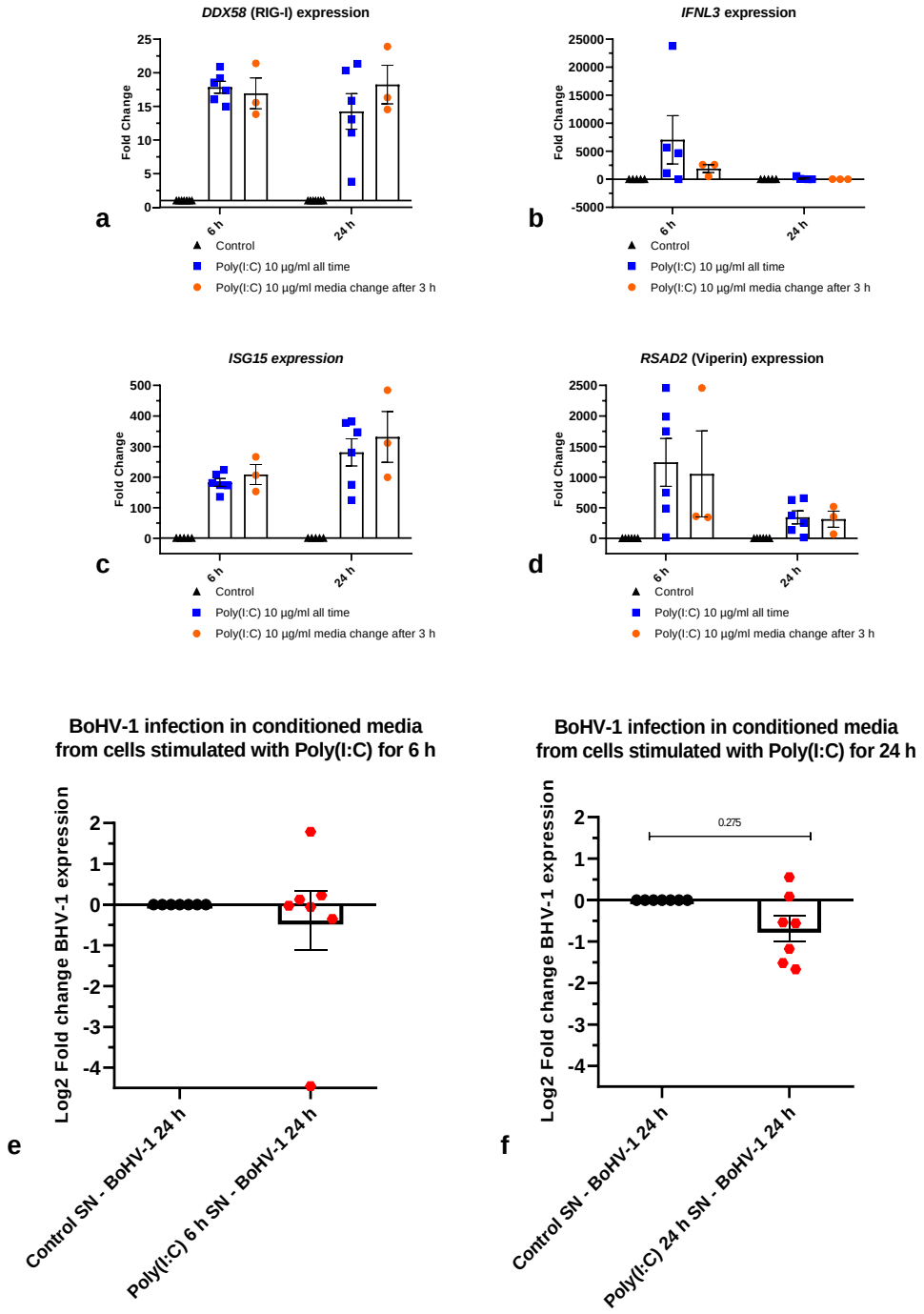

Figure 5.20 Supernatant of tracheal epithelial cells stimulated with Poly(I:C) does not inhibit the replication of live bovine herpes virus 1 in primary tracheal epithelial cells

Confluent primary bovine tracheal epithelial cells were stimulated with Poly(I:C) and the media replaced after the initial first 3 hours of stimulation. The supernatant was transferred to new cells and infected with purified live bovine herpes virus 1. Cells were harvested into Trizol. RNA was extracted and first strand cDNA reverse transcribed. qPCR for BoHV-1 expression was carried out and gene Cq values were normalised to the reference gene H3F3A. Values were normalised to the BoHV-1 infected control. Each data point represents a different animal. Error bars indicate standard error of the mean. Statistical analysis was performed on the 2^-ΔCT values using the Wilcoxon matched-pairs signed rank test; n=7.

5.4.9. Poly(I:C) stimulation inhibits the replication of BoHV-1 in primary tracheal epithelial cells

Having shown that primary bovine epithelial cells upregulate innate antiviral immune genes in response to Poly(I:C) stimulation, we stimulated cells with Poly(I:C) prior to infection with BoHV-1. Interestingly, 24-hour pre-treatment with Poly(I:C) resulted in significantly decreased viral genome presence with a log2 fold change of -5.84. Pre-treatment for 6 hours decreased viral genome presence with a log2 fold change of -7.23 and the simultaneous treatment caused a log2 fold change of -6.82 (**Fig. 5.21 a-c**). Delayed treatment with Poly(I:C) after 18 hours of BoHV-1 infection did not significantly change the viral load compared to the BoHV-1 infection control (**Fig. 5.21 d**).

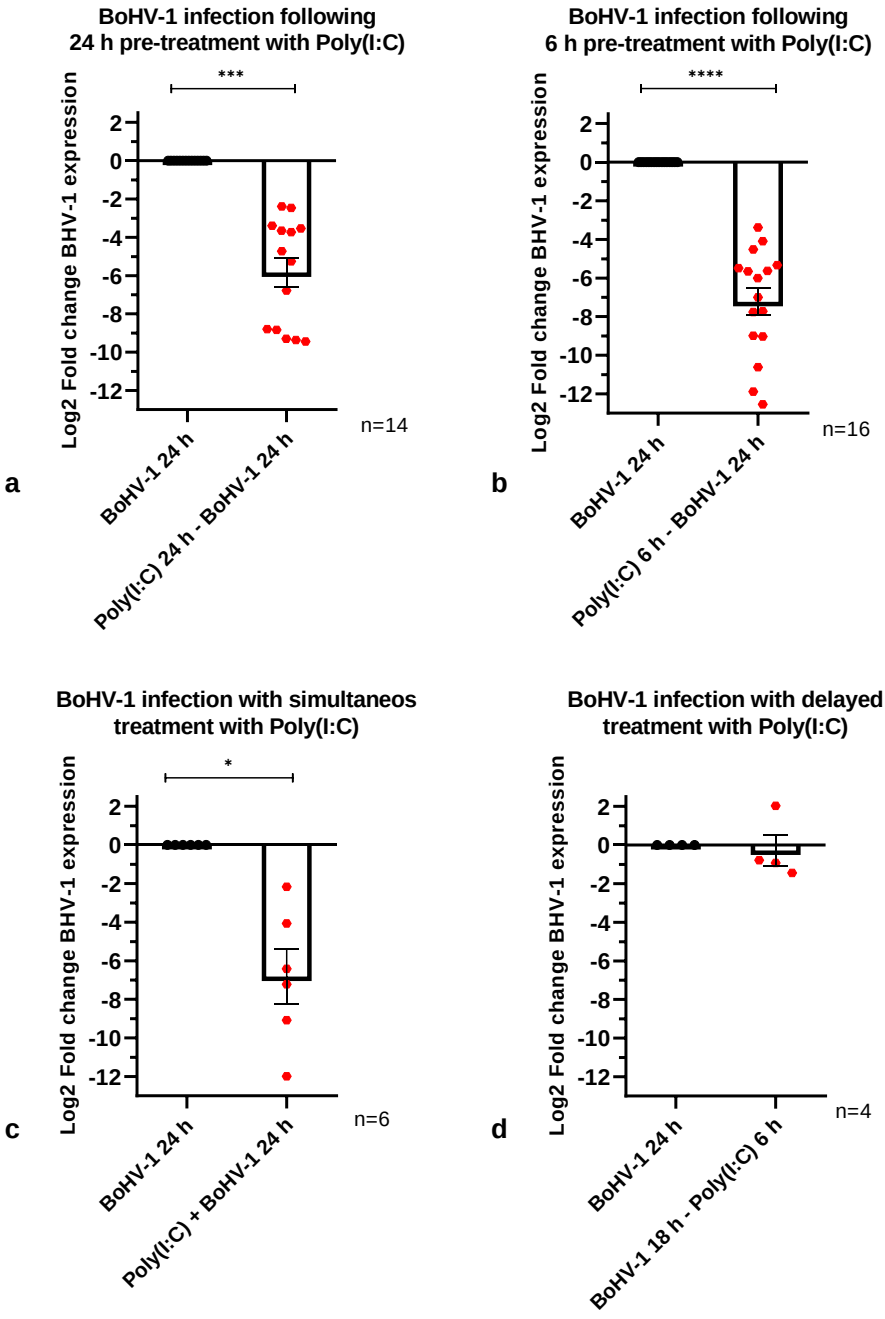

Figure 5.21 Poly(I:C) stimulation inhibits the replication of live bovine herpes virus 1 in primary tracheal epithelial cells

*Confluent primary bovine tracheal epithelial cells were stimulated with Poly(I:C) prior (A-B), simultaneous (C) and after (D) infection with purified live bovine herpes virus 1. Cells were harvested into Trizol. RNA was extracted and first strand cDNA reverse transcribed. qPCR for BoHV-1 expression was carried out and gene Cq values were normalised to the reference gene H3F3A. Values were normalised to the BoHV-1 infected control. Each data point represents a different animal. Error bars indicate standard error of the mean. Statistical analysis was performed on the 2^-ΔCT values using the Wilcoxon matched-pairs signed rank test. Asterisks indicate statistically significant differences relative to the BoHV-1 infected control: *= adjusted p<0.05; **= adjusted p<0.01; ***=adjusted p<0.001; ****=adjusted p<0.0001.*

5.5. Discussion

Our study demonstrates that epithelial cells can detect and respond to viral presence early after infection. We found that increased expression of IFNL3 characterises this early innate antiviral immune activity induced by Poly(I:C), Poly(dA:dT) and 5'triphosphate hairpin RNA. The antiviral state within epithelial cells initiated by the activation of the TLR3 signaling pathway protected against replication of BoHV-1.

In our experiments, stimulation of primary bovine epithelial cells with various synthetic viral mimics was characterised by hypo-responsiveness. We could not detect upregulation of the pro-inflammatory cytokines, chemokines or type I interferons. One important reason for the indolent responsiveness of tracheal epithelial cells is their localisation in constant contact to the environment and commensal bacteria requiring tight regulation of immune and inflammatory activity. Literature proposes that mechanisms in the respiratory system have evolved to keep immune functions under control. Weitnauer and colleagues suggest that epithelial cells modulate the sensitivity of innate immune sensing (Weitnauer et al., 2016). Only if antigens or pathogens exceed a certain threshold of tolerance, will the inhibitory microenvironment switch to a stimulatory one and initiate immune activity. Interestingly, it has been shown that airway epithelial cells are also hyporesponsive towards TLR2 and TLR4 agonists, even though they express these receptors (Ioannidis et al., 2013; Mayer et al., 2007). We found polarised primary tracheal epithelial cells to be less responsive than epithelial cells cultured as monolayers. Epithelial tight junctions are characteristic of polarised airway cells and the restriction of sensor molecules to the inaccessible basolateral side has been discussed as another mechanism of reduced responsiveness (Ioannidis et al., 2013). According to this model, only virulent pathogens, overcoming the physical carrier, can drive extended activation of pro-inflammatory signals. The importance of a functional tight epithelial barrier is displayed in the context of the acute respiratory stress syndrome. The full syndrome develops, if the loss of epithelial cell integrity allows neutrophils to become activated due to getting in contact with bacterial products in the lumen (Yang et al., 2021).

The recent SARS-CoV-2 pandemic has highlighted the importance of type I and III interferons, both potent antiviral cytokines, in the upper respiratory tract. In addition to their beneficial effects early in infection, dysregulation of these interferon families showed significant detrimental roles in patients with COVID-19 (Zanoni, 2021). Therefore, more information regarding the time, localisation and activity of the members of the interferon family is needed to understand the role of interferons in the innate immunity in the respiratory tract. In our experiments using bovine epithelial cells, Poly(I:C) led to a significant upregulation of proinflammatory cytokines and *IFNL3*. However, *IFNB1* and *IFNB3* were not significantly regulated. A study conducted by Ioannidis and colleagues measured IFN production by human airway epithelial cells in response to different synthetic PAMPs and influenza virus. The results indicated that although all TLR ligands tested were capable of inducing airway epithelial cell activation and cytokine production, only Poly(I:C) 10 μg/ml and influenza virus H3N2 stimulation could trigger the production of both IFNB and IFNL protein (Ioannidis et al., 2013).

Our results highlight an important role for IFN-λ at epithelial surfaces. However, the precise mechanism has not been defined. We found that increased expression of IFNL3 characterises the innate immune response in bovine primary tracheal epithelial cells stimulated with Poly(I:C), Poly(dA:dT) and 5'triphosphate hairpin RNA. This suggests an important role for the TLR3/RIG-I pathway for the induction of IFNL in bovine respiratory epithelial cells. In line with these results a study found IFNL but not IFNB or IFNA induced by respiratory virus infection in primary human nasal epithelial cells and the suppression of RIG-I but not MDA5 expression using siRNA significantly reduced IFNL1 production in RSV infected cells (Okabayashi et al., 2011). Viruses infecting the respiratory tract, including influenza A and B virus, RSV and SARS-CoV-2 were more pathogenic and replicated to higher titres in the lungs of mice lacking the functional receptors for type I and type III IFN than mice lacking a single receptor (Mordstein et al., 2010). In the same study, Lassa fever virus infection, which replicates in the liver was not influenced by the IFNL receptor defect (Mordstein et al., 2010), emphasising the complex role of interferons and the special function of IFN within epithelial cells during viral infections.

The infection of a virus can enhance or reduce infection and replication of a second virus. Interestingly, stimulation of epithelial cells with Poly(I:C) prior to live viral challenge inhibited the replication of live BoHV-1 in tracheal epithelial cells, indicating that the activation of the TLR3 signaling pathway is able to cause an antiviral state which is effective against BoHV-1 replication. However, Poly(I:C) stimulation after 18 hours of BoHV-1 infection did not significantly change the viral load. As it is common for respiratory viruses to infect the respiratory tract concurrently or sequentially, virus-virus interactions in this context have been reviewed previously (Piret and Boivin, 2022). As mechanism for reducing the replication for second virus the production of interferons, ISGs, chemokines and cytokines, the blocking of cell surface receptors and the competition for cellular resources have been identified (Piret and Boivin, 2022). On the other hand, an increased IFN and proinflammatory cytokine or reduced secretion of anti-inflammatory mediators can lead to increased disease severity (Piret and Boivin, 2022). Mice infected with respiratory syncytial virus (RSV) prior to influenza A virus (IAV) infection were protected and demonstrated decreased weight loss and increased survival when compared to IAV infection alone. In contrast, IAV infection prior to RSV infection did not change the severity of the pathogenesis compared to IAV infection alone. This highlights the importance of the order in which viral infections occur (Hartwig et al., 2022). Our results demonstrate that our established model of primary epithelial cells can be utilised to characterise the mechanisms of virus-virus interactions at the mucosal level. Further experiments are needed to identify the mechanism by which the shown activation of the TLR3 signaling is inhibiting BoHV-1 replication in primary bovine tracheal epithelial cells.

Our study highlights the importance of epithelial cells for initial innate antiviral activity in the respiratory tract due to their ability to detect and respond quickly to viral infection. Our results using the infection model of primary bovine tracheal epithelial cells support an important role for IFNL3 in innate antiviral immune activity in these cells. We demonstrated protective antiviral activity against BoHV-1 infection in these cells through the activation of the TLR3 signaling pathway. Investigating the antiviral immune responses including animal specific heritable traits explaining the inter-animal variation will lead to further understanding of the antiviral defence mechanisms. This

will help identify specific targets to improve strategies for preventing infection and better targeting respiratory viruses involved in BRD.

Chapter 6. General discussion

The agriculture sector is facing several serious challenges associated with infectious diseases which not only undermine sustainability but also negatively impact on animal welfare and foster a dependence on exogenous antimicrobial usage. Prevention and alternative therapeutic solutions for viral infections, including those caused by BoHV-1, are limited in part by a comparatively limited understanding of livestock host immunity as well as the availability of suitable models for investigating host-pathogen interactions in a physiologically relevant manner. Here, the establishment of a reproducible and physiologically relevant primary cell culture model without the requirement for experimental infection enabled us to reproducibly investigate the innate immune functional capacity of tracheal epithelial cells in response to both synthetic viral ligands as well as purified live BoHV-1.

Collectively, our results exemplify the critical role that bovine respiratory epithelial cells have in the initiation, regulation and resolution of the local immune response to viral infections, as shown in studies involving human and murine subjects. Specifically, we report the significant downregulation of genes involved in the unfolded protein response in BoHV-1 infected epithelial cells, while pre-treatment with Thapsigargin, an inhibitor of the sarco/endoplasmic reticulum Ca^{2+} ATPase was able to counteract this viral mediated downregulation. Quantifying the viral genome presence of BoHV-1 showed that pre-treatment with Tg had protective antiviral activity against BoHV-1 infection, thereby illustrating the importance of the UPR for the antiviral response in these cells. A major finding in our study was that the upregulation of IFN-λ3 and IDO1 expression characterises the early innate antiviral innate immune response to BoHV-1 infection and both are also activated in response to various viral ligands. The antiviral state within epithelial cells initiated by Poly(I:C) stimulation was found to protect against BoHV-1 replication. This inhibition indicates that activation of the TLR3/RIG-like receptor signalling pathway induces an antiviral state effective against BoHV-1 replication in tracheal epithelial cells. Collectively our results contribute to a more comprehensive characterization of innate antiviral immunity of respiratory epithelial cells of the bovine, an important livestock species.

We found that infection with live BoHV-1 stimulated a muted innate immune response based on pan genomic transcriptomic analysis. Proinflammatory cytokine, chemokine and type I IFN genes were not significantly upregulated in our infection model. This could indicate innate immune suppression by BoHV-1 (described in 1.3.4.) which could contribute to the establishment of viral infection. Although cells showed increased responsiveness to synthetic viral analogues, a clear signature of an inflammatory state with upregulation of proinflammatory cytokines and type I IFNs was not apparent. As epithelial cells are in constant contact with the environment and commensal microbes, this hypo-responsiveness could underpin the tight regulation of innate immune activity required in order to avoid chronic inflammation. Related studies have outlined the mechanisms by which epithelial cells modulate their innate immune sensing and are therefore generally hyporesponsive towards prototypical PAMPs (Weitnauer et al., 2016). One discussed mechanism regulating the immune activity in epithelial cells is polarised localisation of PRRs. On human intestinal epithelial cells TLR3 was shown to be localised on the basolateral side, and basolateral stimulation with TLR3 agonists or infection with TLR3 activating viruses led to a higher induction of IFN-β and IFN-λ compared to stimulation via the apical membrane. This regional localisation of PRRs allows intestinal cells to tolerate the presence of commensals on the apical side while being highly responsive against enteric pathogens that have crossed the epithelial barrier (Stanifer et al., 2020b). An increasing number of reports also indicate that TLR signaling is actively suppressed in the airway and in alveolar epithelial cells under homeostatic conditions. Hypo-responsiveness of airway cells has also been observed in relation to both TLR2 and TLR4 expression. Even though the cells express both receptors, stimulation with LPS or Gram-positive bacteria did not result in a strong induction of cytokines. The lack of expression of cofactors, e.g., CD36, MD2 and CD14, has been suggested as a possible mechanism to adjust the sensor threshold to the specific needs of the cell location (Becker et al., 2000; Jia et al., 2004). Similarly alveolar type II cells seem to be hyporesponsive towards LTA and LPS in contrast to type I cells (Wong and Johnson, 2013). It is thought that this tolerance is partially mediated by epigenetic mechanisms after repetitive challenge with the same pathogens (Neagos et al., 2015) or the production of surfactant with anti-inflammatory properties (Sato et al., 2003). Further possible mechanisms causing epithelial cells to switch from tolerance into a

reactive phenotype would be the absolute concentration of antigen or PAMP accumulating on the cell or alternatively the type of antigen or PAMP. Airway epithelial cells are generally hyporesponsive towards prototypical PAMPs, e.g., LPS but do secrete proinflammatory cytokines after Poly(I:C) stimulation (Weitnauer et al., 2016). Another concept are so-called viability-associated PAMPs, where inhalation of dead bacteria does not cause inflammation in contrast to PAMPs only present on viable bacteria which result in immune activation (Mourao-Sa et al., 2013). Furthermore, viral pathogens can lead to cell death of epithelial cells, which concurs with what we observed in our infection model of bovine tracheal epithelial cells infected with BoHV-1. As result of this interference with epithelial cell integrity, pathogens reach the subepithelial compartment and activate immune cells. Necrotic cell death then leads to the release of various alarmins, including IL-33 and IL-1a, which are known to induce an inflammatory response (Fritzsching et al., 2015).

Another cellular response that occurs upon viral infection and is able to induce apoptosis and cytokine secretion in epithelial cells, is the unfolded protein response (UPR), which combines several of the above-mentioned mechanisms to induce inflammatory processes. Our results found genes involved in the UPR to be downregulated in BoHV-1 infected epithelial cells. Human HSV-1 (herpes simplex virus type 1) is known to inhibit the UPR via multiple mechanisms. Even though HSV-1 triggers IRE1 kinase activity, it represses *XBP1* splicing and XBP1 synthesis. The HSV-1 glycoprotein B (gB) binds to PERK and prevents its activation, which leads to limited eIF2α phosphorylation and maintenance of protein synthesis. The HSV-1 protein γ34.5 acts in a fashion that is similar to GADD34 and recruits cellular PP1 phosphatase to eIF2a, resulting in no synthesis of ATF4 (Johnston and McCormick, 2019). Our results indicate that similar to human HSV-1, BoHV-1 modulation of the UPR not only benefits lytic replication but also helps viral evasion of immune surveillance. Since our results demonstrate that pre-treatment with Tg has a protective antiviral activity against BoHV-1 infection, we were able to highlight the importance of the UPR for the antiviral response in bovine respiratory epithelial cells and the possibility to target the UPR as strategy as antiviral treatment.

Bulk RNA sequencing analysis of primary bovine tracheal epithelial cells infected with purified live BoHV-1 revealed (after stringent correction or multiple testing), differential expression of nine genes, whereas qPCR analysis using the same infection model showed various additional genes being differentially expressed throughout this project. One caveat of working with post-mortem tissue is an inability to select specific animals and often being unaware of the health status. Future work should therefore try to minimise inter-sample variation by selecting cattle of similar age, sex, breed. Recent studies in humans are now showing a significant influence of sex on antiviral immune response profiles (Ghosh and Klein, 2017; Regis et al., 2021) which would be of interest to investigate in cattle. Another possible reason for the different gene expression results generated may be the time point after viral infection chosen for the RNA-seq analysis. While we analysed samples of tracheal epithelial cells infected with BoHV-1 at 6 hours post infection via RNAseq, most of our findings of regulated genes were found 24 hours post infection with qPCR analysis. This was the case for example for the downregulation of UPR genes, as well as the upregulation of IFN-λ3 and ISGs. The kinetics of the antiviral immune response has been shown in multiple studies to rapidly change after infection, and therefore our work lays an important foundation for the design of future detailed infection studies using this model.

Our results show that within bovine epithelial cells *IFNL3* and *IDO1* expression were highly upregulated in response to virus infection, suggesting a role of metabolic changes in innate antiviral immunity potentially linked with IFN-λ. However, we found no significant correlation in the gene expressions analysing the upregulation of both in response to Poly(I:C) stimulation. The responsible mechanisms for IFN-γ-mediated IDO1 induction have been well characterised in previous studies. The promoter region of the IDO1 gene contains two interferon-stimulated response elements (ISREs) and three IFN-γ-activated sites and (Raniga and Liang, 2018; Robinson et al., 2003). IDO1 was thought to be primarily an IFN-γ-induced gene, however, other inflammatory mediators were found to enhance the IFN-γ-mediated induction while being ineffective alone. For example, TNF synergistically enhanced IDO1 activity in HeLa cells, an epithelial cervical cancer cell line (Babcock and Carlin, 2000), and IFN-α induced IDO1 expression in dendritic cells (Manlapat et al., 2007). A study in 2015 investigated the effect of IFN-λ

on IDO1 expression in epithelial cells and found IDO1 and IFN-λ expression was upregulated in MLE-15 cells, a mouse tumour lung epithelial cell line, after influenza virus infection. In these cells IDO1 was upregulated by recombinant IFN-λ and IDO1 expression was reduced if IFN-λ was silenced during influenza infection. IDO1 inhibition resulted in a decreased viral load and reduced cellular viability at later time points post infection (Fox et al., 2015). Further experiments with our infection model, including IDO1 inhibition, are needed to unravel the role of IDO1 and its connection to IFN-λ3 in bovine respiratory epithelial cells in the context of BoHV-1 infection.

While we could show that the viral load increased after 24 hours in our cell culture model of primary bovine tracheal epithelial cells, suggesting viral replication in our infection model, the shown effects on gene expressions could be caused by viral presence rather than viral replication itself. Our findings were most present with high virus concentrations of MOI 35 and 70, possibly due to the relative high virus presence. The similar response after stimulation with viral RNA and DNA syntetic analogues indicate the ability of tracheal epithelial cells to respond to viral replication intermediates. In order to investigate the response of epithelial cells to BoHV-1 antigens experiments with heat-inactivated BoHV-1 should be conducted.

The consistent upregulation of IFN-λ3 in bovine respiratory epithelial cells following BoHV-1 infection and after stimulation with various viral analogues, Poly(I:C), Poly(dA:dT) and 3p-hpRNA, highlights the need to investigate its role in the context of viral infections at epithelial surfaces. In order to explore the translation of the mRNA, we carried out multiple approaches. Unfortunately, no IFN-λ ELISA is currently available for use in cattle. The available assays for human IFN-λ did not show any results, likely due to the < 70% identity in protein sequence between the two species. Coomassie brilliant blue stain of cell lysate and concentrated supernatant of primary bovine tracheal epithelial cells stimulated with Poly(I:C) did not show any clear differences between control and stimulated samples. Mass spectrometry analysis was also conducted using concentrated supernatants of samples stimulated for 6 hours with Poly(I:C) but revealed no differentially abundant immune related proteins. Follow on work will investigate the IFNL protein in more detail using mass spectrometry analysis at later time points for the analysis of both cell lysates and supernatants.

Due to the limited number of cell types expressing IFN-λ, its unique functions at mucosal surfaces compared to type I IFNs have been of previous interest. Mouse tracheal epithelial cells with either IFN-λR1 or IFNAR1 knockdown exhibited similar transcription profiles in response to influenza A virus *in-vitro* (Crotta et al., 2013). Studies with mice deficient in IFN-λR1, IFNAR1 or both indicated a degree of redundancy between the two types of IFNs. The mice lacking both receptors were highly susceptible to respiratory infections, whereas a single knock-down led to a similar resistance as the wild type controls to viral infection (Mordstein et al., 2010). Even though IFN-λ seems to have partly redundant functions, many studies show an antiviral function of IFN-λ as a treatment. Inoculation of cattle with a viral vector expressing bovine IFN-λ3 induced systemic antiviral activity and upregulation of ISGs in the upper respiratory tract. Treated animals showed reduced clinical signs and viral shedding in nasal swabs, delaying, and reducing the severity of foot-and-mouth disease (Perez-Martin et al., 2012). Experimentally challenged cattle with BVDV treated with recombinant bovine IFN-λ two days before and two days after infection did not develop clinical symptoms and the virus was not found in nasal secretions or sera. The infected animals treated with recombinant bovine IFN-λ had increased systemic type I IFN levels, indicating an interplay between the two IFN types during viral infections (Quintana et al., 2020). However, concentration, timing, and duration must be carefully considered for IFN therapeutic strategies. Both IFN types have shown to reduce mouse lung epithelial cells proliferation following treatment during influenza infection and IFN-λ additionally compromised cell repair in a TP53-dependent manner. The authors suggest as cause the greater induction of antiproliferative pathways in response to IFN-λ compared to type I IFNs (Major et al., 2020). The stimulation of lung-resident DCs with Poly(I:C) led to a sustained production of IFN-λ causing an impaired epithelial barrier and a severe pathology with *Staphylococcus aureus* superinfection in a mouse model. Wild-type mice with a deficient IFN-λR1 expression were protected against barrier damage and resistant to superinfection with *S. aureus* (Broggi et al., 2020). Another possible mechanism by which IFN-λ could lead to increased susceptibility to secondary bacterial infections is its inhibitory effects on neutrophil migration. The treatment of IFN-λ led to an anti-inflammatory state by restricting the recruitment of neutrophils into joints at the

early stages of arthritis in a mouse model (Blazek et al., 2015). Considering the predisposition of BoHV-1 infected cattle to secondary bacterial infections, our results suggest an important role of IFN-λ in this context in line with the described studies. Future experiments are needed to determine the influence of IFN-λ on the barrier function of bovine tracheal epithelial cells and its possible cause leading to superinfections. An IFN-λ antagonist could potentially help to reduce secondary bacterial infections in the bovine respiratory tract.

We found activation of the TLR3/RIG-like receptor signalling pathway prior to BoHV-1 infection had an inhibitory effect on viral replication in bovine tracheal epithelial cells. As discussed earlier, a previous infection can lead to a primed antiviral state or cause competition for cellular resources, both of which can inhibit a secondary viral infection. For example, it has been shown that respiratory syncytial virus infection increases TLR3 expression in tracheobronchial epithelial cells, leading to increased NFκB activity and production of IL-8 in response to subsequent dsRNA exposure (Groskreutz et al., 2006). The exposure of human nasal epithelium to *S. epidermidis in-vitro* was also shown to increase IFN-λ expression and secreted protein. To examine the effect of *S. epidermidis* on the antiviral immune response, cells were treated with *S. epidermidis* at 8 hours before inoculation of IAV. Results showed that this pre-treatment inhibited influenza A virus replication (Kim et al., 2019).

The term immune adaptation in innate immune cells summarises processes that rapidly and reversible modify properties of the cell in response to the environment. The consequences can be short-term or prolonged after the stimulus. The different processes and outcomes have been referred to with terms such as ‘plasticity’, ‘priming’, ‘training’, ‘exhaustion’ and ‘tolerance’ (Natoli and Ostuni, 2019). The idea of primed innate immunity and the following trained immunity describes the manifestation of protection against reinfection by the same or different pathogen within innate immune cells (Arneth, 2021). If the functional status of the innate immune response remains enhanced after recovery, the status is described as ‘trained immunity’, which is the opposite to tolerance after a severe activation (Netea, 2013). Trained immunity has been mainly investigated in macrophages (Bowdish et al., 2007). However, it is likely

that epithelial cells might also demonstrate trained immunity. Tolerance effects are also described for respiratory epithelial cells, as previously mentioned, which can occur due to the repetitive challenge with the same pathogens (Neagos et al., 2015; Wong and Johnson, 2013). In the case of our observed antiviral effect resulting from priming via TLR3 pathway activation, further experiments are necessary to determine whether the first stimulus after its termination leads to hyper-responsive adaptation. The possible underlying mechanisms causing the hyper-responsive adaptation include the induction of signaling components, transcription factors, metabolic reprogramming and higher chromatin accessibility (Natoli and Ostuni, 2019). A short period of psoriasis-like inflammation altered mouse skin epithelial stem cells to repair a subsequent wound more rapidly at that site. In this way epithelial stem cells can contribute to the persistence of disease by functioning as repositories for allergic inflammatory memories. AIM2 and its downstream effectors, caspase-1 and IL-1β, were found to contribute to the ability to recollect inflammation as well as maintaining chromosomal accessibility (Naik et al., 2017).

Although vaccine development is an important aspect to the ultimate control of bovine respiratory diseases, our results show that the antiviral innate immune response of epithelial cells, e.g., UPR or TLR3/RIG-I signalling, can be influenced in order to impact the outcome of viral infection in the respiratory tract. Several recent therapies have tried to enhance the animal's innate state of disease resistance, especially during periods of stress, such as around weaning or during long distance transport. One example is the DNA-based immunostimulant with the commercial name Zelnate™ (Bayer Animal Health, Shawnee Mission, KS, USA). The intramuscular or intranasal administered bacterial-produced plasmid DNA has been shown to reduce lung pathologies and mortality in cattle experimentally challenged with *M. haemolytica*, which can lead to BRD (Nickell et al., 2016). Another immunomodulatory product, marketed as Amplimune™ (Novavive, Inc, Napanee, Ontario, Canada) is a mycobacterium cell wall fraction originated from the non-pathogenic *Mycobacterium phlei*. It has been applied for prevention of *E. coli* infection in pre-weaned calves; it functions via non-specific activation of the innate immune system after a subcutaneous administration (Masic, 2017). The beneficial effects of these non-specific drugs highlight

the value of more meaningful investigation of specific therapeutic options that might shape the antiviral immune potential of epithelial cells. Our research suggests targeting specific mechanisms, e.g. the UPR, the augmentation of immunometabolic changes or potentially priming of the innate immune response via exposure of viral ligands as possible options to investigate.

Another factor influencing the resistance and susceptibility to a wide variety of diseases are genetic factors. Cattle of the same age and in the same housing conditions vary greatly in their susceptibility to respiratory infections, which suggests some degree of genetic control (Emam et al., 2019). In the context of BRD, quantitative-trait locus mapping has shown two single-nucleotide polymorphisms (SNPs) in the *ANKRA2* gene and the *CD180* gene associated with BRD susceptibility. While *ANKRA2* plays a role in transcription of MHC class II genes, *CD180* is part of the TLR family and is crucial for B-cell responsiveness to LPS (Casas et al., 2011). While there has no SNP being identified in bovine *IFNL3*, SNPs in the IFN-λ locus in the human are associated with antiviral protection. A SNP in the *IL28B* gene, which encodes IFN-λ3, is associated with a difference in HCV drug treatment and the natural clearance of HCV (Thomas et al., 2009). SNPs in the locus of *IFNL3* and *IFNL4* genes in the human have been important marker for responsiveness in chronic hepatitis C (Silva et al., 2021). Identifying hereditable factors accounting for resistance or susceptibility opens the possibility for breeding for relevant traits, especially in livestock species (Ring et al., 2018). Genetic variation in the genes identified here, including in *IFNL3* could augment efforts to breed for cattle with superior antiviral innate immune responses.

In summary, our study highlights the importance of epithelial cells for local innate antiviral activity in the respiratory tract due to their ability to detect and respond to viral infection. Our studies using the infection model of primary bovine tracheal epithelial cells demonstrate the significant innate immune potential of bovine tracheal epithelial cells against viral pathogens characterised by significant *IFNL3* upregulation. We demonstrate protective antiviral potential against viral infection in these cells through activation of the TLR3/RIG-like receptor signalling pathway. Further characterisation of antiviral innate immune potential of respiratory epithelial cells including definition of

the signalling pathways underpinning inter-animal variation will ultimately contribute to breeding and immunotherapeutic strategies capable of preventing and better treatment of BoHV-1 infection in livestock.

Bibliography

Ablasser, A. et al., 2009. RIG-I-dependent sensing of poly(dA:dT) through the induction of an RNA polymerase III-transcribed RNA intermediate. Nat Immunol, 10(10): 1065-72.

Ackermann, M., Engels, M., 2006. Pro and contra IBR-eradication. Veterinary Microbiology, 113(3): 293-302.

Afroz, S., Brownlie, R., Fodje, M., van Drunen Littel-van den Hurk, S., 2016. VP8, the Major Tegument Protein of Bovine Herpesvirus 1, Interacts with Cellular STAT1 and Inhibits Interferon Beta Signaling. J Virol, 90(10): 4889-4904.

Agol, V.I., 2012. Cytopathic effects: virus-modulated manifestations of innate immunity? Trends Microbiol, 20(12): 570-6.

Al-Beltagi, S. et al., 2021a. Emergent SARS-CoV-2 variants: comparative replication dynamics and high sensitivity to thapsigargin. Virulence, 12(1): 2946-2956.

Al-Beltagi, S. et al., 2021b. Thapsigargin Is a Broad-Spectrum Inhibitor of Major Human Respiratory Viruses: Coronavirus, Respiratory Syncytial Virus and Influenza A Virus. Viruses, 13(2): 234.

Al-Haddawi, M., Mitchell, G.B., Clark, M.E., Wood, R.D., Caswell, J.L., 2007. Impairment of innate immune responses of airway epithelium by infection with bovine viral diarrhea virus. Vet Immunol Immunopathol, 116(3-4): 153-62.

Albakova, Z., Armeev, G.A., Kanevskiy, L.M., Kovalenko, E.I., Sapozhnikov, A.M., 2020. HSP70 Multi-Functionality in Cancer. Cells, 9(3).

Alexopoulou, L., Holt, A.C., Medzhitov, R., Flavell, R.A., 2001. Recognition of double-stranded RNA and activation of NF-kappaB by Toll-like receptor 3. Nature, 413(6857): 732-8.

Andreakos, E., Salagianni, M., Galani, I., Koltsida, O., 2017. Interferon-»s: Front-Line Guardians of Immunity and Homeostasis in the Respiratory Tract. Frontiers in Immunology, 8.

Armstrong, L. et al., 2004. Expression of functional toll-like receptor-2 and -4 on alveolar epithelial cells. Am J Respir Cell Mol Biol, 31(2): 241-5.

Arneth, B., 2021. Trained innate immunity. Immunol Res, 69(1): 1-7.

Babcock, T.A., Carlin, J.M., 2000. Transcriptional activation of indoleamine dioxygenase by interleukin 1 and tumor necrosis factor alpha in interferon-treated epithelial cells. Cytokine, 12(6): 588-94.

Babiuk, L.A., Wardley, R.C., Rouse, B.T., 1975. Defense mechanisms against bovine herpesvirus: relationship of virus-host cell events to susceptibility to antibody-complement cell lysis. Infect Immun, 12(5): 958-63.

Baler, R., Dahl, G., Voellmy, R., 1993. Activation of human heat shock genes is accompanied by oligomerization, modification, and rapid translocation of heat shock transcription factor HSF1. Mol Cell Biol, 13(4): 2486-96.

Baños-Lara Mdel, R. et al., 2015. Impact and regulation of lambda interferon response in human metapneumovirus infection. J Virol, 89(1): 730-42.

Barrett, D. et al., 2018. Prevalence of Bovine Viral Diarrhoea Virus (BVDV), Bovine Herpes Virus 1 (BHV 1), Leptospirosis and Neosporosis, and associated risk factors in 161 Irish beef herds. BMC Vet Res, 14(1): 8.

Basset, C., Holton, J., O'Mahony, R., Roitt, I., 2003. Innate immunity and pathogen-host interaction. Vaccine, 21 Suppl 2: S12-23.

Becker, M.N., Diamond, G., Verghese, M.W., Randell, S.H., 2000. CD14-dependent lipopolysaccharide-induced beta-defensin-2 expression in human tracheobronchial epithelium. J Biol Chem, 275(38): 29731-6.

Becker, S., Koren, H.S., Henke, D.C., 1993. Interleukin-8 expression in normal nasal epithelium and its modulation by infection with respiratory syncytial virus and cytokines tumor necrosis factor, interleukin-1, and interleukin-6. Am J Respir Cell Mol Biol, 8(1): 20-7.

Belknap, E.B. et al., 1999. Immunogenicity and protective efficacy of a gE, gG and US2 gene-deleted bovine herpesvirus-1 (BHV-1) vaccine. Vaccine, 17(18): 2297-305.

Bellinghausen, C., Rohde, G.G.U., Savelkoul, P.H.M., Wouters, E.F.M., Stassen, F.R.M., 2016. Viral-bacterial interactions in the respiratory tract. J Gen Virol, 97(12): 3089-3102.

Bem, R.A., Domachowske, J.B., Rosenberg, H.F., 2011. Animal models of human respiratory syncytial virus disease. Am J Physiol Lung Cell Mol Physiol, 301(2): L148-56.

Berghuis, L. et al., 2014. Comparison of innate immune agonists for induction of tracheal antimicrobial peptide gene expression in tracheal epithelial cells of cattle. Vet Res, 45: 105.

Bieback, K. et al., 2002. Hemagglutinin protein of wild-type measles virus activates toll-like receptor 2 signaling. J Virol, 76(17): 8729-36.

Blazek, K. et al., 2015. IFN-λ resolves inflammation via suppression of neutrophil infiltration and IL-1β production. J Exp Med, 212(6): 845-53.

Bowdish, D.M., Loffredo, M.S., Mukhopadhyay, S., Mantovani, A., Gordon, S., 2007. Macrophage receptors implicated in the "adaptive" form of innate immunity. Microbes Infect, 9(14-15): 1680-7.

Boyce, M. et al., 2005. A selective inhibitor of eIF2alpha dephosphorylation protects cells from ER stress. Science, 307(5711): 935-9.

Bridges, J.P., Vladar, E.K., Huang, H., Mason, R.J., 2022. Respiratory epithelial cell responses to SARS-CoV-2 in COVID-19. Thorax, 77(2): 203-209.

Broggi, A. et al., 2020. Type III interferons disrupt the lung epithelial barrier upon viral recognition. Science, 369(6504): 706-712.

Bromberg, Z., Weiss, Y., 2016. The Role of the Membrane-Initiated Heat Shock Response in Cancer. Frontiers in Molecular Biosciences, 3.

Brown, T.T., Jr., Ananaba, G., 1988. Effect of respiratory infections caused by bovine herpesvirus-1 or parainfluenza-3 virus on bovine alveolar macrophage functions. Am J Vet Res, 49(9): 1447-51.

Bryant, N.A., Davis-Poynter, N., Vanderplasschen, A., Alcami, A., 2003. Glycoprotein G isoforms from some alphaherpesviruses function as broad-spectrum chemokine binding proteins. Embo j, 22(4): 833-46.

Buckingham, E.M., Carpenter, J.E., Jackson, W., Grose, C., 2014. Autophagy and the effects of its inhibition on varicella-zoster virus glycoprotein biosynthesis and infectivity. J Virol, 88(2): 890-902.

Bürckstümmer, T. et al., 2009. An orthogonal proteomic-genomic screen identifies AIM2 as a cytoplasmic DNA sensor for the inflammasome. Nat Immunol, 10(3): 266-72.

Cario, E. et al., 2000. Lipopolysaccharide Activates Distinct Signaling Pathways in Intestinal Epithelial Cell Lines Expressing Toll-Like Receptors. The Journal of Immunology, 164(2): 966.

Carneiro, L.C. et al., 2017. Coordinated Role of Toll-Like Receptor-3 and Retinoic Acid-Inducible Gene-I in the Innate Response of Bovine Endometrial Cells to Virus. Front Immunol, 8: 996.

Casas, E., Garcia, M.D., Wells, J.E., Smith, T.P., 2011. Association of single nucleotide polymorphisms in the ANKRA2 and CD180 genes with bovine respiratory disease and presence of Mycobacterium avium subsp. paratuberculosis(1). Anim Genet, 42(6): 571-7.

Caswell, J.L., 2014. Failure of respiratory defenses in the pathogenesis of bacterial pneumonia of cattle. Vet Pathol, 51(2): 393-409.

Chaplin, D.D., 2003. 1. Overview of the immune response. J Allergy Clin Immunol, 111(2 Suppl): S442-59.

Chapwanya, A., Meade, K.G., Doherty, M.L., Callanan, J.J., O'Farrelly, C., 2013. Endometrial epithelial cells are potent producers of tracheal antimicrobial peptide and serum amyloid A3 gene expression in response to E. coli stimulation. Vet Immunol Immunopathol, 151(1-2): 157-62.

Chen, X., Shen, J., Prywes, R., 2002. The luminal domain of ATF6 senses endoplasmic reticulum (ER) stress and causes translocation of ATF6 from the ER to the Golgi. J Biol Chem, 277(15): 13045-52.

Chen, Y.G., Hur, S., 2022. Cellular origins of dsRNA, their recognition and consequences. Nature Reviews Molecular Cell Biology, 23(4): 286-301.

Chen, Y.J. et al., 2010. Heat shock protein 72 is associated with the hepatitis C virus replicase complex and enhances viral RNA replication. J Biol Chem, 285(36): 28183-90.

Ciacci-Zanella, J., Stone, M., Henderson, G., Jones, C., 1999. The latency-related gene of bovine herpesvirus 1 inhibits programmed cell death. J Virol, 73(12): 9734-40.

Cowley, D.J., Clegg, T.A., Doherty, M.L., More, S.J., 2011. Aspects of bovine herpesvirus-1 infection in dairy and beef herds in the Republic of Ireland. Acta Vet Scand, 53(1): 40.

Cozens, D. et al., 2018. Development and optimization of a differentiated airway epithelial cell model of the bovine respiratory tract. Sci Rep, 8(1): 853.

Crotta, S. et al., 2013. Type I and type III interferons drive redundant amplification loops to induce a transcriptional signature in influenza-infected airway epithelia. PLoS Pathog, 9(11): e1003773.

Cullinan, S.B. et al., 2003. Nrf2 is a direct PERK substrate and effector of PERK-dependent cell survival. Mol Cell Biol, 23(20): 7198-209.

da Silva, L.F., Sinani, D., Jones, C., 2012. ICP27 protein encoded by bovine herpesvirus type 1 (bICP27) interferes with promoter activity of the bovine genes encoding beta interferon 1 (IFN-beta1) and IFN-beta3. Virus Res, 169(1): 162-8.

Dalby, B. et al., 2004. Advanced transfection with Lipofectamine 2000 reagent: primary neurons, siRNA, and high-throughput applications. Methods, 33(2): 95-103.

Daugaard, M., Rohde, M., Jäättelä, M., 2007. The heat shock protein 70 family: Highly homologous proteins with overlapping and distinct functions. FEBS Lett, 581(19): 3702-10.

Davies, D. et al., 2008. Toll-like receptor and antimicrobial peptide expression in the bovine endometrium. Reprod Biol Endocrinol, 6: 53.

de Courcey, F. et al., 2012. Development of primary human nasal epithelial cell cultures for the study of cystic fibrosis pathophysiology. Am J Physiol Cell Physiol, 303(11): C1173-9.

Deane, C.A.S., Brown, I.R., 2018. Knockdown of Heat Shock Proteins HSPA6 (Hsp70B') and HSPA1A (Hsp70-1) Sensitizes Differentiated Human Neuronal Cells to Cellular Stress. Neurochem Res, 43(2): 340-350.

Deng, Z. et al., 2016. An Investigation of the Innate Immune Response in Bovine Mammary Epithelial Cells Challenged by Prototheca zopfii. Mycopathologia, 181(11-12): 823-832.

Devireddy, L.R., Jones, C.J., 1999. Activation of caspases and p53 by bovine herpesvirus 1 infection results in programmed cell death and efficient virus release. J Virol, 73(5): 3778-88.

Di Teodoro, G. et al., 2018. Respiratory explants as a model to investigate early events of contagious bovine pleuropneumonia infection. Vet Res, 49(1): 5.

Dolganiuc, A. et al., 2004. Hepatitis C core and nonstructural 3 proteins trigger toll-like receptor 2-mediated pathways and inflammatory activation. Gastroenterology, 127(5): 1513-24.

Duan, Y. et al., 2014. HspA1A facilitates DNA repair in human bronchial epithelial cells exposed to Benzo[a]pyrene and interacts with casein kinase 2. Cell Stress Chaperones, 19(2): 271-9.

Ellis, J.A., 2009. Update on viral pathogenesis in BRD. Animal Health Research Reviews, 10(2): 149-153.

Emam, M., Livernois, A., Paibomesai, M., Atalla, H., Mallard, B., 2019. Genetic and Epigenetic Regulation of Immune Response and Resistance to Infectious Diseases in Domestic Ruminants. Vet Clin North Am Food Anim Pract, 35(3): 405-429.

Fenwick, M.L., Walker, M.J., 1978. Suppression of the synthesis of cellular macromolecules by herpes simplex virus. J Gen Virol, 41(1): 37-51.

Fox, J.M., Crabtree, J.M., Sage, L.K., Tompkins, S.M., Tripp, R.A., 2015. Interferon Lambda Upregulates IDO1 Expression in Respiratory Epithelial Cells After Influenza Virus Infection. J Interferon Cytokine Res, 35(7): 554-62.

François-Newton, V. et al., 2011. USP18-based negative feedback control is induced by type I and type III interferons and specifically inactivates interferon α response. PLoS One, 6(7): e22200.

Fritzsching, B. et al., 2015. Hypoxic epithelial necrosis triggers neutrophilic inflammation via IL-1 receptor signaling in cystic fibrosis lung disease. Am J Respir Crit Care Med, 191(8): 902-13.

Fulton, R.W., Pearson, N.J., 1980. Interferon production by bovine tracheal organ cultures infected with bovid herpesvirus 1 strains. Canadian journal of comparative medicine : Revue canadienne de medecine comparee, 44(4): 447-452.

Galani, I.E. et al., 2017. Interferon-λ Mediates Non-redundant Front-Line Antiviral Protection against Influenza Virus Infection without Compromising Host Fitness. Immunity, 46(5): 875-890.e6.

Gallo, O., Locatello, L.G., Mazzoni, A., Novelli, L., Annunziato, F., 2021. The central role of the nasal microenvironment in the transmission, modulation, and clinical progression of SARS-CoV-2 infection. Mucosal Immunol, 14(2): 305-316.

Galvan, V., Roizman, B., 1998. Herpes simplex virus 1 induces and blocks apoptosis at multiple steps during infection and protects cells from exogenous inducers in a cell-type-dependent manner. Proc Natl Acad Sci U S A, 95(7): 3931-6.

Gebhardt, A., Laudenbach, B.T., Pichlmair, A., 2017. Discrimination of Self and Non-Self Ribonucleic Acids. J Interferon Cytokine Res, 37(5): 184-197.

Ghosh, S., Klein, R.S., 2017. Sex Drives Dimorphic Immune Responses to Viral Infections. J Immunol, 198(5): 1782-1790.

Gondaira, S. et al., 2018. Innate immune response of bovine mammary epithelial cells to Mycoplasma bovis. J Vet Sci, 19(1): 79-87.

Groskreutz, D.J. et al., 2006. Respiratory syncytial virus induces TLR3 protein and protein kinase R, leading to increased double-stranded RNA responsiveness in airway epithelial cells. J Immunol, 176(3): 1733-40.

Guillot, L. et al., 2005. Involvement of toll-like receptor 3 in the immune response of lung epithelial cells to double-stranded RNA and influenza A virus. J Biol Chem, 280(7): 5571-80.

Hanon, E. et al., 1996. Inactivated bovine herpesvirus 1 induces apoptotic cell death of mitogen-stimulated bovine peripheral blood mononuclear cells. J Virol, 70(6): 4116-20.

Hariharan, M.J., Nataraj, C., Srikumaran, S., 1993. Down regulation of murine MHC class I expression by bovine herpesvirus 1. Viral Immunol, 6(4): 273-84.

Hartwig, S.M., Miller, A.M., Varga, S.M., 2022. Respiratory Syncytial Virus Provides Protection against a Subsequent Influenza A Virus Infection. J Immunol, 208(3): 720-731.

He, B., Gross, M., Roizman, B., 1997. The gamma(1)34.5 protein of herpes simplex virus 1 complexes with protein phosphatase 1alpha to dephosphorylate the alpha subunit of the eukaryotic translation initiation factor 2 and preclude the shutoff of protein synthesis by double-stranded RNA-activated protein kinase. Proc Natl Acad Sci U S A, 94(3): 843-8.

He, S., Han, J., 2020. Manipulation of Host Cell Death Pathways by Herpes Simplex Virus. Curr Top Microbiol Immunol.

Health, A.S.o.A., 2020. Preview: Economic Effects of Bovine Respiratory Disease. Journal of Animal Science, 98(2).

Hedges, S., de Man, P., Linder, H., Kooten, C.V., Edén, C.S., 1990. Interleukin-6 is secreted by epithelial cells in response to Gram-negative bacterial challenge. In: MacDonald, T.T. et al. (Eds.), Advances in Mucosal Immunology: Proceedings of the Fifth International Congress of Mucosal Immunology. Springer Netherlands, Dordrecht, pp. 144-147.

Hedges, S.R., Agace, W.W., Svanborg, C., 1995. Epithelial cytokine responses and mucosal cytokine networks. Trends in Microbiology, 3(7): 266-270.

Heil, F. et al., 2004. Species-specific recognition of single-stranded RNA via toll-like receptor 7 and 8. Science, 303(5663): 1526-9.

Hemmi, H. et al., 2000. A Toll-like receptor recognizes bacterial DNA. Nature, 408(6813): 740-5.

Henderson, G., Zhang, Y., Jones, C., 2005. The Bovine herpesvirus 1 gene encoding infected cell protein 0 (bICP0) can inhibit interferon-dependent transcription in the absence of other viral genes. J Gen Virol, 86(Pt 10): 2697-2702.

Hetz, C. et al., 2006. Proapoptotic BAX and BAK modulate the unfolded protein response by a direct interaction with IRE1alpha. Science, 312(5773): 572-6.

Hewitt, R.J., Lloyd, C.M., 2021. Regulation of immune responses by the airway epithelial cell landscape. Nat Rev Immunol: 1-16.

Hewson, C.A., Jardine, A., Edwards, M.R., Laza-Stanca, V., Johnston, S.L., 2005. Toll-like receptor 3 is induced by and mediates antiviral activity against rhinovirus infection of human bronchial epithelial cells. J Virol, 79(19): 12273-9.

Hinkley, S., Ambagala, A.P., Jones, C.J., Srikumaran, S., 2000. A vhs-like activity of bovine herpesvirus-1. Arch Virol, 145(10): 2027-46.

Hogan, B.L. et al., 2014. Repair and regeneration of the respiratory system: complexity, plasticity, and mechanisms of lung stem cell function. Cell Stem Cell, 15(2): 123-38.

Hoorn, B., 1964. Respiratory Viruses in Model Experiments. Acta Oto-Laryngologica, 57(sup188): 138-144.

Hornung, V. et al., 2006. 5'-Triphosphate RNA is the ligand for RIG-I. Science, 314(5801): 994-7.

Huemer, H.P., Larcher, C., van Drunen Littel-van den Hurk, S., Babiuk, L.A., 1993. Species selective interaction of Alphaherpesvirinae with the "unspecific" immune system of the host. Arch Virol, 130(3-4): 353-64.

Huérfano, S., Šroller, V., Bruštíková, K., Horníková, L., Forstová, J., 2022. The Interplay between Viruses and Host DNA Sensors. Viruses, 14(4).

Ioannidis, I., Ye, F., McNally, B., Willette, M., Flaño, E., 2013. Toll-like receptor expression and induction of type I and type III interferons in primary airway epithelial cells. Journal of virology, 87(6): 3261-3270.

Jensen, K.E., Neal, A.L., Owens, R.E., Warren, J., 1963. INTERFERON RESPONSES OF CHICK EMBRYO FIBROBLASTS TO NUCLEIC ACIDS AND RELATED COMPOUNDS. Nature, 200: 433-4.

Jensen, S., Thomsen, A.R., 2012. Sensing of RNA Viruses: a Review of Innate Immune Receptors Involved in Recognizing RNA Virus Invasion. Journal of Virology, 86(6): 2900.

Jia, H.P. et al., 2004. Endotoxin responsiveness of human airway epithelia is limited by low expression of MD-2. Am J Physiol Lung Cell Mol Physiol, 287(2): L428-37.

Johnston, B.P., McCormick, C., 2019. Herpesviruses and the Unfolded Protein Response. Viruses, 12(1).

Jones, C., 2003. Herpes simplex virus type 1 and bovine herpesvirus 1 latency. Clin Microbiol Rev, 16(1): 79-95.

Jones, C., 2013. Bovine Herpes Virus 1 (BHV-1) and Herpes Simplex Virus Type 1 (HSV-1) Promote Survival of Latently Infected Sensory Neurons, in Part by Inhibiting Apoptosis. J Cell Death, 6: 1-16.

Jones, C., 2019. Bovine Herpesvirus 1 Counteracts Immune Responses and Immune-Surveillance to Enhance Pathogenesis and Virus Transmission. Front Immunol, 10: 1008.

Jones, C. et al., 2006. Functional analysis of bovine herpesvirus 1 (BHV-1) genes expressed during latency. Vet Microbiol, 113(3-4): 199-210.

Jung, J., Zeng, H., Horng, T., 2019. Metabolism as a guiding force for immunity. Nature Cell Biology, 21(1): 85-93.

Kalinowski, A. et al., 2018. Respiratory syncytial virus activates epidermal growth factor receptor to suppress interferon regulatory factor 1-dependent interferon-lambda and antiviral defense in airway epithelium. Mucosal Immunology, 11(3): 958-967.

Kato, H. et al., 2005. Cell type-specific involvement of RIG-I in antiviral response. Immunity, 23(1): 19-28.

Kato, H. et al., 2006. Differential roles of MDA5 and RIG-I helicases in the recognition of RNA viruses. Nature, 441(7089): 101-5.

Kaur, G., Dufour, J.M., 2012. Cell lines: Valuable tools or useless artifacts. Spermatogenesis, 2(1): 1-5.

Kawai, T., Akira, S., 2007. Antiviral signaling through pattern recognition receptors. J Biochem, 141(2): 137-45.

Kawai, T. et al., 2005. IPS-1, an adaptor triggering RIG-I- and Mda5-mediated type I interferon induction. Nat Immunol, 6(10): 981-8.

Keil, G.M., 2000. Fusion of the green fluorescent protein to amino acids 1 to 71 of bovine respiratory syncytial virus glycoprotein G directs the hybrid polypeptide as a class II membrane protein into the envelope of recombinant bovine herpesvirus-1. J Gen Virol, 81(Pt 4): 1051-5.

Keuser, V. et al., 2004. Improved antigenic methods for differential diagnosis of bovine, caprine, and cervine alphaherpesviruses related to bovine herpesvirus 1. J Clin Microbiol, 42(3): 1228-35.

Kim, H.J. et al., 2019. Nasal commensal Staphylococcus epidermidis enhances interferon-λ-dependent immunity against influenza virus. Microbiome, 7(1): 80.

Kirchhoff, J., Uhlenbruck, S., Goris, K., Keil, G.M., Herrler, G., 2014. Three viruses of the bovine respiratory disease complex apply different strategies to initiate infection. Vet Res, 45: 20.

Kline, M.P., Morimoto, R.I., 1997. Repression of the heat shock factor 1 transcriptional activation domain is modulated by constitutive phosphorylation. Mol Cell Biol, 17(4): 2107-15.

Klinkhammer, J. et al., 2018. IFN0» prevents influenza virus spread from the upper airways to the lungs and limits virus transmission. eLife, 7.

Kobayashi, H. et al., 2017. Development of an in vitro immunobiotic evaluation system against rotavirus infection in bovine intestinal epitheliocytes. Benef Microbes, 8(2): 309-321.

Koppers-Lalic, D. et al., 2001. The UL41-encoded virion host shutoff (vhs) protein and vhs-independent mechanisms are responsible for down-regulation of MHC class I molecules by bovine herpesvirus 1. J Gen Virol, 82(Pt 9): 2071-2081.

Kotenko, S.V. et al., 2003. IFN-lambdas mediate antiviral protection through a distinct class II cytokine receptor complex. Nat Immunol, 4(1): 69-77.

Kurt-Jones, E.A. et al., 2000. Pattern recognition receptors TLR4 and CD14 mediate response to respiratory syncytial virus. Nat Immunol, 1(5): 398-401.

Laloli, L. et al., 2022. Time-resolved characterization of the innate immune response in the respiratory epithelium of human, porcine, and bovine during influenza virus infection. Front Immunol, 13: 970325.

Lang, B.J. et al., 2021. The functions and regulation of heat shock proteins; key orchestrators of proteostasis and the heat shock response. Arch Toxicol, 95(6): 1943-1970.

Latz, E., Xiao, T.S., Stutz, A., 2013. Activation and regulation of the inflammasomes. Nature Reviews Immunology, 13(6): 397-411.

Laulajainen-Hongisto, A., Toppila-Salmi, S.K., Luukkainen, A., Kern, R., 2020. Airway Epithelial Dynamics in Allergy and Related Chronic Inflammatory Airway Diseases. Front Cell Dev Biol, 8: 204.

Lazear, H.M., Nice, T.J., Diamond, M.S., 2015. Interferon-λ: Immune Functions at Barrier Surfaces and Beyond. Immunity, 43(1): 15-28.

Lazear, H.M., Schoggins, J.W., Diamond, M.S., 2019. Shared and Distinct Functions of Type I and Type III Interferons. Immunity, 50(4): 907-923.

Levings, R.L., Roth, J.A., 2013. Immunity to bovine herpesvirus 1: I. Viral lifecycle and innate immunity. Anim Health Res Rev, 14(1): 88-102.

Lindner, P., Christensen, S.B., Nissen, P., Møller, J.V., Engedal, N., 2020. Cell death induced by the ER stressor thapsigargin involves death receptor 5, a non-autophagic function of MAP1LC3B, and distinct contributions from unfolded protein response components. Cell Communication and Signaling, 18(1): 12.

Liu, P. et al., 2007. Retinoic acid-inducible gene I mediates early antiviral response and Toll-like receptor 3 expression in respiratory syncytial virus-infected airway epithelial cells. J Virol, 81(3): 1401-11.

LM, R.E.-A., Thomas, C., Luke, J., J, A.W., Brownlie, J., 2015. Enhanced neutralising antibody response to bovine viral diarrhoea virus (BVDV) induced by DNA vaccination in calves. Vaccine, 33(32): 4004-12.

Loneragan, G.H., Dargatz, D.A., Morley, P.S., Smith, M.A., 2001. Trends in mortality ratios among cattle in US feedlots. Journal of the American Veterinary Medical Association, 219(8): 1122-1127.

Lorenz, I. et al., 2011. Calf health from birth to weaning. III. housing and management of calf pneumonia. Ir Vet J, 64(1): 14.

Lovato, L., Inman, M., Henderson, G., Doster, A., Jones, C., 2003. Infection of cattle with a bovine herpesvirus 1 strain that contains a mutation in the latency-related gene leads to increased apoptosis in trigeminal ganglia during the transition from acute infection to latency. J Virol, 77(8): 4848-57.

Lund, J.M. et al., 2004. Recognition of single-stranded RNA viruses by Toll-like receptor 7. Proc Natl Acad Sci U S A, 101(15): 5598-603.

Lundberg, A.M. et al., 2007. Key differences in TLR3/poly I:C signaling and cytokine induction by human primary cells: a phenomenon absent from murine cell systems. Blood, 110(9): 3245-52.

Ma, Y. et al., 2016. A species-specific activation of Toll-like receptor signaling in bovine and sheep bronchial epithelial cells triggered by Mycobacterial infections. Mol Immunol, 71: 23-33.

Madin, S.H., McKercher, D.G., York, C.J., 1956. Isolation of the infectious bovine rhinotracheitis virus. Science, 124(3225): 721-2.

Madrigal-Estebas, L., Doherty, D.G., O'Donoghue, D.P., Feighery, C., O'Farrelly, C., 2002. Differential expression and upregulation of interleukin-1alpha, interleukin-1beta and interleukin-6 by freshly isolated human small intestinal epithelial cells. Mediators Inflamm, 11(5): 313-9.

Maggioncalda, J., Mehta, A., Su, Y.H., Fraser, N.W., Block, T.M., 1996. Correlation between herpes simplex virus type 1 rate of reactivation from latent infection and the number of infected neurons in trigeminal ganglia. Virology, 225(1): 72-81.

Mahlakõiv, T., Hernandez, P., Gronke, K., Diefenbach, A., Staeheli, P., 2015. Leukocyte-derived IFN-α/β and epithelial IFN-λ constitute a compartmentalized mucosal defense system that restricts enteric virus infections. PLoS Pathog, 11(4): e1004782.

Major, J. et al., 2020. Type I and III interferons disrupt lung epithelial repair during recovery from viral infection. Science (New York, N.y.), 369: 712 - 717.

Malhotra, J.D., Kaufman, R.J., 2007. The endoplasmic reticulum and the unfolded protein response. Seminars in Cell & Developmental Biology, 18(6): 716-731.

Manlapat, A.K., Kahler, D.J., Chandler, P.R., Munn, D.H., Mellor, A.L., 2007. Cell-autonomous control of interferon type I expression by indoleamine 2,3-dioxygenase in regulatory CD19+ dendritic cells. Eur J Immunol, 37(4): 1064-71.

Marcello, T. et al., 2006. Interferons alpha and lambda inhibit hepatitis C virus replication with distinct signal transduction and gene regulation kinetics. Gastroenterology, 131(6): 1887-98.

Marin, M.S. et al., 2014. Toll-like receptor activation and expression in bovine alpha-herpesvirus infections. Res Vet Sci, 96(1): 196-203.

Masic, A., 2017. Effect of a Non-Specific Immune Stimulant (Amplimune™) on the Health and Production of Light Feedlot Calves. Journal of Dairy, Veterinary & Animal Research, 6.

Matassov, D., Kagan, T., Leblanc, J., Sikorska, M., Zakeri, Z., 2004. Measurement of apoptosis by DNA fragmentation. Methods Mol Biol, 282: 1-17.

Mateu, E., Martin, M., 2001. Why is anti-microbial resistance a veterinary problem as well? J Vet Med B Infect Dis Vet Public Health, 48(8): 569-81.

Mayer, A.K. et al., 2007. Differential recognition of TLR-dependent microbial ligands in human bronchial epithelial cells. J Immunol, 178(5): 3134-42.

Medzhitov, R., Janeway, C., Jr., 2000. Innate immune recognition: mechanisms and pathways. Immunol Rev, 173: 89-97.

Mesev, E.V., LeDesma, R.A., Ploss, A., 2019. Decoding type I and III interferon signalling during viral infection. Nat Microbiol, 4(6): 914-924.

Mihaylova, V.T. et al., 2018. Regional Differences in Airway Epithelial Cells Reveal Tradeoff between Defense against Oxidative Stress and Defense against Rhinovirus. Cell Rep, 24(11): 3000-3007.e3.

Mitchell, G.B., Al-Haddawi, M.H., Clark, M.E., Beveridge, J.D., Caswell, J.L., 2007. Effect of corticosteroids and neuropeptides on the expression of defensins in bovine tracheal epithelial cells. Infect Immun, 75(3): 1325-34.

Mogensen, T.H., 2009. Pathogen recognition and inflammatory signaling in innate immune defenses. Clin Microbiol Rev, 22(2): 240-73, Table of Contents.

Mordstein, M. et al., 2010. Lambda interferon renders epithelial cells of the respiratory and gastrointestinal tracts resistant to viral infections. J Virol, 84(11): 5670-7.

Mosier, D., 2015. Review of BRD pathogenesis: the old and the new. Animal Health Research Reviews, 15(2): 166-168.

Mourao-Sa, D., Roy, S., Blander, J.M., 2013. Vita-PAMPs: signatures of microbial viability. Adv Exp Med Biol, 785: 1-8.

Muir, A. et al., 2004. Toll-like receptors in normal and cystic fibrosis airway epithelial cells. Am J Respir Cell Mol Biol, 30(6): 777-83.

Mukherjee, A. et al., 2009. Retinoic acid-induced gene-1 (RIG-I) associates with the actin cytoskeleton via caspase activation and recruitment domain-dependent interactions. J Biol Chem, 284(10): 6486-94.

Munn, D.H., Mellor, A.L., 2013. Indoleamine 2,3 dioxygenase and metabolic control of immune responses. Trends Immunol, 34(3): 137-43.

Murawski, M.R. et al., 2009. Respiratory syncytial virus activates innate immunity through Toll-like receptor 2. J Virol, 83(3): 1492-500.

Muylkens, B., Thiry, J., Kirten, P., Schynts, F., Thiry, E., 2007. Bovine herpesvirus 1 infection and infectious bovine rhinotracheitis. Vet Res, 38(2): 181-209.

Naik, S. et al., 2017. Inflammatory memory sensitizes skin epithelial stem cells to tissue damage. Nature, 550(7677): 475-480.

Nalubamba, K.S., Gossner, A.G., Dalziel, R.G., Hopkins, J., 2007. Differential expression of pattern recognition receptors in sheep tissues and leukocyte subsets. Vet Immunol Immunopathol, 118(3-4): 252-62.

Natoli, G., Ostuni, R., 2019. Adaptation and memory in immune responses. Nat Immunol, 20(7): 783-792.

Neagos, J. et al., 2015. Epigenetic Regulation of Tolerance to Toll-Like Receptor Ligands in Alveolar Epithelial Cells. Am J Respir Cell Mol Biol, 53(6): 872-81.

Nelson-Rees, W.A., Daniels, D.W., Flandermeyer, R.R., 1981. Cross-contamination of cells in culture. Science, 212(4493): 446-52.

Netea, M.G., 2013. Training innate immunity: the changing concept of immunological memory in innate host defence. Eur J Clin Invest, 43(8): 881-4.

Newcomer, B.W., Cofield, L.G., Walz, P.H., Givens, M.D., 2017. Prevention of abortion in cattle following vaccination against bovine herpesvirus 1: A meta-analysis. Prev Vet Med, 138: 1-8.

Ng, T.F. et al., 2015. A metagenomics and case-control study to identify viruses associated with bovine respiratory disease. J Virol, 89(10): 5340-9.

Nicholas, B. et al., 2006. Shotgun proteomic analysis of human-induced sputum. Proteomics, 6(15): 4390-401.

Nickell, J. et al., 2016. Efficacy and safety of a novel DNA immunostimulant in cattle. The Bovine Practitioner, 50: 10-20.

O'Grady, L., O'Neill, R., Collins, D., Clegg, T., More, S., 2008. Herd and within-herd BoHV-1 prevalence among Irish beef herds submitting bulls for entry to a performance testing station. Ir Vet J, 61(12): 809-15.

O'Neill, L.A., Golenbock, D., Bowie, A.G., 2013. The history of Toll-like receptors - redefining innate immunity. Nat Rev Immunol, 13(6): 453-60.

O'Neill, L.A., Kishton, R.J., Rathmell, J., 2016. A guide to immunometabolism for immunologists. Nat Rev Immunol, 16(9): 553-65.

Ogata, M. et al., 2006. Autophagy is activated for cell survival after endoplasmic reticulum stress. Mol Cell Biol, 26(24): 9220-31.

Okabayashi, T. et al., 2011. Type-III interferon, not type-I, is the predominant interferon induced by respiratory viruses in nasal epithelial cells. Virus Res, 160(1-2): 360-6.

Okumura, R., Takeda, K., 2017. Roles of intestinal epithelial cells in the maintenance of gut homeostasis. Exp Mol Med, 49(5): e338.

Osman, R., Gonzalez-Cano, P., Brownlie, R., Griebel, P.J., 2017. Induction of interferon and interferon-induced antiviral effector genes following a primary bovine herpesvirus-1 (BHV-1) respiratory infection. J Gen Virol, 98(7): 1831-1842.

Parliament, E., 2011.

Perez-Martin, E. et al., 2012. Bovine type III interferon significantly delays and reduces the severity of foot-and-mouth disease in cattle. J Virol, 86(8): 4477-87.

Pfefferkorn, E.R., 1984. Interferon gamma blocks the growth of Toxoplasma gondii in human fibroblasts by inducing the host cells to degrade tryptophan. Proc Natl Acad Sci U S A, 81(3): 908-12.

Piret, J., Boivin, G., 2022. Viral Interference between Respiratory Viruses. Emerg Infect Dis, 28(2): 273-281.

Proud, D., Leigh, R., 2011. Epithelial cells and airway diseases. Immunol Rev, 242(1): 186-204.

Quintana, M.E. et al., 2020. Interferon lambda protects cattle against bovine viral diarrhea virus infection. Vet Immunol Immunopathol, 230: 110145.

Rabbani, M.A.G., Ribaudo, M., Guo, J.-T., Barik, S., Sandri-Goldin, R.M., 2016. Identification of Interferon-Stimulated Gene Proteins That Inhibit Human Parainfluenza Virus Type 3. Journal of Virology, 90(24): 11145-11156.

Radons, J., 2016. The human HSP70 family of chaperones: where do we stand? Cell Stress Chaperones, 21(3): 379-404.

Raghunath, A., Panneerselvam, L., Sundarraj, K., Perumal, E., 2018. Heat Shock Proteins and Endoplasmic Reticulum Stress. In: Asea, A.A.A., Kaur, P. (Eds.), Heat Shock Proteins and Stress. Springer International Publishing, Cham, pp. 39-78.

Ramirez, V.P., Stamatis, M., Shmukler, A., Aneskievich, B.J., 2015. Basal and stress-inducible expression of HSPA6 in human keratinocytes is regulated by negative and positive promoter regions. Cell Stress Chaperones, 20(1): 95-107.

Raniga, K., Liang, C., 2018. Interferons: Reprogramming the Metabolic Network against Viral Infection. Viruses, 10(1).

REED, L.J., MUENCH, H., 1938. A SIMPLE METHOD OF ESTIMATING FIFTY PER CENT ENDPOINTS12. American Journal of Epidemiology, 27(3): 493-497.

Reed, S.E., 1969. Persistent respiratory virus infection in tracheal organ cultures. British journal of experimental pathology, 50(4): 378-388.

Regis, E. et al., 2021. Sex differences in innate anti-viral immune responses to respiratory viruses and in their clinical outcomes in a birth cohort study. Sci Rep, 11(1): 23741.

Ring, S.C. et al., 2018. Genetic variability in the humoral immune response to bovine herpesvirus-1 infection in dairy cattle and genetic correlations with performance traits. J Dairy Sci, 101(7): 6190-6204.

Robinson, C.M., Shirey, K.A., Carlin, J.M., 2003. Synergistic transcriptional activation of indoleamine dioxygenase by IFN-gamma and tumor necrosis factor-alpha. J Interferon Cytokine Res, 23(8): 413-21.

Roche, W.R., Montefort, S., Baker, J., Holgate, S.T., 1993. Cell adhesion molecules and the bronchial epithelium. Am Rev Respir Dis, 148(6 Pt 2): S79-82.

Roizman, B., Gu, H., Mandel, G., 2005. The first 30 minutes in the life of a virus: unREST in the nucleus. Cell Cycle, 4(8): 1019-21.

Rotem, Z., Cox, R.A., Isaacs, A., 1963. Inhibition of virus multiplication by foreign nucleic acid. Nature, 197: 564-6.

Saha, S.K. et al., 2006. Regulation of antiviral responses by a direct and specific interaction between TRAF3 and Cardif. Embo j, 25(14): 3257-63.

Saira, K., Zhou, Y., Jones, C., 2007. The infected cell protein 0 encoded by bovine herpesvirus 1 (bICP0) induces degradation of interferon response factor 3 and, consequently, inhibits beta interferon promoter activity. J Virol, 81(7): 3077-86.

Santoro, M.G., Amici, C., Rossi, A., 2010. Role of Heat Shock Proteins in Viral Infection. Prokaryotic and Eukaryotic Heat Shock Proteins in Infectious Disease, 4: 51-84.

Sasai, M. et al., 2006. NAK-associated protein 1 participates in both the TLR3 and the cytoplasmic pathways in type I IFN induction. J Immunol, 177(12): 8676-83.

Sato, M. et al., 2003. Direct binding of Toll-like receptor 2 to zymosan, and zymosan-induced NF-kappa B activation and TNF-alpha secretion are down-regulated by lung collectin surfactant protein A. J Immunol, 171(1): 417-25.

Sayers, R.G., 2017. Associations between exposure to bovine herpesvirus 1 (BoHV-1) and milk production, reproductive performance, and mortality in Irish dairy herds. J Dairy Sci, 100(2): 1340-1352.

Schmittgen, T.D., Livak, K.J., 2008. Analyzing real-time PCR data by the comparative C(T) method. Nat Protoc, 3(6): 1101-8.

Schoggins, J.W., 2019. Interferon-Stimulated Genes: What Do They All Do? Annu Rev Virol, 6(1): 567-584.

Schoggins, J.W., Rice, C.M., 2011. Interferon-stimulated genes and their antiviral effector functions. Curr Opin Virol, 1(6): 519-25.

Schroten, H. et al., 2001. Potential role of human brain microvascular endothelial cells in the pathogenesis of brain abscess: inhibition of Staphylococcus aureus by activation of indoleamine 2,3-dioxygenase. Neuropediatrics, 32(4): 206-10.

Sehgal, P. et al., 2017. Inhibition of the sarco/endoplasmic reticulum (ER) Ca(2+)-ATPase by thapsigargin analogs induces cell death via ER Ca(2+) depletion and the unfolded protein response. J Biol Chem, 292(48): 19656-19673.

Sha, Q., Truong-Tran, A.Q., Plitt, J.R., Beck, L.A., Schleimer, R.P., 2004. Activation of airway epithelial cells by toll-like receptor agonists. Am J Respir Cell Mol Biol, 31(3): 358-64.

Shaban, M.S. et al., 2021. Multi-level inhibition of coronavirus replication by chemical ER stress. Nature Communications, 12(1): 5536.

Shaw, A.E. et al., 2017. Fundamental properties of the mammalian innate immune system revealed by multispecies comparison of type I interferon responses. PLoS Biol, 15(12): e2004086.

Sheppard, P. et al., 2003. IL-28, IL-29 and their class II cytokine receptor IL-28R. Nat Immunol, 4(1): 63-8.

Shi, Y. et al., 1998. Identification and characterization of pancreatic eukaryotic initiation factor 2 alpha-subunit kinase, PEK, involved in translational control. Mol Cell Biol, 18(12): 7499-509.

Shoemaker, M.L. et al., 2009. Differential expression of the type I interferon pathway during persistent and transient bovine viral diarrhea virus infection. J Interferon Cytokine Res, 29(1): 23-35.

Silva, A.M.V.d. et al., 2021. Interferon-lambda 3 and 4 Polymorphisms Increase Sustained Virological Responses and Regulate Innate Immunity in Antiviral Therapy With Pegylated Interferon-Alpha. Frontiers in Cellular and Infection Microbiology, 11.

Smirnova, N.P. et al., 2012. Development of fetal and placental innate immune responses during establishment of persistent infection with bovine viral diarrhea virus. Virus Res, 167(2): 329-36.

Sommereyns, C., Paul, S., Staeheli, P., Michiels, T., 2008. IFN-lambda (IFN-lambda) is expressed in a tissue-dependent fashion and primarily acts on epithelial cells in vivo. PLoS Pathog, 4(3): e1000017.

Spear, P.G., 2004. Herpes simplex virus: receptors and ligands for cell entry. Cell Microbiol, 6(5): 401-10.

Spurzem, J.R. et al., 1995. Bovine herpesvirus-1 infection reduces bronchial epithelial cell migration to extracellular matrix proteins. Am J Physiol, 268(2 Pt 1): L214-20.

Standiford, T.J. et al., 1990. Interleukin-8 gene expression by a pulmonary epithelial cell line. A model for cytokine networks in the lung. The Journal of Clinical Investigation, 86(6): 1945-1953.

Stanifer, M., Guo, C., Doldan, P., Boulant, S., 2020a. Importance of Type I and III Interferons at Respiratory and Intestinal Barrier Surfaces. Frontiers in Immunology, 11.

Stanifer, M.L. et al., 2020b. Asymmetric distribution of TLR3 leads to a polarized immune response in human intestinal epithelial cells. Nat Microbiol, 5(1): 181-191.

Su, Y.-S., Hwang, L.-H., Chen, C.-J., 2021. Heat Shock Protein A6, a Novel HSP70, Is Induced During Enterovirus A71 Infection to Facilitate Internal Ribosomal Entry Site-Mediated Translation. Frontiers in Microbiology, 12.

Taha-Abdelaziz, K. et al., 2016. Regulation of tracheal antimicrobial peptide gene expression in airway epithelial cells of cattle. Vet Res, 47: 44.

Takanashi, N. et al., 2013. Advanced application of bovine intestinal epithelial cell line for evaluating regulatory effect of lactobacilli against heat-killed enterotoxigenic Escherichia coli-mediated inflammation. BMC Microbiol, 13: 54.

Takaoka, A. et al., 2007. DAI (DLM-1/ZBP1) is a cytosolic DNA sensor and an activator of innate immune response. Nature, 448(7152): 501-5.

Takaoka, A., Yanai, H., 2006. Interferon signalling network in innate defence. Cell Microbiol, 8(6): 907-22.

Takeuchi, O., Akira, S., 2010. Pattern recognition receptors and inflammation. Cell, 140(6): 805-20.

Tavalai, N., Stamminger, T., 2009. Interplay between Herpesvirus Infection and Host Defense by PML Nuclear Bodies. Viruses, 1(3): 1240-64.

Taylor, G., 2017. Animal models of respiratory syncytial virus infection. Vaccine, 35(3): 469-480.

Thomas, D.L. et al., 2009. Genetic variation in IL28B and spontaneous clearance of hepatitis C virus. Nature, 461(7265): 798-801.

Thompson, A.J., Locarnini, S.A., 2007. Toll-like receptors, RIG-I-like RNA helicases and the antiviral innate immune response. Immunol Cell Biol, 85(6): 435-45.

Thompson, M.R., Kaminski, J.J., Kurt-Jones, E.A., Fitzgerald, K.A., 2011. Pattern recognition receptors and the innate immune response to viral infection. Viruses, 3(6): 920-40.

Török, Z. et al., 2014. Plasma membranes as heat stress sensors: from lipid-controlled molecular switches to therapeutic applications. Biochim Biophys Acta, 1838(6): 1594-618.

Trapp, S., Osterrieder, N., Keil, G.M., Beer, M., 2003. Mutagenesis of a bovine herpesvirus type 1 genome cloned as an infectious bacterial artificial chromosome: analysis of glycoprotein E and G double deletion mutants. J Gen Virol, 84(Pt 2): 301-306.

Turin, L., Russo, S., Poli, G., 1999. BHV-1: New Molecular Approaches to Control a Common and Widespread Infection. Molecular Medicine, 5.

Tyrrell, D.A., Bynoe, M.L., 1965. CULTIVATION OF A NOVEL TYPE OF COMMON-COLD VIRUS IN ORGAN CULTURES. Br Med J, 1(5448): 1467-70.

Ubeda, M. et al., 1996. Stress-induced binding of the transcriptional factor CHOP to a novel DNA control element. Mol Cell Biol, 16(4): 1479-89.

Unterholzner, L., 2013. The interferon response to intracellular DNA: why so many receptors? Immunobiology, 218(11): 1312-21.

Unterholzner, L. et al., 2010. IFI16 is an innate immune sensor for intracellular DNA. Nat Immunol, 11(11): 997-1004.

van Drunen Littel-van den Hurk, S., Tikoo, S.K., van den Hurk, J.V., Babiuk, L.A., Van Donkersgoed, J., 1997. Protective immunity in cattle following vaccination with conventional and marker bovine herpesvirus-1 (BHV1) vaccines. Vaccine, 15(1): 36-44.

Vareille, M., Kieninger, E., Edwards, M.R., Regamey, N., 2011. The airway epithelium: soldier in the fight against respiratory viruses. Clin Microbiol Rev, 24(1): 210-29.

Voynow, J.A., Rubin, B.K., 2009. Mucins, mucus, and sputum. Chest, 135(2): 505-512.

Wan, Q., Song, D., Li, H., He, M.L., 2020. Stress proteins: the biological functions in virus infection, present and challenges for target-based antiviral drug development. Signal Transduct Target Ther, 5(1): 125.

Wang, J., Alexander, J., Wiebe, M., Jones, C., 2014. Bovine herpesvirus 1 productive infection stimulates inflammasome formation and caspase 1 activity. Virus Res, 185: 72-6.

Wang, J., Li, F., Tian, Z., 2017. Role of microbiota on lung homeostasis and diseases. Sci China Life Sci, 60(12): 1407-1415.

Wang, J., Matsukura, S., Watanabe, S., Adachi, M., Suzaki, H., 2007. Involvement of Toll-like receptors in the immune response of nasal polyp epithelial cells. Clin Immunol, 124(3): 345-52.

Wang, Q. et al., 2009. Role of double-stranded RNA pattern recognition receptors in rhinovirus-induced airway epithelial cell responses. J Immunol, 183(11): 6989-97.

Warren, L.M., Babiuk, L.A., Campos, M., 1996. Effects of BHV-1 on PMN adhesion to bovine lung endothelial cells. Vet Immunol Immunopathol, 55(1-3): 73-82.

Weitnauer, M., Mijosek, V., Dalpke, A.H., 2016. Control of local immunity by airway epithelial cells. Mucosal Immunol, 9(2): 287-98.

Werner, E.R. et al., 1989. Parallel induction of tetrahydrobiopterin biosynthesis and indoleamine 2,3-dioxygenase activity in human cells and cell lines by interferon-gamma. Biochem J, 262(3): 861-6.

Whitsett, J.A., Alenghat, T., 2015. Respiratory epithelial cells orchestrate pulmonary innate immunity. Nat Immunol, 16(1): 27-35.

Wileman, B.W., Thomson, D.U., Reinhardt, C.D., Renter, D.G., 2009. Analysis of modern technologies commonly used in beef cattle production: conventional beef production versus nonconventional production using meta-analysis. J Anim Sci, 87(10): 3418-26.

Winkler, M.T., Doster, A., Jones, C., 1999. Bovine herpesvirus 1 can infect CD4(+) T lymphocytes and induce programmed cell death during acute infection of cattle. J Virol, 73(10): 8657-68.

Wong, M.H., Johnson, M.D., 2013. Differential response of primary alveolar type I and type II cells to LPS stimulation. PLoS One, 8(1): e55545.

Wu, J. et al., 2013. Cyclic GMP-AMP is an endogenous second messenger in innate immune signaling by cytosolic DNA. Science, 339(6121): 826-30.

Xing, Z. et al., 2011. Host immune and apoptotic responses to avian influenza virus H9N2 in human tracheobronchial epithelial cells. Am J Respir Cell Mol Biol, 44(1): 24-33.

Xu, X. et al., 2012. Bovine herpes virus type 1 induces apoptosis through Fas-dependent and mitochondria-controlled manner in Madin-Darby bovine kidney cells. Virol J, 9: 202.

Yang, S.-C., Tsai, Y.-F., Pan, Y.-L., Hwang, T.-L., 2021. Understanding the role of neutrophils in acute respiratory distress syndrome. Biomedical Journal, 44(4): 439-446.

Yang, Z. et al., 2015. Bovine TLR2 and TLR4 mediate Cryptosporidium parvum recognition in bovine intestinal epithelial cells. Microb Pathog, 85: 29-34.

Yao, Y., Wang, H., Liu, Z., 2020. Expression of ACE2 in airways: Implication for COVID-19 risk and disease management in patients with chronic inflammatory respiratory diseases. Clin Exp Allergy, 50(12): 1313-1324.

Ye, L. et al., 2019a. Interferon-» enhances adaptive mucosal immunity by boosting release of thymic stromal lymphopoietin. Nature Immunology, 20: 593-601.

Ye, L., Schnepf, D., Staeheli, P., 2019b. Interferon-λ orchestrates innate and adaptive mucosal immune responses. Nat Rev Immunol, 19(10): 614-625.

Yoneyama, M. et al., 2005. Shared and unique functions of the DExD/H-box helicases RIG-I, MDA5, and LGP2 in antiviral innate immunity. J Immunol, 175(5): 2851-8.

Yoneyama, M. et al., 2004. The RNA helicase RIG-I has an essential function in double-stranded RNA-induced innate antiviral responses. Nat Immunol, 5(7): 730-7.

Yoshida, H., Matsui, T., Yamamoto, A., Okada, T., Mori, K., 2001. XBP1 mRNA is induced by ATF6 and spliced by IRE1 in response to ER stress to produce a highly active transcription factor. Cell, 107(7): 881-91.

Yoshida, R., Hayaishi, O., 1978. Induction of pulmonary indoleamine 2,3-dioxygenase by intraperitoneal injection of bacterial lipopolysaccharide. Proc Natl Acad Sci U S A, 75(8): 3998-4000.

Yoshida, R., Imanishi, J., Oku, T., Kishida, T., Hayaishi, O., 1981. Induction of pulmonary indoleamine 2,3-dioxygenase by interferon. Proc Natl Acad Sci U S A, 78(1): 129-32.

Zanoni, I., 2021. Interfering with SARS-CoV-2: are interferons friends or foes in COVID-19? Current Opinion in Virology.

Zbinden, C., Pilo, P., Frey, J., Bruckmaier, R.M., Wellnitz, O., 2015. The immune response of bovine mammary epithelial cells to live or heat-inactivated Mycoplasma bovis. Vet Microbiol, 179(3-4): 336-40.

Zhang, P., Su, C., Jiang, Z., Zheng, C., 2017. Herpes Simplex Virus 1 UL41 Protein Suppresses the IRE1/XBP1 Signal Pathway of the Unfolded Protein Response via Its RNase Activity. J Virol, 91(4).

Zhang, S.Y. et al., 2007. TLR3 deficiency in patients with herpes simplex encephalitis. Science, 317(5844): 1522-7.

Zhou, X. et al., 2022. HSPA6 is Correlated With the Malignant Progression and Immune Microenvironment of Gliomas. Front Cell Dev Biol, 10: 833938.

Zhou, Z. et al., 2007. Type III interferon (IFN) induces a type I IFN-like response in a restricted subset of cells through signaling pathways involving both the Jak-STAT pathway and the mitogen-activated protein kinases. J Virol, 81(14): 7749-58.

Zhu, L. et al., 2009. Rhinovirus-induced major airway mucin production involves a novel TLR3-EGFR-dependent pathway. Am J Respir Cell Mol Biol, 40(5): 610-9.

A. Appendices

A.1. List of reagents, materials and instruments used

Table A.1 General reagents used with manufacturer details

Reagent	Company	Location
Cell isolation and culture		
Accutase cell detachment solution	Biolegend	San Diego, CA, USA
Amphotericin B solution	Sigma-Aldrich	Poole, UK
Bovine Serum Albumin	Sigma-Aldrich	Poole, UK
Dulbecco's Modified Eagle's Medium (DMEM)	Gibco (Thermo Fisher Scientific)	Paisley, UK
Dimethyl Sulfoxide (DMSO)	Sigma-Aldrich	Poole, UK
Distilled, sterile, nuclease-free water	Gibco (Thermo Fisher Scientific)	Paisley, UK
Eagle's Minimum Essential Medium (MEM)	Gibco (Thermo Fisher Scientific)	Paisley, UK
Ethanol	Sigma-Aldrich	Poole, UK
thylenediaminetetraacetic acid (EDTA)	Sigma-Aldrich	Poole, UK
Fetal bovine serum (FBS)	Gibco (Thermo Fisher Scientific)	Paisley, UK
Formalin, neutral buffered, 10%	Sigma-Aldrich	Poole, UK
Horse serum	Gibco (Thermo Fisher Scientific)	Paisley, UK
Industrial methylated spirits (IMS)	Lennox	Dublin, Ireland

Insulin-Transferrin-Selenium-Ethanolamine (ITS-X) solution	Gibco (Thermo Fisher Scientific)	Paisley, UK
LHC-9 Medium	Gibco (Thermo Fisher Scientific)	Paisley, UK
Matrigel basement membrane matrix	Thermo Fisher Scientific	Paisley, UK
Methanol	Sigma- Aldrich	Poole, UK
Paraformaldehyde, 4%	Sigma- Aldrich	Poole, UK
Penicillin-Streptomycin	Invitrogen (Biosciences)	Carlsbad, CA, USA
Phosphate buffered saline (PBS), sterile	Gibco (Thermo Fisher Scientific)	Paisley, UK
Sodium chloride	Sigma- Aldrich	Poole, UK
Sucrose	Sigma- Aldrich	Poole, UK
Trypan blue	Sigma-Aldrich	Poole, UK
Trypsin 0.25%	Sigma-Aldrich	Poole, UK
Molecular biology		
100bp DNA ladder	Invitrogen (Thermo Fisher Scientific)	Paisley, UK
Acetone	Sigma-Aldrich	Poole, UK
Agarose	Sigma-Aldrich	Poole, UK
Ammonium bicarbonate, bioultra	Merck	Darmstadt, Germany
Chloroform	Sigma-Aldrich	Poole, UK
Ethanol, molecular grade	Sigma-Aldrich	Poole, UK
HotStar Master Mix PCR kit	Qiagen	Crawley, UK
Isopropanol/2-propanol	Sigma-Aldrich	Poole, UK
Oligo dT Primers	Qiagen	Crawley, UK
Omniscript cDNA synthesis kit	Qiagen	Crawley, UK

PCR clean-up kit	Promega	Wisconsin, USA
Power Up SYBR Green Master Mix	Applied Biosystems (Thermo Fisher Scientific)	Paisley, UK
Primer	Integrated DNA technologies	Coralville, IA, USA
RNAlater	Sigma-Aldrich	Poole, UK
SybrSafe DNA gel stain 10,000X	Invitrogen (Thermo Fisher Scientific)	Paisley, UK
Trichloroacetic acid, bioultra >= 99.5	Merck	Darmstadt, Germany
TRIzol	Ambion (Thermo Fisher Scientific)	Paisley, UK
Urea for Biochemistry	Merck	Darmstadt, Germany
Water for chromatography (LC-MS Grade), LiChrosolv®	Merck	Darmstadt, Germany
SDS PAGE		
4-Morpholineethane-sulfonic acid (MES)	Sigma-Aldrich	Poole, UK
Acrylamide	National Diagnostics	USA
APS	Sigma-Aldrich	Paisley, UK
Bromophenol blue	Sigma-Aldrich	
Coomassie Brilliant Blue R-250 Staining Solution	Bio-Rad	California, USA
DL-Dithiothreitol (DDT)	Sigma-Aldrich	Paisley, UK
Glycerol	Sigma-Aldrich	
PageRuler™ Prestained Protein Ladder 10-180 kDa	Thermo Fisher Scientific	Paisley, UK
SDS	Fisher Chemicals	Paisley, UK
Temed	Sigma-Aldrich	Poole, UK
TRIS	Sigma-Aldrich	Poole, UK

Histological processing and immunohistochemical staining		
EnVision IHC detection kit	Dako (Agilent Technologies)	Santa Clara, CA, USA
Hydrogen peroxide	Sigma-Aldrich	Poole, UK
Surgipath mounting medium	Leica Biosystems	Newcastle, UK
Assay kits		
Pierce™ BCA Protein Assay Kit	Thermo Fisher Scientific	Paisley, UK
CellTiter-Blue® Cell Viability Assay	Promega	Wisconsin, USA
LDH-Glo™ Cytotoxicity Assay	Promega	Wisconsin, USA
MTT Assay	Sigma-Aldrich	Poole, UK
Preomics iST Sample Preparation Kit 8x precipitated protein	Preomics	Martinsried, Germany

Table A.2 General materials used with manufacturer details

Reagent	Company	Location
Cell isolation and culture		
10 ml plastic pipettes	Cruinn Diagnostics (Greiner)	Dublin, Ireland
12 well flat bottom tissue culture plates	Cruinn Diagnostics (Cellstar)	Dublin, Ireland
24 well flat bottom tissue culture plates	Cruinn Diagnostics (Cellstar)	Dublin, Ireland
25 ml plastic pipettes	Cruinn Diagnostics (Greiner)	Dublin, Ireland
5 ml plastic pipettes	Cruinn Diagnostics (Greiner)	Dublin, Ireland
6-well flat bottom tissue culture plates	Cruinn Diagnostics (Cellstar)	Dublin, Ireland
70 µm filters	Falcon	NY, USA
96 well flat bottom tissue culture plates	Cruinn Diagnostics (Cellstar)	Dublin, Ireland
Cryovials	VWR (Nunc Inc.)	Radnor, PA, USA
Dissection Scissors	Thermo Fisher Scientific	Paisley, UK
Forceps with teeth	Thermo Fisher Scientific	Paisley, UK
Hanging culture transwell inserts 0.4 µm	Millipore	Burlington, MA, USA
Petri dishes	Greiner Bio-One	Kremsmünster, Austria
T175 Tissue culture flask	Cruinn Diagnostics (Cellstar)	Dublin, Ireland
T75 Tissue culture flask	Cruinn Diagnostics (Cellstar)	Dublin, Ireland

Molecular biology		
96 well plates for qPCR	Thermo Fisher Scientific	Paisley, UK
Optical adhesive film	Applied Biosystems (Thermo Fisher Scientific)	Paisley, UK
Stainless steel beads 5mm	Qiagen	Crawley, UK
P10/P20/P200/P1000 sterile, nuclease-free filtered pipette tips	Thermo Fisher Scientific	Paisley, UK
1.5/2.0 ml nuclease-free, sterile micro centrifuge tubes	Thermo Fisher Scientific	Paisley, UK
0.2 ml nuclease-free micro centrifuge tubes	Sarstedt	Numbrecht, Germany
Histological processing and immunohistochemical staining		
EZ SLIDE 4 well glass culture slides	Millipore	Burlington, MA, USA
Glass slides	Thermo Fisher Scientific	Paisley, UK
Microtome blade	Feather	Japan
Surgipath cassettes	Leica Biosystems	Wetzlar, Germany

Table A.3 List of reagents used for in-vitro stimulation and siRNA treatments

Reagent	Company	Location
Stimulations		
3p-hpRNA	Invivogen	San Diego, CA, USA
IFNB1, Bos taurus	Kingfisher Biotech	St. Paul, MN, USA
Lipofectamine 2000	Thermo Fisher Scientific	Paisley, UK
LPS from *Escherichia coli*, Serotype O55:B5	ENZO Life Sciences (Fisher)	Farmingdale, NY, USA
LyoVec™	Invivogen	San Diego, CA, USA
Poly(dA:dT)/ LyoVec™	Invivogen	San Diego, CA, USA
Poly(I:C) HMW	Invivogen	San Diego, CA, USA
Poly(I:C) HMW/LyoVec™	Invivogen	San Diego, CA, USA
Thapsigargin	Thermo Fisher Scientific	Paisley, UK
siRNA treatments		
Lipofectamine RNAi Max	Thermo Fisher Scientific	Paisley, UK
Opti-MEM media	Gibco (Thermo Fisher Scientific)	Paisley, UK
bt-DDX58 5’ – GUACAAAGUUUCAGGCAUUUU – 3’	Merck	Darmstadt, Germany
bt-IFNAR1 5’ – CUUCAAAUGCUGAGAGAAAUU – 3’	Merck	Darmstadt, Germany
bt-IFNLR1 5’ – AGGAAGGGACUAAGAACAAUU – 3’	Merck	Darmstadt, Germany
bt-TLR3 5’ – CAUCUGAAGUUGACGCAAAUU – 3’	Merck	Darmstadt, Germany
Scramble siRNA 5’ – UGGUUUACAUGUCGACUAA – 3’	Dharmacon	Lafayette, USA

Table A.4 List of antibodies used

Reagent	Supplier	Isotype	Concentration
Vimentin	Sigma-Aldrich	Mouse	1:100
Cytokeratin	Dako	Mouse	1:100
IgG1 Isotype Control from murine myeloma	Sigma-Aldrich	Mouse	1:100

Table A.5 Equipment and software used with manufacturer details

Equipment	Company	Location
Aperio ScanScope Imager	Leica Biosystems	Newcastle, UK
Aperio ScanScope Imager Software	Leica Biosystems	Newcastle, UK
VersaMax Microplate reader	Molecular Devices	San Jose, CA, USA
Epithelial Volt-ohm meter	World Precision Instruments	Hertfordshire, UK
FastQC https://www.bioinformatics.babraham.ac.uk/projects/fastqc/		
Gel Logic 200 imaging system	Kodak	Rochestor, NY, USA
GraphPad Prism 8.0.1 for Windows	Graphpad Software Inc.	San Diego, CA, USA
Microtome	Leica Biosystems	Newcastle, UK
Nanodrop spectrophotometer	Thermo Fisher Scientific	Paisley, UK
Olympus BX51 upright microscope	Leica Biosystems	Newcastle, UK
Olympus IX81 inverted microscope	Leica Biosystems	Newcastle, UK
Perseus https://maxquant.net/perseus/	Max Planck Institute of Biochemistry	Martinsried, Germany
Rstudio 1.4.1717 http://www.rstudio.com/	Integrated Development Environment for R	Boston, MA
StepOne Plus Real time PCR	Thermo Fisher Scientific	Paisley, UK
StepOne Software v.2.3	Thermo Fisher Scientific	Paisley, UK
Techne Prime Thermocycler	Bibby Scientific	Staffordshire, UK
Tissue Lyser II	Qiagen	Crawley, UK

A.2. Coomassie brilliant blue stain of cell lysate and supernatant of primary bovine tracheal epithelial cells stimulated with Poly(I:C)

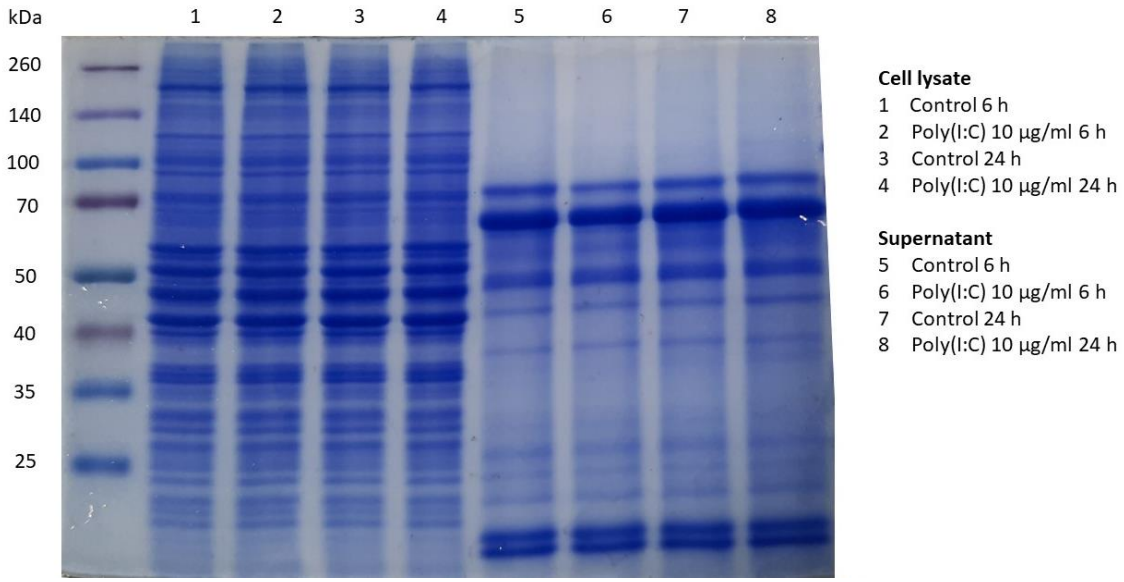

Figure A.1 Coomassie brilliant blue stain of cell lysate and supernatant of primary bovine tracheal epithelial cells stimulated with Poly(I:C)

Bovine tracheal epithelial cells were stimulated for 6 or 24 hours with 10 µg/ml Poly(I:C). The protein pellets obtained from the TCA protein precipitation from cell culture supernatants were resuspended or cells scrapped off in loading buffer. A 14% resolving gel, topped with a 4% stacking gel were used for electrophoresis. Coomassie Brilliant Blue R-250 Staining Solution was used to stain for proteins.

A.3. Mass spectrometry analysis of supernatant of tracheal epithelial cells stimulated with Poly(I:C)

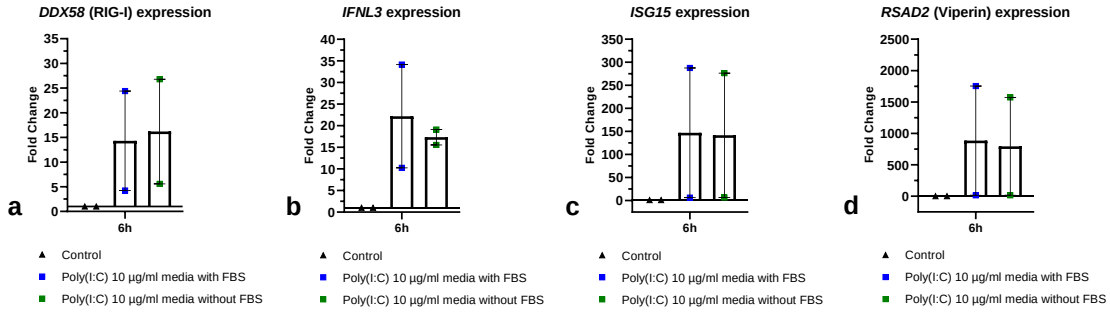

Figure A.2 Fetal bovine serum (FBS) absence in the media does not influence the upregulation of the genes DDX58, IFNL3, ISG15 or RSAD2 in bovine tracheal epithelial cells stimulated with Poly(I:C)

Bovine tracheal epithelial cells were stimulated for 6 hours with 10 µg/ml Poly(I:C) in media with or without 10% FBS. Cells were harvested into Trizol, RNA was extracted and first strand cDNA reverse transcribed. qPCR was carried out and gene Cq values were normalised to the reference gene H3F3A and values normalised to the untreated control. Each data point represents a different animal. Error bars indicate standard error of the mean; n=2.

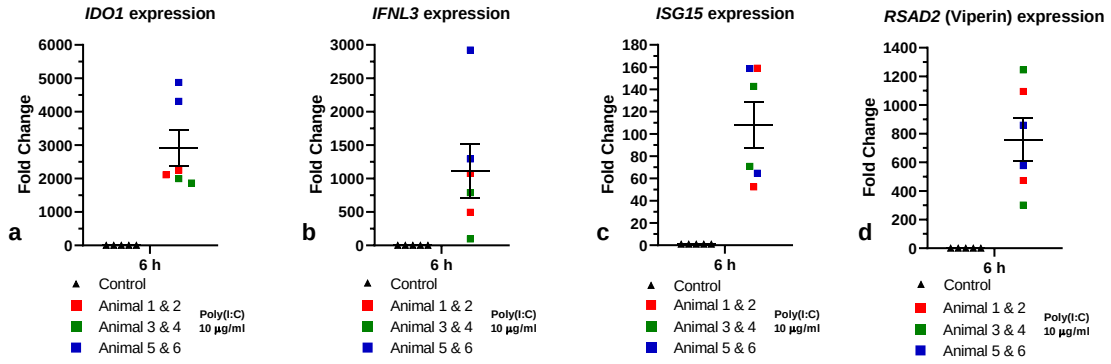

Figure A.3 Upregulation of the genes IDO1, IFNL3, ISG15 and RSAD2 in bovine tracheal epithelial cells stimulated with Poly(I:C) from which supernatants were used for mass spectrometry analysis

Bovine tracheal epithelial cells were stimulated for 6 hours with 10 µg/ml Poly(I:C) in media without FBS. Cells were harvested into Trizol, RNA was extracted and first strand cDNA reverse transcribed. qPCR was carried out and gene Cq values were normalised to the reference gene H3F3A and values normalised to the untreated control. Each data point represents a different animal. Error bars indicate standard error of the mean. For subsequent mass spectrometry analysis two animals each got pooled.

Table A.6 Mass spectrometry analysis results of supernatant from primary bovine epithelial cells unstimulated vs. Poly(I:C) 10 µg/ml for 6 hours (significant results only)

Protein name	log2 FC	FC	-log p-value	adj. p-value
ELAV-like protein	-1.30793333	0.40389905	3.57894	0.142119
Keratin, type II cytoskeletal 1	-2.10126667	0.23305354	2.27493	0.958331
Guanine nucleotide-binding protein G(o) subunit alpha	-0.18766667	0.87802464	2.13011	0.958331
RNA-binding protein 8A	1.55706667	2.94254946	2.00882	0.958331
Glucosamine-6-phosphate isomerase 2	0.2781	1.21259687	1.76076	0.958331
Annexin A1	0.45736667	1.37303335	1.55292	0.958331
Tropomyosin alpha-1 chain	1.32166667	2.49954702	1.53453	0.958331
Uncharacterized protein/Hydroxyacyl-CoA dehydrogenase	-1.8933	0.26919061	1.52094	0.958331
Ubiquitin carboxyl-terminal hydrolase isozyme L1	0.28676667	1.21990319	1.50564	0.958331
Hemopexin	0.4903	1.40473695	1.44887	0.958331
Cytoplasmic aconitate hydratase	-0.55303333	0.68158556	1.36935	0.958331
Talin 1	-0.42656667	0.74403033	1.33105	0.958331
Myelin P2 protein	0.21596667	1.1614819	1.30594	0.958331

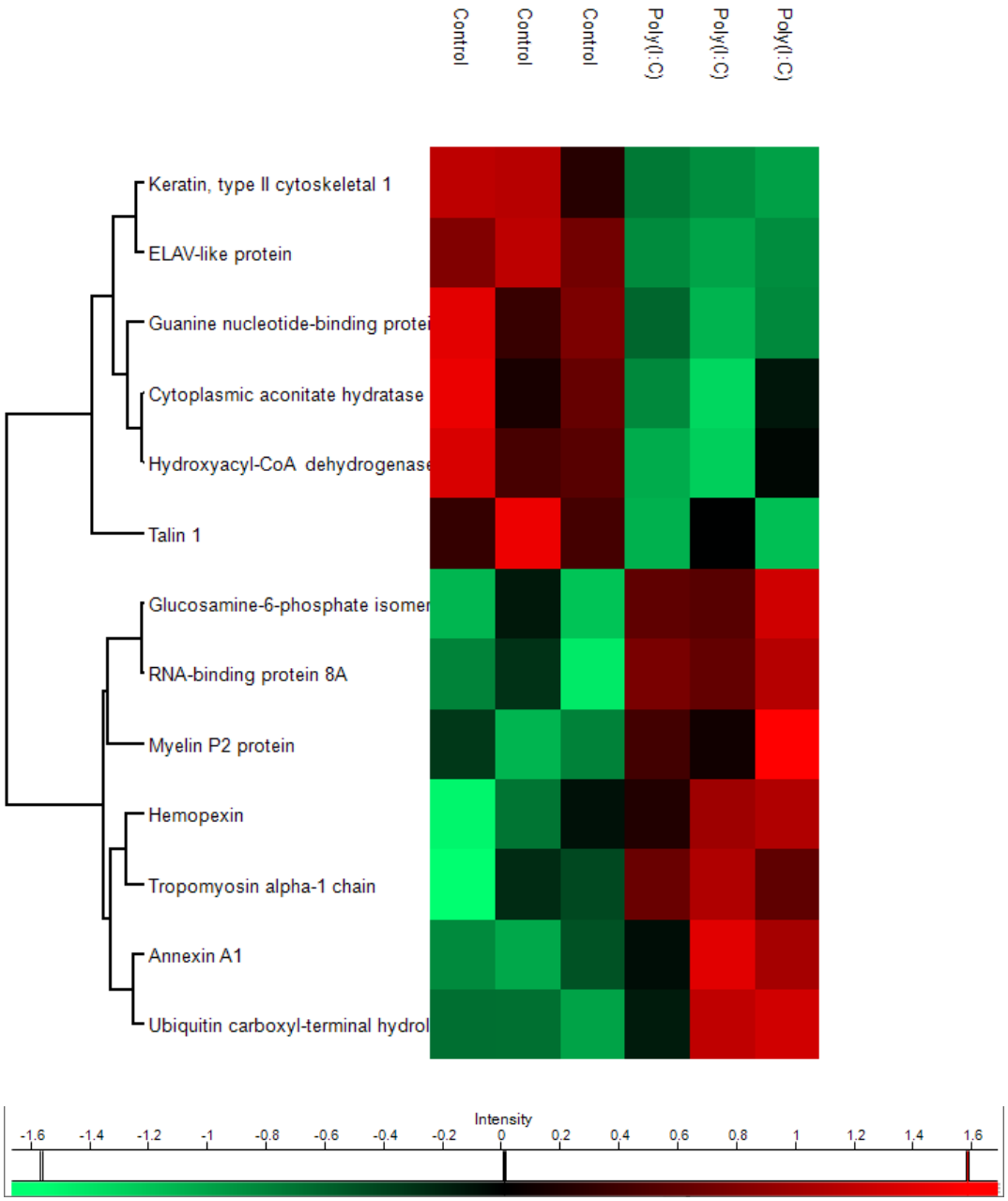

Figure A.4 Heat map of significantly different expressed proteins in supernatants from primary bovine epithelial cells unstimulated vs. Poly(I:C)

Mass spectrometry analysis results of supernatant from primary bovine epithelial cells unstimulated vs. Poly(I:C) 10 µg/ml for 6 hours. Analysis was conducted with the program Perseus applying a two sample t-test. Significant results were defined by p-value ≤ 0.05.

A.4. Gene expression of interferons and interferon-stimlated genes in bovine tracheal epithelial cells infected with BoHV-1 after pre-stimlation with Poly(I:C)

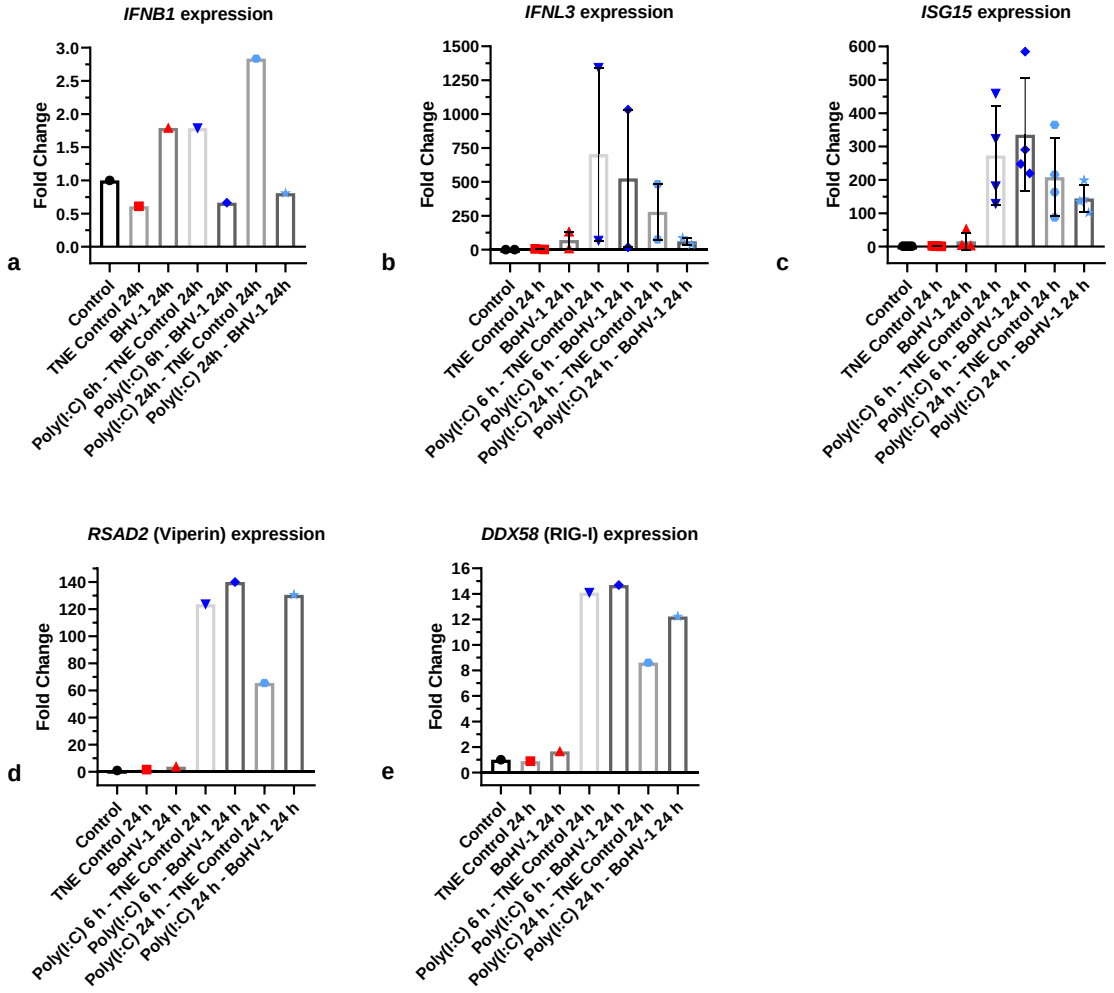

Figure A.5 Poly(I:C) pre-stimulation does not influence the gene expression in response to BoHV-1 infection in tracheal epithelial cells

Confluent primary bovine tracheal epithelial cells were stimulated with Poly(I:C) prior infection with purified live BoHV-1. Cells were harvested into Trizol. RNA was extracted and first strand cDNA reverse transcribed. qPCR was carried out and gene Cq values were normalised to the reference gene H3F3A. Values were normalised to the untreated control. Each data point represents a different animal. Error bars indicate standard error of the mean.

A.5. Poly(I:C) pre-stimulation does not influence the gene expression in response to LPS stimulation in bovine tracheal epithelial cells

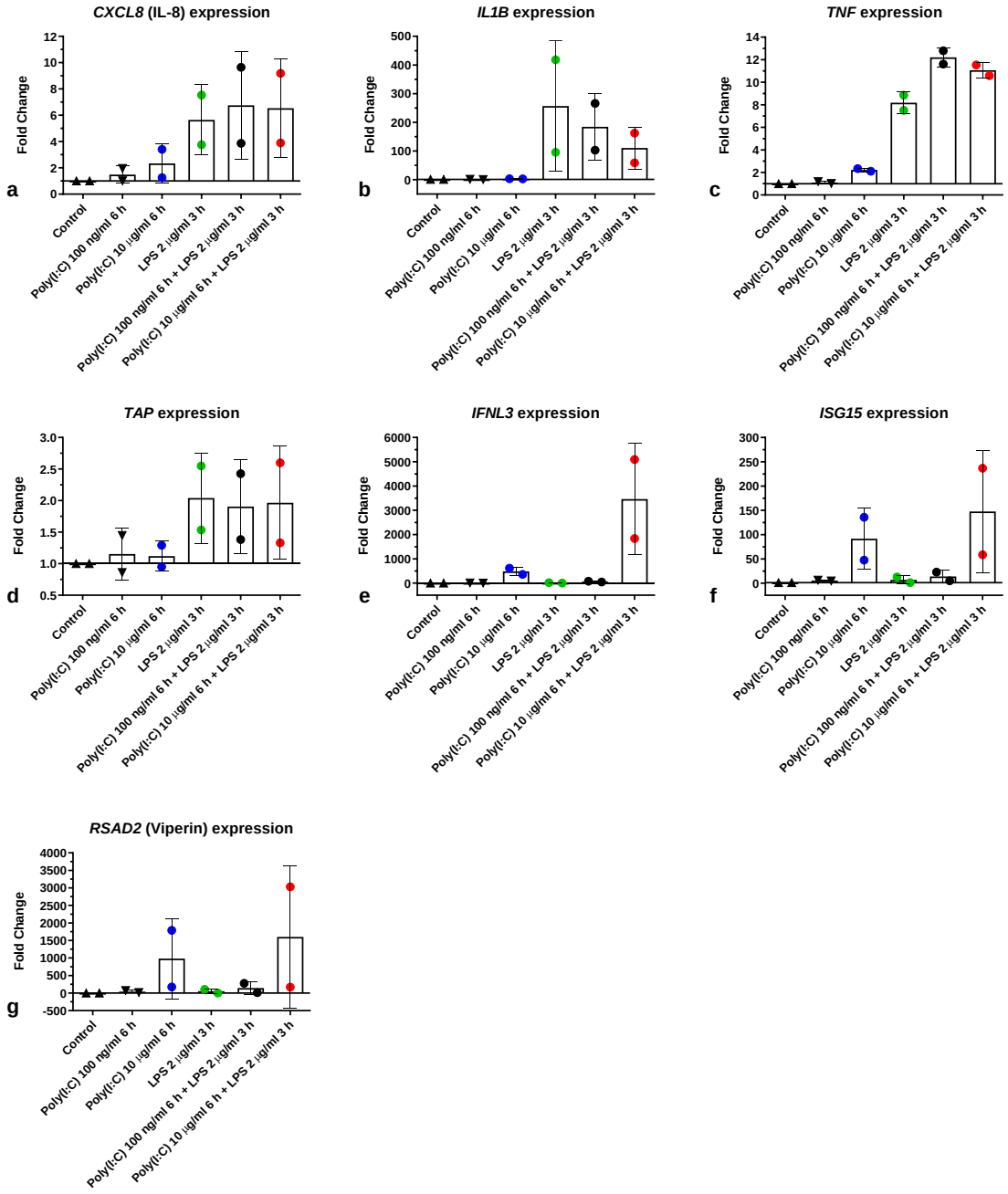

Figure A.6 Poly(I:C) pre-stimulation does not influence the gene expression in response to LPS stimulation in tracheal epithelial cells

Confluent primary bovine tracheal epithelial cells were stimulated with Poly(I:C) prior stimulation with LPS. Cells were harvested into Trizol. RNA was extracted and first strand cDNA reverse transcribed. qPCR was carried out and gene Cq values were normalised to the reference gene H3F3A. Values were normalised to the untreated control. Each data point represents a different animal. Error bars indicate standard error of the mean.

A.6. BoHV-1 infection does not influence the gene expression in response to LPS stimulation in bovine tracheal epithelial cells

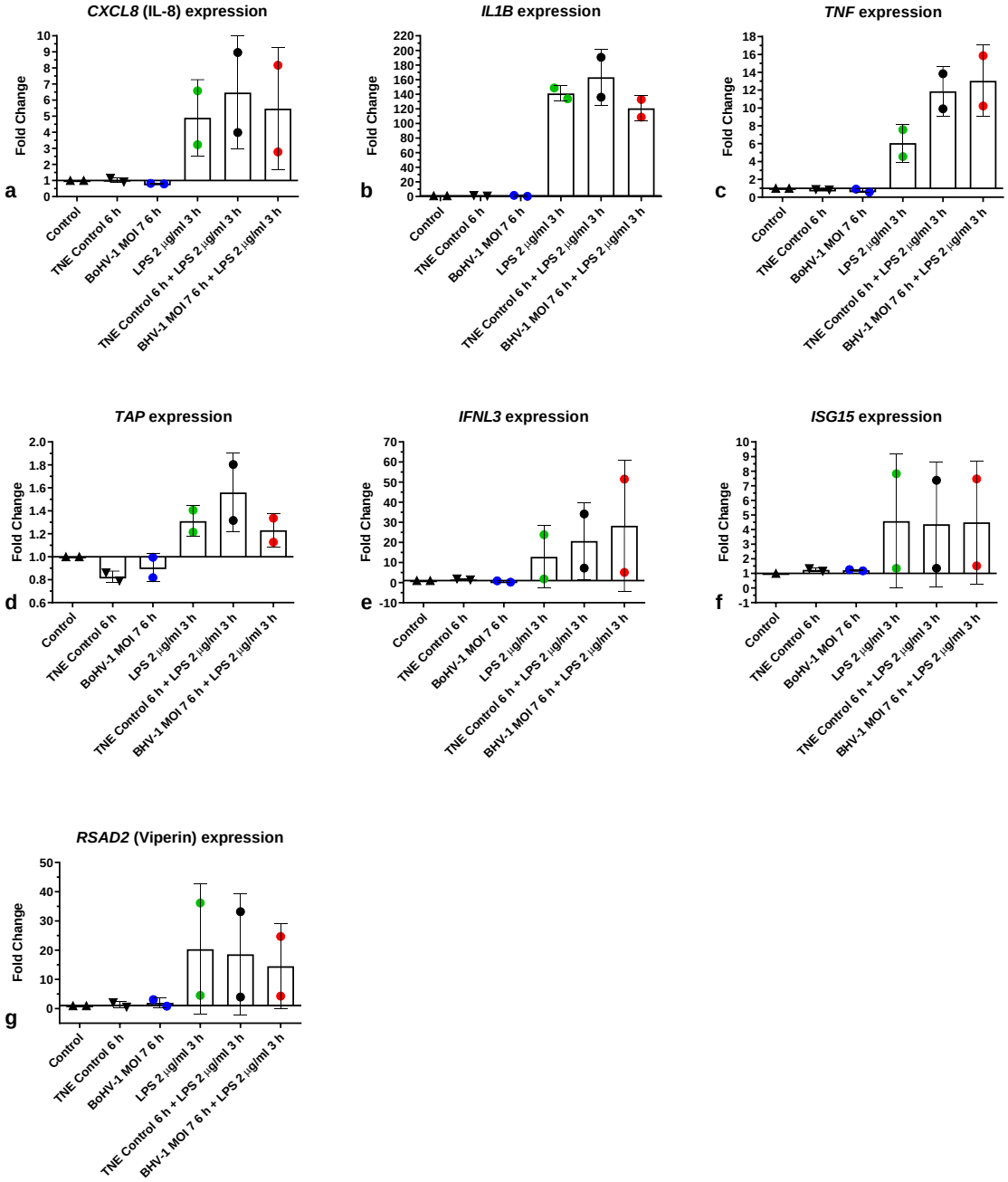

Figure A.7 BoHV-1 infection does not influence the gene expression in response to LPS stimulation in tracheal epithelial cells

Confluent primary bovine tracheal epithelial cells were infected with BoHV-1 prior stimulation with LPS. Cells were harvested into Trizol. RNA was extracted and first strand cDNA reverse transcribed. qPCR was carried out and gene Cq values were normalised to the reference gene H3F3A. Values were normalised to the untreated control. Each data point represents a different animal. Error bars indicate standard error of the mean.